Liquid chromatographic analysis of geological organic substances of industrial importance

By

Thelma-Jean Whelan

UNIVERSITY OF TECHNOLOGY SYDNEY

This thesis is submitted in fulfilment of the requirements for
the degree of Doctor of Philosophy

2005

CERTIFICATE OF AUTHORSHIP

I herby certify that the work in this thesis has not previously been submitted for a degree nor has it been submitted as part of requirements for a degree. I also certify that this thesis has been written by me and that to the best of my knowledge it contains no previously published material. Any help that I have received in my research work and the preparation of this thesis itself has been acknowledged. In addition, I certify that all sources of information and literature used are indicated in this thesis.

Signature of candidate

Production Note:
Signature removed prior to publication.

Thelma-Jean Whelan

ACKNOWLEDGMENTS

I would like to thank Professor Mick Wilson for his supervision, encouragement and support over the past three years. I would not have gotten to this point without his help. I will always be grateful for the opportunities you have given me and consider it a privilege to have worked with you.

Dr Kamali Kannangara, thank you for all your help, support and friendship. It has been a privilege working with you. To the past and present members of the research group, thank you for your friendship and encouragement.

Dr Andrew Shalliker and his research group at UWS, thank you for your friendship, support and encouragement. It has been great working with you all. Your advice and guidance over the past year and a half have been very much appreciated.

I would also like to acknowledge my supervisor Brian Reedy for his contributions to this project and to my colleagues at UTS, thanks for all your support and encouragement over the years.

To my friends, thank you for your support, encouragement and for listening to me. Your friendship is invaluable!

Most importantly I would like to thank my husband Lindsay and my Dad, Mum, Anna, Andrew and my two nieces for their love, support, encouragement and for believing in

me.   They have been with me throughout the three years and I could not have completed this without them and their prayers.   I am very blessed to have all of you in my life. Thank you particularly to Lindsay, who over the last months of my thesis was there with me, supporting me loving me and not letting me quit. Thank you for your patience and for believing in me. I love you!

Finally, to my Lord and saviour, the creator of everything, thank you for giving me this opportunity.   All that I am and all that I do is because of you and the Grace that you have shown me.

Do you not know? Have you not heard?
The Lord in the everlasting God, the Creator of the ends of the earth.
He will not grow tired or weary and his understanding no one can fathom.
He gives strength to the weary and increases the power of the weak.
Even youths grow tired and weary and young men stumble and fall;
but those who hope in the Lord will renew their strength.
They will soar on wings like eagles; they will run and not grow weary,
they will walk and not be faint.

Isaiah 40:28-31

TABLE OF CONTENTS

LIST OF FIGURES

LIST OF TABLES

ABSTRACT

Soluble organic species called humic substances are important in the Bayer process due to their adverse effect on the industrial scale production of alumina from bauxite. During the Bayer process the bauxite is subjected to a high temperature caustic digestion using sodium hydroxide. Most of the organic matter associated with the bauxite (up to 0.3%) ends up in the liquor. The soluble organic species can accumulate in the process liquor as the caustic solution is recycled for the digestion of fresh bauxite after the precipitation of the aluminium hydroxide trihydrate. In this work the humic substances were extracted from the Bayer process liquor obtained from a refinery plant operation at Kwinana Alcoa, Western Australia. The whole fraction as well as sub fractions obtained from a continuous solvent extraction were characterised by elemental and ash analysis, infrared spectroscopy, nuclear magnetic resonance spectroscopy and gas chromatography/mass spectrometry. High-performance liquid chromatography was used to further investigate the composition and structure of Bayer humic substances.

In this study a one-dimensional HPLC separation was developed for Bayer humic substances that achieved a level of separation previously unreported in the literature. The one-dimensional HPLC method separated the Bayer humic substances into compound classes. The analysis of solvent fractions allowed further assignment of the separation. Small molecules and three discrete clusters of macromolecules were observed that are believed to represent micellar like aggregates of different amounts of polar groups as supported by the results of the NMR, FTIR and GC/MS analyses. Within these clusters there was some degree of further resolution. Certain stable

configurations of molecular weights that are controlled by polarity through intramolecular binding were observed which provided strong evidence for a supramolecular structure to humic material rather than the existence of random conformational material.

To further enhance the one-dimensional separation, model compounds were studied to find the most appropriate reversed phase column for the separation of the type of compounds found in humic substances. Five new generation columns were studied with the Phenomenex Synergi polar-RP column found to offer the best performance in terms of separation. This column was later used in the development of the two-dimensional HPLC separation.

Finally, a two-dimensional reversed phase HPLC separation was successfully developed for the separation of Bayer humic substances using novel methodology developed in our laboratories, which successfully resolved uniform band profiles that showed promise of being essentially pure individual components. With the aid of mass spectrometric analysis of three second dimensional bands, the results of the separation strongly supported a host guest model for these compounds. It was concluded that small molecules are held in some way in some supramolecular structure by larger molecules (host guest complexes). The results suggested that the lower molecular weight material is capable of holding small guests more than larger molecular weight material making the supposition that the micellar host guest model is more probable than a model where hosts hide within the guests.

CHAPTER 1

Introduction

1.1. ALUMINA INDUSTRY

1.1.1. The Australian alumina industry

Over the past decades the aluminium industry in Australia has emerged to become a large industry of economic importance both in the national and international markets. In 2001 Australia produced 39% of the world's bauxite and almost 33% of the world's alumina, making it the largest producer of bauxite and alumina in the world [1]. Bauxite production in Australia in 2001 was in excess of 53.3 million tonnes of bauxite and was the world's fifth largest producer of aluminium, accounting for 8.7% of world's primary aluminium production that year [1].

It was in 1955 that the Australian aluminium industry started production from a smelter in Bell Bay, Tasmania using imported supplies of bauxite [2]. Not long after, bauxite deposits of a sufficient size and grade to support an aluminium industry were discovered and developed near Weipa in Queensland marking the beginning of the Australian bauxite industry. It was estimated in 1988 that Australia had bauxite stocks of over half a billion (10^{12}) tonnes with major bauxite reserves located in the Darling Ranges (Western Australia), Gove (Northern Territory) and Weipa (Queensland) [2]. Today the Australian aluminium industry consists of five bauxite mines, six alumina refineries, six primary aluminium smelters, twelve extrusion mills and four rolled product (sheet, plate and foil) mills [1].

The six alumina refineries are located mainly in Western Australia with one each in Queensland and the Northern Territory. In 2001, the six alumina refineries produced over 16.2 million tonnes of alumina, which makes Australia the worlds largest alumina producer [1]. Approximately 80% of Australia's alumina is exported with the remaining alumina shipped to Australian smelters. The majority of the world's alumina (90%) is used to make aluminium however it does have several other uses including applications in chromatography, water purification, pharmaceuticals, as a catalyst in the formation of refractory materials and as a dehydrating agent [2].

1.1.2. Bauxite

In weathered materials aluminium accumulates in clay minerals or in purely aluminous minerals such as gibbsite, boehmite and diaspore, which are the principal minerals of bauxite. Bauxite is a general term for a rock composed of hydrated aluminium oxides and is the material from which alumina is made. It was discovered 175 years ago by Pierre Berthier, a French mineralogist and is the only workable ore of aluminium [3].

The most popular model proposed for bauxite ore genesis is that bauxite is a residual sedimentary material formed by selective concentration of alumina after the dissolution of carbonate and silicate rocks in subtropical regions. High rainfall areas with pronounced dry seasons such as tropical monsoon and some Mediterranean climates produce saturation and drying of the surface, which results in intensive weathering. This intensive weathering leaches most of the minerals from the top few metres of the soil and leaves the insoluble components such as iron and aluminium oxides, clay

minerals and quartz. This weathered product is termed laterite. Bauxite is laterite enriched in aluminium and most deposits are of the post-Mesozoic age (225-70 Ma).

The quantity of the various minerals in bauxite deposits depends on age. Young bauxite deposits are mostly gibbsite, and with age gibbsite changes to boehmite and diaspore. Gibbsite occurs in monoclinic crystals in bauxites that are mostly of tertiary (70 Ma) or younger age [3, 4]. Boehmite occurs in orthorhombic crystals in bauxites that are found in deposits of Tertiary and Upper Cretaceous (100-70 Ma) age [3, 4]. Diaspore occurs in orthorhombic crystals in bauxites of older deposits and metamorphic rocks formed by high pressure and elevated temperature [3, 4].

The mineralogical properties of bauxites largely determine the processing conditions for the recovery of alumina. Diaspore is the most difficult to process, and boehmite is more difficult to process than gibbsite. To be classified as economical to mine by today's technology, the bauxite grade must contain over 27% of aluminium oxides [3]. In addition, the amount of inert material, iron oxides, titanium dioxide and non-reactive quartz determines the size of the separation circuits for the removal of this material (collectively termed red mud). These circuits can be very expensive and hence have an impact on economic viability. Furthermore, the quantity of kaolinite and reactive silica largely determines whether bauxite is classified as commercial or not. At present if bauxite contains more than 8% silica it is classed as "not commercial" to process [5]. One final important consideration in bauxite processing is the organic matter content. Significantly, Australian bauxite has the highest organic matter content in the world (0.05-0.5% w/w) [2]. The organic matter has numerous adverse effects on the process, which are discussed later in this chapter.

1.1.3. Bayer Process

In 1888, an Austrian chemist named Karl Josef Bayer discovered the Bayer process and patented it [2]. The Bayer process [2] is used for the industrial-scale production of alumina from the ore bauxite. This process involves a processing plant that is essentially a three-stage device for heating and cooling bauxite in a large recirculating stream of a highly alkaline solution.

In the first major stage, bauxite is added to 3.5-5 M sodium hydroxide at high temperatures (145-245°C) in sealed vessels, termed digesters. The product liquor, which is supersaturated in sodium aluminate, is filtered to remove insoluble residues, such as oxides of silicon, iron and titanium and a geo-organic fraction, humin. This dark red residue is termed "red mud". Although the insoluble organics (humin) are removed in this fraction, alkali soluble organic degradation products remain in the process liquor and accumulate on recycling [6-8].

For a Bayer process plant to operate cost-effectively, different temperatures and molarities of sodium hydroxide are used due to the variability of alumina found in bauxites (Equations (1.1)-(1.3)). For gibbsite (γ-$Al_2O_3.3H_2O$), 3.5 M NaOH, and temperatures of 135-150°C are used. Thus;
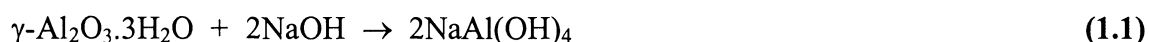
$$\gamma\text{-}Al_2O_3.3H_2O + 2NaOH \rightarrow 2NaAl(OH)_4 \tag{1.1}$$

For boehmite (γ-Al$_2$O$_3$.H$_2$O), 3.5 M NaOH and temperatures of 205-245°C are used. Hence;

$$\gamma\text{-Al}_2\text{O}_3.\text{H}_2\text{O} + 2\text{NaOH} + 2\text{H}_2\text{O} \rightarrow 2\text{NaAl(OH)}_4 \qquad \textbf{(1.2)}$$
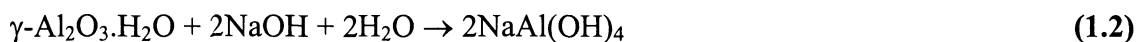
and for diaspore (α-Al$_2$O$_3$.H$_2$O), 5 M NaOH and higher temperatures are common. Hence;

$$\alpha\text{-Al}_2\text{O}_3.\text{H}_2\text{O} + 2\text{NaOH} + 2\text{H}_2\text{O} \rightarrow 2\text{NaAl(OH)}_4) \qquad \textbf{(1.3)}$$

Some modern plants are being designed for use at higher temperatures.

The next and most critical stage of the process involves cooling the product liquor to approximately 90°C and seeding it to precipitate aluminium hydroxide 'trihydrate'. This involves careful control of conditions to achieve high yields and a good quality product. It is at this point that soluble organic matter contributes detrimentally to the process through suppression of precipitation yields, incorporation of sodium ions, excessive liquor foaming, evolution of odours, increased liquor viscosity and density and effects on alumina crystallisation and agglomeration [6-8].

After precipitation in the third and final stage, precipitated aluminium hydroxide is calcined at 1200°C to produce alumina (Al$_2$O$_3$). Once again, the organics have an adverse effect on the process causing dusting and decolourisation of the final product.

While a number of technologies have been considered for removing the organics such as photoxidation, prior fractionation of bauxite and post liquor burning, they are all expensive [2] even though organics have been estimated to be responsible for a loss of as much as 20% of production. The organic matter affects the process at a number of points in the Bayer process and these will be described in detail later in this chapter.

1.1.4. Crystallisation

Crystallisation of alumina from a strongly alkaline solution involves the conversion of the aluminate ion $(AlO_4)^-$ which has tetrahedral geometry to octahedral alumina trihydrate $Al_2O_3.3H_2O$. The process by which this occurs is poorly understood although there has been suggestions that the aluminate ion dimerises and then addition occurs across the dimer to form a species with octahedral coordination [9].

1.1.4.1. Nucleation

A greater understanding of the process can be gained by studying the formation of alumina species at lower pH [10-11]. It is clear that species form polymers either in mildly acidic or mildly basic solution. These alumina species may be specific such as the Al_{13} species, which consists of one tetrahedral aluminium surrounded by twelve octahedral species or long polymer chains some of which are colloidal i.e. nanoscale. Five-coordinated aluminium may also be formed transitorily [11]. It would seem logical therefore that nucleation occurs with a number of these species coordinating together so that dimensions of molecules are microsize rather than nanosize. Organic

matter with highly electronegative groups coordinate to Al^{3+} species thereby interfering with the process.

1.1.4.2. Crystal Growth

A second source of interference occurs during the crystal growth. As the lattice forms, organic molecules may adsorb on the surface and need to be displaced for further aluminium species to precipitate. These organic molecules may occlude thereby creating lattice defects, or the displacement process may slow down the entire crystallisation. Further, these organic molecules may act as nuclei for other impurities or may prevent individual crystals agglomerating together. Thus some of the compounds present hamper the precipitation of aluminium hydroxide by adversely altering the desired product size distributions and by increasing the amounts of impurities in the product crystals. Organic matter can also affect the crystallisation of other materials in solution such as sodium oxalate, which needs to be removed.

The most important organic contaminant found in highest yield in Bayer liquors is sodium oxalate [12]. There are numerous references in literature on the effects of sodium oxalate on the Bayer process [6, 13-15]. At sufficiently high concentrations sodium oxalate may precipitate as fine needles onto which the aluminium hydroxide 'trihydrate' co-precipitates. Once the concentration of sodium oxalate is high enough, oxalate crystal nuclei form suddenly in the liquor resulting in what is termed "oxalate showers". These nuclei then allow for gibbsite nucleation onto the oxalate surface. This results in a product that is considered useless. However the presence of some

organic matter species in Bayer liquor are beneficial in this role (although detrimental in others) in that they may stabilise the sodium oxalate in solution hence reducing the likelihood of the above process.

Whilst it may be thought that oxalate removal can be achieved just by calcination since oxalate can readily be decomposed by heat to carbon dioxide. In fact the sodium oxalate is decomposed to carbon dioxide; however the final alumina product is contaminated with high levels of sodium. This creates very small particles of alumina as the sodium reduces proper calcined particle agglomeration and finely sized alumina ($< 11 \ \mu m^2$) is not acceptable as a material for alumina production.

In order to control the sodium oxalate concentration a side-stream process in which sodium oxalate is precipitated from the spent liquor is used. The liquor and precipitate are vacuum filtered then passed through a fabric filter press. The resultant liquor now has a sodium oxalate concentration of approximately 2.0 g/L compared with 4.0 g/L prior to oxalate precipitation.

For the purposes of this study we were interested in analysing the sodium hydroxide soluble geo-organic matter that accumulates during the Bayer process. This fraction is referred to as Bayer humic substances.

1.2. HUMIC SUBSTANCES

1.2.1. Soil and aquatic humic substances

Humic substances are vital to our environment, playing an important role in terrestrial and aquatic ecosystems. The term 'humic substances' is given to a mixture of relatively high molecular weight, yellow to black organic compounds of aromatic and aliphatic nature that are formed by secondary synthesis reactions (humification) during the chemical and biological degradation of plant and animal litter and from synthetic activities of microorganisms [16-18].

The exact structure of humic substances has been the source of much debate. Present knowledge proposes humics as complex macromolecular substances that contain aromatic, phenolic, quinonic, and heterocyclic building blocks that are randomly condensed or linked by aliphatic, oxygen, nitrogen or sulfur bridges. Aliphatic, glucidic, aminoacidic and lipidic surface chains are present in the macromolecule in addition to chemically active functional groups such as carboxylic, as well as phenolic and alcoholic hydroxyls, and carbonyls, that make the humic polymer acidic [18-20]. Hydrophilic and hydrophobic sites are also present. Further studies have suggested that within this macromolecular structure there are voids capable of occluding lower molecular weight material. These small molecules appear to be held in the macromolecular matrix by either hydrogen bonding or in the case of alkanes, trapped in molecular voids, making them guests to the host structure (Host-guest theory) [21].

Humic substances can be divided into three main fractions according to their solubility in water at various pH's. Fulvic acids are the fraction that is soluble at all pH's and consists on average of smaller molecular weight compounds. Humic acids are the fraction that is soluble in dilute alkaline solutions and insoluble below pH 2, with higher molecular weight compounds being present in this fraction. The last fraction is humin, which is insoluble in both acidic and alkaline media [16, 18].

Humic substances have a number of valuable roles in nature. They are known to be chelating agents, on occasions being responsible for the transport of a wide range of metal ions both in soils and waters. They can have an impact on fertility by affecting the availability of a wide range of cations [22]. The run-off of cations can be prevented by the chelating nature of humic substances, allowing soils to store more useful cations [21]. The presence of humic substances is not always of a beneficial nature. In water they generate colour and affect taste and therefore need to be removed by purification. In addition, due to their chelating capacity, industrial processes that involve surface activity can be inhibited by the presence of humic substances.

Humic substances comprise approximately 60-70% of the total organic carbon found in soils and 40-60% of the dissolved organic carbon occurring in water [19]. Nevertheless, our knowledge of the structural features and conformational behaviour of humic substances is still limited, with their basic chemical nature and reactivity poorly understood [23]. Their physical and chemical properties are all closely related to their functionality, size, molecular weight, molecular weight distribution and conformation. Since the discovery of humic substances, structural, functional, compositional and behavioural data has been collected using techniques such as nuclear magnetic

resonance (NMR) spectroscopy [24-35], infrared spectroscopy (IR) [25-26, 28-29, 36-38], elemental analysis [25-26, 28-29, 37], scanning electron microscopy (SEM) [25, 30, 37], gas chromatography/mass spectroscopy (GC/MS) [24, 29, 39-45], liquid chromatographic methods such as capillary electrophoresis (CE) [46-48] and capillary zone electrophoresis (CZE) [49-51], and size-exclusion chromatography (SEC) [52-66].

1.2.2. Bayer humic substances

As noted previously, the humics enter the Bayer process during the formation of alumina from bauxite ore via dissolution in concentrated sodium hydroxide (3.5-5 M) at high temperatures. Up to 3% of the organic matter associated with the bauxite ends up in the liquor, although some insolubles are removed with the red mud [2]. The soluble organic species can accumulate in the process liquor, as the caustic solution is recycled for the digestion of fresh bauxite after the precipitation of the aluminium hydroxide trihydrate.

The bauxite entering the process contains essentially two types of organic matter. The first type is derived from large vascular plant root systems that penetrate deep into the bauxite deposits from overlying trees. These systems contain largely lignin (up to 26% w/w) and carbohydrates (up to 60% w/w). The dissolution of these components under lower temperature Bayer process conditions has been reported [67-68].

The second type of organic matter is geo-organic matter/humic substances, which has accumulated over the history of the bauxite deposit through geochemical and bacterial

transformation of plant and animal matter [12, 52]. These include alkali soluble species that enter and impinge on the process, and any alkali insoluble organic material (humin) being removed with the red mud. These materials are not all plant derived, as many other alkanes and alkenes, polycondensed aromatics, high nitrogen and long chain fatty acids [12, 52, 67-71] can originate from bacteria and fungi. The presence of charcoal-like material termed "char" from ancient forest fires has also been observed in soils and humic extracts [69-71] and bauxite [72]. Tests carried out on one of the "char" samples suggest that it is largely insoluble and is expected to be removed along with red mud [72].

Given the significance of the organic matter content to the process, industrial confidentiality restricts reports in open literature on organic matter distribution in individual bauxite deposits throughout Australia. However there is at least one report on the organic matter in bauxite and this shows it is similar to that found in many soils [73].

1.2.3. Host guest theory

It is clear that a myriad of chemical compounds of different molecular weights make up the organic matter in soils and would therefore end up in bauxite. For organic matter produced in reducing environments, such as coal and lignite, a Host Guest theory has been proposed based on solubility and reactivity [74-75]. ^{1}H NMR spectral data also revealed the existence of two groups of molecules in bituminous coals with different molecular rigidities, i.e. rigid large hosts and smaller mobile guests, although there

would be rapidly moving groups in hosts such as methyl groups which blur the distinction.

It is also probable that these assemblies could exist in soils and in bauxite [21]. Despite attempts to remove low molecular weight organic matter by dialysis, specific molecular weight fractions have revealed the presence of low molecular weight organic matter [21]. These host-guest interactions may occur in a variety of humic macromolecular compounds in the environment. The exact mechanism of entrapment is not known but it is likely that the organic guest molecules are included in the host molecule via formation of intermolecular interactions such as hydrogen bonding [56, 65-66]. Physical entrapment in the large host structure is also possible.

Chelation to metal ions may be another method through which organic guest molecules are entrapped. This may be a mechanism of breaking intra or intermolecular interactions, which may create voids or indeed a mechanism of forming other voids. Chelation to metal ions may release guests or entrap others. Energetically the destruction of host-guest complexes is expected to be less demanding than the destruction of covalent bonds. Indeed it has been demonstrated that humic substances undergo facile degradation with UV radiation rather than polymerisation [76-79]. It can be envisioned that a series of events occur including oxidation of host component phenols to quinones that removes any possibility of hydrogen bonding and then the subsequent release of small molecular weight guests.

1.2.4. Organic Fractionation

1.2.4.1. Organics in red mud

During the digestion stage of the Bayer process, most of the organics in the bauxite dissolve but some organic matter is insoluble. The insoluble organic matter is removed from the process with the red mud waste product as an organic rich material on heater tubes in the shell-side of heat exchangers, or adsorbed on aluminium hydroxide precipitate and the sodium oxalate by-product. Sometimes organic matter is also observed in precipitation tank scale and with oxalate-gibbsite co-precipitated fine particles.

It is worthwhile observing the differences in chemical structure between the organic matter that was insoluble in sodium hydroxide that ends up in the red mud, with the organic matter in the original bauxite as this provides an insight into the changes taking place during digestion. However, simple pyrolysis-GC/MS is insufficient to compare the two components in the red mud and bauxite because the iron oxide, not the alumina species, catalyse the decomposition of the organics [80].

The methanol soluble products are different in the red mud and bauxite as shown by pyrolysis analysis. The pyrolysis products from the methanol solubles from the red mud has been shown to contain various alkanes, alkenes, aromatic carboxylic acids, and aliphatic carboxylic acids. Some examples include methyl benzoate, methyl esters of saturated C_4 - C_{20} carboxylic acids and C_{11} - C_{23} alkenes. Few aromatic compounds

were seen in the extracts [80].   Some of the species released from the red mud have also been found to be released from the bauxite when it was analysed under the same conditions, however the compounds were present in very different amounts.   These results highlight that the composition of the organic matter in the bauxite and red mud are intrinsically different.

It appears from the above results that the dissolution of organic matter in the Bayer process is selective.   That is, the molecular structure of the organic matter in the red mud differs from that in the bauxite and from the soluble compounds that dissolve in the Bayer liquor.   It is particularly surprising that some of the most polar compounds including the short chain carboxylic acids concentrate in the red mud despite their solubility in sodium hydroxide.   These results suggest that the red mud acts as an adsorbent for these compounds.

1.2.4.2. Other insoluble Organics

Insoluble organic matter is removed at several other stages of the Bayer process including as an organic rich material on heater tubes in the shell-side of heat exchangers, on aluminium hydroxide precipitated crystals, the sodium oxalate by-product, as well as in precipitation tank scale and with oxalate-gibbsite co-precipitated fine particles.   Table 1.1 summarises the results of the ^{13}C CP/MAS NMR analysis of insoluble organic matter removed during the Bayer process.

Table 1.1: ^{13}C CP/MAS NMR analysis of the insoluble organic matter in deposits from a refinery operating at 250-255°C.

	C-Alkyl 0-50 (ppm)	O-Alkyl 50-100 (ppm)	Aromatic 100-160 (ppm)	Carboxylic 160-190 (ppm)	Carbonyl 190-220 (ppm)
	%	%	%	%	%
Deposits					
Heat exchanger scale	60.0	0	40.0	0	0
Sodium oxalate	13.0	0	33.5	53.5	0
Aluminium hydroxide	22.5	0	35.5	42.0	0
Precipitation tank scale	28.6	0	55.8	15.6	0
Oxalate-gibbsite co-precipitation fines	25.7	0	34.9	39.4	0

After digestion, the first cooling event occurs at the heat exchanger units. Here organic matter forms on the shell-side of heater tubes and contains enough carbon to be analysed by ^{13}C CP/MAS NMR. The material is highly aromatic, and the aromaticity [fraction of carbon that is aromatic, (f_a)] is 0.40 [80]. The absence of carboxylic carbon at or about 175 ppm chemical shift shows that this material is not humic like. Pyrolysis-GC/MS data on the same material identified the sample as having the composition of a light pitch or tar.

Solid-phase sodium oxalate plays a minor role in the sodium content of product alumina, but it has a critical role in gibbsite nucleation in precipitation operations, determining crystal size and particle numbers [20-21]. The presence of organic matter in the Bayer liquor stabilises the oxalate in solution to some extent, however once oxalate precipitation begins the oxalate surface adsorbs some of the organics from the liquor promoting further precipitation. This phenomena, known as 'oxalate showers', disturbs the orderly precipitation of aluminium hydroxide causing excess nucleation leading to fines in the circuit and poor quality alumina with a high sodium content [20-21]. Most alumina refineries use an oxalate removal circuit to control the process and minimise the impact of this material. As a result, the crystallised oxalate is also a material that removes insoluble organic material from the Bayer process.

Crystallised aluminium hydroxide also contains insoluble organic material. These aluminophilic organics play a role in the poisoning of the Bayer process by altering the growth of gibbsite crystals from the Bayer liquor. The solid state ^{13}C NMR spectra of the insoluble carbon in the sodium oxalate and aluminium hydroxide are similar. The

NMR spectra contain three main regions - a distinct aromatic region (100-150 ppm), a less intense aliphatic region consisting of carbon substituted with electron donating groups (50-100 ppm) and a series of peaks in the region between 160-180 ppm due to the presence of carboxylic carbon and oxalate [80].

Sodium oxalate and aluminium hydroxide produced several common pyrolysis products including alkanes, alkenes and long chain aliphatic carboxylic acids (predominantly with C_{14} to C_{16} carbon chain lengths), as well as short chain (C_4-C_7) aliphatic mono-, di- and tri- carboxylic acids. The main difference is that the aluminium hydroxide pyrolysates also contain large amounts of fluorene, biphenyl and methyl-substituted naphthalenes, as well as low concentrations of methyl-substituted phenanthrenes and anthracenes and two alkanes, C_{20} and C_{21}.

Oxalate-gibbsite co-precipitation fines are a network of aluminium hydroxide and sodium oxalate crystals that do not settle from the Bayer liquor. This product gives rise to pyrolysis products including alkanes, alkenes, aromatic compounds including substituted benzenes, alkylbenzenes, napthalenes as well as substituted anthracenes, phenanthrenes and fluorenes. The solid state ^{13}C NMR spectrum of the oxalate-gibbsite co-precipitation fines showed the presence of aliphatic and aromatic carbon. NMR spectra of oxalate-gibbsite co-precipitation fines showed a range of structural groups including aromatic and methoxy carbons [80]. The presence of such a wide range of chemical groups may poison further precipitation and growth of the crystals. This may explain why sodium oxalate fines prevent the growth of sufficiently large enough crystals of aluminium hydroxide to be settled from the Bayer process by gravity separation.

Precipitation tank scale contains both precipitated sodium oxalate and aluminium hydroxide. The ^{13}C NMR spectrum of the precipitation tank scale appeared quite similar to the NMR spectra obtained for dissolved organic matter with the proportions of the different carbon types also being similar [80].

1.2.5. Organics in solution

1.2.5.1. Process differences due to temperature

Typical concentrations of organics in Bayer liquors that are extracted from the bauxite into the Bayer process liquor during digestion, range from a few grams per litre up to 40 g/L, [6] with molecular weights from less than 100 Da to greater than 300 kDa [24, 81]. As already noted this geo-organic matter causes numerous problems in the operation of alumina refineries. The compositions of organic materials obtained from a low temperature Bayer refinery (145-150 °C) and a high temperature refinery (250-255 °C) have been compared [24, 81].

Typical chemical compositions of the organic molecular weight fractions are detailed in Tables 1.2 and 1.3 but they will vary with refinery [24, 81]. Table 1.3 also shows elemental compositions of whole liquor organics prior (pregnant) and post (spent) precipitation of alumina hydrate. Table 1.3 shows the smallest molecular weight fraction, <1.2 kDa, accounting for 87% of the recovered organic material from a refinery operating at 250-255 °C. Structurally the <1.2 kDa fraction contains mainly hydroxybenzene carboxylic acids [24, 81]. The 12-25 kDa and 25-50 kDa fractions

Table 1.2: ^{13}C CP/MAS NMR analysis of molecular weight fractions of soluble organic matter from a refinery operating at 250-255°C.

	C-Alkyl 0-50 (ppm)	O-Alkyl 50-100 (ppm)	Aromatic 100-160 (ppm)	Carboxylic 160-190 (ppm)	Carbonyl 190-220 (ppm)
	%	%	%	%	%
Molecular weight fractions (kDa) in solution					
<1.2	20.6	2.4	52.9	23.1	1.0
1.2-6	22.4	4.3	55.9	16.7	0.7
6-12	18.8	10.9	56.8	12.2	1.3
12-25	13.0	6.6	62.9	16.2	1.4
25-50	11.8	8.4	58.3	20.6	1.2
50-100	14.6	0.1	67.3	16.9	1.1
100-300	23.2	7.2	58.7	10.1	0.9
>300	26.3	6.9	58.7	7.8	0.4

Table 1.3: Yields, pH and elemental analysis of the Bayer humic substances fractions (dry ash free basis) from a refinery operating at 250-255°C.

Fraction No.	Molecular weight fraction (kDa)	%C	%H	%N	%S	%O Difference	O/C	H/C	N/C	S/C	pH at 5g/litre in water	Mass yield (%)[a]
PL[b]	<1.2 to >300	56.32	3.67	0.36	0.23	39.42	0.53	0.78	0.0055	0.0015	2.43	100.00
SL[b]	<1.2 to >300	53.13	3.58	0.11	0.11	43.07	0.61	0.80	0.0018	0.00078	2.39	100.00
1	<1.2	50.79	4.22	0.56	0.17	44.26	0.65	0.99	0.0095	0.0013	2.48	87.0
2	1.2-6	48.25	3.78	1.87	0.32	45.78	0.71	0.93	0.033	0.0025	2.96	3.3
3	6-12	54.32	4.23	3.22	0.60	37.62	0.52	0.93	0.051	0.0041	3.39	0.6
4	12-25	53.87	3.67	1.39	0.44	40.62	0.57	0.81	0.022	0.0031	2.90	1.6
5	25-50	55.58	5.41	3.69	0.42	34.90	0.47	1.16	0.057	0.0028	3.79	1.0
6	50-100	48.85	4.05	4.92	0.68	41.50	0.64	0.99	0.086	0.0052	3.99	3.8
7	100-300	49.13	4.85	5.92	0.99	39.11	0.60	1.18	0.10	0.0075	4.64	0.7
8	>300	54.52	3.78	2.05	0.42	39.24	0.54	0.83	0.032	0.0029	4.36	2.0

a) The weight of fraction over total weight of material recovered. b) PL = pregnant liquors, SL = spent liquors

appear to resemble material more akin to kerogen, while the highest molecular weight organic material (>300 kDa) behaves as a soluble char [24, 81].

Table 1.3 shows that the pH of the organic fractions varies between 2.39 and 4.64. The two whole organic fractions, from the pregnant and spent liquors, as well as the <1.2 kDa fraction are the most acidic. The pH of each fraction generally increases with increasing molecular weight, however the 12-25 kDa fraction is an exception. The pH of the fractions is an important factor during precipitation testing as this affects local ionic strengths of the Bayer solutions, which has an impact on oxalate stability, and precipitation yields.

1.2.5.2. Small molecular weight molecules

The amount of less than 1.2 kDa molecules is highly dependent on temperature, bauxite geological history and species of native plant matter as previously described. This is the most acidic fraction containing the highest proportion of carboxylic carbon (20%, 145 °C and 23.1%, 245°C), compared with >300 kDa higher molecular weights (9.8%, 145 °C and 7.8%, 245°C) [69-72]. Much of this fraction comprises of very low molecular weight species, such as oxalate and lactic, acetic and formic acids and a range of benzene carboxylic acids [6-8]. They are well documented by Lever [13]. Table 1.4 shows comparative py-GC/MS data between compounds found in the lowest molecular weight fraction isolated from a low temperature (145°C) [24] and high temperature (245°C) [81] processes which shows clear differences in volatiles upon pyrolysis.

Table 1.4: Comparison of py-GC/MS data at 450°C between low molecular weight (<1.2 kDa) fraction from a low temperature and high temperature Bayer liquor. Selective relative abundance (%) to phenol.

Compound	Low temperature process (145°C) <1.2 kDa	High temperature process (245°C) <1.2 kDa
Toluene	35.3	
1,2-dimethylbenzene	44.9	
1,2,3-trimethylbenzene	27.7	
5-methoxy-2-methyl-1H-indole	90.1	99
4-hydroxybenzonitrile		51
Phenol	100	100
2-methylphenol	16.8	
3-methylphenol	31.8	
2-methoxyphenol	55.5	
2-naphthalenol		125
2-coumaranone	54.4	63
2-methyl -1,3-isobenzofurandione		61
4-hydroxyphenyl-1-pentanone		23
1H-isoindole-1,3(2H)-dione		87
4,7-dimethyl-1,3-isobenzofurandione		170
5,6-dimethyl-1,3-isobenzofurandione		59
Benzoic acid	50.1	83
3-methylbenzoic acid	29.2	41
4-methylbenzoic acid	34.0	
4-methyl-1,2-benzenecarboxylic acid		100
3-hydroxy-4-methylbenzoic acid		287
Trimethylbenzaldehyde	49.3	

The presence and thus the formation of compounds in the low molecular weight fractions isolated from Bayer liquors are Bayer plant dependent. Interestingly, Table 1.3 shows that the high temperature process contains a higher proportion of ketones, diones and nitrogen containing compounds. This is in contradiction with the low temperature process in which methylbenzenes, phenols, and benzoic acids predominate. Temperature may play a role in this discrepancy, in that high temperatures produce more highly oxidised species. However, it is also likely that the differing geo-histories of the bauxite deposits produce different organic inputs to the processes.

1.2.5.3. Intermediate molecular weight molecules

There is little literature on the interaction of intermediate (1.2-100 kDa) molecular weight humic substances with alumina, although it is known that this material plays an important role in the Bayer process.

Attempts have been made to characterise and quantify these intermediate organic molecules present in the Bayer liquor by using a number of chromatographic techniques. GC/MS spectral analysis has been successfully used to identify and quantitate a number of smaller molecular components such as monocyclic aromatic carboxylic acids, alkanes and fatty acids [24, 81]. Liquid chromatographic (LC) analysis of the less volatile humic acid component has been less successful. LC methods for the monitoring of known organic and inorganic ions that accumulate in the process liquor have been reported [82-83]. Any further reported attempts at analysing the humic acids found in the Bayer liquor has been restricted to the quantitative analysis

of the humic acids present [84]. Therefore the development of a High-Performance Liquid Chromatographic (HPLC) method for resolving these intermediate molecular weight components into molecular entities or even compound classes would be of considerable industrial importance.

1.2.5.4. Large molecular weight molecules

The higher molecular weight organics (>50 kDa), although present in low concentrations in Bayer process liquor have a range of structures. The largest molecular weight organic matter is char-like [69-72]. In principle because they are large compounds it would be expected that these would have large surface covering effects and therefore inhibit precipitation in this way. As hosts they may also contain many guests, which might be prevented from playing a role in precipitation. They effectively can alter the equilibrium concentration between an adsorbing guest on a crystal surface and a free guest in solution. Char-like materials can be in the original bauxite [72] but solubility studies suggest that this material ends up largely as insolubles in the red mud. Thus these char-like materials are probably also synthesised in the process.

1.2.5.5. Host guests in Bayer liquor extracts

A myriad of chemical compounds of different molecular weights compose the organic mixture that makes up the organic matter in Bayer liquors. Many have extremely high molecular weights with values for some components as high as 300 kDa. Dialysis of

humic organic matter separates the material into molecular weight fractions or more correctly, fractions that can pass through specifically sized pores. Despite attempts to separate organic matter into molecular weight fractions by dialysis, specific higher molecular weight fractions were obtained that still contained low molecular weight organic material. Material of molecular weight of 50 kDa or greater have voids in its packing quite capable of occluding smaller molecular weight material so that the smaller materials are in fact guests. It was clear that these small molecules appeared to be bound too much larger macromolecules by physical entrapment and/or hydrogen bonding.

As noted earlier in this chapter, one new finding for oxidising environments is the concept of host-guest structures where smaller molecules reside within a framework of a macromolecular host primarily derived from lignin [85]. The guests within the host cannot be removed by physical separation techniques. The structure of the host can be determined by py-GC/MS and NMR techniques. Differential thermal analysis, calorimetry, methylation and NMR data can be used to identify the guests. Some of the guests are probably held by hydrogen bonding but others are true prisoners, for example, alkanes and hence have no binding sites.

1.3. INSTRUMENTAL TECHNIQUES FOR THE ANALYSIS OF HUMIC SUBSTANCES

The present knowledge of the structure and composition of humic substances is the result of decades of study with various analytical tools. With advancements in technology, important information has been gained on the structure of humic substances using techniques such as nuclear magnetic resonance (NMR) spectroscopy, Fourier transform infrared (FTIR) spectroscopy, pyrolysis-gas chromatography/mass spectrometry (py-GC/MS), X-ray methods and other functional group analysis techniques. Of particular importance has been the contribution of NMR spectroscopy, py-GC/MS and FTIR spectroscopy to the understanding of the structure and composition of humic materials. It is not intended to detail these here but nevertheless it is necessary to indicate their use.

1.3.1. Nuclear Magnetic Resonance spectroscopy analysis of humic substances

The development of NMR spectroscopy in geochemistry over the last two decades has seen advancements in the knowledge of the structure and composition of humic substances. ^{1}H, ^{13}C, ^{15}N and ^{31}P NMR spectroscopy have all been used to analyse humic substances.

Solution ^{1}H NMR was the first form of NMR used for the study of humic substances, with Schnitzer and Barton in 1963 studying the structure of a methylated soil humic

acid [17, references within]. In 1978 Wilson et al. [86], using high-field (270MHz) techniques, obtained a detailed spectra for soil humic acids. However, the application of ^{1}H NMR to humic substances has been limited due to the poor resolution of resonance groups and the presence of a large dominating residual water peak. Over the past few years, effective techniques have been developed to suppress the water signal allowing the distribution of hydrogen types to be determined [87-88].

Solid state ^{13}C NMR is the most widely used in the study of humic material. With the development of cross-polarization magic-angle spinning (CP-MAS) experiments the undesirable line broadening associated with earlier solid ^{13}C NMR was improved. Hatcher et al. (1980) [89], Wilson et al. (1981) [90] and Preston and Ripmeester (1982) [91] were some of the first to use CP-MAS ^{13}C NMR to analyse humic material. The ^{13}C NMR spectrum can be divided into regions that correspond to specific chemical classes. The characteristic regions of the ^{13}C NMR for humic materials are the aliphatic carbon (0-50 ppm), methoxyl C-O carbon (50-60 ppm), carbohydrate C-O carbon (60-100 ppm), aromatic carbon (100-150 ppm), phenolic and aromatic ether carbon (145-160 ppm), C=O carbon of carboxyl and ester groups (160-190 ppm) and C=O ketonic carbon (190-210 ppm) [18]. Today NMR spectroscopy has become a method of choice for the analysis of humic substances.

A number of studies have been reported on the NMR analysis of Bayer humic substances. Baker et al. [73] compared the composition of humics extracted from bauxite and the Bayer liquor using ^{13}C NMR. Wilson et al. (1998) [92] used ^{13}C NMR to study Bayer humics that precipitated with the aluminium hydroxide cake at pH 7. Wilson et al. (1999) [24] looked at the chemical composition of size-exclusion fractions

of low-temperature Bayer humic substances using solid-state ^{13}C NMR and ^{1}H NMR. Smeulders et al. [80] used ^{13}C NMR to examine the structure of molecular weight fractions of high temperature Bayer humic substances. ^{13}C NMR was used by Ellis et al. [68] to look at the degradation of angiosperm and gymnosperm under laboratory simulated Bayer process conditions.

1.3.2. Pyrolysis - gas chromatography/mass spectrometry analysis of humic substances

Py-GC/MS combines the high separation efficiency of GC with the identifying power of MS. This technique is based on the thermal degradation of a macromolecular sample in an inert atmosphere to form molecules of a lower mass suitable for GC/MS analysis [42].

Nagar [93], Wershaw et al. [94] and Kimber et al. [95-96] were some of the first to report the use of py-GC/MS to study the structure and composition of humic substances in the late 1960's, early 1970's. However, it was not until the mid 1980's that the most significant discoveries were made using py-GC/MS by Saiz-Jimenez and de Leeuw [42] who revealed that humic substances contained groups originating from lipids, polysaccharides, proteins and lignins. More than 300 pyrolysis products were identified and possible origins for each compound were assigned [97-98]. Later studies provided evidence suggesting that humic substances can also contain highly aliphatic plant biopolymers originating from algal and plant cell walls and/or plant cuticles and barks [42]. Numerous other studies using py-GC/MS to examine the structural

characteristics of humic substances have been performed, with many suggesting that humic materials consist of aromatic rings that are connected by long, flexible aliphatic chains that may be highly carboxylated [42, 99-100].

Over the past few years a number of advances have been made to the py-GC/MS technique for the analysis of humic substances. These advances were driven by some of the limitations in the technique. During pyrolysis carboxylic acids decarboxylate, yielding the corresponding alkanes and alkenes so that the structural units containing carboxyl groups are not detected [41]. Another limitation occurs due to the pyrolysis temperature, as the behaviour of the humic substances is highly dependant on the temperature selected [41]. To overcome these limitations, Challinor (1989) [101] introduced a technique for the simultaneous pyrolysis and methylation of polar groups using tetramethylammonium hydroxide (TMAH) as a derivatizing reagent. It was found that the presence of the strongly basic TMAH promotes hydrolytic ester and ether cleavage during pyrolysis [102].

Saiz-Jimenez et al. first applied the use of TMAH in the methylation pyrolysis of humic fractions [102, references within] and the results were compared with those obtained by conventional pyrolysis. Methylation was found to substantially change the pattern of pyrolysis, producing a cleaner chromatogram due to less structural fragmentation and provided higher sensitivity. Methylation pyrolysis with TMAH has now been employed in numerous studies of humic substances.

Bayer humic substances have been studied by py-GC/MS. Wilson et al. [24] in 1999 used this technique to analyse low-temperature molecular weight Bayer humic fractions,

which was followed by a study of the high-temperature molecular weight Bayer humic fractions by Smeulders et al. [81]. Py-GC/MS with in situ methylation was used to analyse insoluble organic compounds found in the Bayer process [80].

Although py-GC/MS does provide detailed structural information, it can provide a distorted picture due to the thermal degradation of some structures. The interpretation of pyrolytic experimental results may be misleading as in many cases the naturally occurring units may have been altered before or after release from the macromolecular structure [102]. Despite its limitations and pitfalls, py-GC/MS and its modifications are probably one of the best techniques that have been applied to the structural analysis of humic substances and when combined with other characterisation techniques such as NMR and FTIR spectroscopy, important structural and compositional information can be gained.

1.3.3. Infrared spectroscopy analysis of humic substances

Infrared (IR) spectroscopy analysis has contributed substantially to the knowledge of the chemistry of humic substances. For the structural and analytical study of organic molecules the medium IR region between 4000 and 400 cm^{-1} was found to be of greatest interest [18]. The energy absorbed in this region by an organic molecule is converted into molecular vibrational energy. The IR spectrum of organic molecules consists of two types of vibrational bands, stretching vibrational modes and bending or deformation vibrational modes. Using IR spectroscopy, information can be gained on the presence of specific functional groups present within a molecule, based on each

absorption band corresponding to a particular vibration of a given bond that occurs at a given frequency [18]. The main absorption bands have been assigned and are in the regions of 3450-3000 cm^{-1} (hydrogen-bonded OH), 3080-3030 cm^{-1} (aromatic C-H stretching), 2950-2840 cm^{-1} (aliphatic C-H stretching), 1725-1710 cm^{-1} (C=O stretching of COOH, aldehydes and ketones), 1620-1600 cm^{-1} (aromatic C=C stretching, COO-symmetric stretching), 1400-1380 cm^{-1} (OH deformation and C-O stretching of phenolic OH, C-H deformation of CH_2 and CH_3 groups, COO- antisymmetric stretching), 1260-1200 cm^{-1} (C-O stretching and OH deformation of COOH, C-O stretching of aryl ethers and phenols), 1170 cm^{-1} (C-OH stretching of aliphatic O-H) and 975-775 cm^{-1} (out-of-plane bending of aromatic C-H) [18].

IR spectroscopy has been used in the research of humic substances for the gross characterisation of important functional groups, for analysing the effects of chemical modifications such as methylation and acetylation, for the detection of any changes in the structure or composition of humic substances after hydrolysis or thermal degradation, to determine the presence or absence of inorganic impurities and for investigating the interaction between metal ions or pesticides with humic substances.

Stevenson and Goh [103] classified IR spectra of humic substances into three general types on the basis of typical bands relating to specific functional groups and structure entities. Type I spectra are typical of humic acids. Type II spectra are typical of fulvic acids. Type III in addition to the bands shown in the spectra of type I and II, displays additional bands, some indicating the presence of proteins and carbohydrates. Kumada et al. [18, references within] made a more comprehensive classification of IR spectra of

humic substances classifying them into 4 major types that are based on relative intensities of specific bands [16, 18].

A number of studies have been reported on the use of FTIR for the analysis of Bayer humic substances. Wilson et al. [24] analysed the structure of low-temperature molecular weight Bayer humic fractions. Smeulders et al. [81] used FTIR to compare the structure of high-temperature Bayer humics in molecular weight fractions.

1.4. LIQUID CHROMATOGRAPHY

1.4.1. Definition of chromatography

For centuries, techniques related to chromatography have been used to separate materials such as dye extracts from plants. However, it was not until 1906 that Michael Tswett first used the term *'chromatography'* to describe his work on the separation of coloured plant pigments into bands on a column made of chalk [104]. Since then chromatography has progressed considerably and is now an accepted technique used in many fields of science including chemistry, biology, pharmaceutical, medical, quality control and environmental studies.

In 1993 the International Union of Pure and Applied Chemistry (IUPAC) defined chromatography as;

'Chromatography is a physical method of separation in which the components to be separated are distributed between two phases, one of which is stationary while the other moves in a definite direction.' [104]

Liquid chromatography (LC) is the term used to describe any chromatographic procedure in which the mobile phase is a liquid [105]. High-performance liquid chromatography (HPLC) is the term used to describe a liquid chromatographic method in which the liquid mobile phase is mechanically pumped through a column that contains the stationary phase [105]. HPLC is a term typically used to refer to modern liquid chromatographic methods.

1.4.2. Parameters of HPLC

Four major parameters are used in chromatography to describe and measure the operation of a chromatographic system: retention factor, selectivity, resolution and efficiency [105]. The efficiency of a chromatographic system is optimised to obtain the best possible separation, the retention factor of a column should be enough so that the solutes are retained and the column should have the appropriate selectivity to resolve the analytes of interest [105].

1.4.2.1. Retention Factor

The retention factor (capacity factor) k describes the ability of a stationary phase to retain components and is a direct measure of the strength of the interaction of the sample with the packing material [104-105]. k is defined by the expression [106];

$$k = \frac{t_R - t_0}{t_0} \tag{1.4}$$

where t_R is the retention time of a specific solute and t_0 is the retention time of a non-retained species [104-107]. Although the retention factor of a column is to a large degree a function of the packing material, it can be manipulated to a degree by adjusting the solvent strength. The optimum range for k, which is between 1 and 10 can be achieved by adjusting the solvent strength. The higher the retention factor of the column, the greater is its ability to retain solutes.

1.4.2.2. Selectivity

The selectivity describes how effectively a chromatographic system can separate two species. The selectivity (α) of a column for two species 1 and 2 is defined as [106];

$$\alpha = \frac{k_1}{k_2} \tag{1.5}$$

where k_1 and k_2 are the retention factors of species 1 and 2. The selectivity (α) of a column is largely a function of the stationary phase and by definition must always be greater than unity, with no separation possible if $\alpha = 1$. An increase in separation selectivity translates to an increase in resolution. To some extent the separation selectivity can be improved by changing the stationary phase or adjusting the mobile phase, temperature, mobile phase pH or by the addition of special chemical additives. The separation selectivity should be as large as possible while maintaining k values in the optimum range of $1 \leq k \geq 10$ [106].

1.4.2.3. Efficiency

The efficiency of a column is measured by the population distibution, a function of that is defined as the number of theoretical plates (N). An increase in the number of theoretical plates can be achieved by increasing the column length, decreasing the stationary phase particle size or by adjusting the mobile phase velocity so as to change the column pressure, thus increasing the efficiency of the column [106].

1.4.2.4. Resolution

The resolution (R_s) of a column is a term used for the quantitative measure of a columns ability to separate two solute bands. It is affected by the selectivity (α), efficiency (N) and retention capacity (k) of the column with the resolution equation describing the relationship between these factors. The resolution of a column can be describe by the following equation [106];

$$R_s = \frac{1}{4}\sqrt{N}\left(\frac{\alpha - 1}{\alpha}\right)\left(\frac{k}{1+k}\right)$$

(1.6)

1.4.3. Liquid chromatographic modes of separation

The success of modern day HPLC as an analytical technique can be largely attributed to the variety of separation mechanisms (modes) that are available. The most significant modes of liquid chromatographic separation are normal phase, reversed phase, ion-exchange and size-exclusion chromatography.

1.4.3.1. Normal phase

Normal phase chromatography is the oldest of the chromatographic modes [108]. For this separation mode a polar stationary phase is employed with a less polar mobile phase used to elute the analytes. In a normal phase chromatographic system, neutral solutes in solution are separated based on their polarity, with the polar solutes being retained on the column for longer. As the mobile phase is less polar than the stationary phase, increasing the polarity of the mobile phase results in a decrease in the retention of the solute [105, 109]. Typical stationary phases for normal phase chromatographic systems are chemically bonded stationary phases that have polar functional groups. On these types of stationary phases, elution is carried out with relatively non-polar solvents such as ethyl ether, chloroform and n-hexane [107].

1.4.3.2. Reversed phase

Reversed phase chromatography is the most widely used chromatographic mode accounting for over 75% of all HPLC separations [108]. The term 'reversed phase' is used to denote a chromatographic system that is in essence the reverse of normal phase chromatography with a non-polar stationary phase and a polar mobile phase. With this separation mode, the more polar a solute, the lower the retention [108-109]. An increase in the polarity of the mobile phase results in an increase in the retention of the solute. Reversed phase chromatographic systems use chemically bonded stationary phases that have non-polar functional groups. Typically water is used as the base solvent for most reverse phase separations with a less polar solvent such as methanol or acetonitrile added to adjust the solvent strength [105, 108].

1.4.3.3. Ion-exchange

Ion-exchange chromatography refers to the separation of analytes according to their differences in electric charge, which is governed by the electrostatic attraction of the ionic solutes in solution to the "fixed ions" of opposite charge on the stationary phase support [105]. Ion-exchange supports can be classified into anion-exchangers or cation-exchangers according to the nature of the ionic functional groups on the stationary phase. Ion chromatography, a form of ion-exchange chromatography, is widely used in the analysis of inorganic anions, cations, and low molecular weight, water-soluble organic acids and bases [105, 108]. Retention in ion chromatography is

governed by the pH of the mobile phase, ionic strength, temperature and the type and concentration of buffer ions in the mobile phase [107].

1.4.3.4. Size-exclusion

In size-exclusion chromatography solutes are separated as a result of their permeation into solvent-filled pores within the column packing [108]. In this chromatographic mode of separation, the packing material consists of small silica or polymer particles that contain a uniform network of pores into which solvent or solute molecules can diffuse [107]. The first to elute are molecules that are larger than the average pore size of the packing as they are excluded and thus in essence have no retention. Molecules that are significantly smaller than the pore size of the packing are able to penetrate the pore network, thus being retained for longer and are last to elute. In size-exclusion chromatography secondary adsorption effects such as chemical or physical interaction between the analytes and stationary phase are avoided.

1.4.4. Multidimensional Chromatography

1.4.4.1. Limitations of one-dimensional HPLC separations

High-performance liquid chromatography (HPLC) is widely used today for the separation and identification of a variety of sample matrices. However, despite the advances in instrumentation and column technology, HPLC still cannot completely resolve samples that are complex in nature. It has been shown that single

chromatographic separation systems often fail to separate even the simplest of complex samples largely as a result of the random distribution of peaks throughout the separation [110-111].

In a one-dimensional HPLC separation a component mixture is displaced along a single axis where a single separation mechanism is employed. Giddings [112] in 1967 developed peak capacity, a concept for measuring the resolving power of a one-dimensional system. Peak capacity is a term used to define the maximum number of peaks that can fit next to each other in the available separation space, assuming that the component peaks follow one another at exactly the right distance to yield the minimum stated resolution [112]. For example, if we were to have a peak capacity of 100 it tells us that 100 single component peaks are evenly distributed to fit in the allowed retention volume range. This theoretical approach however falls short of the practical reality of the separation with component chromatographic peaks of complex mixtures falling randomly along the chromatogram.

To account for this random distribution, Davis and Giddings in 1983 developed the component overlap theory using Poisson statistics [110-111, 113]. This theory predicted that if the component peaks were uniformly spaced, the maximum number of randomly distributed peaks that could be separated is only approximately 37% of the theoretical limit and single component peaks only 18% under the most favourable conditions. The theory also showed that a chromatogram must be approximately 95% vacant in order to provide 90% probability that a given component of interest will appear as an isolated peak [110]. Further experimental studies by Davis and Giddings [111] using complex samples showed the peak spacing to be random which was in

agreement with their previous theoretical models. A number of other studies have also demonstrated the randomness of component peaks in complex samples including the work of Guiochon et al. [114-115].

For complex mixtures HPLC separations will be limited by the statistical possibilities discussed above. For a single column, inadequate resolution of all the components may occur.

1.4.4.2. Multidimensional HPLC separations

In multidimensional separations, mixture components are displaced along two axes of separation, providing larger physical spaces in which components of complex mixtures can be separated, therefore increasing the separation capability of a chromatographic system [116-118]. According to Giddings there are two conditions that define a multidimensional separation [116]. The first criteria is that a multidimensional separation is one in which the components of a mixture are subjected to two or more separation steps (mechanisms) where their displacements depend on different factors. Secondly, in a multidimensional separation, when two components are substantially separated in any single step, they remain separated until the completion of the separative operation.

An ideal multidimensional separation system should consist of two or more separation systems that are coupled together providing a separation environment in which two or more different retention mechanisms are employed. This would generate orthogonal

retention behaviour of the solutes in each dimension, thus maximising the peak capacity of the system [118]. In theory, the maximum peak capacity of a multidimensional system is the product of the peak capacities of the individual dimensions [119]. However, in practice this maximum theoretical peak capacity is difficult to obtain. For a two-dimensional HPLC system, the degree to which the two different separation mechanisms in each dimension differ can be described by the informational orthogonality of the two-dimensional system. Informational orthogonality can be used to optimise a multidimensional separation and can be calculated using information theory [120]. Slonecker et al. [120] describes the use of information theory for calculating the informational orthogonality of two-dimensional chromatographic separations.

Multidimensional HPLC techniques may be coupled or non-coupled. Non-coupled techniques are where the columns are not physically joined and require manual manipulation between columns and coupled techniques are where the columns in each dimension are connected by switching valves or traps [108]. Due to advances in instrumentation, coupled techniques are more popular with automated systems providing increased analysis times with minimal operation. A coupled multidimensional system is distinct from joining two different columns in series. A system in which the columns are in series provides little advantage over a one-dimensional HPLC separation. In coupled multidimensional HPLC separations, either all or a portion of the eluent from the first dimension may be switched to the second dimension or to a trapping column. When only a portion of the sample separated in the first dimension is transported to the second dimension, the process is referred to as

"heart-cutting" [117, 121], whereas in a comprehensive multidimensional system all the components of the sample mixture are subjected to separation in both dimensions [121]. For two-dimensional HPLC separations, heart-cutting techniques are the most popular.

As there are a large number of possible combinations of chromatographic systems, there is enormous variability in the types of multidimensional separation systems that are available. Bushey and Jorgenson [122] separated protein standards and serum proteins using a comprehensive two-dimensional HPLC method with UV detection. The system used a microbore cation exchange column in the first dimension and a size-exclusion column in the second. The eluent from the first dimension filled one of two loops, which were of equal size, using an eight-port switching valve. In one position, eluent from the first dimension column was loaded into one loop while the second pump forced the contents of the other loop onto the column in the second dimension. The entire first column eluent was analysed on the second column by the time of the completion of the first column separation.

Murphy et al. [123] used a combination of normal phase and reversed phase HPLC in a two-dimensional LC system to separate alcohol ethoxylates. Using the two-dimensional system they were able to separate alcohol ethoxylates into their alkyl and ethylene oxide components. The results of the two-dimensional method were compared with one-dimensional techniques where it was clearly shown that there was an increase in the selectivity using the two-dimensional technique.

A mixture of peptides resulting from the enzymatic digestion of a protein were easily separated using a two-dimensional liquid chromatographic system which used size-

exclusion chromatography followed by reversed phase chromatography [124]. The

interface between the two dimensions was comprised of two reversed phase columns in

parallel rather than storage loops allowing the use of conventional analytical diameter

columns. Following the two-dimensional chromatographic separation an electrospray

mass spectrometer was used to detect the peptide fragments. Other examples of

multidimensional chromatographic separations techniques have been reported [125-

133].

1.4.5. Liquid chromatographic analysis of Bayer humic substances

There is very little literature published on the liquid chromatographic analysis of Bayer

humic substances. A limited number of liquid chromatographic methods have been

successfully developed for the monitoring of known simple organic and inorganic ions

that accumulate in the process liquor. Jackson in 1995 [83] compared ion

chromatography (IC) and capillary electrophoresis (CE) for the analysis of oxalate,

which is of prime importance as its stability and removal can control refinery

productivity, as well as chloride and sulfate. For oxalate, IC produced consistently

higher results than CE due to the presence of chromatographic interferences and overall

reported a lower precision for replicate samples compared to CE. CE also allowed the

simultaneous determination of oxalate, chloride and sulfate, whereas IC did not due to

significant chromatographic interferences. Overall this study found that CE was the

preferable technique to IC, allowing the complete resolution of all the ions from the

matrix in a run time of less than 6 minutes.

Haddad et al. [49] developed a capillary zone electrophoresis (CZE) method for the simultaneous separation of chloride, sulfate, oxalate, malonate, fluoride, formate, phosphate, carbonate and acetate in Bayer liquors. Optimal running conditions were established and all inorganic and organic anionic components were fully resolved. Harakuwe et al. [82] further investigated the use of CZE for the routine determination of oxalate in Bayer liquors. The effect of changes in conditions, such as temperature, electrolyte composition and applied voltage were studied. It was demonstrated that CZE is an appropriate technique for routine analysis of complicated sample matrices, such as Bayer liquors.

Any further reported attempts at analysing the humic acids found in the Bayer liquor has been restricted to the quantitative analysis of the humic acids present. Susic et al. [84] reported the first use of a HPLC method with fluorometric detection for the quantitative humic acid analysis of Bayer liquor. The method used was adapted from a method that has been routinely used for determining the humic acid content in environmental samples. The reversed phase method provided a rapid quantitative analysis of the humics present in the Bayer liquor that eluted within 10 minutes as a single, sharp peak.

1.5. THIS WORK

As noted above little work has been done to analyse the complex nature of Bayer humic substances by HPLC. While GC/MS has identified small molecular weight material, the molecular analysis of material of molecular weights above 1200 Da has yet to be achieved by HPLC or other analytical techniques. Many individual compounds of molecular weights greater than 1200 Da may be particularly poisonous. The identification of individual components by HPLC will help in identifying the source of these compounds. Further, new and economically viable methodology could then be developed for their removal that would have a beneficial effect for the Australian alumina industry.

In this thesis we examined humic substances that were extracted from Bayer liquor obtained from a refinery plant operation at Kwinana Alcoa, Western Australia and attempted to separate the compounds by HPLC. A one-dimensional HPLC separation was developed that achieved the best reported separation of Bayer humic substances to date. Model compounds were studied to further develop the HPLC separation. Finally, a two-dimensional reversed phase HPLC separation was successfully developed for the separation of Bayer humic substances using novel methodology developed in our laboratories. This technique allowed us to successfully resolve what appears to be essentially pure individual components.

CHAPTER 2

Experimental

2.1. BAYER HUMIC SUBSTANCES

The following section details the methods of extraction of the humic substances from the Bayer liquor and fractionation of the extracted humic substances by a continuous solvent extraction.

2.1.1. Extraction of humic substances from the Bayer liquor

The humic substances were isolated from the Bayer process liquor using a method that was described by Wilson et al. [24, 81]. This extraction method is similar to that described by Sihombing et al. [40]. Figure 2.1 illustrates the extraction process, which is described below.

An aliquot of Bayer liquor (200 mL) from digestion of bauxite at 145-150°C at the Kwinana Alcoa refinery, Western Australia was diluted at volume ratio of about 1 to 10 (v/v) with distilled water and acidified to pH 1.5 with 1:1 (v/v) hydrochloric acid-water mixture. The soluble fulvic acid fraction was decanted and then filtered through a glass microfibre paper (Whatman 15.0 cm GF/C) and filtered again through a sintered glass filter (porosity 4) to remove undissolved particles in the acidified Bayer liquor. The pH of the precipitated humic acid fraction was gradually increased to 4 with sodium hydroxide (1 M) to solubilise the humic acid. This solution and the fulvic acid solution were combined and adsorbed onto an XAD-7 resin as described below.
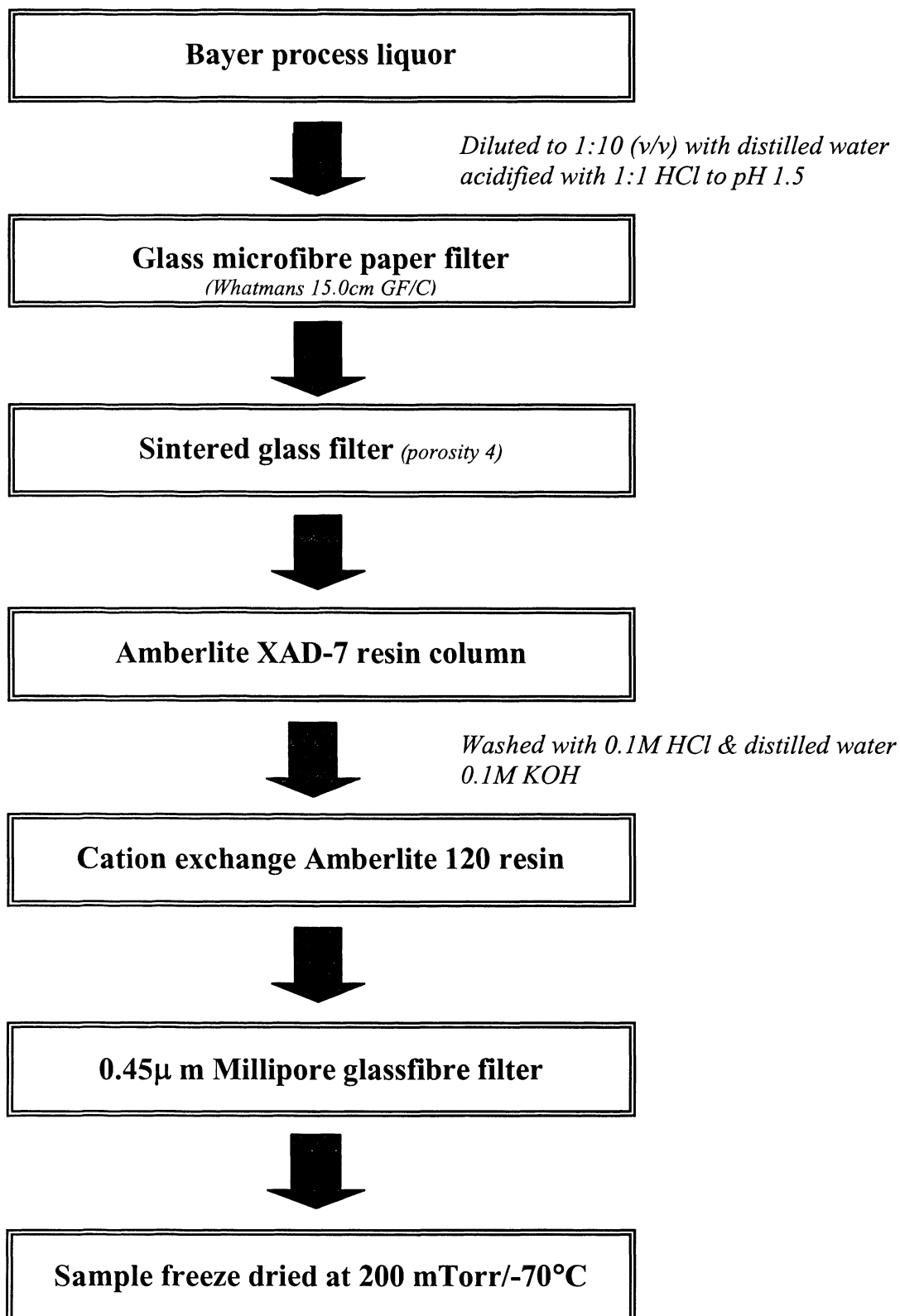
Figure 2.1: Diagram illustrating the extraction and isolation of the Bayer humic substances.

Extraction of the humic substances in the Bayer liquor was then carried out on a pre-washed and acidified Amberlite XAD-7 resin column (6 x 2 cm, 200 g resin). The humic substances in the acidified Bayer liquor solution (above) (1 L) were absorbed on the column by passing the solution through the XAD-7 column at a flow rate of approximately 1 mL/minute until the outlet liquor became yellow in colour. The column was washed with 2 L of 0.1 M hydrochloric acid, and then with 1 L of doubly distilled deionised water until the pH of the outlet water was neutral. The column was eluted with 0.1 M KOH solution (450 mL) and the concentrated (brown coloured) humic substances were collected (400 mL). The protonated form of the Bayer humic substances was obtained by passing 200 mL of the alkaline humic substances solution through a pre-washed (doubly distilled-deionised water) cation exchange resin (Amberlite 120, 60 cm x 2 cm). The humic substances were washed from the column with one column volume of doubly distilled deionised water (120 mL) to yield the protonated form (humic and fulvic acids). The procedure was repeated twenty times using 200 mL aliquots of the initial Bayer liquor solution, and the solutions combined to form 2.4 L of combined solution. This solution was then filtered through a 0.45 μm Millipore glass fibre filter and 16 aliquots of 60 mL were removed for molecular weight separation. The rest of the material was freeze dried and stored. The yield of organic material from the Bayer liquor was 11.6 g/L

2.1.2. Solvent extraction of Bayer humic substances

A continuous solvent extraction procedure with varying solvent polarity was used to separate the bulk Bayer humic substances into four fractions. The Bayer humic

substances [2 g] was placed in a glass microfibre extraction thimble [19 x 90 mm] and used in a Soxhlet extractor. The extraction was carried out starting with diethyl ether [150 mL], then ethyl acetate [150 mL], isopropyl alcohol [150 mL] and finally with milli-Q water [150 mL], with each solvent being allowed to extract for over 12 hrs. The diethyl ether, ethyl acetate and isopropyl alcohol extracts were rotor evaporated to dryness and dried under vacuum over night while the water extract was freeze dried.

2.2. CHARACTERISATION OF BAYER HUMIC SUBSTANCES

The following section details the techniques used to characterise the humic substances extracted from the Bayer liquor and the fractions collected from the solvent extraction of the Bayer humic substances.

2.2.1. Elemental Analysis

Carbon, hydrogen and nitrogen analyses were carried out on the Bayer humic substances. Other elements were not measured. The Microanalytical Unit of the Australian National University, Canberra, performed all elemental analyses in-house.

The carbon, hydrogen and nitrogen compositions were determined using a Carlo Erba EA1108 CHNS-O Elemental Analyser after vacuum drying for 4 hr in an oven at 60°C. Oxygen was calculated by difference.

2.2.2. pH Analysis

The pH of the entire Bayer humic substances was obtained by redissolving the humic sample (50 mg) in 10 mL distilled water to make up a solution of 5.0 g/L. The pH was measured at 25°C on a Radiometer Pacific Copenhagen pH meter using a glass electrode. The pH meter was calibrated using standard buffer solutions at pH 4.00 and pH 7.00.

2.2.3. Ash analysis

The ash content of the entire Bayer humic substances was determined using a TA instrument, SDT (simultaneous differential techniques) 2960. The Bayer humic sample (2.82 mg) was evenly packed into an open 170 μL platinum crucible, which was placed in the furnace under an air atmosphere with a flow rate of 35 mL/minute. The furnace was programmed to rapidly heat to 600°C, after which it was programmed to ramp to 1200°C at a rate of 30°C/minute. The furnace was then held at 1200°C for 5 minutes and then cooled to 35°C with air. The ash content of the Bayer humic sample was found to be negligible.

2.2.4. Fourier transform infrared spectroscopy

Fourier transform infrared (FTIR) spectra were recorded from 4000 to 400 cm^{-1} using a Nicolet Magna-IR 760 spectrometer with 64 scans and a resolution of 4 cm^{-1} in a dry nitrogen atmosphere.

Samples were prepared as potassium bromide (KBr) discs with a diameter of 16 mm by grinding 2 mg of Bayer humic sample and the fractions from the continuous solvent extraction with 250 mg of KBr. BDH laboratory grade KBr for infrared spectroscopy, oven dried at 120°C, was used for all samples. Sample disks were analysed immediately to avoid disks being affected by atmospheric water. Background spectra of the compartmental air was collected and the FTIR sample spectra was ratioed to the collected background to eliminate interfering peaks that were due to atmospheric water and carbon dioxide.

2.2.5. Nuclear magnetic resonance spectroscopy

2.2.5.1. Solution state ^1H NMR

Solution state ^{1}H NMR spectra were recorded on a Bruker DRX 300 MHz instrument fitted with field gradient coils. The Bayer humic substances (2 mg) and the fractions from the continuous solvent extraction (2 mg) were dissolved in dimethyl sulfoxide-d$_6$ (DMSO-d$_6$, 99.8 Atom % D, Aldrich, 0.6 mL). The clear amber solution was removed by pipette to a 5 mm NMR tube. The choice of solvent DMSO-d$_6$ was based on

complete solubility of Bayer humic sample and better resolution of the proton peaks especially the exchangeable protons.

All spectra were recorded at a temperature of 300 K unless a higher temperature (320 K) was used to distinguish the exchangeable protons (hydrogens attached to oxygen and/or nitrogen atoms). At higher temperatures, the exchangeable protons are shielded (peaks shift to a lower chemical shift) because of the weakening of the hydrogen bonding. All non decoupled proton experiments were obtained with a 90° pulse of 7.4 μs, 4000 sweep width, recycle delay of 2 s and an acquisition time of 4.09 s. The data was collected in 8 K of memory and then Fourier transformed using line-broadening factors of 0.3 Hz. The chemical shifts are referenced externally to a solution of tetramethylsilane (TMS; 0 ppm).

2.2.5.2. Solution state ^1H-^1H NMR

Two-dimensional NMR spectroscopy experiments such as ^1H-^1H homonuclear correlation spectroscopy (COSY) spectra were obtained in order to confirm the spin-spin coupling between the protons and to assist in assignments. Acquisition parameters for the ^1H-^1H COSY 2-D NMR experiments included a spectral width of 4000 Hz, recycle delay of 2 s, 1024 data points (time domain) and 16 scans per experiment.

2.2.5.3. Solid state ^{13}C NMR

Solid state ^{13}C Cross Polarisation Magic Angle Spinning Nuclear Magnetic Resonance (CP/MAS NMR) spectra were obtained on a Bruker DPX200W Advance 200 MHz instrument operating at 50.3 MHz. Approximately 200 mg of the Bayer humic sample and the fractions from the continuous solvent extraction were analysed using the cross-polarisation technique with magic-angle spinning (CP/MAS). The solid samples (powdered) were packed into a 4 mm zirconia rotor with a Kel-F cap and the rotors were spun at the magic angle ($54.74°$). Spinning speed was 5 kHz and spectra were recorded at ambient temperature. Pulse widths of 4 μs were used, with a 2 s recycle time and a contact time of 1.5 ms, 20,480 scans were collected in 16k points and Fourier transformed with a line broadening of 20 Hz to obtain the frequency domain spectrum. The chemical shifts were expressed relative to tetramethylsilane (TMS) using adamantane as an external reference (the CH_2 peak of adamantane was assigned to 38.3 ppm downfield from the 0.00 ppm TMS peak). The frequency domain ^{13}C spectrum was analysed to determine approximately the different structural groups present using established literature methods.

2.2.6. Gas chromatography/ mass spectrometry analysis

Solvent fractions of the Bayer humic substances collected using the extraction technique described above were methylated and analysed by GC/MS. Approximately 0.5 mg of the Bayer humic sample and each of the four solvent fractions were placed in 2 mL glass ampoules. An aliquot (100 μL) of a solution made from 5 mL of 25%

tetramethylammonium hydroxide in methanol and 1 mL of 0.05% (w/v) of an internal standard, C19 alkane, in methanol was added. The methanol was evaporated to dryness under vacuum and the ampoules were sealed under vacuum. The ampoules were placed in an oven at 200°C for 30 minutes. After cooling the ampoules were opened and thoroughly washed out with dichloromethane (~ 100 µL). The solution was then analysed by GC/MS.

A HP 5890 GC/MS interfaced to a HP 5970 mass selective detector was used. An aliquot (1 µL) of the solution was injected onto a DB5MS capillary column (30 m x 0.25 mm I.D). The oven was programmed to have an initial temperature of 60°C. After an initial holding time of 5 minutes, the oven was heated at a rate of 5°C/minute to 290°C. Mass spectral analysis was carried out in full scan mode over a range of m/z 60-600 Da.

2.3. ONE-DIMENSIONAL HIGH-PERFORMANCE LIQUID CHROMATOGRAPHIC ANALYSIS

In the following section, details are given on the instrumentation and experimental conditions used in the liquid chromatographic analysis of the Bayer humic substances using a one-dimensional HPLC method.

2.3.1. Chemicals

HPLC grade methanol, acetonitrile was obtained from Mallinckrodt Australia. Formic acid (BDH) was analytical grade (98%) and was purchased from Sigma-Aldrich. Tetrabuytlammonium hydroxide low UV reagent (PIC® A) was purchased from Waters Australia.

2.3.2. Instrumentation

One-dimensional HPLC separations were performed using a Waters 2690 Alliance system equipped with a Waters 996 Photo Diode Array (PDA) detector and Waters Millennium[32] 4.00 software run using a Pentium 3 processor. All mobile phases were vacuumed degassed using the online degasser and the columns were held at 30°C using the inbuilt column heater.

2.3.3. Sample preparation and chromatographic separation conditions

Separations were performed on a Waters Nova-pak C18, 4 μm particle size, 3.9 x 150 mm (60 Å pore size) column at a flow rate of 0.5 mL/min. The Bayer humic sample was re-dissolved in water:methanol [80/20; v/v] using an ultrasonic bath (5 minutes) and 50 μL of the solution (concentration 1500 mg/L) was injected. All chromatograms were analysed over the wavelength range of 190 to 400 nm. The mobile phase composition (acetonitrile, water, formic acid, tetrabuytlammonium hydroxide) and the

elution program (isocratic and gradient) varied throughout this study. All the four samples obtained from the continuous solvent extraction procedure were subjected to a similar HPLC analysis.

2.4. REVERSED PHASE COLUMN STUDY FOR THE SEPARATION OF HUMIC STANDARDS

In this section, the details of the instrumentation and experimental conditions for the study of the resolving power of five new generation reversed phase columns are given. A set of twenty-four standards comprising of a mix of polycarboxylic acids and polyphenol compounds were used as models for humic substances.

2.4.1. Chemicals

HPLC grade methanol was obtained from Mallinckrodt Australia. Formic acid (BDH) was analytical grade (98%) and was purchased from Sigma-Aldrich. The polycarboxylic acids and polyphenol compounds used in this study are identified in Figure 2.2. They ranged in molecular weight from 90 to 218 Da and were purchased from Sigma-Aldrich, Australia.
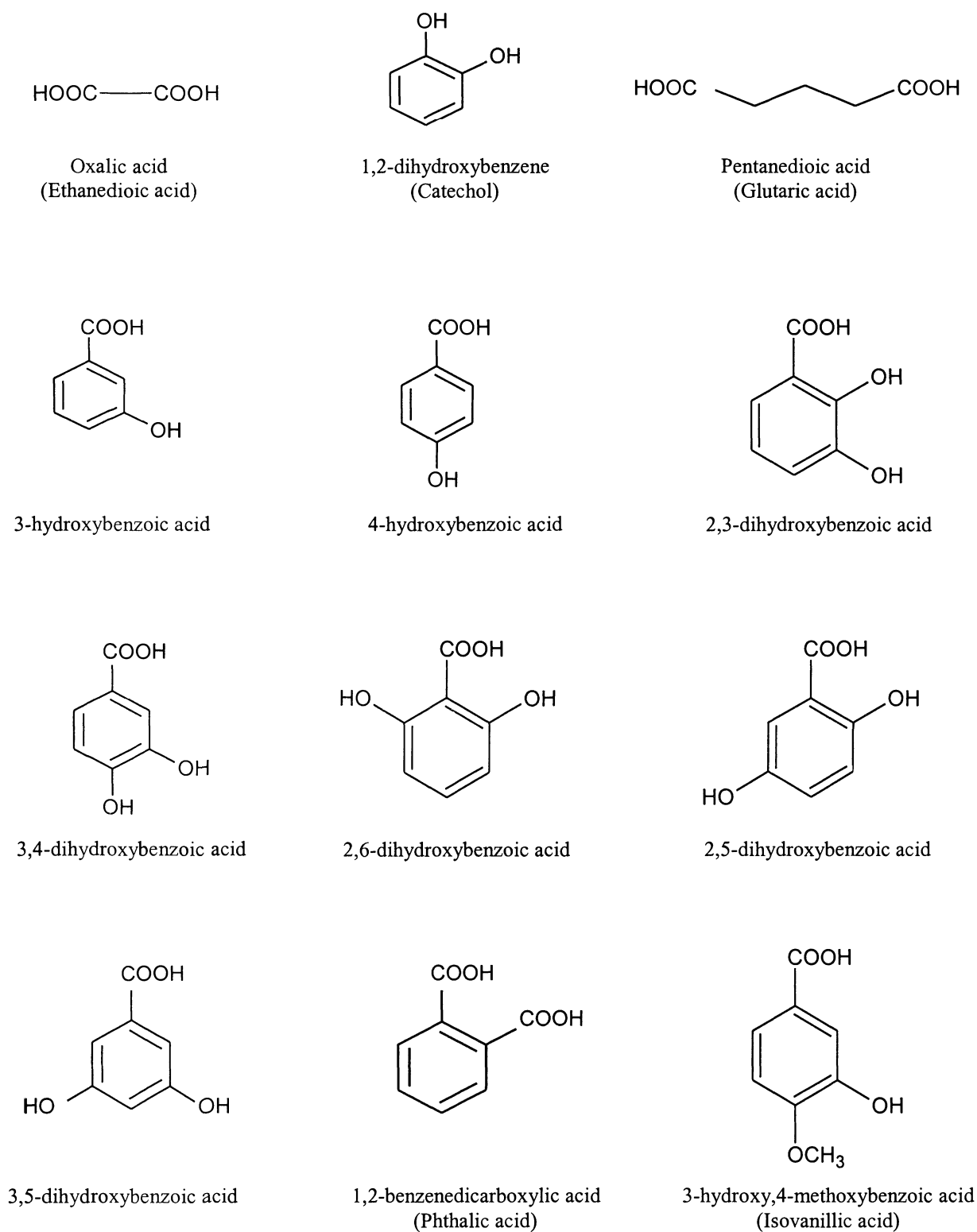
Figure 2.2: Structures of the polycarboxylic acids and polyphenol compounds used in reversed phase column study.

2,4,6-trihydroxybenzoic acid

3,4,5-trihydroxybenzoic acid
(Gallic acid)

2,3,4-trihydroxybenzoic acid

Octanedioic acid
(Suberic acid)

3,4-dimethoxybenzoic acid
(Veratric acid)

Sorbitol

4-Hydroxyisophthalic acid

5-hydroxyisophthalic acid

3,5-dimethoxy,4-hydroxybenzoic acid

1,2,4-benzenetricarboxylic acid
(Trimellitic acid)

1,2,3-benzenetricarboxylic acid

1,2,4,5-benzenetetracarboxylic acid
(Pyromellitic acid)
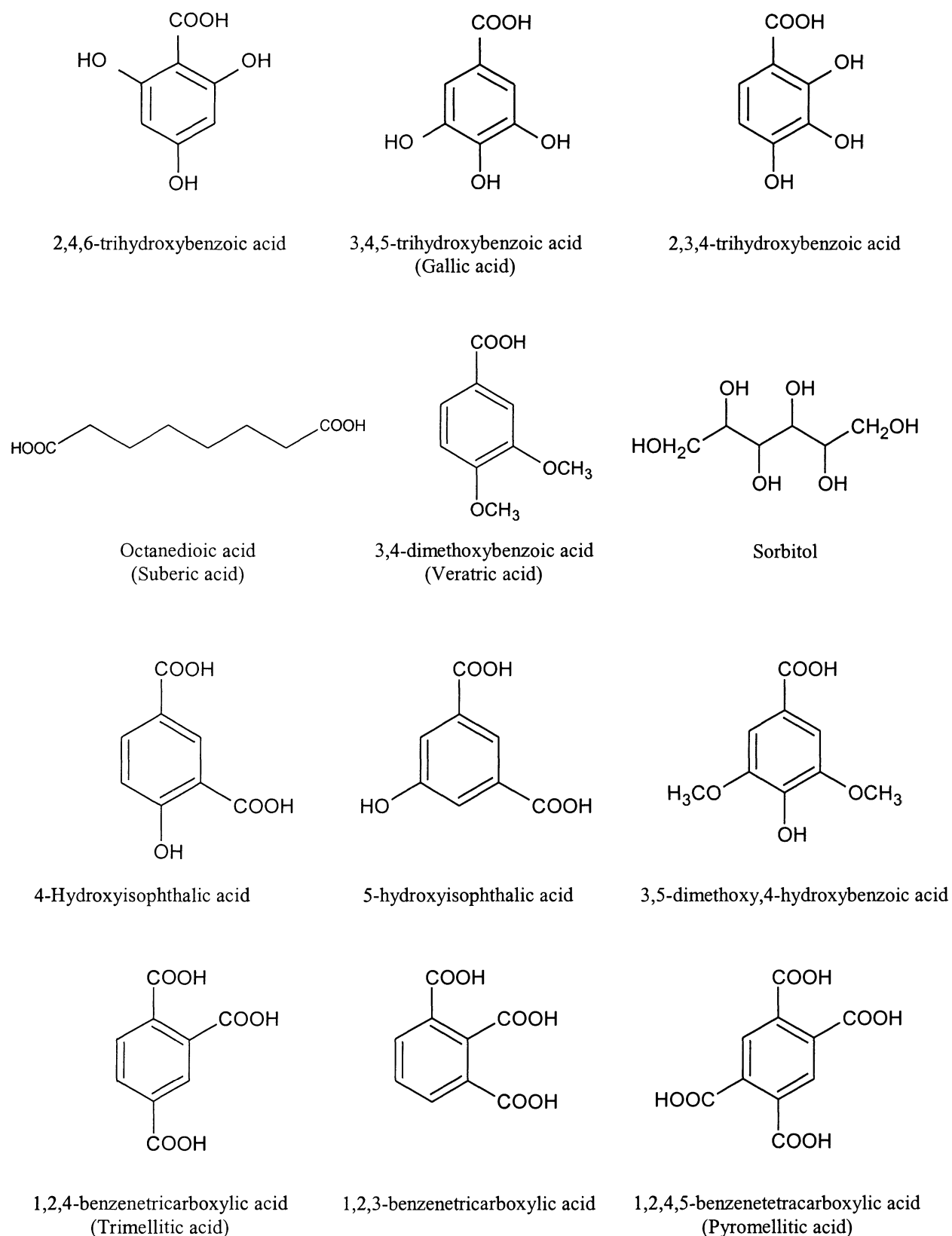
Figure 2.2 (continued): Structures of the polycarboxylic acids and polyphenol compounds used in reversed phase column study.

2.4.2. Instrumentation

A Waters LC system was used for all chromatographic separations and included a 717plus autosampler, 600 pump and controller, 2487 dual wavelength detector and Millennium software run using a Pentium 4 1.60 GHz processor. Five reversed phase columns were chosen for this work, a Phenomenex Luna C18 (150 x 4.6 mm, 5 μ), Phenomenex Luna Cyano (150 x 4.6 mm, 5 μ), Waters XTerra™ RP$_{18}$ (150 x 4.6 mm, 5 μ), Phenomenex Aqua C18 (150 x 4.6 mm, 5 μ) and a Phenomenex Synergi Polar-RP (150 x 4.6 mm, 4 μ). A justification of the columns chosen for this study is discussed later in Chapter 5.

2.4.3. Sample preparation and chromatographic separation conditions

A set of twenty-four standards containing a mix of polycarboxylic acids and polyphenols were used in this study. The identity and structure of these compounds are given in Figure 2.2. The polycarboxylic acids and polyphenol compounds chosen as standards for this study were dissolved in methanol/water [50:50, v/v]. The concentration of the individual standards were 1000 mgL^{-1} except for oxalic acid, glutaric acid, 4-hydroxybenzoic acid, 2,6-dihydroxybenzoic acid, suberic acid and sorbitol that were made to a concentration of 2500 mgL^{-1}(due to low absorbance).

All separations on the five reversed phase columns were carried out using different mobile phase mixtures consisting of methanol and 0.1% formic acid. The flow rate

was set at 1.5 mL/min for all separations and 5 µL duplicate injections were performed

for each standard. All reversed phase columns were thermostated to 40°C and UV

detection was set at 220 nm.

2.5. TWO-DIMENSIONAL HPLC SEPARATION OF BAYER

HUMIC SUBSTANCES

To improve on the one-dimensional HPLC separation of Bayer humic substances a two-

dimensional HPLC method was developed. In the section below, the two-dimensional

HPLC conditions are described and the analysis of bands collected in the second

dimension by mass spectrometry reported.

2.5.1. Chemicals

HPLC grade methanol was obtained from Mallinckrodt Australia. Formic acid (BDH,

AR grade, 98%), sodium nitrate (Univar, AR grade) and blue dextran (average

molecular weight 2,000,000 Da) were purchased from Sigma-Aldrich.

2.5.2. Instrumentation

A two-dimensional reversed-phase HPLC system was designed for the separation of the

Bayer humic substances, which consisted of a Waters LC system. The system included

---

a 717plus autosampler, two 600-pump and controllers, two 2487 dual wavelength detectors and two 6-port, 2-position switching valves. Column switching was achieved using 6-port 2-position switching valves fitted with micro-electric two position valve actuators (Valco Instruments Co. Inc., Houston, TX, USA). The Waters Millenium[32] 4.00 software controlled the switching valves. All mobile phases for this system were helium degassed.

2.5.3. Sample preparation and chromatographic separation conditions

The Bayer humic sample was dissolved in water/methanol [80/20; v/v] using an ultrasonic bath (5 minutes) and was made up to a concentration of 6 mg/mL. Injection volumes were 250 μL. All chromatograms were extracted at 280 nm. The first separation process utilised a Phenomenex BioSep-SEC-S2000 column, 300 x 7.8 mm, running a mobile phase of sodium nitrate (0.05 M) at a flow rate of 2.5 mL/min. The manufacturer reports the exclusion range of the BioSep-S2000 column as being 1,000-300,000 Da. The interstitial column volume (V_o) and the total of the interstitial column volume plus the pore volume (V_t) were determined by injecting blue dextran (2 mg/mL) and acetone respectively. The second separation process utilised a Phenomenex Synergi polar-RP column, 150 x 4.6 mm, running a curved gradient (4) of formic acid (0.1%) and acetonitrile at a flow rate of 2.0 mL/min.

The eluting size-exclusion band was cut at 200 μL intervals across the entire band with each cut transferred using the switching valves that were programmed to periodically 'heart-cut' the solute from the first dimension to the second dimension for subsequent

separation. In total ninety different sections were cut from the first dimension and separated in the second, with a total analysis time (90 × 200 μL fractions) in the order of seven days of continuous operation.

2.5.4. Liquid chromatography/ mass spectrometry analysis of two-dimensional HPLC fractions

For identification purposes the most intense bands in the second dimension of the multidimensional HPLC method were collected using the analytical two-dimensional HPLC method that was developed for further analysis by mass spectrometry. The experiment was repeated at an analytical scale twenty five times to collect enough of each sample for mass spectrometric analysis. They were then freeze dried and made up to 50 μL in methanol/water [10/90; v/v] for mass spectrometric analysis using flow injection.

A VG-Quattro II triple quadrupole mass spectrometer (Micromass, Altrincham, UK), which was fitted with an electrospray source, was used to collect negative ion ESI mass spectra and Masslynx software was used for data acquisition and processing. Instrumental parameters such as a capillary voltage of 2.5 kV, a source temperature of 80°C and a sampling cone of 30 V were used. The collision gas was argon with a collision energy of 10 V and quadrupole resolution settings to achieve unit mass resolution (50% FWHM) were used. Spectra were recorded in MCA mode and were background subtracted and smoothed.

Samples were introduced to the source via flow injection of a mobile phase from a Hewlett-Packard 1090 LC at a flow rate of 10 µL/min. The mobile phase was methanol/water [50/50; v/v]. Each second dimension band was collected approximately 25 times using the analytical two-dimensional HPLC method that was developed. Full scan mass spectra of the two-dimensional Bayer humic bands were recorded by flow injection of 10 µL of the sample and scanning over a range m/z 100-700 Da for 30 seconds using a scan time of 3 seconds. Product ion spectra obtained under collision-induced decomposition (CID) conditions were also collected. Product ion spectra were recorded over the mass range m/z 20-320 Da with a scan time of 1 second. Aliquots (10 µL) of the sample solution were flow injected and spectra recorded for 1 minute. The resolution of the first quadrupole was lowered slightly to increase ion transmission while retaining unit mass resolution for both quadrupoles.

CHAPTER 3

Characterisation of the Bayer humic substances

3.1. INTRODUCTION

This chapter describes the characterisation of the Bayer humic substances studied in this work using non-chromatographic techniques. These include elemental analysis, ^1H NMR, ^1H-^1H homonuclear correlation (COSY) NMR, ^{13}C solid-state CP/MAS NMR and FTIR spectroscopy, which were used to gather information on chemically different structural and functional groups present in the Bayer humic substances. This preliminary characterisation was further extended with a detail characterisation of solvent fractions extracted from the Bayer humic substances discussed later in Chapter 4.

3.2. ELEMENTAL COMPOSITION

Table 3.1 summarises the results of the elemental, atomic ratios and pH analysis of the Bayer humic substances. Elemental analysis of the Bayer humic substances provided information on the distribution of major elements such as C, H, N and O composition. The elemental composition of the Bayer humic substances was 50.25% C, 4.24% H, 0.67% N and 44.84% O by difference (sulphur levels were found to be negligible). These values are comparable to those found in the literature for Bayer humic substances. The atomic ratios of O/C, H/C and N/C can be used to identify the type of humic substance, with the ratios

Table 3.1: Elemental and pH analysis of the Bayer humic substances.

% C	% H	% N	% O Difference	O/C	H/C	N/C	pH at 5g/L in water
50.25	4.24	0.67	44.84	0.67	1.01	0.0114	2.41

reported in Table 3.1 also similar to those reported in literature for Bayer humic substances.

3.3. ANALYSIS OF BAYER HUMIC SUBSTANCES BY NMR

3.3.1. Solution state ^{1}H NMR

Figure 3.1 shows the ^{1}H NMR spectrum obtained in deuterated dimethylsulphoxide (DMSO-d$_6$). The NMR spectrum represents two main regions, the aliphatic (0-6 ppm) and the aromatic (7-10 ppm) regions.

The individual resonances with relatively high intensities with chemical shifts of 8.63, 8.03, 7.95, 7.51, 5.65, 3.79, 2.49, 2.35, 2.19, 2.07, 1.90, 1.47, 1.24 and 1.05 ppm are labelled A to N sequentially. Many of these peaks have been previously assigned in other humic substances [87-88]. The signals at 3.79 and 2.49 ppm (peak F and G respectively) were attributed to water in DMSO and methyl signals of trace amounts of non-deuterated DMSO respectively. The signals at 8.63 ppm (A) and 1.9 ppm (K) were assigned to hydrogen of formate (HCOO$^-$) and the methyl group of acetate (CH$_3$COO$^-$) respectively.

The presence of a number of singlets between 7 to 9 ppm can be attributed to isolated proton spin systems, most likely to be on substituted aromatic rings. The protons on an
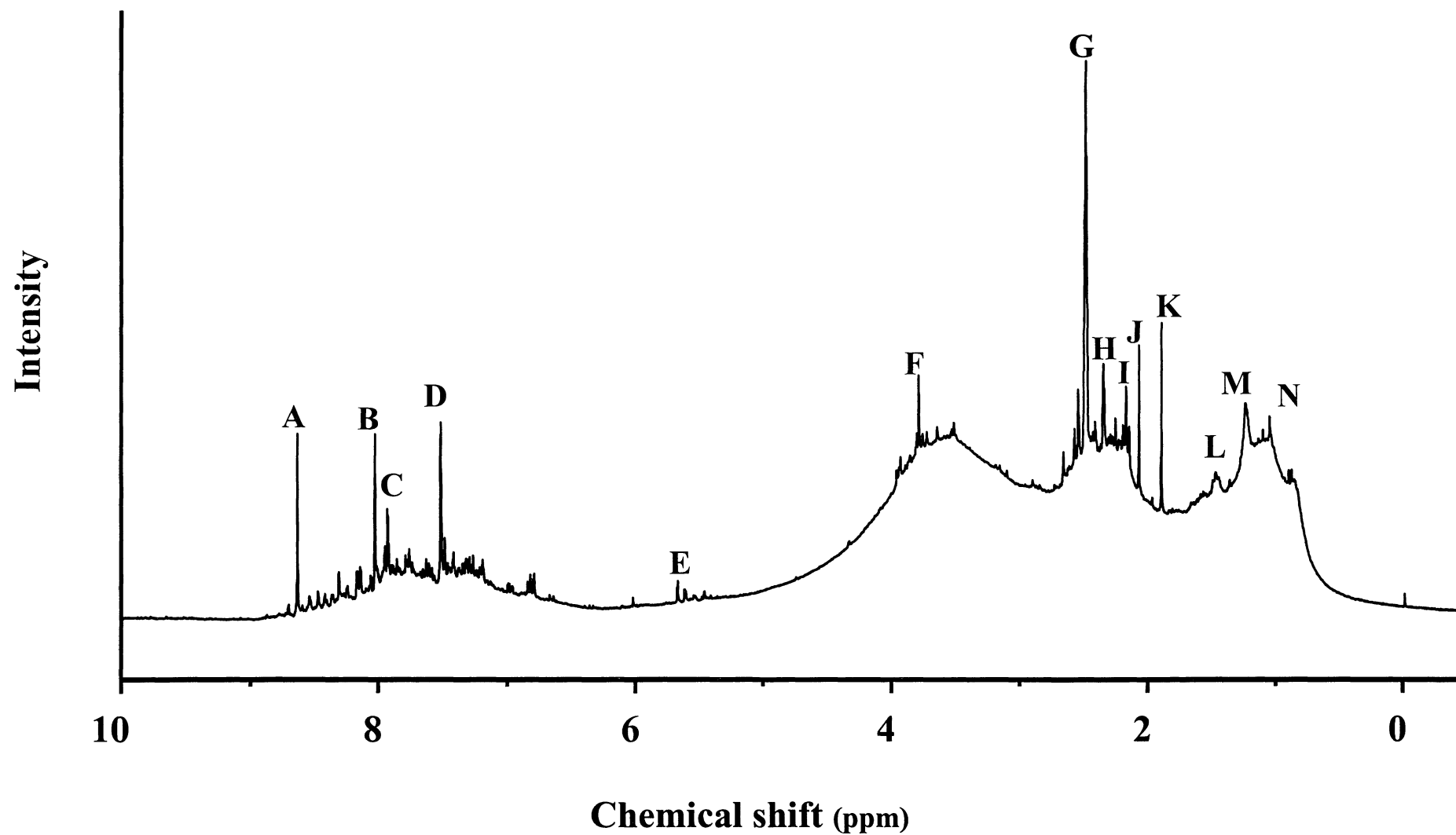
Figure 3.1: Solution ^1H NMR spectrum of the Bayer humic substances. Resonances A-N are assigned in the text.

aromatic ring with electron donating substitutions such as ethers and hydroxy groups

will be shielded and will therefore appear between 6.5 to 7 ppm. Some alkene protons

are observed at 5.6 ppm (peak E, Figure 3.1). Despite the broad peak between 3-4 ppm

it can be seen that there were a number of smaller peaks that indicated the presence of

protons attached to carbons directly bonded to electronegative groups such as ether and

alkoxy groups in the humic macromolecules or from furan-type molecules. The

hydrofurans, which are formed during the Bayer process from the rearrangement of

carbohydrates, will have the protons in this region.

3.3.2. Solution state ^{1}H-^{1}H NMR

The ^{1}H-^{1}H homonuclear correlation (COSY) NMR spectrum is shown in Figures 3.2

and 3.3 and revealed information on the extent of the spin-spin coupling among the

protons. Figure 3.2 shows the aliphatic region between 0.8 and 2.4 ppm and Figure 3.3

the aromatic region between 6.5 and 8.5 ppm.

The aliphatic region, between 0.8 to 2.4 ppm exhibits two distinct correlations. These

peaks are obscured by the broad hump in the region. The triplet at 2.19 ppm in Figure

3.2 (see peak I, Figure 3.1) is coupled to the protons (multiplet) at 1.47 ppm and the

protons at 1.47 ppm are further coupled to protons at 1.24 ppm. Although the splitting

pattern of the peak at 1.24 ppm is not visible due to superimposition of the broad peak,

it is most likely to be a terminal methyl group. The triplet at 2.19 ppm can be attributed

to methylene protons in close proximity to an electron-withdrawing group such as
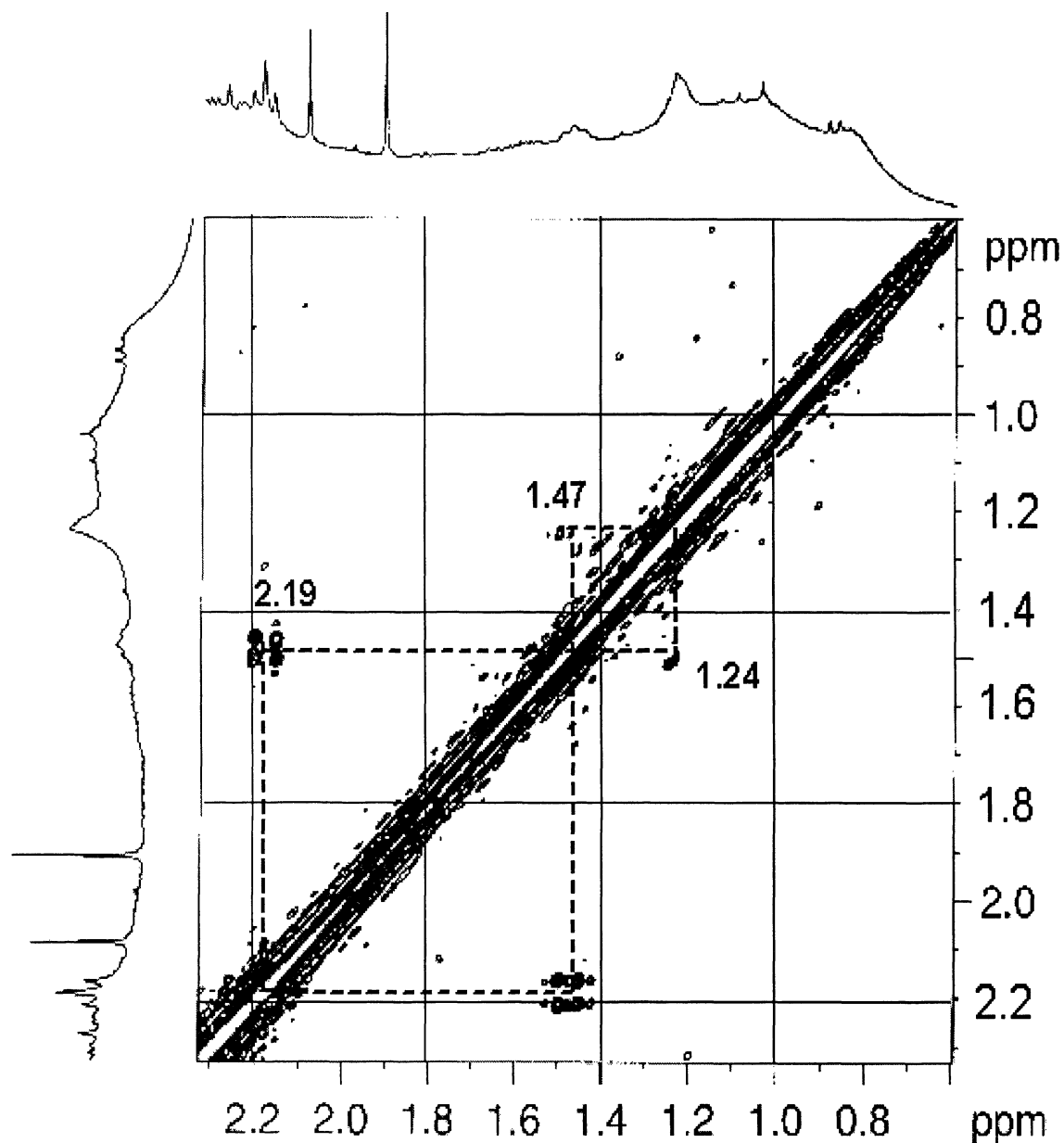
Figure 3.2: ^{1}H-^{1}H Homonuclear 2-D-correlation (COSY) spectrum of the aliphatic region of the Bayer humic substances. Assignments are described in the text.
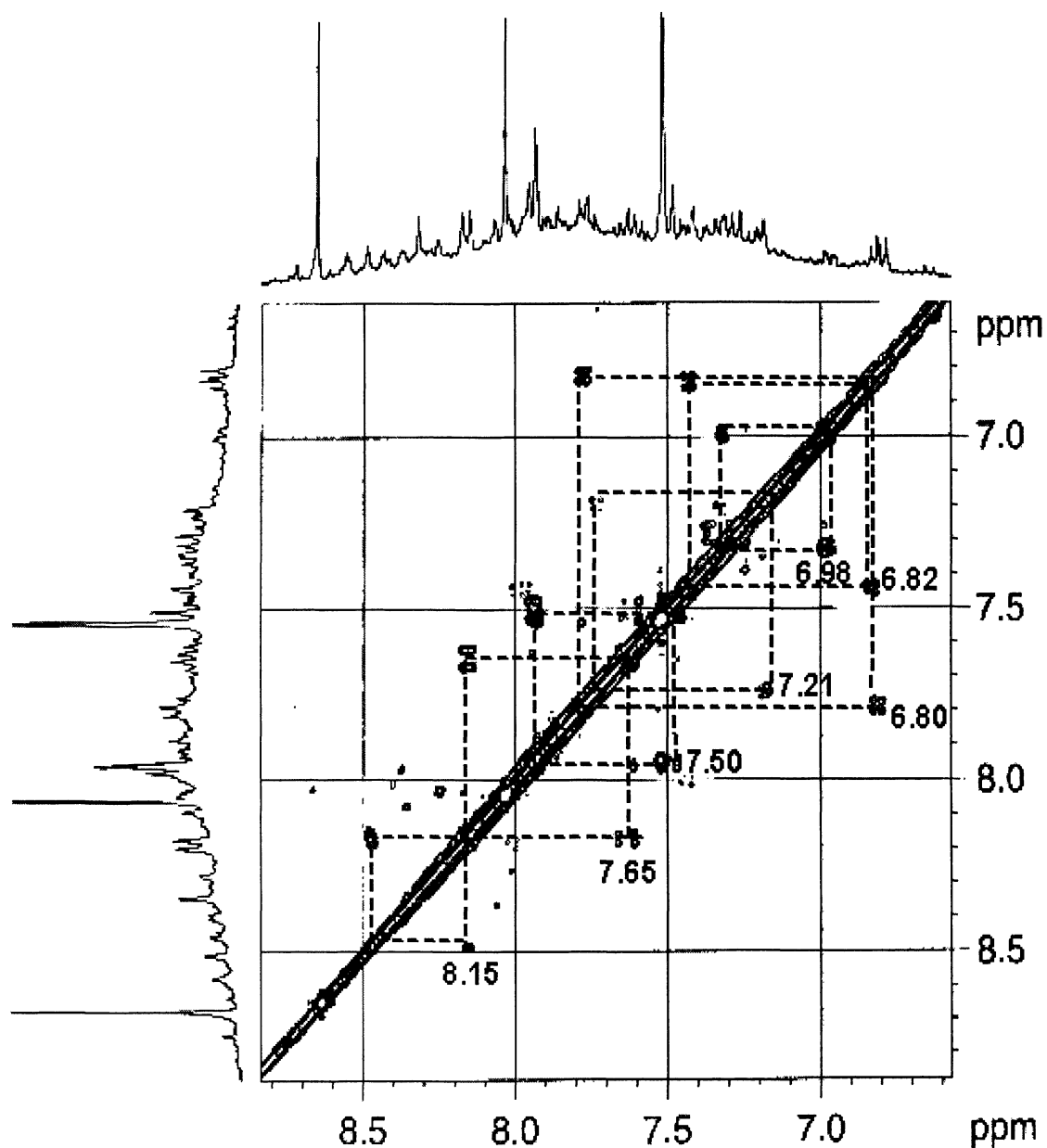
Figure 3.3: ^{1}H-^{1}H Homonuclear 2-D-correlation (COSY) spectrum of the aromatic region of the Bayer humic substances. Assignments are described in the text.

carboxylic acid. The singlets at 2.07 and 1.90 ppm (peaks J, K Figure 3.1) are not present in Figure 3.2 (a small noise peak or underlying resonance is present in trace amounts) and hence can be assigned to proton isolated methyl ketone substituent, i.e. CH_3-CO-C- and acetate, i.e. CH_3COO^- respectively.

There were several correlations observed in the aromatic region including two sets of doublets at 6.80 and 6.82. Figure 3.3 shows correlations to protons at 7.75 and 7.43 ppm respectively. It is most likely that 6.80 and 7.75 ppm are the protons on 4-hydroxybenzoic acid and 6.82 and 7.43 ppm belong to the adjacent protons of 3,4-dihydroxybenzoic acid. In both instances the proton adjacent to the hydroxy group will be shielded and hence will appear high field. Another correlation between the protons at 7.50 and 7.95 ppm suggest an electron deshielded environment and was assigned to 1,2-benzene dicarboxylic acid. The singlet at 8.03 ppm belongs to isolated, electron-deficient protons and was assigned to 1,3 benzene dicarboxylic acid.

The symmetry of the molecule gives rise to only a single peak in the NMR spectrum. The doublet peak at 8.15 ppm in Figure 3.3 and the other two protons at 8.47 and 7.65 ppm showed the 1,3,4-trisubstituted benzene ring system where the proton at 8.15 ppm is coupled to both the protons at 8.47 and 7.65 ppm.

In summary, the results of the 1D and 2D ^1H NMR spectra give information on the type and pattern of substitution of the protons in the molecular components.

3.3.3. Solid state ^{13}C NMR

The ^{13}C solid-state CP/MAS NMR spectrum is shown in Figure 3.4. Using literature values carbons belonging to different functional groups were assigned and are summarised in Table 3.2.

The spectrum showed four broad regions, that can be assigned to aliphatic carbon groups unsubstituted with O (C-alkyl, 0 to 50 ppm), carbon of a methoxy group, (55 ppm) and all other aliphatic carbons attached to alkoxy, hydroxy groups (O-alkyl, 50-100 ppm), carbons with two alkoxy groups and aromatic carbons (acetal and aromatic, 100-160 ppm) and the carbonyl carbons in carboxyl groups (160-190 ppm) [87-88]. Table 3.2 also indicates the % composition of the different carbon groups in the Bayer humic sample, which has been calculated based on the integration of the different regions in the ^{13}C solid-state NMR spectrum.

Table 3.2: Estimates of the proportions of different carbon types in the Bayer humic substances as measured by Solid-State ^{13}C NMR spectroscopy.

	C-alkyl	O-alkyl	Acetal, Aromatic	Carboxyl
Chemical Shift (ppm)	0-50	50-100	100-160	160-190
% Composition	42.4	5.4	31.3	20.9
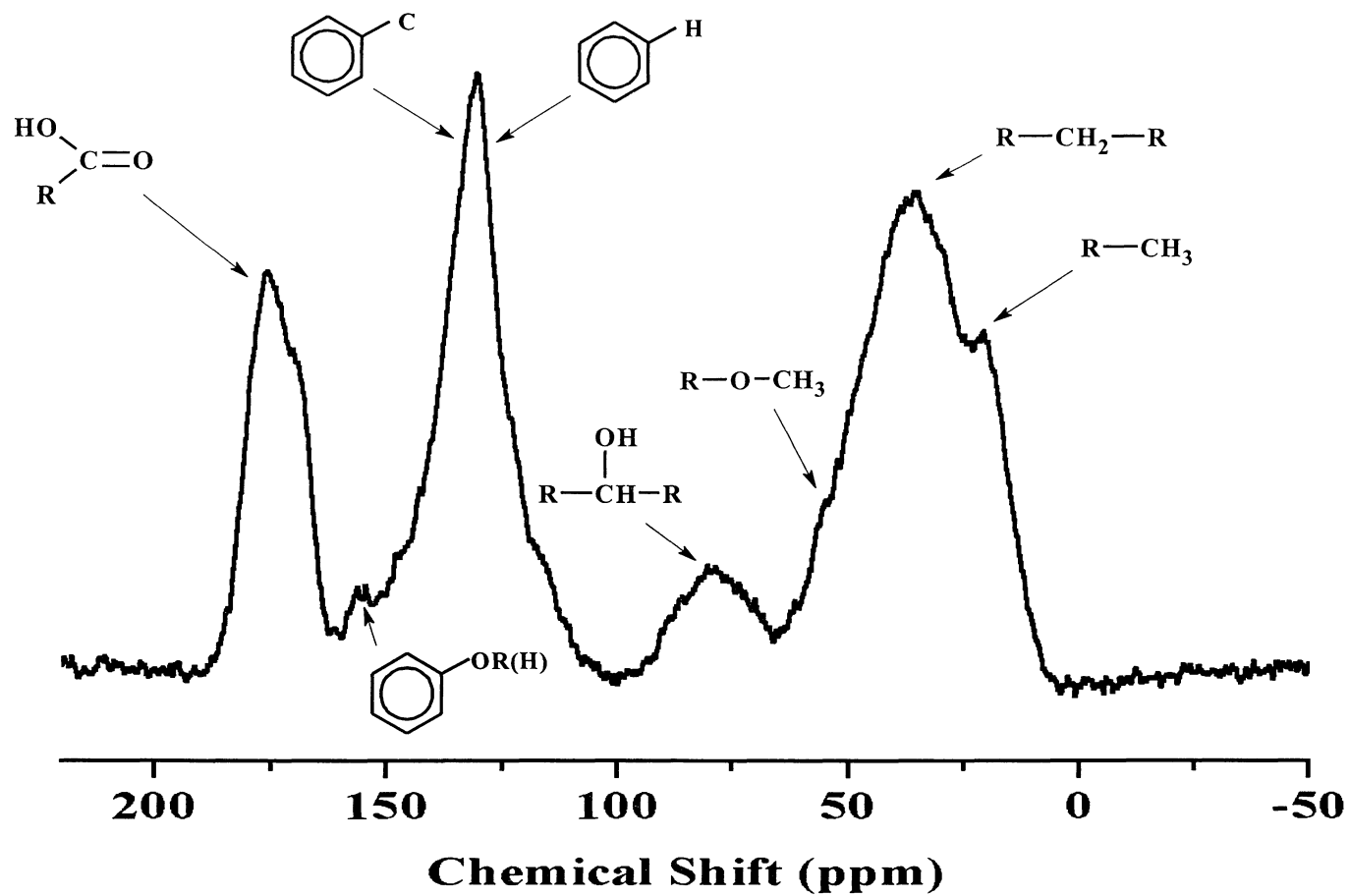
Figure 3.4: Cross polarisation (contact time of 1 ms) ^{13}C solid-state NMR spectrum of the Bayer humic substances. Structural groups are assigned.

3.4. ANALYSIS OF BAYER HUMIC SUBSTANCES BY FTIR

Figure 3.5 shows the FTIR spectra of the Bayer humic substances. Overall the FTIR spectrum reflected the preponderance of oxygen-containing functional groups, that is, COOH, OH and C=O in the humic material.

The broad absorption at 3433 cm^{-1}(A) is due to the O-H stretching of the H-bonded OH groups. The bands in the region of 2900-3000 cm^{-1}(B) are attributed to the antisymmetric and symmetric stretching vibrations of aliphatic C-H bonds in CH_3 and CH_2 groups and is a common feature in most humic samples. The distinct band at 1709 cm^{-1} (C) is the C=O stretching vibration, which is due to carboxyl groups present in the Bayer humic sample. The band at 1616 cm^{-1}(D) is due to C=C vibration of aromatic compounds, the hydrogen-bonded C=O of carbonyl or quinones and the COO$^-$ symmetric stretching. The absorption band at 1403 cm^{-1} (E) can be assigned as the OH deformation and C-O stretching of phenolic OH, C-H deformation of CH_2 and CH_3 groups and the COO$^-$ antisymmetric stretching. The broad band at 1237 cm^{-1} (F) is attributed to C-O stretching and the OH deformation of COOH groups and stretching of aryl ethers and phenols. The weak bands at 933 cm^{-1} (G) and 772 cm^{-1} (H) are due to the out-of-plane bending of the aromatic C-H and C-H of the long-chain aliphatics [14, 87-88].
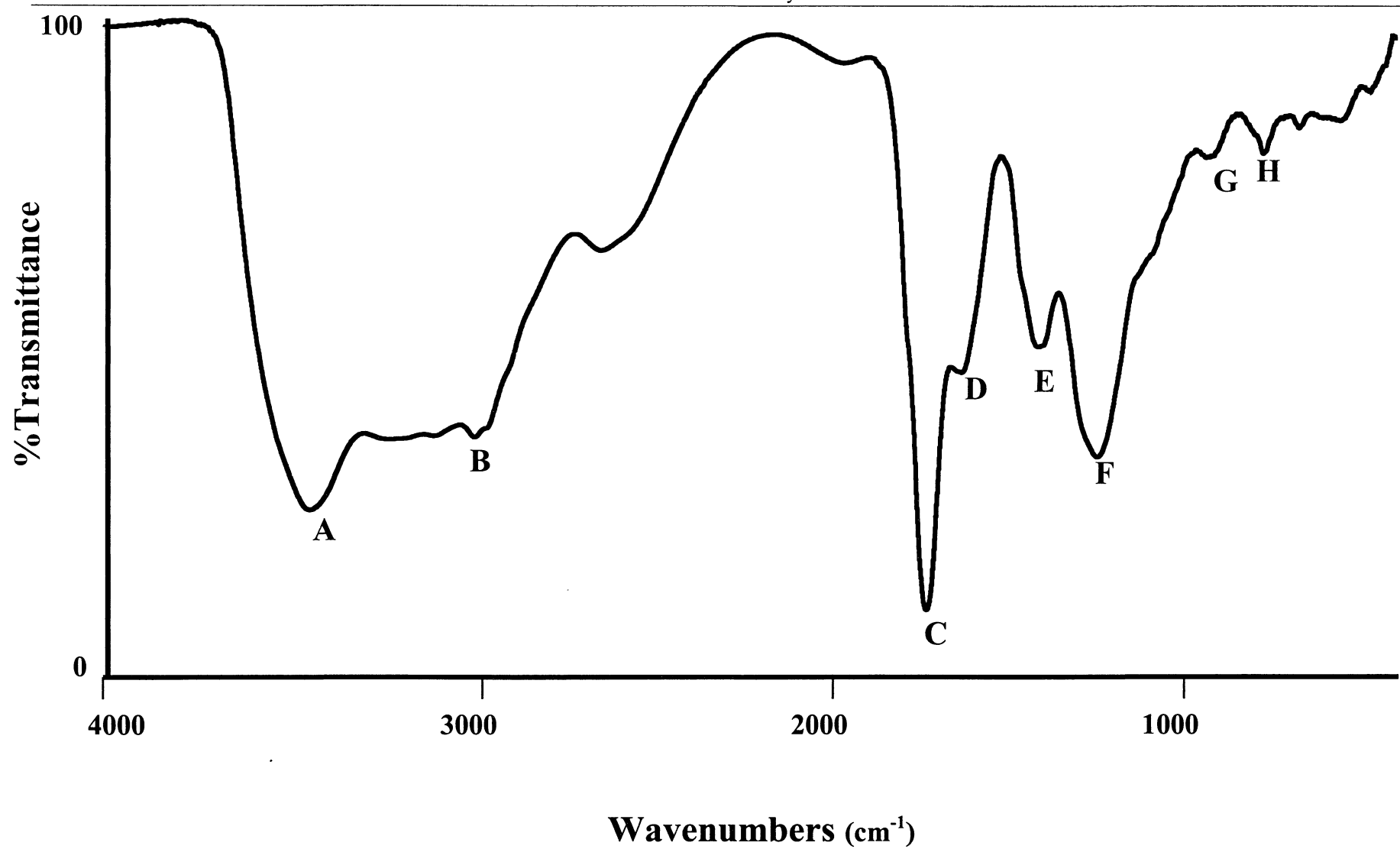
Figure 3.5: Fourier transform Infra-red (FTIR) spectrum of the Bayer humic substances.

3.5. CONCLUSIONS

The structure, functional group content and elemental composition of the Bayer humic substances were identified by elemental analysis, ^{1}H NMR, ^{1}H-^{1}H NMR, ^{13}C NMR and FTIR.

The 1D and 2D ^{1}H NMR spectra gave information on the type and pattern of substitution of the protons in the molecular components. The ^{13}C NMR spectrum showed a high percentage composition of C-alkyl (42.2%) and acetal and aromatic carbon (31.3%). The FTIR spectrum showed a predominance of oxygen-containing functional groups such as carboxyl or hydroxyl groups, which was supported by the ^{13}C NMR spectrum that indicated that the Bayer humic substances contained 20.9% carboxyl carbon. The results of the elemental, atomic ratios and acidity analysis of the Bayer humic substances were comparable to those found in literature.

CHAPTER 4

Development of a reversed phase high-performance liquid chromatographic method for the analysis of Bayer humic substances

4.1. INTRODUCTION

This chapter deals with the conventional high-performance liquid chromatographic (HPLC) separation of Bayer humic substances. As noted in Chapter 1, low molecular weight organic molecules such as formate, acetate, oxalate and simple aromatic polycarboxylic acids and phenols can be readily measured by HPLC techniques or by gas chromatography/mass spectrometry (GC/MS) after methylation. However the analysis of material of molecular weights above 1200 Da has yet to be achieved by HPLC. Many individual compounds of molecular weights greater than 1200 Da may be particularly poisonous to the Bayer process. There identification by HPLC will allow methodology to be developed for their removal.

There are a limited number of references in the literature on the liquid chromatographic (LC) analysis of humic substances found in Bayer liquors. LC analysis of the humic acid component of Bayer liquors has so far not been reported although LC methods have been successfully developed for the monitoring of known simple organic and inorganic ions that accumulate in the process liquor. Oxalate, which is of prime importance as its stability and removal can control refinery productivity, as well as chloride and sulfate, have been analysed using either ion chromatography (IC) or capillary electrophoresis (CE) [82-83]. Any further reported attempts at analysing the humic acids found in the Bayer liquor have been restricted to the quantitative analysis of the humic acids present. Susic et al. [84] reported the first use of a HPLC method with fluorometric detection for the quantitative humic acid analysis of a Bayer liquor. A method by which the humic acid concentration could be routinely monitored was

supposedly developed however not all humic material fluoresces and therefore this method offered limited full detection.

The work presented in this Chapter aimed to develop a one-dimensional HPLC method that would separate some of the larger organic species (>1200 Da) present into compound classes. HPLC is routinely used for the determination of ionic and non-ionic compounds, although HPLC of ionic samples tends to be more complicated and difficult to interpret. Therefore several strategies were employed to simplify the analysis of ionic samples. As noted in Chapter 1, there is a choice of three HPLC modes of separation: reversed phase, ion-suppression and ion-pair chromatography. Reversed phase HPLC is usually the most appropriate starting point due to its simplicity compared to the other modes of separation. If reversed phase chromatography proves to be inadequate, the application of ion-suppression or the addition of an ion-pairing reagent would then be considered.

4.2. REVERSED PHASE HPLC SEPARATION

Due to the wide range of applicability, convenience, and the ease with which the selectivity and retention factor can be altered with the manipulation of the aqueous mobile phase, reversed phase chromatography was used as the starting point for developing a method for the separation of the Bayer humic sample. A water/methanol and a water/acetonitrile gradient were run and compared. The water/acetonitrile

gradient offered the best separation in terms of resolution and was therefore used throughout the rest of the method development. Initially a water/ acetonitrile gradient was used, running isocratic for 10 minutes on water and then running a linear gradient from 100% water to 100% acetonitrile at a rate of change of 1% per minute. The chromatogram in Figure 4.1 shows that the majority of the Bayer humic sample eluted in the first 20 minutes, close to the void. From this result normal reversed phase chromatography was seen to be inadequate for separating the Bayer humic sample and therefore another mode of separation was required.

4.3. ION-SUPPRESSION HPLC SEPARATION

Ionic samples are normally separated by ion-exchange or ion-pair chromatography but reversed phase chromatography can be used if the sample contains weak acids or weak bases in addition to neutral compounds. In cases where the sample contains weak acids or weak bases, it is possible to alter the chromatographic retention by adjusting the pH of the eluent with the addition of a buffer to the mobile phase. This mode of separation termed "ion-suppression", controls chromatographic retention through suppression of the ionisation of an ionic sample. The ionisation of an acid or the protonation of a base is suppressed by adjusting the pH, thereby allowing the sample to be chromatographed on a reversed phase column using a mobile phase mixture of methanol or acetonitrile plus a buffer solution, increasing the retention of the sample [134].
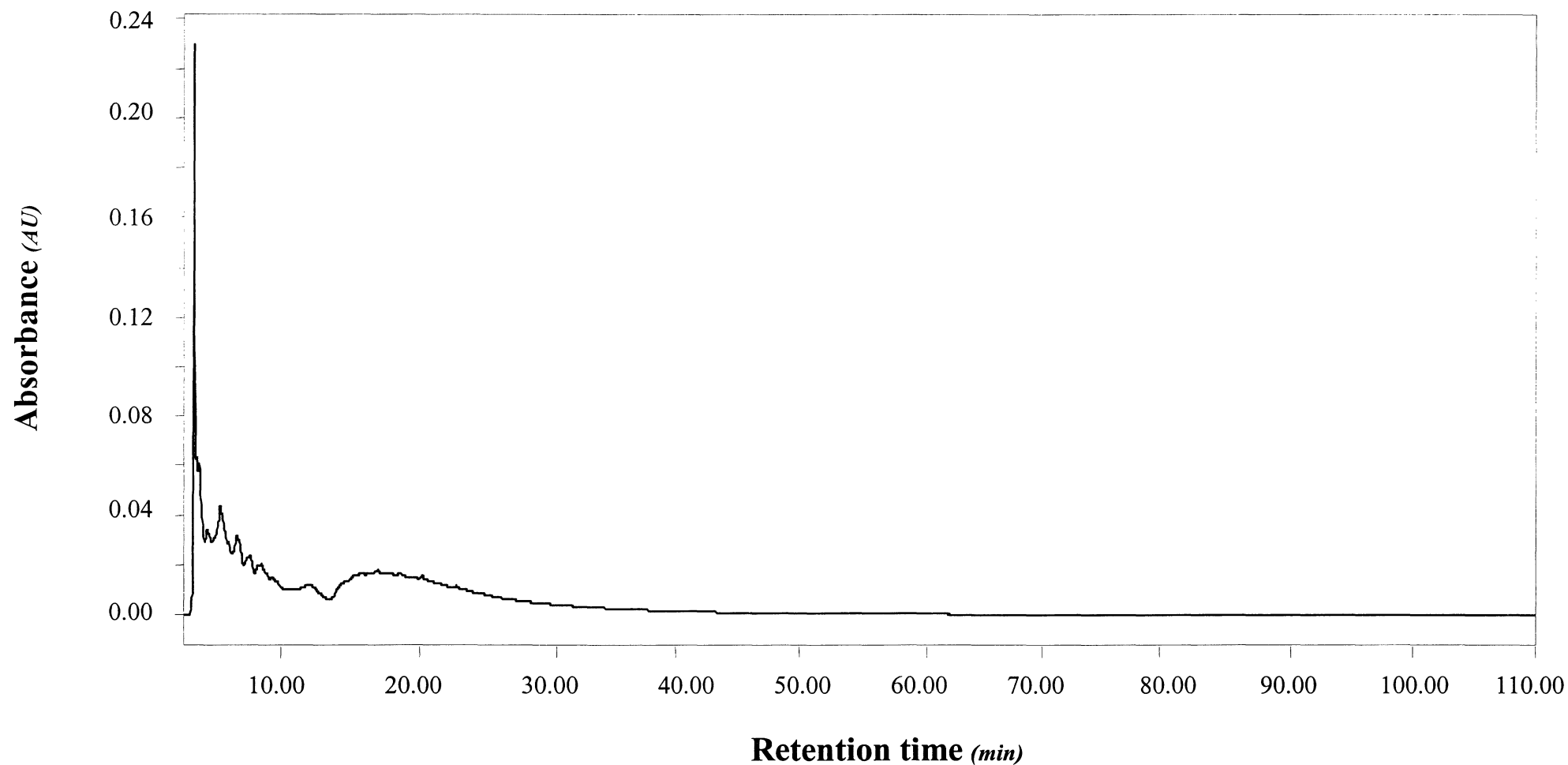
Figure 4.1: HPLC separation of the Bayer humic sample using reversed phase chromatography with a linear water/acetonitrile gradient at a rate of change of 1% min^{-1}. AU=arbitrary units

In the current analysis the pH of the aqueous component of the mobile phase was adjusted to a lower pH with 1% formic acid, which suppressed the ionisation of the weak acid solutes, allowing improved retention on the hydrophobic stationary phase. A 1% formic acid/acetonitrile gradient was used, running isocratically for 10 minutes on 1% formic acid and then a linear gradient from 1% formic acid to 100% acetonitrile at a rate of change of 1% per minute. The chromatogram in Figure 4.2 shows the humics from the Bayer liquor being retained for longer, allowing further separation to occur. By adjusting the pH of the mobile phase the ionic equilibrium of the Bayer humic sample would have been adjusted to the neutral form, increasing its retention on the hydrophobic stationary phase. The ionised form of the Bayer humic sample would elute more rapidly in comparison to its neutral form due to the greater affinity the polar ionised form would have to the polar aqueous phase, while the neutral form would have a greater affinity for the hydrophobic stationary phase of the Nova-pak C18 column.

Whilst the majority of the sample eluted after 20 minutes with some resolution achieved the separation was still poor. To improve the separation the gradient was altered by decreasing the gradient rate of change firstly to 0.5% per minute, then 0.25% per minute and finally to a 0.17% per minute. These changes had little effect on the separation and did not improve the overall resolution, indicating that another mode of separation such as ion-pair chromatography would be more appropriate.
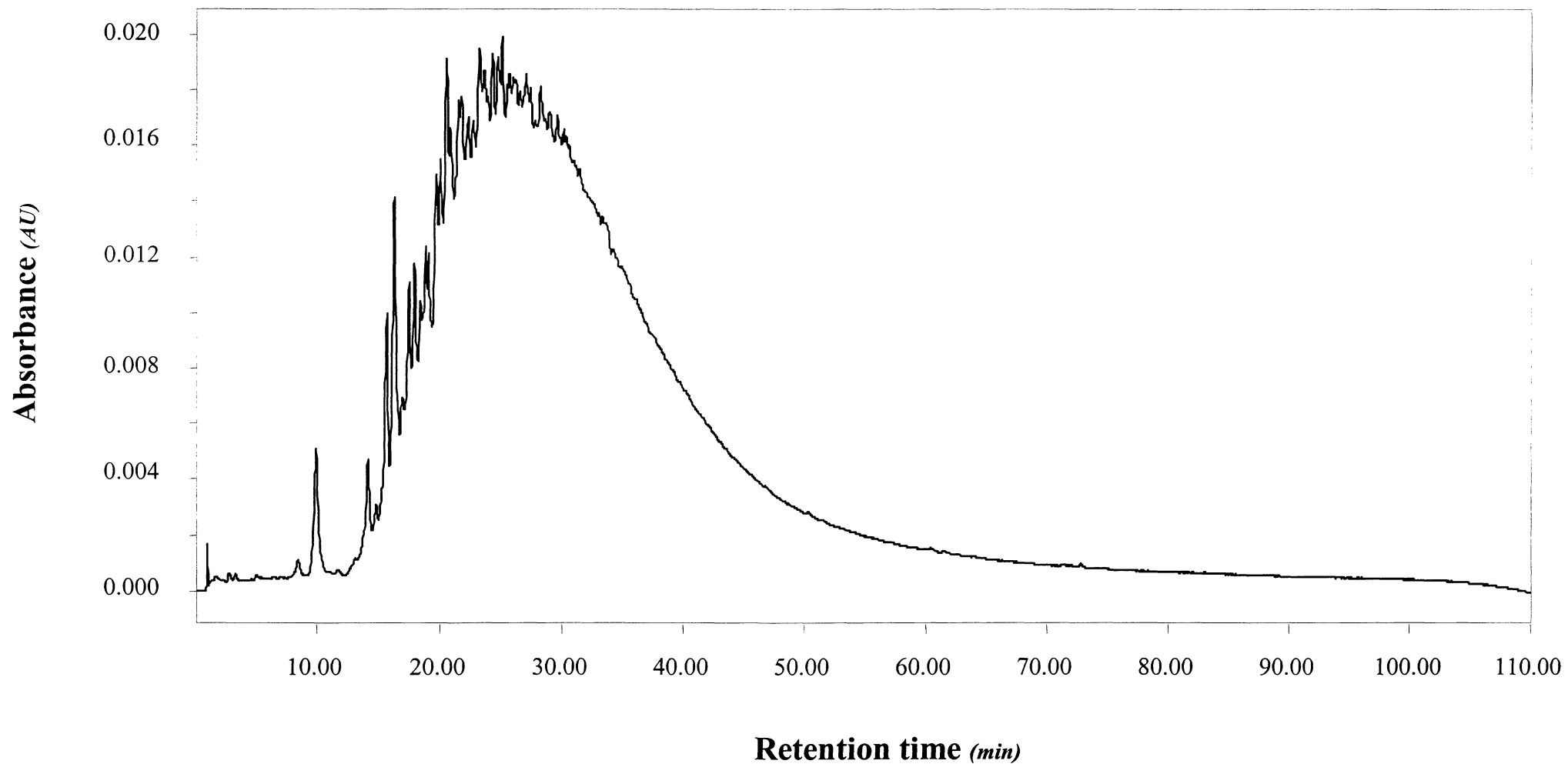
Figure 4.2: HPLC separation of the Bayer humic sample using ion-suppression chromatography with a linear 1% formic acid/acetonitrile gradient at a rate of change of 1% min^{-1}. AU=arbitrary units

---

Liquid chromatographic analysis of geological organic substances of industrial importance

4.4. ION-PAIR HPLC SEPARATION

In cases where the sample contains strong acids or bases and in the case of polar solutes of small molecules, the method of ion-suppression may not be adequate [134-135]. Improved control of retention and selectivity on a reversed phase column in these cases is obtained with the application of an ion-pairing reagent [136].

Ion-pair chromatography is an extension of the principles discussed for ion-suppression chromatography. An organic water-soluble ionic compound (ion-pairing reagent) is added to the mobile phase and forms an ion-pair with a sample component of the opposite charge. Addition of an ion-pairing reagent can alter the retention of the ionic compounds in the sample but will not affect the retention of the neutral compounds [134-135]. Uncertainty still exists over the retention mechanism of this mode of separation, however it is believed that an electrical double-layer is formed at the stationary phase surface by the lipophilic ion-pairing reagent ions forming a dynamic equilibrium with the eluent and stationary phases [134-137]. It is generally observed that the retention of the oppositely charged solute ions increases with the increased concentration and hydrophobicity of the pairing ion in the mobile phase and can be further altered by adjusting the percentage of the organic eluent or the pH [136].

For organic acids the added ion-pairing reagent is a strong base, which in this case was tetrabutylammonium hydrogen sulfate, referred to as PIC A. A gradient was run using PIC A [5 mM]/acetonitrile, running isocratically for 10 minutes on PIC A [5 mM] and then a linear gradient from PIC A [5 mM] to 75% acetonitrile at a rate of change of 1%

per minute. The resulting chromatogram in Figure 4.3 shows that greater resolution was achieved using PIC A with the humics from the Bayer liquor eluting over the first 50 minutes of the run. According to separation principles the neutral solutes in the Bayer humic sample would have passed through the double layer relatively unaffected. Solutes that had an opposite charge to the ion-pairing reagent in the Bayer humic sample would increase in retention due to an attraction with the electrostatic layer. The solutes in the Bayer humic sample with the same charge as the ion-pairing reagent would decrease in retention due to repulsion from the electrostatic layer.

Comparing all three modes of separation, ion-pair chromatography displayed significantly greater selectivity compared to the two other chromatographic modes discussed. The humics from the Bayer liquor were retained for longer and greater resolution was achieved. As ion-pair chromatography offered the greatest potential to vary the separation selectivity, time was further spent in developing this method.

To improve on the initial separation seen in Figure 4.3 where a PIC A [5 mM]/acetonitrile gradient was used, the gradient rate of change was decreased from 1% per minute to 0.17% per minute. The resulting separation is shown in Figure 4.4. By decreasing the gradient rate of change the Bayer humic sample was retained for longer, increasing the interaction of the sample with the stationary phase and eluent. This resulted in greater resolution being achieved, particularly in the first 200 minutes of the chromatographic run.
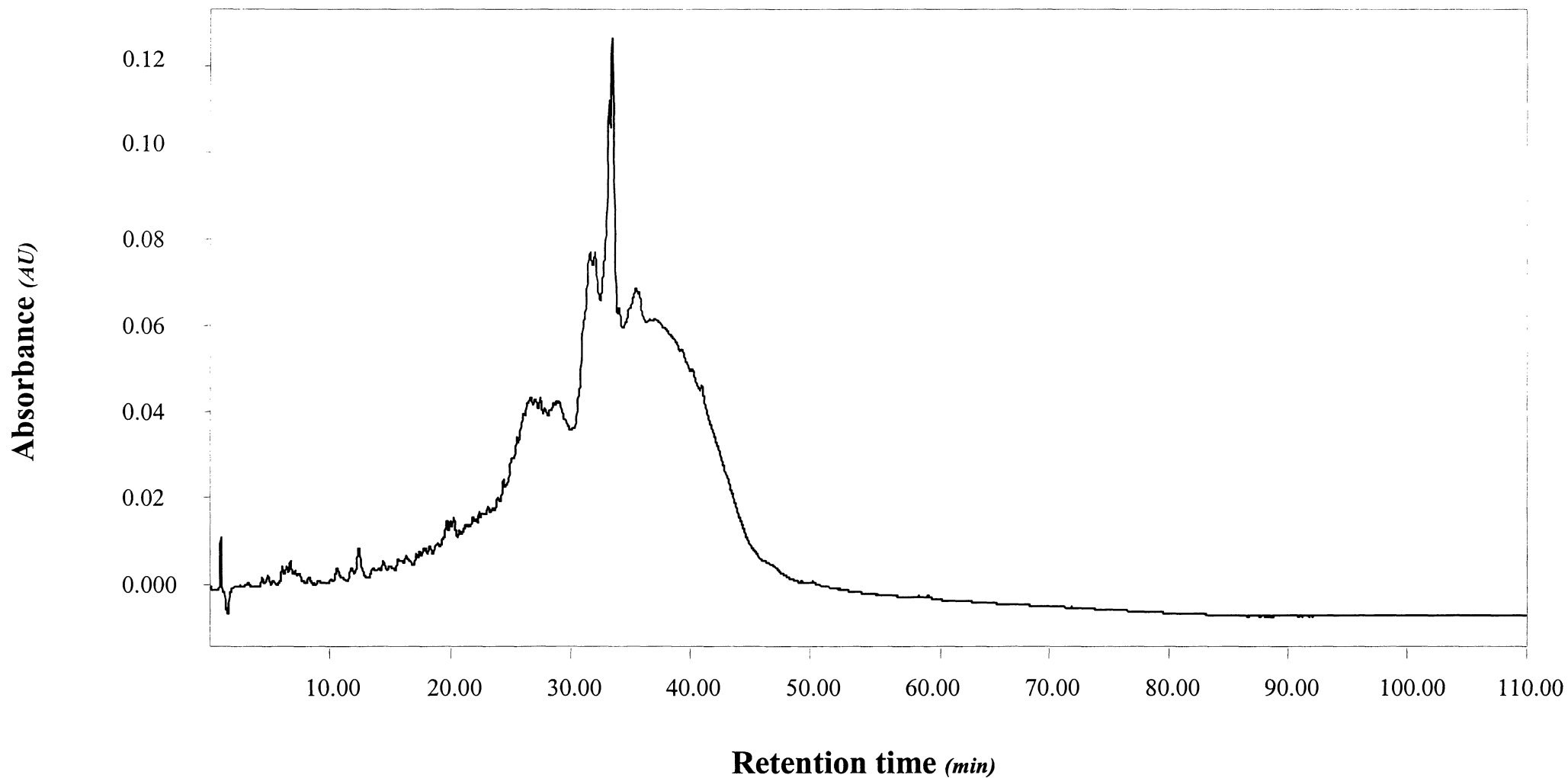
Figure 4.3: HPLC separation of the Bayer humic sample using ion-pair chromatography with linear PIC A/acetonitrile gradient at a rate of change of 1% min^{-1}. AU=arbitrary units
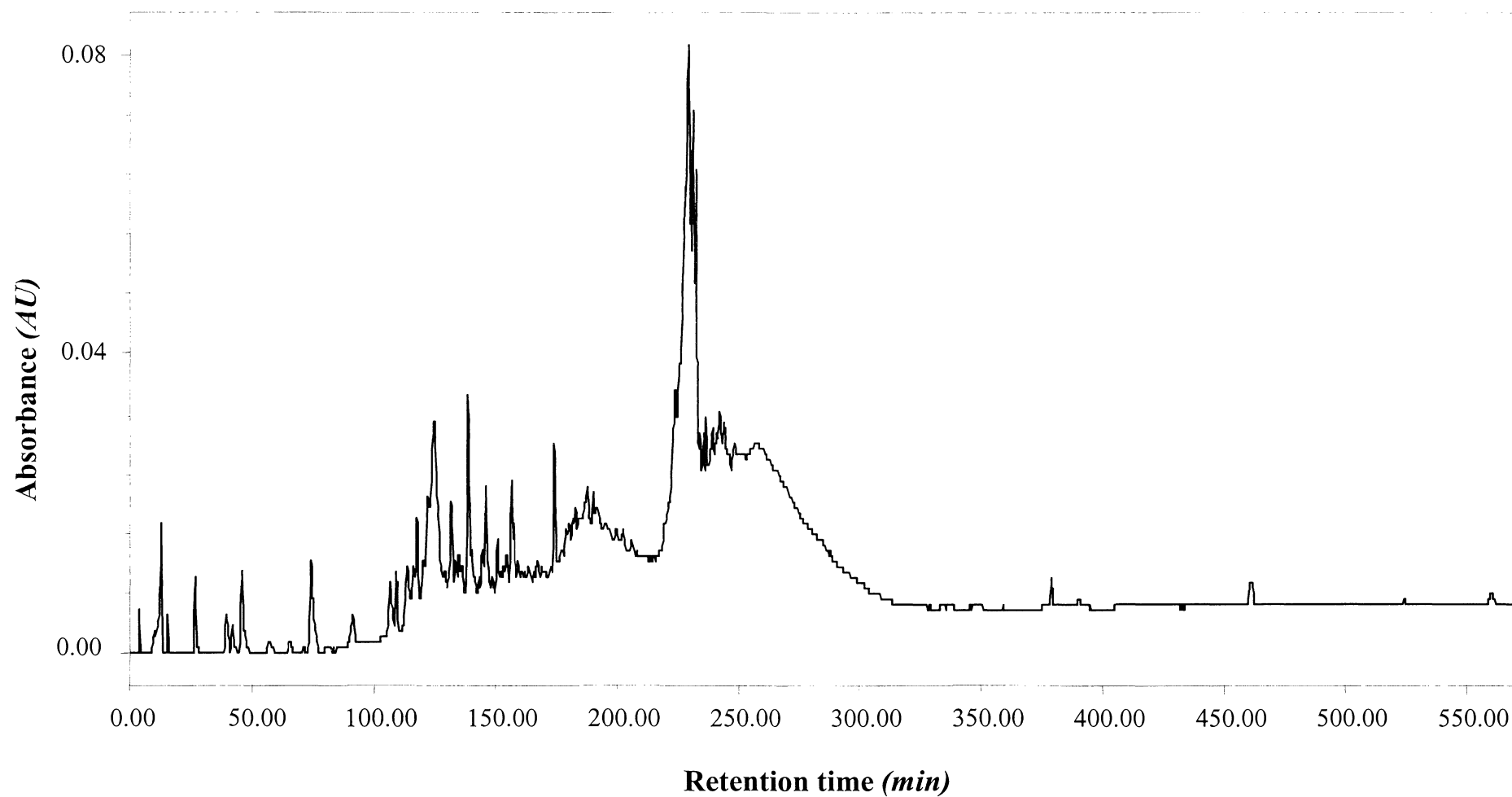
Figure 4.4: HPLC gradient separation of the Bayer humic sample using ion-pair chromatography with linear PIC A/acetonitrile gradient at a rate of change of 0.17% min^{-1}. AU=arbitrary units

A step gradient was then developed to further improve on this result. Figure 4.5 shows the HPLC separation achieved when the gradient was run using PIC A [5 mM]/acetonitrile, running isocratically for 30 minutes on PIC A [5 mM] and then a linear gradient from 100% PIC A [5 mM] to 20% acetonitrile at a rate of change of 0.1% per minute. The gradient rate of change was then decreased to further separate the compounds that eluted in the first 200 minutes in the previous chromatogram. The solvent composition was held at 80% PIC A [5 mM] and 20% acetonitrile for 60 minutes then the gradient was continued running from 80% PIC A [5 mM] and 20% acetonitrile to 60% PIC A [5 mM] and 40% acetonitrile at a rate of change of 0.083% per minute. The solvent composition was then held for a further 120 minutes. The resulting separation in Figure 4.5 shows that greater separation was achieved in the first 250 minutes but little difference was observed in the separation between 250 to 650 minutes. It appears that the relatively polar lower molecular weight material present in the Bayer humic sample is being resolved at the start of the chromatogram, with the rest of the Bayer humic sample eluting much later. These smaller molecules are those seen by NMR and are the parent molecules to those observed by GC/MS analysis.

Figure 4.6 shows the optimum separation achieved, with respect to resolution, for the Bayer humic sample. There is a slight loss of resolution in the separation in Figure 4.6 compared to the separation under the conditions shown in Figure 4.5. The separation shown in Figure 4.6 however is the optimum as it achieved base line resolution for four groupings; the highly resolved material 0-100 minutes, a second grouping of material 100-200 minutes, the partly resolved material at 250-280 minutes and the hump from 280-500 minutes. These four groups Group 1, 2, 3 and 4 respectively
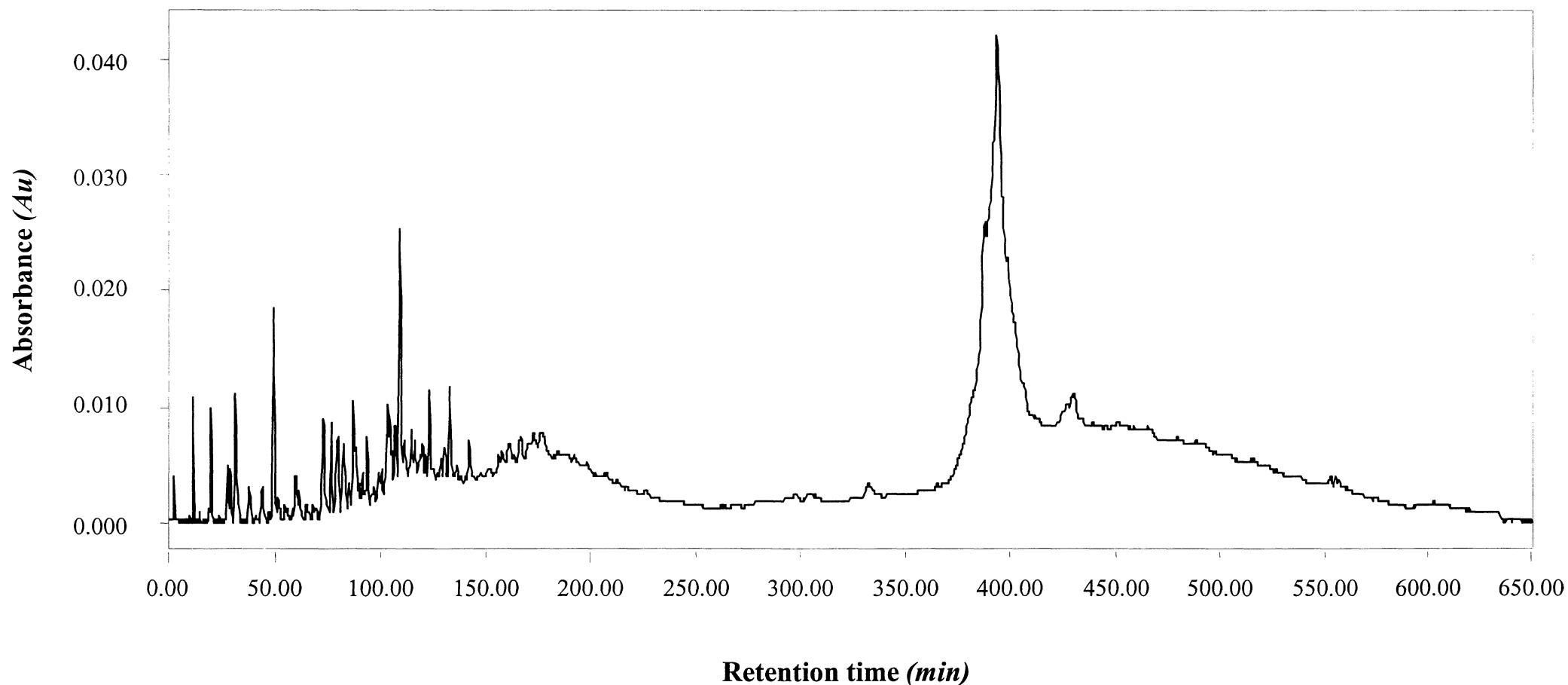
Figure 4.5: Development of a stepwise gradient for the separation of the Bayer humic sample. Isocratic PIC A [5 mM] for 30 min followed by a linear gradient from 100 % PIC A [5 mM] to 20% acetonitrile at 0.10% min^{-1}, then the gradient was held at 80% PIC A [5 mM] and 20% acetonitrile for 60 min, the gradient was continued running from 80% PIC A [5 mM] and 20% acetonitrile to 60% PIC A [5 mM] and 40% acetonitrile at 0.083% min^{-1}. The gradient was then held for 120 minutes. AU=arbitrary units
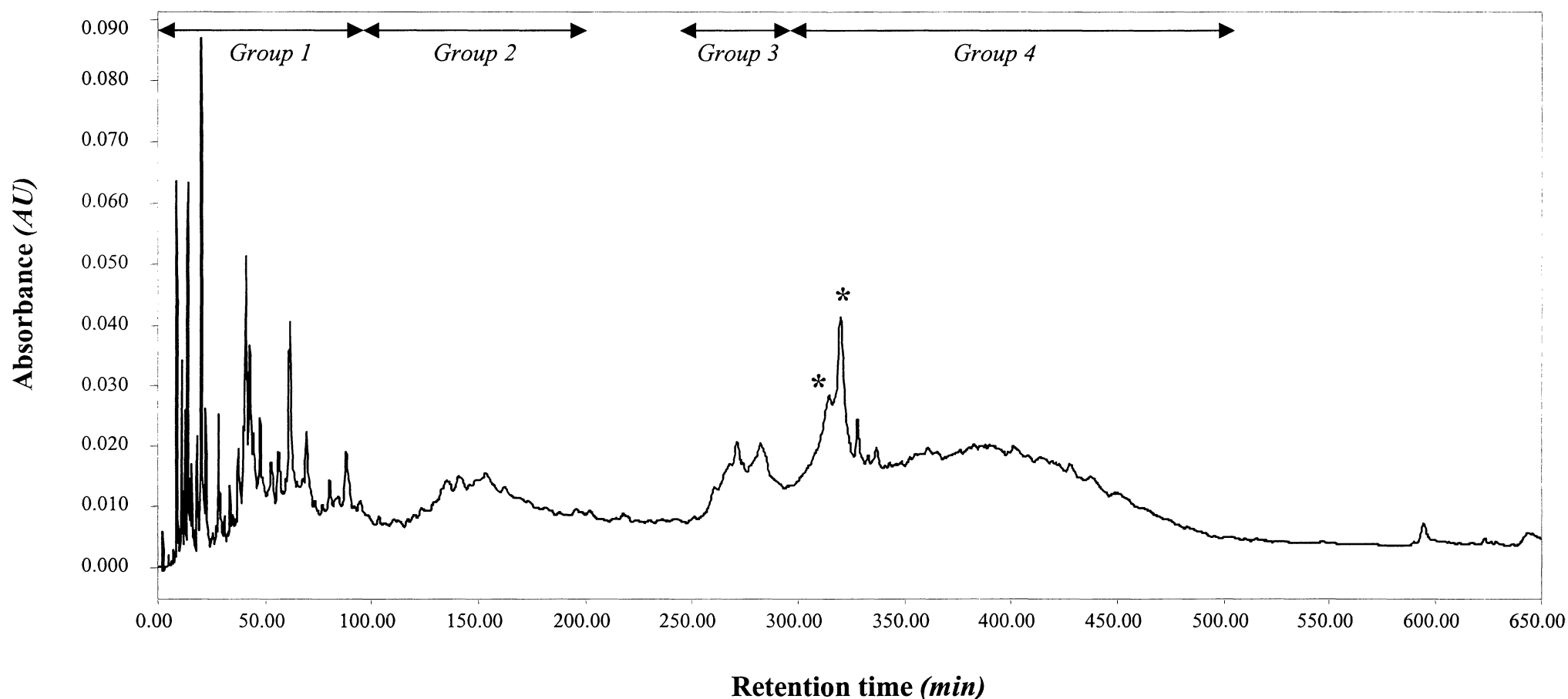
Figure 4.6: Optimum HPLC separation of the Bayer humic sample. Isocratic PIC A [5 mM]/acetonitrile for 10min followed by a linear gradient from 100% PIC A[5 mM] to 18% acetonitrile at 0.056% min^{-1}, then 82% PIC A [5 mM] and 18% acetonitrile to 57% PIC A [5 mM] and 43% acetonitrile at 0.083% min^{-1} then 50% PIC A [5 mM] and 50% acetonitrile for 5min. AU=arbitrary units. * =solvent change artefact

---

are shown in Figure 4.6. To achieve the separation in Figure 4.6 a gradient was run using PIC A [5 mM]/acetonitrile, running isocratically for 10 minutes on PIC A [5 mM] and then a linear gradient from 100% PIC A [5 mM] to 18% acetonitrile at a rate of change of 0.056% per minute. The gradient continued running from 82% PIC A [5 mM] and 18% acetonitrile to 57% PIC A [5 mM] and 43% acetonitrile at a rate of change of 0.083% per minute. The gradient was then changed to 50% PIC A [5 mM] and 50% acetonitrile over 5 minutes and the solvent composition was then held for 10 minutes. The chromatogram showed that substantial separation was achieved in the first 300 minutes with a number of peaks baseline resolved. It also displayed an improvement on the separation between 300 to 650 minutes. The reproducibility of this method was tested by repeating the separation in triplicate. The optimum separation was found to be reproducible.

The separation in Figure 4.6 is highly significant since it represents the first recorded liquid chromatographic method in which Bayer humic substances that contained higher molecular weight material have been separated into different groups, which will be discussed later in this Chapter with the analysis of the Bayer humic solvent extracted fractions. It is interesting to note that the Bayer humic substances did not elute as a continuum, but rather as clusters of peaks. These clusters could represent some form of molecular aggregation based on their size and/or polarity. The Bayer humic sample eluting as clusters of peaks rather than a continuum as seen in Figure 4.6, could reflect the fact that only certain configurations of molecular structures are warranted. The reason(s) for formation of such aggregates and their corresponding molecular weights are important parameters to consider, as these will provide valuable information on the chemical dynamics of Bayer humic substances.

4.5. SOLVENT EXTRACTION OF THE BAYER HUMIC SUBSTANCES

To assist in interpreting the complexity of the optimum separation of the Bayer humic substances seen in Figure 4.6, the humic sample was extracted with a series of solvents of different polarities. The components in individual solvent fractions were then characterised by GC/MS, NMR and FTIR spectroscopy and were separated using the optimum HPLC method.

The Bayer humic substances were separated based on solubility using a continuous solvent extraction of the Bayer humic sample with organic solvents in a Soxhlet apparatus. The extent of solubility of the Bayer humic substances was tested using a number of solvents ranging in polarity. Diethyl ether, ethyl acetate, isopropyl alcohol and water were chosen as the most appropriate solvents for the extraction. Using a glass microfibre extraction thimble the Bayer humic substances were extracted into four fractions, from the least polar solvent to the most polar solvent and resulted in fractions of a lesser degree of complexity.

Table 4.1 summarises the solvents and percentage mass yields. The majority of the Bayer humic substances (54%) were extracted in the first fraction with the least polar solvent, diethyl ether. The second largest yielding extracted fraction (25%) was the last fraction, which was extracted with the most polar solvent, water. The third fraction extracted with isopropyl alcohol gave a yield of 13%. The lowest yielding fraction (8%) was the second fraction that was extracted with ethyl acetate. Each of the

Table 4.1: Solvents used for the continuous solvent extraction of the Bayer humic substances and the % yields.

Fraction Number	Solvent	Mass yield (w/w, %)
F1	Diethyl Ether	54
F2	Ethyl Acetate	8
F3	Isopropyl Alcohol	13
F4	Water	25

fractions were then characterised by GC/MS, FTIR and NMR spectroscopy and were separated using the optimum HPLC method.

The FTIR spectra of the solvent fractions are shown in Figure 4.7. Significant changes in the spectra are indicated in Figure 4.7 and occurred at 1700, 1600, 1400 and 1200 cm^{-1}. Differentiation occurs primarily in the number of carboxylic acid groups observed in the FTIR spectra. A decrease in the intensity of the absorption band at 1700 cm^{-1} can be seen in all four fractions from least polar fraction to the most polar. This indicates a decrease in the content of carboxylic groups (C=O stretch at 1700 cm^{-1}) from the diethyl ether fraction (F1) (Figure 4.6 (b)) to the water fraction (F4) (Figure 4.6 (e)). The reduction coincides with a change in magnitude of the C-O stretching vibration at 1260 cm^{-1}. The water fraction (F4) displayed a considerable reduction in the carboxylic acid functional groups present compared with the diethyl ether fraction (F1). Therefore it can be concluded that the water soluble extract contains the least number of polar groups. This may seem strange but it should be appreciated that the solubility of humic materials is controlled by association, so small molecules that can aggregate by arranging their polar groups internally to produce a more hydrophobic complex are more soluble in organic solvents [23]. Although the FTIR analysis of the solvent fractions did provide information on the carbonyl content on a quantitative level, it did not provide information on the overall polarity of the Bayer humic solvent fractions. Further analysis of the solvent fractions by solid-state ^{13}C NMR spectroscopy however will provide information on the overall distribution of the carbon containing functional groups present in the solvent fractions.
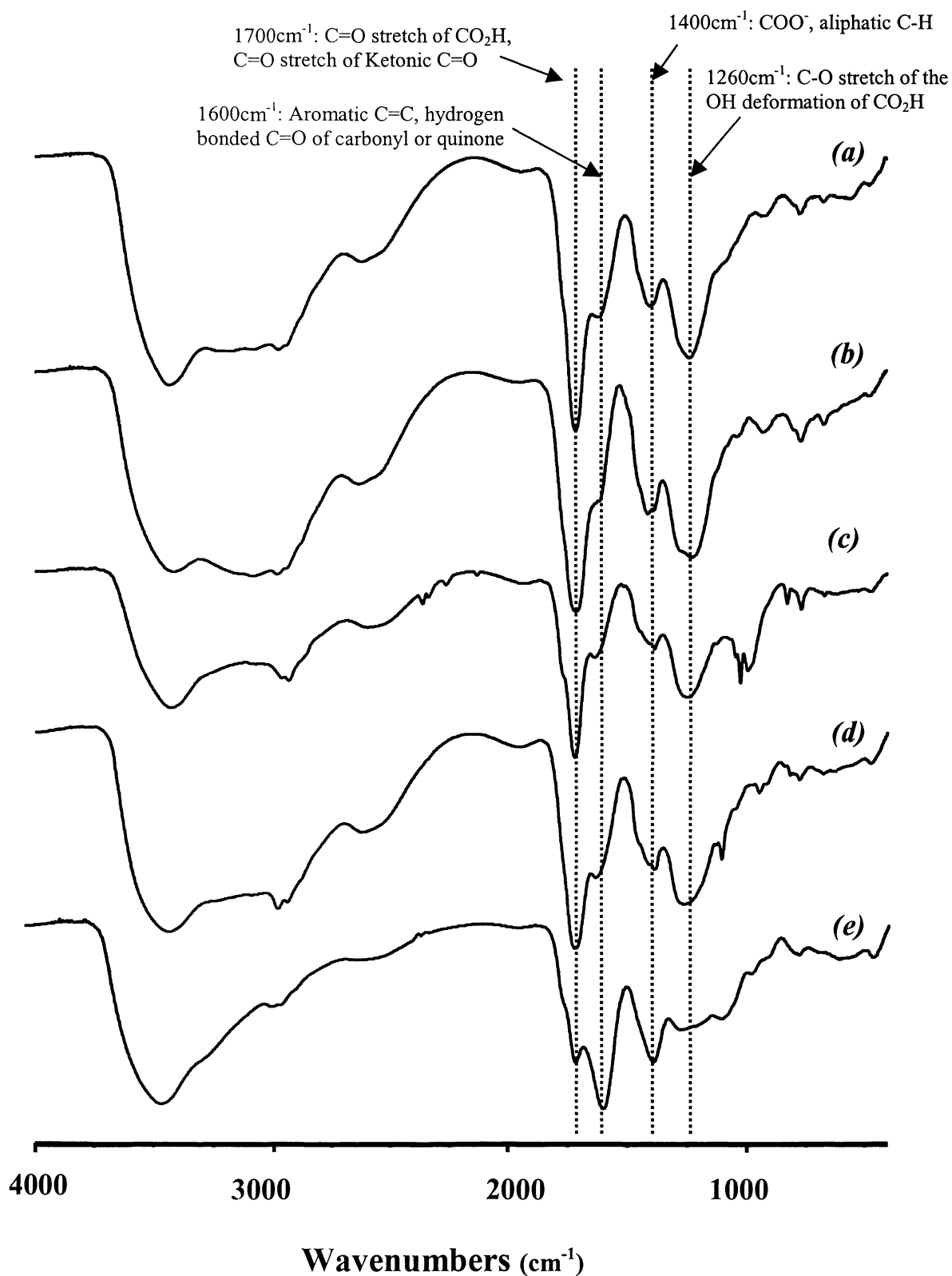
Figure 4.7: FTIR spectra of the solvent fractions: (a) Bayer humic sample, (b) diethyl ether fraction, (c) ethyl acetate fraction, (d) isopropyl alcohol fraction and (e) water fraction.

^{1}H NMR spectra data shows the variability of the components during the extraction (Figure 4.8). A typical ^{1}H NMR spectrum of humic acids shows only broad resonances due to the large number of environments of the protons in substances of such high molecular weight. Examination of the proton ^{1}H NMR spectra (Figure 4.8) in this case showed a number of discrete resonances particularly in solvent fractions F1 and F2, indicating the presence of low molecular weight molecules. Greater detail of the aliphatic and aromatic regions in the ^{1}H NMR spectra can be seen in Figures 4.9 and 4.10 respectively.

The spectrum of the Bayer humic sample showed a broad hump with numerous sharp resonances superimposed in the aromatic region extending from 6-8.8 ppm (Figure 4.10). This was also observed in solvent fractions F1 and F2. The lack of discrete resonances in the aromatic region for solvent fractions F3 and F4 indicate that they contain a very small amount of aromatic protons. Low molecular weight compounds previously identified in Bayer liquors such as lactate and formate were observed [8, 13, 87]. It is clear that the small molecules concentrated in the diethyl ether fraction (F1) and with increasing solvent polarity these are removed. Protons on carbons adjacent to functional groups such as COOH resonating in the region 2-3 ppm also decreased (Figure 4.9). However, it should be pointed out that ^{1}H NMR spectral data only provides information on the hydrogen containing chemical constituents and therefore it is necessary to determine the distribution of substituted carbon constituents by solid state ^{13}C NMR spectral data which will be discussed later in this chapter. All of the chemical features observed in the ^{1}H NMR data such as reduction in the hydrogen
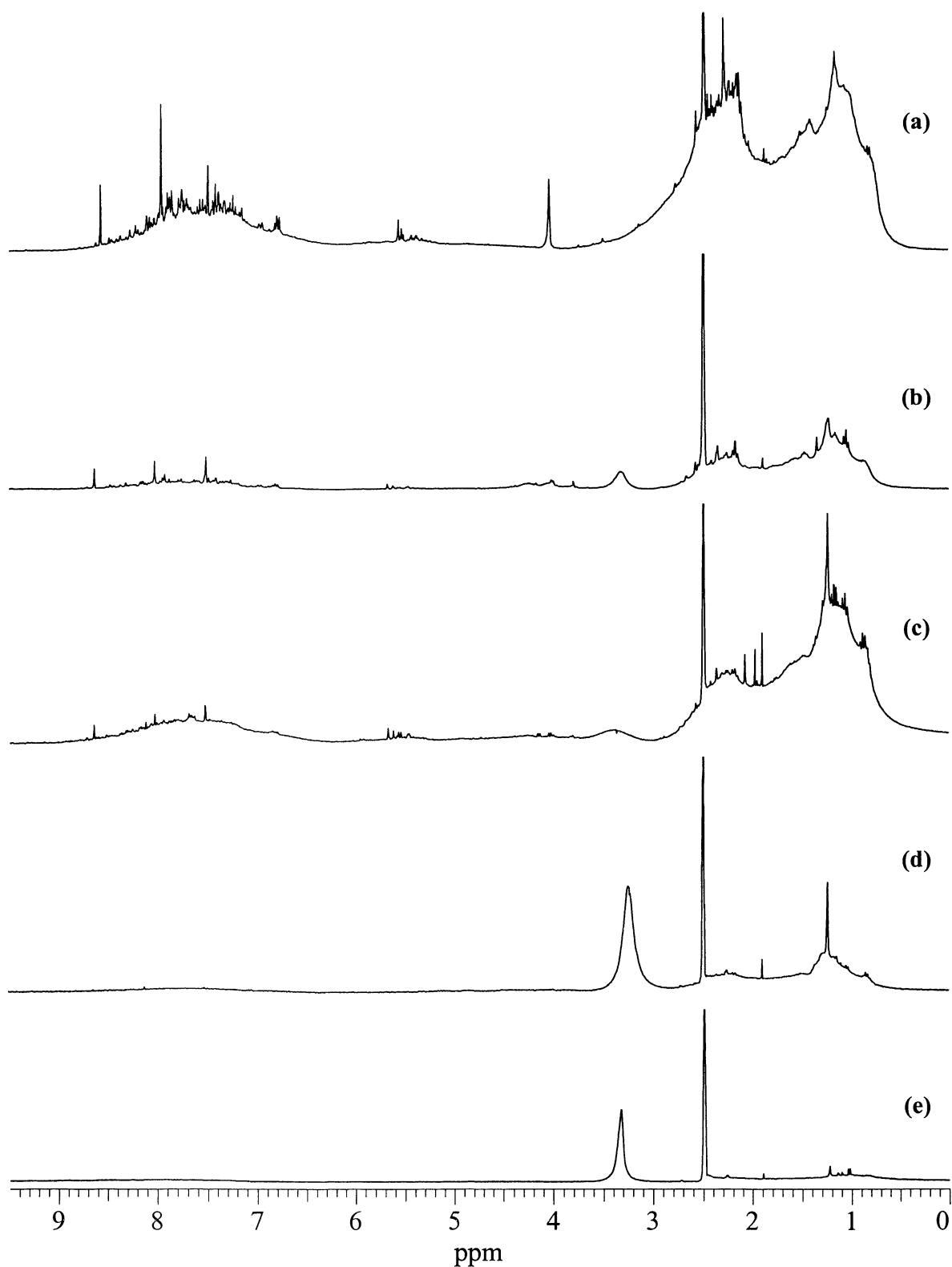
Figure 4.8: Solution ^{1}H NMR spectra of the solvent fractions: (a) Bayer humic sample, (b) diethyl ether fraction, (c) ethyl acetate fraction, (d) isopropyl alcohol fraction and (e) water fraction.
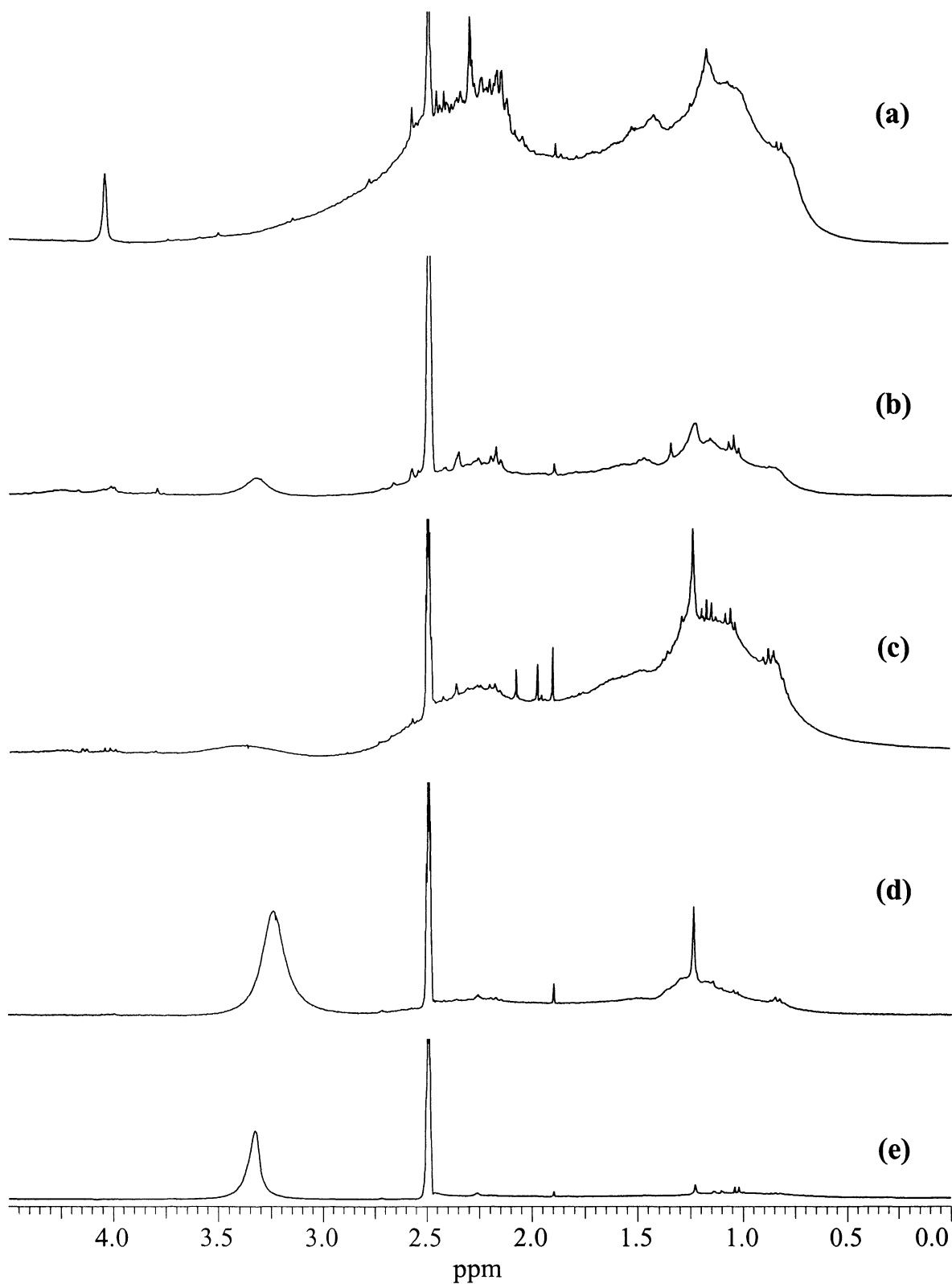
Figure 4.9: Solution ^{1}H NMR spectra of the solvent fractions – aliphatic region: (a) Bayer humic sample, (b) diethyl ether fraction, (c) ethyl acetate fraction, (d) isopropyl alcohol fraction and (e) water fraction.
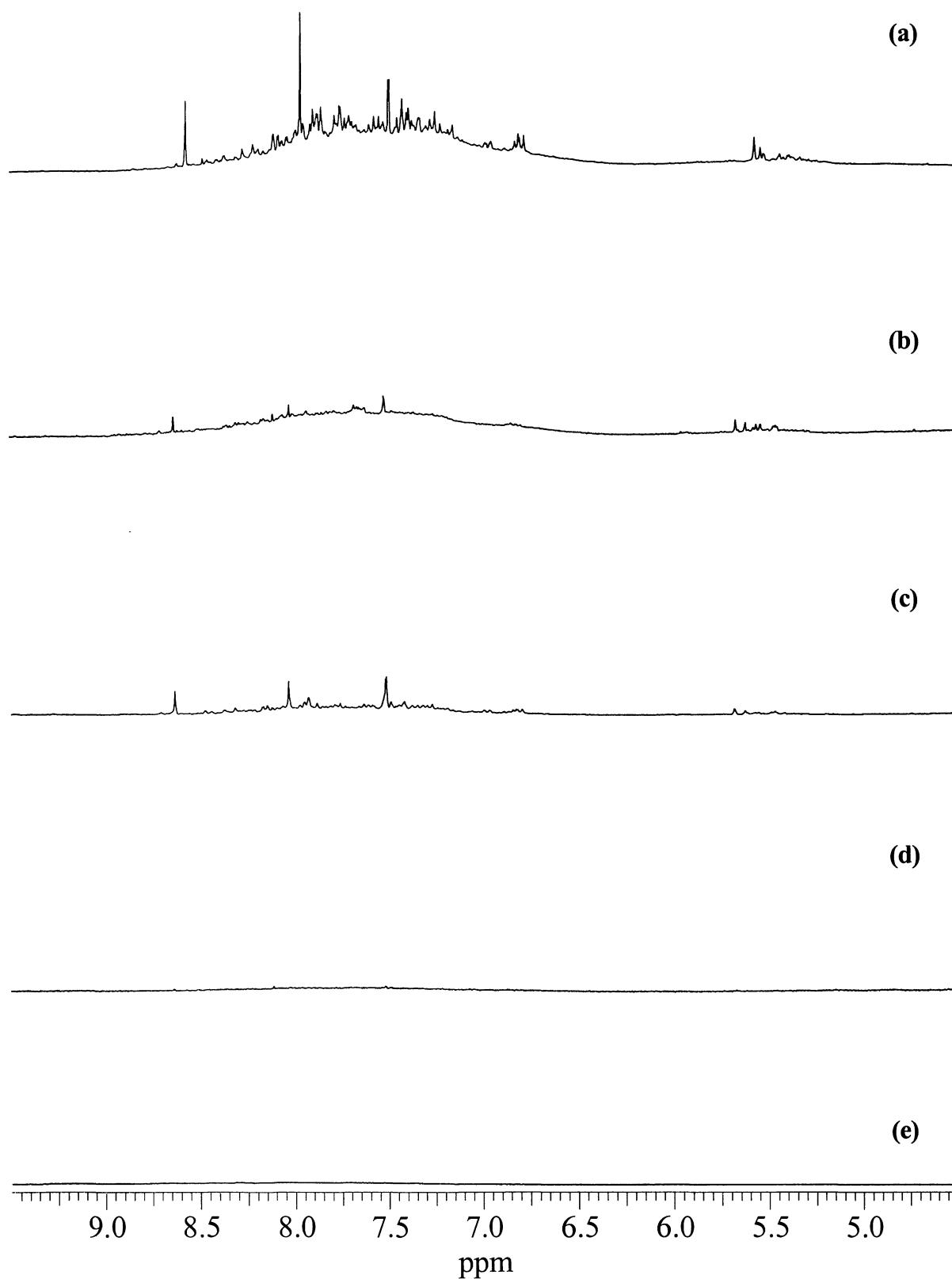
Figure 4.10: Solution ^{1}H NMR spectra of the solvent fractions – aromatic region: (a) Bayer humic sample, (b) diethyl ether fraction, (c) ethyl acetate fraction, (d) isopropyl alcohol fraction and (e) water fraction.

substituted carbons, polar functional groups such as ethers and carboxylic acids, are consistent with the FTIR spectroscopic data. It is difficult to further assign the compounds present based on ^{1}H NMR of humic acids and its fractions alone, but some of the molecular identities can be obtained from the analysis of the methylated fractions by GC/MS.

The four extracted solvent fractions and the Bayer humic sample were methylated using the procedure described used by Smeulders et al. [80] and analysed by GC/MS. Figure 4.11 shows the GC/MS spectra of the methylated samples. The GC/MS data shown in Figure 4.11 will only show small molecules since the larger molecules will be involatile. The results support the ^{1}H NMR data since the greatest concentration of small molecules are in the least polar fractions. Compounds identified in Figure 4.11 are assigned in Figure 4.11 from (1) - (15) and are summarised in Table 4.2.

The ^{13}C data is also supportive of the FTIR, ^{1}H NMR and GC/MS data. The frequency domain ^{13}C spectra for each extract was analysed to approximately determine the different structural groups present using the established literature methods previously mentioned. Table 4.3 summarises the functional group assignments and indicates the % composition of the different carbon groups in the Bayer humic sample and the carboxyl ratios calculated based on the integration of the different regions in the ^{13}C solid-state NMR spectra.

The carboxyl content follows the order expected. The carboxyl group is partly resolved into two groups at 175 and 180ppm, with the aromatic carboxylic acids assigned to the
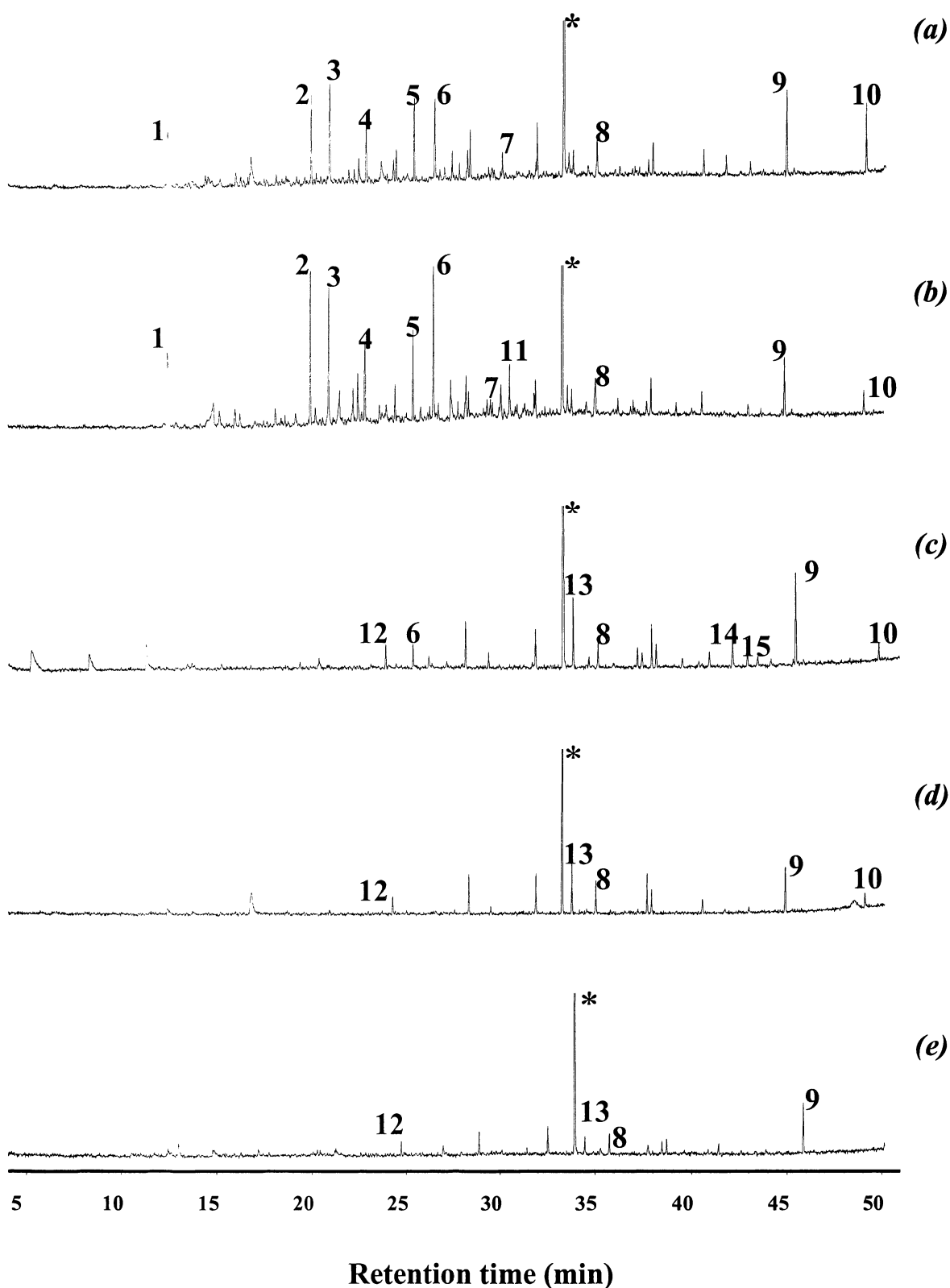
Figure 4.11: GC/MS of methylated solvent fractions: (a) Bayer humic sample, (b) diethyl ether fraction, (c) ethyl acetate fraction, (d) isopropyl alcohol fraction and (e) water fraction. See Table 4.2 for chemical assignments.

Table 4.2: GC/MS spectra chemical assignments for Bayer humic substances and solvent fractions.

Assignment	Identified compounds	Bayer humic substances	F1	F2	F3	F4
(1)	benzoic acid methyl ester	✓	✓			
(2)	3-methoxybenzoic acid methyl ester	✓	✓			
(3)	4-methoxybenzoic acid methyl ester	✓	✓			
(4)	octanedioic acid dimethyl ester	✓	✓			
(5)	nonanedioic acid dimethyl ester	✓	✓			
(6)	3,4-methoxybenzoic acid dimethyl ester	✓	✓	✓		
(7)	3,4-dihydro-5-methoxy-3,8-dimethyl-1(2H)-naphthalenone	✓	✓			
(8)	octadecanoic acid methyl ester	✓	✓	✓	✓	✓
(9)	1,2-benzenedicarboxylic acid bis(2-ethylhexyl) methyl ester	✓	✓	✓	✓	✓
(10)	squalene	✓	✓	✓	✓	
(11)	3,5-di-tert-butyl-4-hydroxybenzaldehyde		✓			
(12)	1,4-benzenedicarboxylic acid methyl ester			✓	✓	✓
(13)	hexadecanoic acid methyl ester			✓	✓	✓
(14)	1,2-benzenedicarboxylic acid butyl phenylmethyl ester			✓		
(15)	hexanedioic acid bis(2-ethylhexyl) methyl ester			✓		
*	nonadecane (Internal standard)	✓	✓	✓	✓	✓

Table 4.3: Percentage composition of different carbon types in the Bayer humic substances as measured by solid-state ^{13}C NMR spectroscopy.

	% Composition				
	C-alkyl	**O-alkyl**	**Acetal, Aromatic**	**Carboxyl**	**Carboxyl ratio**
Chemical Shift (ppm)	0-50	50-100	100-160	160-190	180/ 175ppm
Humic Substance	42.4	5.4	31.3	20.9	1.22
F1 Diethyl ether fraction	35.7	5.4	33.9	25.0	0.8
F2 Ethyl acetate fraction	39.4	5.5	31.3	23.8	0.9
F3 Isopropyl alcohol fraction	36.5	6.2	35.0	22.5	1.0
F4 Water fraction	37.4	4.6	41.3	16.7	2.0

a) Solvent peaks have not been integrated

higher chemical shift (this is also evident in ^{13}C solid-state NMR spectrum for the whole Bayer humic substances shown in Chapter 3). The diethyl ether fraction (F1) contains more of the 175 ppm and the water fraction (F4) more of the 180 ppm [138]. This could be hydrogen bonded or deshielded carboxylic acids. Hydrogen bonding deshields the COOH group, which is in agreement with the data if the material in the diethyl ether fraction (F1) is complexed in hydrogen bonded structures, intramolecularly or in supramolecular structures, while that in the water fraction (F4) is free to bond with the water [138]. However, keep in mind the water fraction is more aromatic, as evident both from the NMR and FTIR spectra (as seen by comparing the relative intensities of the 1616 cm^{-1} absorption due to C=C vibrations). These differences could be due to different amounts of aromatic and aliphatic bound carboxylic acid groups respectively.

Of particular interest are the ratios of carbons present in each of the solvent fractions as shown by the ^{13}C NMR results in the region of 0-50 ppm, which can be considered to be relatively hydrophobic and the carbons between 50-190 ppm, which can be considered to be containing relatively hydrophilic functional groups. On examination of ratios of hydrophobic to hydrophilic carbons in Table 4.3 it can be seen that there is very little difference in the ratios between the most polar to the least polar fractions. For solvent fraction F1 carbons in the hydrophobic region (0-50 ppm) accounted for 35.7% which is very similar to the hydophobic carbons in solvent fraction F4 that accounted for 37.4%. The hydrophilic carbons (50-190 ppm) also reported similar results with the total carbon content in solvent fractions F1 and F4 accounting for 64.3% and 62.6% respectively. However, what is remarkable is that there does not exist a greater difference in these ratios for the Bayer humic solvent fractions. The presence of hydrophobic material in

the solvent fractions extracted with polar solvents and the hydrophilic material in the solvent fractions extracted with non-polar solvents can possibly be attributed to the 'self assembly' of functional groups within the Bayer humic substances. This will be discussed further later in this chapter.

The chromatograms of the solvent soluble fractions were obtained using the conditions developed above and are shown in Figure 4.12. Not surprisingly the small molecular weight material concentrates in the diethyl ether fraction (F1) as seen from the spectroscopic data and is retained the least. The material eluting at retention times above 300 minutes appears to concentrate in the more polar fractions, although they have greater retention than the material eluting in the non-polar fractions. The material in these polar fractions contain associated organic material that is relatively carboxyl group poor but still containing similar abundance of hydrophobic constituents, which is confirmed by the spectroscopic data and explains why they elute later in the chromatographic run even though they were extracted in the more polar solvents.

Our results allow some degree of assignment to optimum HPLC separation developed in Figure 4.6. Interestingly it appears that the more functionalised material elutes first. Hence the separation that was developed as shown in Figure 4.6 is highly significant since it represents the first recorded chromatograph in which Bayer humic substances that contain high molecular weight material have been separated into groups of different functionality. It also demonstrates that the material is not randomly polymeric and there are discrete structural types that chromatograph differently. It is also noteworthy that the material eluting around 150 minutes concentrates in the diethyl ether fraction (F1), which was shown by GC/MS, NMR and FTIR spectroscopy to contain relatively
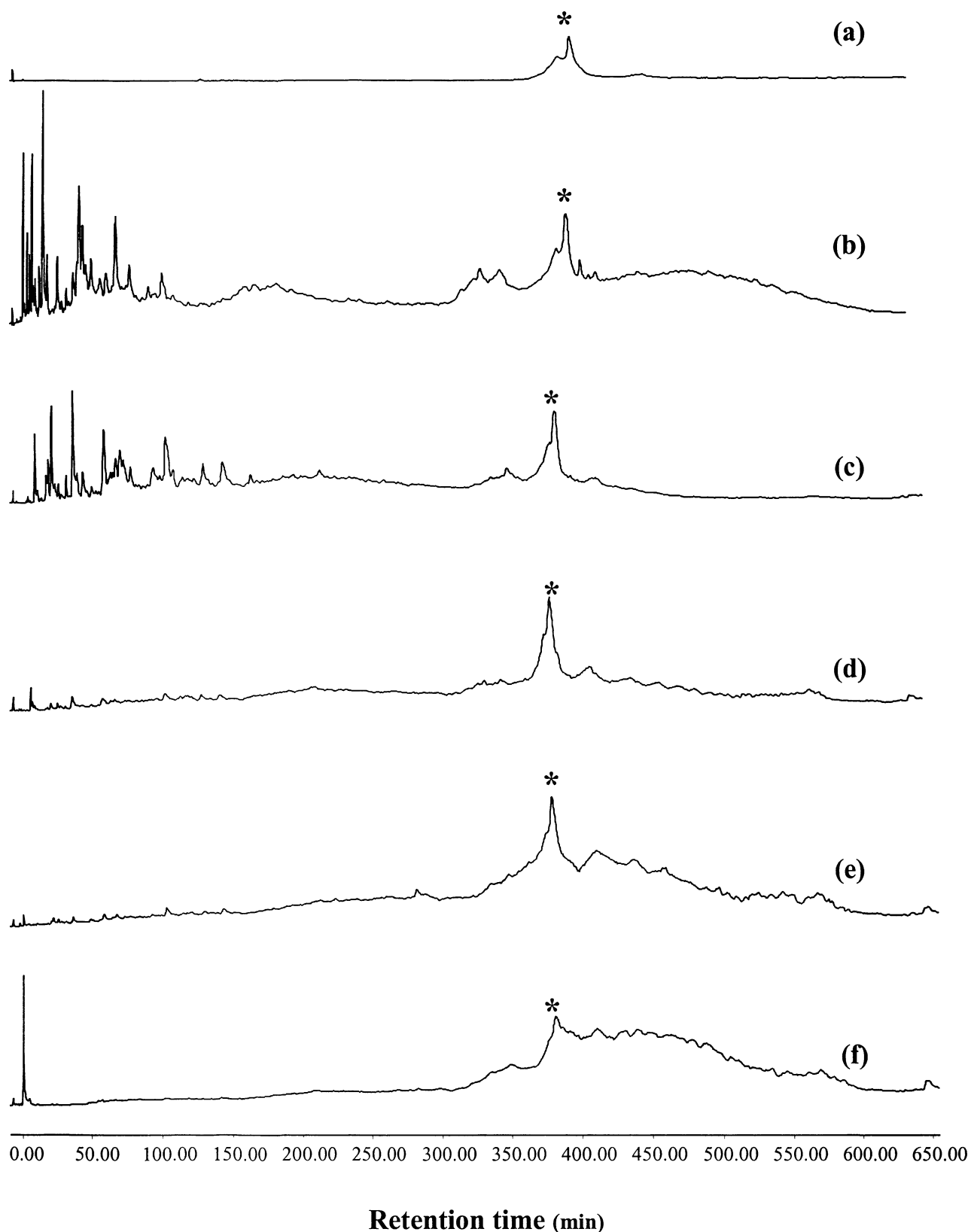
Figure 4.12: HPLC of fractions. (a) Blank, (b) Bayer humic sample, (c) diethyl ether fraction, (d) ethyl acetate fraction, (e) isopropyl alcohol fraction and (f) water fraction. *=solvent change artefact.

polar smaller molecular weight material. The results demonstrate that the compounds containing greater percentage of carboxylic acid functional groups but relatively similar hydrophobic carbon constituents dissolve in the diethyl ether fraction (F1) rather than the water fraction. This is a reflection of the fact that compounds containing the carboxylic acid groups have a considerable amount of hydrophobic character allowing those to be soluble in relatively non-polar solvents, such as diethyl ether. In other words, in more non-polar solvents, the hydrophobic nature of the humic material controls its solubility. It is possible that these carboxylic acid groups form both intermolecular and intramolecular hydrogen bonding with carboxyl and other polar functionality present in the humic material. The structure is therefore somewhat micellar with non-polar groups externally structured or at least there is a core of functionalised groups with the hydrophobic groups to the outside. Whether this micelle is one coiled molecule or a number bound supramolecularly is unknown.

It is not surprising therefore that the separated clusters in the chromatograms of molecules around 0-100, 100-200, 250-280 and 280-500 minutes behave as they do. They represent micellar like aggregates of different amounts of polar groups. It must be that only certain configurations are stable other wise the chromatograph in Figure 4.6 would be a continuum. Therefore we propose two structural models. Firstly small molecules are entrapped in a complex of larger molecules, which will be referred to as a "hidden host guest model" as illustrated in Figure 4.13 (a). Alternatively, small molecules are interbound to each other, which will be referred to as a "micellar host guest model" as illustrated in Figure 4.13 (b). Although there has been a general
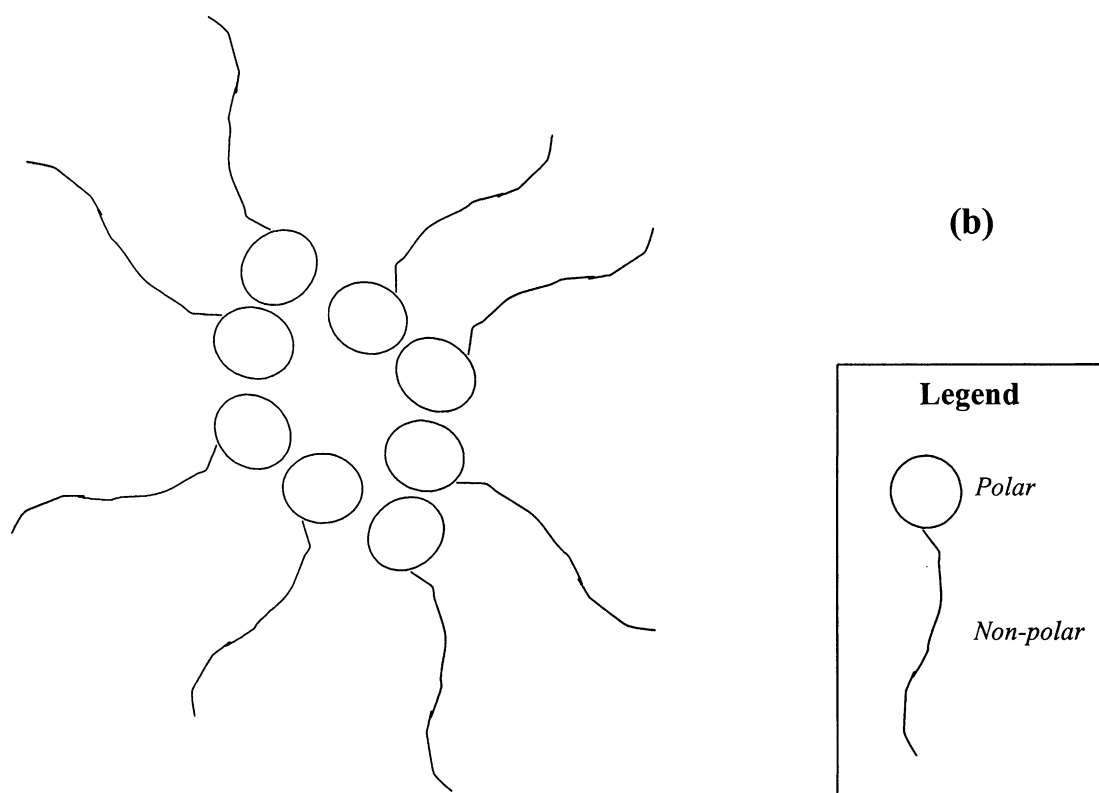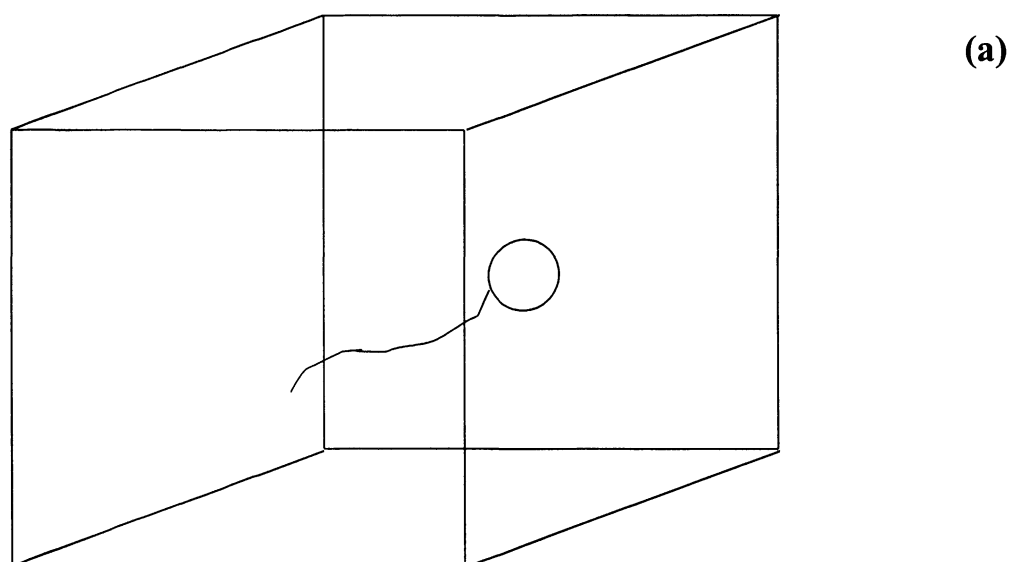
Figure 4.13: Diagrammatic representation of the proposed "hidden host guest model" (a) and "micellar host guest model" (b).

acceptance of aggregate structures in humic materials controlling conformation [23, 56, 60, 62], this is an important result since it is the first recorded evidence for a supramolecular structure to Bayer humic substances. An outstanding problem is to determine the molecular weight of these supramolecular clusters since there must be only certain defined molecular clusters allowable and why they cluster as they do. The results do suggest if the complexes are micellar they consist of collected aggregates of small and large molecules rather than small molecules hidden inside large molecules, not with standing the hosting of alkanes as described by Smeulders et al. [85]. Both these models will be discussed further in Chapter 6.

4.6. CONCLUSIONS

A high-performance liquid chromatographic method was developed which separated the Bayer humic substances into compound classes. The optimum separation was achieved by running a gradient using PIC A [5 mM]/acetonitrile, running isocratically for 10 minutes on PIC A [5 mM] and then a linear gradient from 100% PIC A [5 mM] to 18% acetonitrile at a rate of change of 0.056% per minute. The gradient continued running from 82% PIC A [5 mM] and 18% acetonitrile to 57% PIC A [5 mM] and 43% acetonitrile at a rate of change of 0.083% per minute. The gradient was then changed to 50% PIC A [5 mM] and 50% acetonitrile over 5 minutes. The solvent composition was then held for 10 minutes.

Solvent separation of the Bayer humic substances yielded fractions of different complexity that were then correlated with the optimum separation achieved as shown in Figure 4.6. Surprisingly the fraction extracted with the least polar solvent, diethyl ether (F1), contained polar material and the fraction extracted with the most polar solvent, water (F2), contained non-polar material as shown by the results of the NMR, FTIR and GC/MS analyses. It was also clear from the NMR and GC/MS results that the small molecular weight material concentrated in the diethyl ether fraction (F1). The most polar material concentrating in the least polar solvents provided evidence to support that the Bayer humic substances have a micellar like structure in that polar groups are concentrated to avoid solvent interaction in fractions soluble in the least polar solvents. Whether this micelle is one coiled molecule or a number bound supramolecularly is unknown however two structural models were proposed based on the results, "hidden host guest model" and the "micellar host guest model". Both structural models will be further discussed later in Chapter 6.

Small molecules and three discrete clusters of macromolecules were observed. Within these clusters there is some degree of further resolution. It must be that only certain configurations are stable otherwise the separation would show a continuum of peaks rather than clusters. Four discrete groupings were observed (Figure 4.6) which represent certain stable configurations of molecular weights that could be controlled by polarity through intramolecular binding and are strong evidence for a supramolecular structure to Bayer humic substances rather than the existence of random conformational material.

Despite having developed a one-dimensional HPLC separation for Bayer humic substances that achieved a level of separation previously unreported in the literature, this method was still not ideal with a number of limitations. The separation did take over ten hours and even then limited resolution was achieved as the peak capacity of the separation system was vastly exceeded. It also used an involatile ion-pairing reagent that made the method incompatible with mass spectrometry (MS). Limited information can be gained using a photodiode array detector whereas MS would provide greater information on the structure of the Bayer humic substances. This separation did however highlight the complexity of the isolation problem. It showed that Bayer humic substances are too complex to separate using a one-dimensional HPLC separation and that a multidimensional approach to the separation problem would be required. To improve on the one-dimensional HPLC separation developed in this Chapter, a two-dimensional HPLC separation that expanded the peak capacity of the system was further developed and will be discussed later in Chapter 6.

CHAPTER 5

Study of the selectivity of reversed phase columns for the separation of small compounds as humic mimics

5.1. INTRODUCTION

The results presented within Chapter 4 demonstrated that conventional high-performance liquid chromatographic (HPLC) techniques employing a C18 column could be further enhanced to improve the separation of Bayer humic substances. However, these separations were far from ideal. This does not mean that further chromatographic development is of no value as there have been a number of advances in column technology since the development of the C18 column. The supply of spherical, smaller particulate matter, new hybrid packing materials, optimised surface modifications, as well as advances in column packing, have all led to improvements in this separation technique [139-141]. In addition, due to advances in column technology the reproducibility of column packing and the mechanical stability of the packed bed are no longer a concern [142-148].

Little work has been done using these new types of reversed phase columns for the separation of humic substances. Nevertheless since reversed phase HPLC is commonly used for the analysis of polycarboxylic acids and polyphenols (the types of compounds commonly found in humic substances) and there exists some relevant literature in related fields. The retention of polycarboxylic acids and polyphenols in reversed phase HPLC is highly dependent on the degree to which these type of compounds are ionised and therefore changes in the pH of the mobile phase can affect the separation [139].

There are many types of reversed bonded-phase stationary phases available today, the most common of which is the C18 or C8. A C18 column is packed with bonded

octyldecyl siloxane stationary phase material. Cyano and nitrile columns are often used for more polar solutes and can be operated in reversed phase or normal-phase mode. Both these columns therefore may be useful for the separation of humic substances. The propyl phenyl column could also be used for the separation of humic substances as it often finds use as an alternative to the C18 column and can take advantage of π–π type interactions. Moreover the continual search for new and improved stationary phases has led to new bonded phase supports that have alleviated some of the limitations of the traditional silica-based packing materials, such as improving the pH stability and minimising interactions with residual surface hydroxyl groups which could further advance the liquid chromatographic separation of humic substances.

The new hybrid packing materials now available, such as the Waters XTerra™ column have the advantages of both silica and polymer packing materials. They are stable over a wider pH range, with a working range of pH 1 to 12 and have a high efficiency, mechanical strength and high temperature stability [139]. There have also been a number of advances in the design of stationary phases that can help retain polar analytes under highly aqueous conditions including hydrophilic, polar-encapped and polar-enhanced stationary phases and polar-embedded alkyl phases [149].

The majority of reversed phase liquid chromatographic separations of humic substances use the traditional C18 column. Therefore there are great opportunities in exploring the potential of these new column phases for the separation of humic substances. However without a systematic approach to evaluating these new phases for the separation of

polycarboxylic acids and polyphenols, the overall approach would be random and unstructured. While there is some literature available on the separation of these types of compounds, it is scarce. In this study we compared the resolving power of five new generation stationary phases that were selected according to their potential differences in retention mechanism hence facilitating possible changes in selectivity, band shape and performance. Using a set of twenty-four standards comprising a mix of polycarboxylic acids and polyphenol compounds, we compared the five columns by taking the retention data for each column and using information theory (IT) and factor analysis to determine the degree of correlation between the four different columns and a conventional C18 column. The objective of this study was to find the most appropriate reversed phase column for the separation of the type of compounds found in humic substances. This column would later be used in the development of a two-dimensional HPLC separation for Bayer humic substances.

The approach used here was to compare the columns firstly in terms of their retention behaviour using information theory and factor analysis, secondly by the physical shape of the eluting bands and finally comparing the elution order of the bands.

5.2. COMPARISON OF RETENTION BEHAVIOUR

5.2.1. Information theory

Chemical compounds can be identified by the measurement of properties that depend on their chemical nature [150]. In the case of chromatography the property used to assist

in the identification of a compound is retention. Different methods of chromatography such as different types of modes of separation or chromatographic columns can yield different amounts of information. Information theory gives the tools to assess these amounts and thus allows a mathematical evaluation of the methods of separation [151-153].

Firstly, retention data for each column is normalised according to equation (5.1) [120, 152, 154]. This yields scaled retention factors (X_a) that allow independent systems to be directly compared.

$$X_a = \frac{Rt_i - Rt_0}{Rt_f - Rt_0}$$ (5.1)

In equation 5.1, Rt_i is the retention time of any solute (i), Rt_f is the retention time of the last eluting solute and Rt_0 is the retention time of an unretained solute.

In information theory, "information" is defined as a measure of the uncertainty of the incidence of an event [152]. In this instance, the "information" or "informational entropy", I, is a measure of the reduction in the uncertainty about the nature of the substance and is a quantity that is measured in units of bits [120]. Information theory allows a mathematical evaluation of qualitative methods by the calculation of the expected or average amount of information obtained from an analysis [153].

The informational entropy of a measurement, I, is a probabilistic quantity described by equation (5.2)

$$I = \sum_k (-p_k \log_2 p_k) \qquad\qquad (5.2)$$

where p_k is the probability of the incidence of a single possible result, k, out of n possible results [120, 152]. For example, in the case of a liquid chromatographic separation a resulting chromatogram may exhibit n possible peaks that are assumed to be completely resolved and have the probabilities p_k where $k=1,2,...,n$. Therefore, p_k is the probability of the appearance of a chromatographic peak k at a particular retention time.

The "similarity " of data between different modes of separation between two dimensions in a multidimensional separation, or between different types of chromatographic columns can then be calculated using the informational entropy. In this study it was used to provide a qualitative numerical description of the retention behaviour of a number of new generation reversed phase liquid chromatographic columns.

In the case of comparing two different types of chromatographic columns, the informational entropy is first calculated from the normalised retention time data for the first chromatographic column, $I(k)$, and then the second chromatographic column, $I(k,l)$, where k and l represent the two columns being compared [120]. This is achieved by summing the informational entropy for each normalised retention time (X_a). For example, if you had a chromatographic separation that contained 20 components, ten with X_a factors of 0.2, four with X_a factors 0.6 and six with X_a factors 0.8, then the total informational entropy for that separation would be [120];

$$I = \left(-\frac{10}{20}\log_2 \frac{10}{20} \right) + \left(-\frac{4}{20}\log_2 \frac{4}{20} \right) + \left(-\frac{6}{20}\log_2 \frac{6}{20} \right) \tag{5.3}$$

If no correlation exists between the two chromatographic columns being compared, k and l, the informational entropy is described by equation (5.4) [120];

$$I(k,l) = \sum_{j=1}^{n} I(j) \tag{5.4}$$

However, in reality it is highly unlikely that there would be no correlation between the two chromatographic columns. When there exists some correlation the total informational entropy is described by equation (5.5) [120];

$$I(1,2,3,\ldots,n) < \sum_{j=1}^{n} I(j) \tag{5.5}$$

The information of a correlated state can be calculated by substituting equation (5.5) into equation (5.4) and results in equation (5.6);

$$I(1,2,3,\ldots,j) = \sum_{j=1}^{n} I(j) - I(1;2;3\ldots;j) \tag{5.6}$$

where $I(1;2;3;\ldots;j)$ is the mutual information which represents correlation [120]. To compare the informational entropy of the two chromatographic columns k and l, the fractional informational content, $h(k,l)$, is calculated by [120];

$$h(k,l) = 1 - \frac{I(k;l)}{I(k,l)} = 1 - \frac{mutual\,information}{total\,2D\,informational\,entropy} \qquad \textbf{(5.7)}$$

where $I(k;l)$ represents the mutual information between the chromatographic columns k and l, and $I(k,l)$ the total informational entropy. The informational similarity $H(k,l)$ of the two chromatographic columns can then be calculated by [120];

$$H(k,l) = [1 - h^2(k,l)]^{1/2} \qquad \textbf{(5.8)}$$

Informational similarity of the two chromatographic columns, $H(k,l)$, is a measure of the degree of solute crowding of the sample components being separated on a normalised 2-D retention plot, with a value of unity indicating high solute crowding, while a value of zero no solute crowding and utilising all of the separation space [120, 155]. A normalised 2-D retention plot is where the normalised retention factors, calculated using equation (5.1), of the sample components separated on column 1 are plotted against the normalised retention factors of the sample components separated on column 2.

The percentage-synentropy is another important IT parameter for determining the orthogonality (the divergent retention behaviour) between any two liquid chromatographic columns. The %synentropy is the 2-D informational entropy that is contributed equally from both columns and is a system attribute used to determine the retention mechanism equivalency between two different columns [120, 155]. This allows a comparison of the retention mechanisms of the stationary phases chosen in this study for the separation of the polycarboxylic acids and polyphenol compounds.

Percentage synentropy is calculated by dividing the informational entropy from data diagonally aligned on the normalised retention plots by the total 2-D informational entropy [120]. An X_a factor variance of $\pm$ 0.05 from the main diagonal of a normalised 2-D retention plot was assumed when using the informational entropy for the calculation of %synentropy. In this study the %synentropy was used as a comparative measurement of the retention mechanism equivalency. A 0 %synentropy value indicates that there is no retention mechanism equivalency between the two chromatographic systems, whereas a value of 100 %synentropy indicates complete retention mechanism equivalency between the two chromatographic systems.

Information theory is further demonstrated later in this chapter where it is used to assist in evaluating the retention behaviour of five new generation reversed phase liquid chromatographic columns for the separation of polycarboxylic acids and polyphenol compounds. Informational similarity and %synentropy values for all of the experiments investigated here are reported in Table 5.2.

5.2.2. Factor analysis

Factor analysis is a mathematical tool that is used to examine a wide range of data sets, taking large amounts of data and resolving them into distinct patterns of occurrence that can be used to indicate any type of correlation or relationship between variables [156-157]. A geometric approach to factor analysis as described by Gray et al. and Liu et al. [155, 158], can be applied to the chromatographic data. Using this geometric approach

to factor analysis correlations between different factors and their variables can be determined and then displayed in a geometric manner. In this case, factor analysis provided a different approach to evaluating the extent to which the retention behaviour of the five new generation liquid chromatographic columns differed.

In this study, pairs of chromatographic columns were compared resulting in two sets of retention data. Each set of retention data can be considered as an independent vector that represents the interaction between the solutes, mobile phase and stationary phase [155]. For example, if we compare two different columns, column A and column B, two sets of retention data are generated for each column. This can be represented in a matrix form K;

$$K = \begin{vmatrix} k_{11} & k_{12} & ... & k_{1n} \\ k_{21} & k_{22} & ... & k_{2n} \end{vmatrix} \tag{5.9}$$

where k_{12} is the normalised retention data of the second component separated on the first column, A. A geometric approach to factor analysis enables the calculation of correlations between a pair of vectors. In order to find the angles between the vectors the cross product of the normalised matrix represented in equation (5.9) needs to be formed where the entries in the matrix must be scaled so that their mean is zero and their variance one [157-158]. This results in a correlation matrix that has as its elements the cosines of the angles between vectors. The scaled matrix can be calculated using equation (5.10);

$$k'_{nn} = \frac{k_{ij} - m_i}{s_i} \qquad (5.10)$$

where m_i is the mean of the original entries of the ith vector, s_i is the standard deviation of the original entries in the ith vector and k is the value of each retention time of the components. The new scaled matrix is represented by K' and the transposed matrix by K'^T. The sample by sample correlation matrix is then calculated by equation (5.11) [158];

$$C = \left(\frac{1}{N-1}\right) K'^T K' \qquad (5.11)$$

where N is the number of entries found in each data vector. A square diagonal matrix where $C_{12} = C_{21}$ is produced with the matrix acting as a quantitative measure of the vector correlations as seen in equation (5.12) [158].

$$C = \begin{vmatrix} 1 & C_{12} \\ C_{21} & 1 \end{vmatrix} \qquad (5.12)$$

Equation (5.12) is important as it enables us to define the degree of retention correlation between any two columns. For example when comparing the first column, 1, and second column, 2, perfect correlation would exist when $C_{12} = 1$ and a truly orthogonal separation would be obtained when $C_{12} = 0$ as C_{12} is the cosine of any two unit length vectors [158]. The retention correlations, C, for each of the cases investigated here are

reported in Table 5.2 and are a measure of the orthogonality of the two chromatographic columns.

The peak spreading angle matrix between each of the two retention vectors can be calculated using equation (5.13).

$$\beta_{nk} = \cos^{-1} C_{nk} \tag{5.13}$$

The peak spreading angle β is a relative measure of the theoretical retention space used [155, 158]. As the spreading angle β approaches 0 the more correlated the two liquid chromatographic columns are and the stronger the relationship between retention mechanisms of the two columns. A spreading angle of 90 indicates a total orthogonal separation.

The peak spreading matrix for the comparison of two chromatographic columns is represented in equation (5.14);

$$\beta = \begin{vmatrix} 0 & \beta_{12} \\ \beta_{21} & 0 \end{vmatrix} \tag{5.14}$$

where $\beta_{12} = \beta_{21}$ is the correlation or spreading angle between the retention axis in the orthogonal retention space [158]. The correlation matrix generated using equations (5.9) – (5.12) provides a measure of the interaction between the stationary phase and a chosen parameter for a group of solutes and this information is useful in aiding the

selection of a column or in the optimisation of a particular separation [158]. Values for the peak spreading angle (β) calculated for each of the cases investigated here are reported in Table 5.2 and will be discussed later in this chapter.

An estimation of the theoretical peak capacity for the separation between the two chromatographic columns that are truly orthogonal can be calculated using equation (5.16);

$$N_t = N_1 \times N_2 \qquad \text{(5.16)}$$

where N_t is the theoretical peak capacity and N_1 and N_2 the peak capacities obtained on the first column and the second column. However, a certain degree of correlation will always exist and the actual peak capacity of the system is found to be less than N_t. Values for theoretical peak capacity, N_t, for all the cases studied here are reported in Table 5.2.

Figure 5.1 shows a geometric plot, which is a visual representation of the practical or effective peak capacity between the two liquid chromatographic columns under comparison. The area that is defined by the grid represents the separation space. The angles α, β and γ depicted in Figure 5.1 can be calculated using equations (5.16) – (5.18) [158].

$$\alpha = \alpha'(1 - 2\beta / \pi) \qquad \text{(5.16)}$$

$$\alpha' = \tan^{-1}(N_2 / N_1) \qquad \text{(5.17)}$$

$$\gamma = \pi / 2 - \alpha - \beta \tag{5.18}$$

The effective area or the practical peak capacity, N_p, is calculated using equation (5.19) [158];

$$N_p = N_t - (A - C) \tag{5.19}$$

where A and C represent the unavailable area depicted in Figure 5.1 resulting from correlation and they are calculated using equations (5.20) and (5.21) [158].

$$A = \frac{1}{2} N_2^2 \tan(\gamma) \tag{5.20}$$

$$C = \frac{1}{2} N_1^2 \tan(\alpha) \tag{5.21}$$

Values for the practical peak capacity, Np, investigated here are reported in Table 5.2. This geometric approach to factor analysis is further demonstrated below and assisted in evaluating the retention behaviour of five new generation reversed phase liquid chromatographic columns for the separation of polycarboxylic acids and polyphenol compounds.
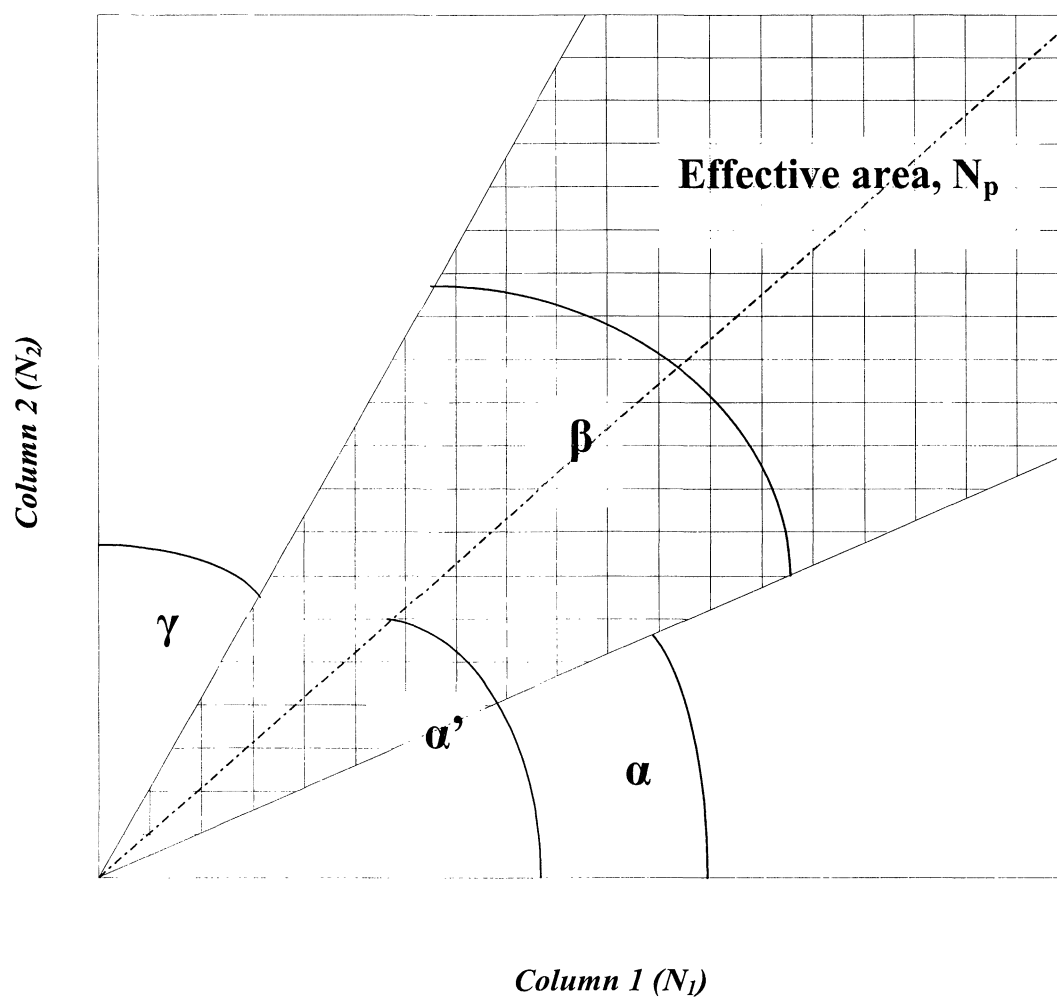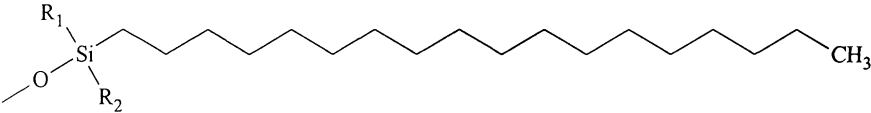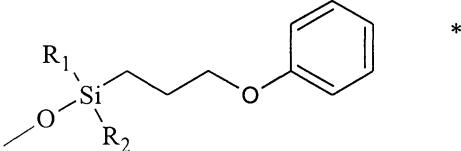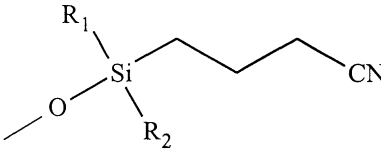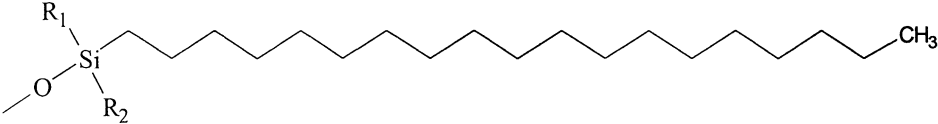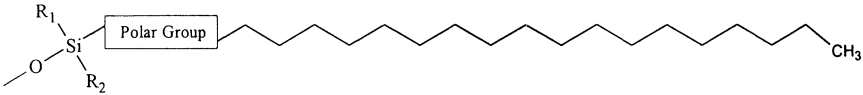
Figure 5.1: Geometric plot visually representing the practical or effective peak capacity between the two chromatographic columns under comparison.

5.2.3. Reversed phase column comparison using information theory and factor analysis

This study compared the Phenomenex Luna Cyano, Waters XTerra™ RP$_{18}$, Phenomenex Aqua C18 and Phenomenex Synergi polar-RP columns with the Phenomenex Luna C18 column used as the reference. The ultimate aim of the study was to find an alternative reversed phase column to be used in the development of a multidimensional HPLC method for the separation of Bayer humic substances. Table 5.1 summarises the bonded stationary phase supports used in this study.

The Phenomenex Luna C18 was picked as the reference for this study due to the popularity of the C18 stationary phase. The reference Phenomenex Luna C18 column offers high quality silica that improves the structural stability of the silica particles and the stability of the column bed and contains dense bonded phase coverage and enhanced endcapping to improve peak shape as well as an extended pH working range of 1.5 to 10. The Phenomenex Luna Cyano was picked for this study because of the probable difference in retention mechanism compared to a C18 column. The Luna Cyano column is made using the same silica base as the Luna C18, but with a pH working range of 1.5 to 7.0. The Phenomenex Aqua C18 column is packed using a bonded phase akin to the C18, but incorporates polar endcapping. It was chosen for the possible differences that this polar endcapping group could have on the retention mechanism of the polycarboxylic acids and polyphenol compounds.

Table 5.1: List of bonded stationary phase supports used in this study.

Column	Structure
Phenomenex Luna C18	
Phenomenex Synergi polar-RP	*
Phenomenex Luna Cyano	
Phenomenex Aqua C18	
Waters XTerra™ RP₁₈	

* With polar encapping

The Synergi polar-RP column was also manufactured by Phenomenex, and is essentially an ether-linked phenyl base with polar endcapping. The Synergi polar-RP phase was chosen for this study as it was specifically developed for separating extremely polar, aromatic analytes or mixtures, and is reported to improve the peak shape of both acids and bases and is stable in 100% aqueous conditions. Unfortunately, both the Aqua C18 and Synergi polar-RP phases are not available on Luna silica.

The Waters XTerra™ RP$_{18}$ column was the only non-Phenomenex column employed in this study and was chosen due to its unique new generation stationary phase that provides a number of advantages. This new generation stationary phase material is a silicon organic/inorganic hybrid, made by reacting methyl triethoxy silane with tetraethoxy silane to form methyl polyethoxy silane. The methyl groups are incorporated into the silica backbone, improving the pH stability of the structure over that of conventional silica used in reversed phase columns. The silicon-oxygen backbone provides the packing with the mechanical strength normally associated with silica supports [139]. The XTerra™ RP$_{18}$ stationary phase contains a monofunctional silane with an embedded carbamate group [139].

To compare the resolving power of a conventional C18 column with the other four columns and to determine the retention mechanism equivalency between these columns, the set of twenty-four standards containing a mix of polycarboxylic acids and polyphenols described in Chapter 2 were used. These are listed again in Figure 5.2 for convenience. For each column a method was developed to separate the twenty-four standards using a mobile phase mixture consisting of methanol and formic acid (0.1%).

The mobile phase compositions for each of the columns were methanol:formic acid (0.1%) [20:80; v/v] for the Luna C18 column; methanol:formic acid (0.1%) [10:90; v/v] for the Luna Cyano column; methanol:formic acid (0.1%) [10:90; v/v] for the XTerra™ RP$_{18}$ column; methanol:formic acid (0.1%) [20:80; v/v] for the Aqua C18 column; and methanol:formic acid (0.1%) [20:80; v/v] for the Synergi polar-RP column. These mobile phase compositions were chosen such that the minimum retention factor of the least resolved solute was 0.15 and the maximum retention factor of the most strongly retained compound was 20. While we acknowledge a retention factor of 20 is excessive, such conditions were required in order to gain some degree of resolution between the less retained species. Gaining resolution for the early eluting compounds consequently increased the retention factor of the later eluting species.

Using the Phenomenex Luna C18 column as the reference for comparing each of the four chromatographic columns, information theory (IT) and factor analysis were then used to determine whether there was any orthogonality or correlation between the four different columns in comparison to the conventional C18 column. Table 5.2 lists the system attributes used to determine the measure of orthogonality or correlation for each of the columns studied compared with the Luna C18 column. This information was then used to determine if there was any differences in retention mechanism and hence possible changes in selectivity, band shape and performance between these columns. To compensate for differences between the columns, such as manufacturer, base silica and particle size, the retention data was normalised according to Equation 5.1, allowing independent systems to be directly compared. In all cases, the retention time of the solvent front was used as the retention time of an unretained solute.
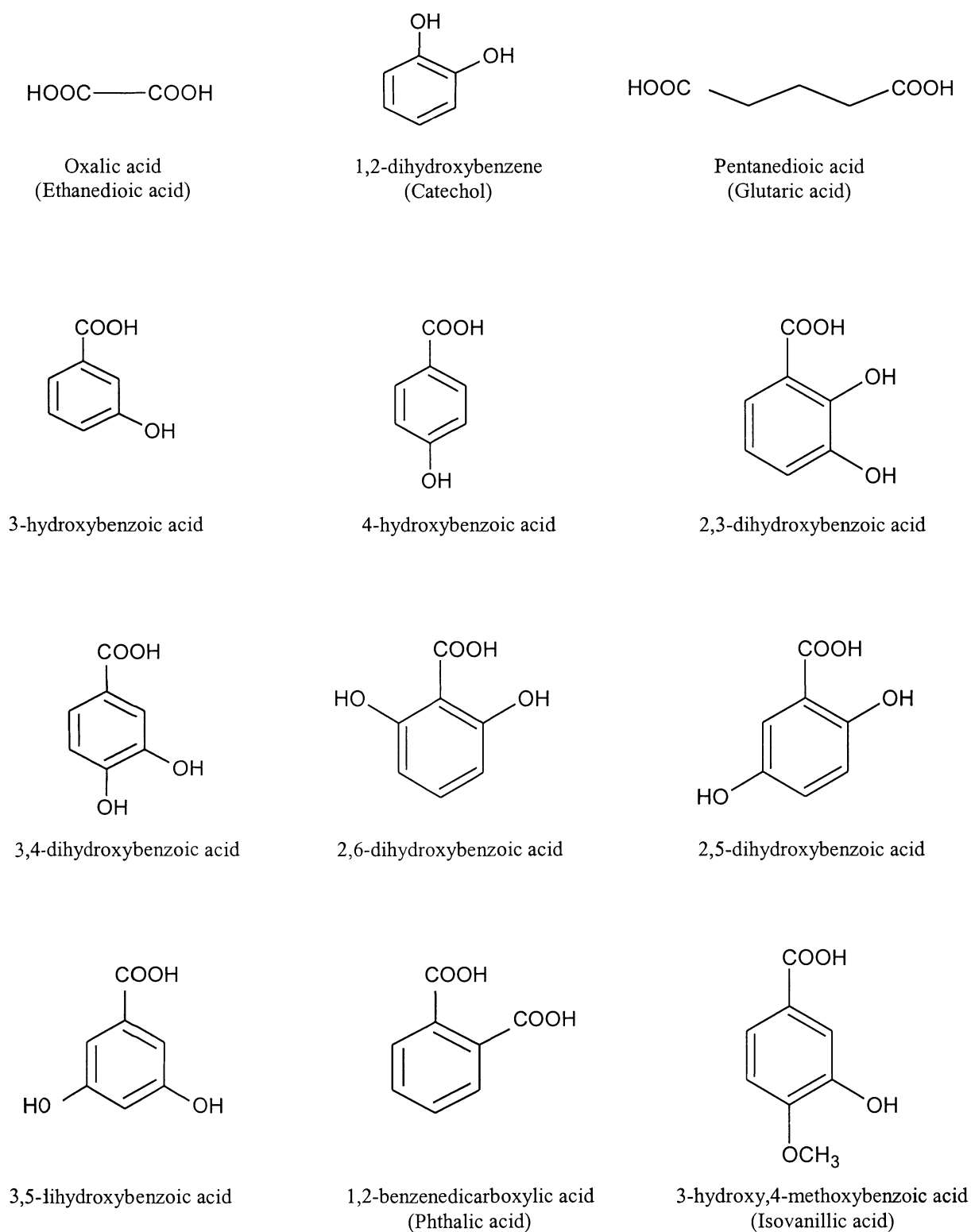
Figure 5.2: Structures of the polycarboxylic acids and polyphenol compounds used in this study *(repeat of Figure 2.2)*.

2,4,6-trihydroxybenzoic acid

3,4,5-trihydroxybenzoic acid
(Gallic acid)

2,3,4-trihydroxybenzoic acid

Octanedioic acid
(Suberic acid)

3,4-dimethoxybenzoic acid
(Veratric acid)

Sorbitol

4-Hydroxyisophthalic acid

5-hydroxyisophthalic acid

3,5-dimethoxy,4-hydroxybenzoic acid

1,2,4-benzenetricarboxylic acid
(Trimellitic acid)

1,2,3-benzenetricarboxylic acid

1,2,4,5-benzenetetracarboxylic acid
(Pyromellitic acid)
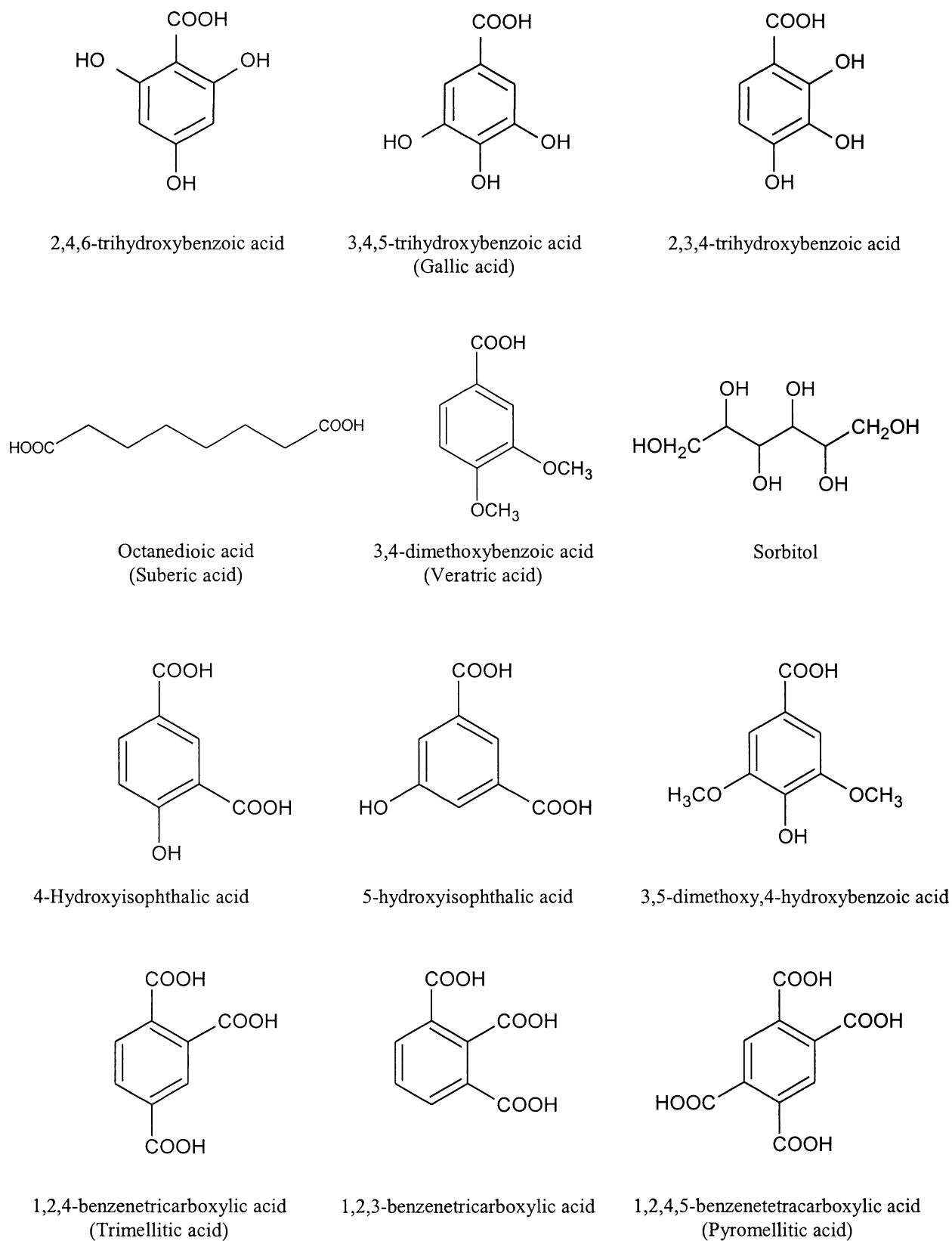
Figure 5.2 (continued): Structures of the polycarboxylic acids and polyphenol compounds used in this study *(repeat of Figure 2.2).*

Table 5.2: System attributes used to determine the measure of orthogonality for the four chromatographic columns compared with the Luna C18 column.

Attributes	Luna C18/Luna Cyano	Luna C18/ XTerra™ RP$_{18}$	Luna C18/Aqua C18	Luna C18/Synergi polar-RP
Informational similarity	0.98	1.00	0.99	0.99
Percentage synentropy *	12.5	34.0	72.1	50.0
Peak spreading angle (β) degrees	55.9	37.0	31.1	45.0
Theoretical peak capacity (N$_t$)	361	380	380	380
Practical peak capacity (N$_p$)	250	191	166	225
Correlation (c)	0.56	0.80	0.86	0.70
% usage	69.3	50.2	43.5	59.0

* A X_a factor variance of $\pm$ 0.05 of the normalised retention factor (X_a) was assumed when using the informational entropy for the calculation of % synentropy

Figure 5.3 shows a plot of the transformed retention data for the comparison of the Luna C18 column with the Luna Cyano column. Each of the plotted points represents the normalised elution time of each of the standards. Using informational theory (IT) to assist in the interpretation of the retention data obtained we can make a comparison of the resolving power of each of the columns in relation to the Luna C18 column. Several authors have applied the principles of IT to chromatography for component identification, optimisation and stationary phase comparisons [120, 154-155, 158]

In calculating the informational similarity, the standard compounds were considered to be separated when there X_a values (calculated using Equation (5.1)) differed by more than 0.01 X_a [120, 155]. Table 5.2 reports the informational similarity (calculated using Equation (5.8)) between the Luna C18 column and the Luna Cyano column as 0.98 indicating a high degree of solute crowding. This can also be seen on examination of the normalised plot in Figure 5.3.

The %synentropy is the 2-D informational entropy (a probabilistic quantity) that is contributed equally from both columns and was described earlier in this Chapter [120, 155]. In this study the %synentropy was used as a comparative measurement of the retention mechanism equivalency. Percentage synentropy was calculated by dividing the informational entropy from data diagonally aligned on the normalised retention plots by the total 2-D informational entropy [120]. When comparing the Luna C18 and Luna Cyano columns the %synentropy was found to be 12.5% indicating that there was only a limited degree of retention mechanism equivalency between the two columns.
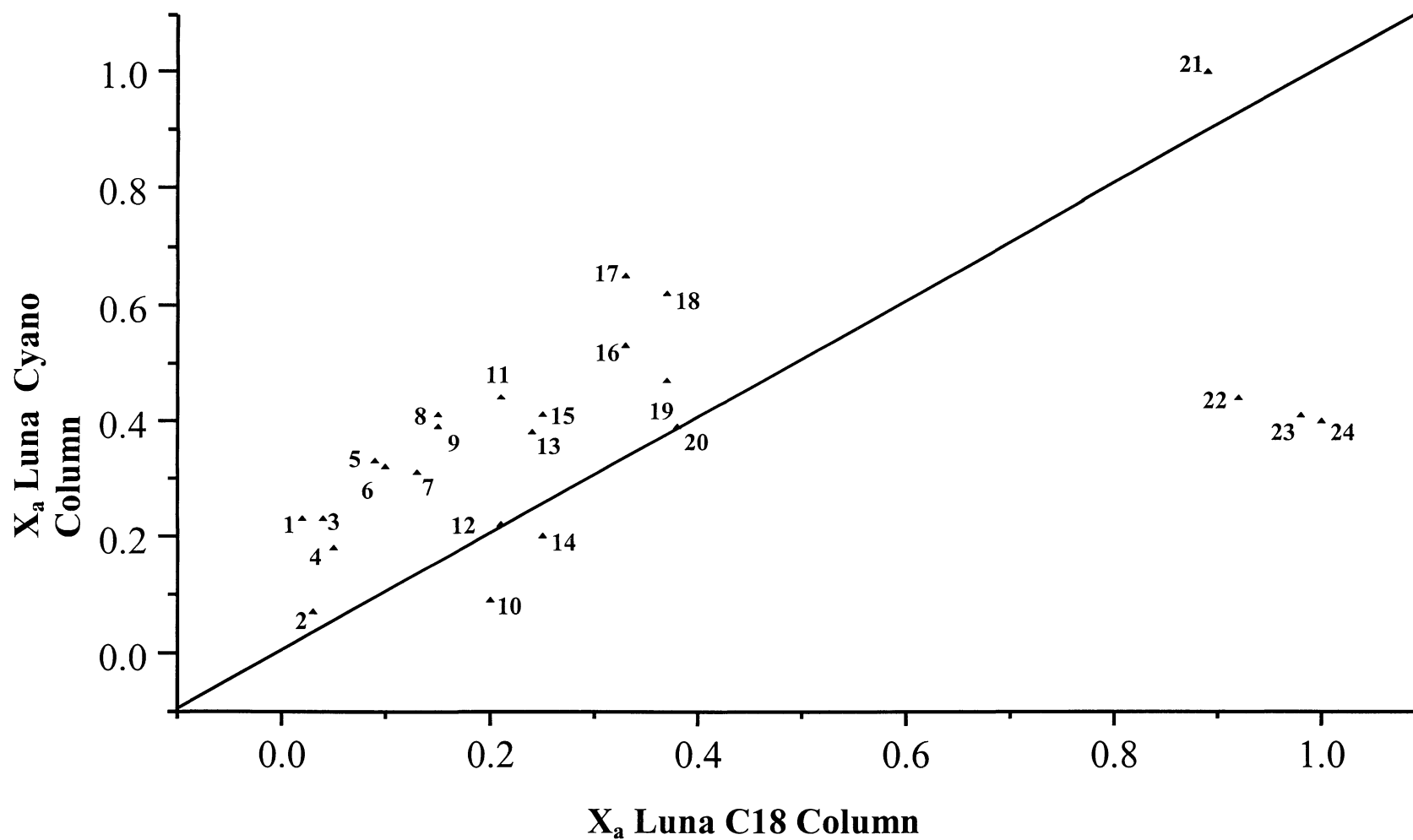
Figure 5.3: Normalised plot of the Luna C18 column versus the Luna Cyano column, number according to order of elution on the Luna C18.

Factor analysis can also be used to aid in the comparison of the retention behaviour on different stationary phases, indicating the similarity of the chromatographic information provided. This technique has been used to determine correlations between different factors and their variables, displaying this in a geometric fashion. Using correlation matrices the practical peak capacity of the separation space defined by employing both columns in the separation process was calculated and then plotted. While this expression of peak capacity is for the most part a meaningless term in one-dimensional chromatography, it does find use in that each of the columns are compared to the same reference column. Hence expansion (or compression) of the number of expected separated compounds can be used to gauge the change in separation equivalency.

A geometric plot of the practical peak capacity of the Luna C18 column versus the practical peak capacity of the Luna Cyano column is illustrated in Figure 5.4. The spreading angle (β) indicated in Figure 5.4 and reported in Table 5.2, is a measure of the separation space utilisation. Complete utilisation of the theoretical separation space is represented by a spreading angle (β) of 90 . As the spreading angle decreases the correlation between the two columns increases. In the comparison between the Luna C18 and Luna Cyano columns the spreading angle was moderately high at 55.9 (see Table 5.2). The peak capacity for each column was calculated from the normalised retention data with a value of one peak capacity unit being assigned to each normalised peak that was separated by a X_a factor of 0.01 [155]. The theoretical peak capacity was then determined by multiplying the peak capacities of both of the columns being compared (equation 5.16). In the comparison between the Luna C18 and Luna Cyano
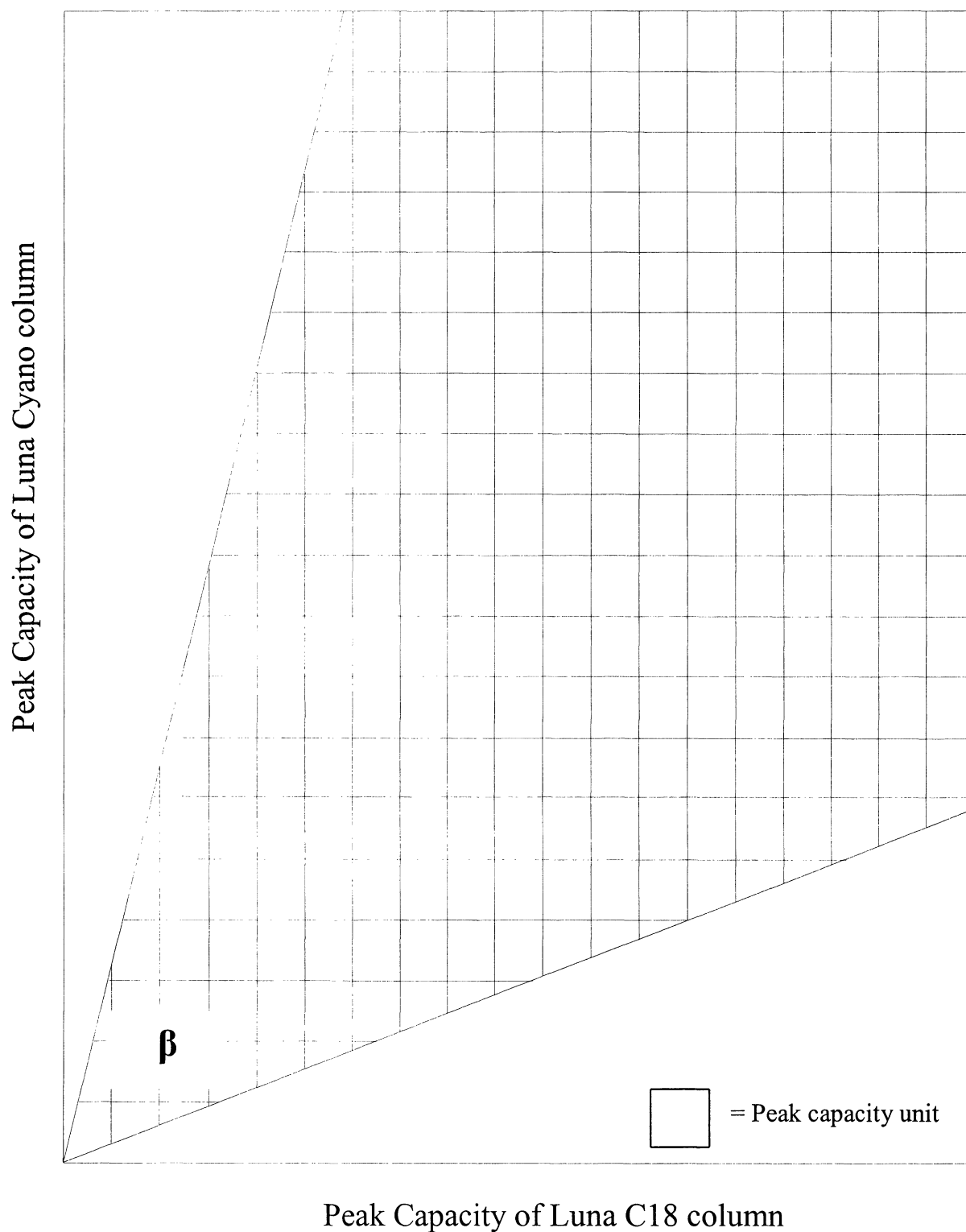
Figure 5.4: Geometric plot showing the practical peak capacity for the Luna C18 column versus the Luna Cyano column.

columns, the practical peak capacity was 250 and the theoretical was found to be 361. The retention correlation coefficient was determined to be 0.56, which represented 69.3% usage of the separation space. A value of 1.00 represents complete correlation; conversely a correlation of 0.00 indicates perfect orthogonality.

The Luna C18 column and the XTerra™ RP$_{18}$ column performance are compared in Figure 5.5. The normalised retention plot of this couple was similar to that of the Luna C18/ Luna Cyano couple with both displaying a small degree of scatter. However on closer inspection of the data scatter it could be seen that there were significant changes in selectivity for compounds on an individual basis. The informational similarity between the Luna C18 and the XTerra™ RP$_{18}$ was 1.00, which was the highest degree of solute crowding of any of the column comparisons. There was some selectivity equivalency between the Luna C18 and the XTerra™ RP$_{18}$ as indicated by a %synentropy value of 34%. The peak-spreading angle, calculated using geometric factor analysis, had decreased to 37.0 and can be seen represented on the geometric plot of the practical peak capacities of both of these columns shown in Figure 5.6. Comparison of the Luna C18 and XTerra™ RP$_{18}$ columns showed that the practical peak capacity was 191 and the theoretical peak capacity was 380. This represented a 50.2% usage of the separation space, equating to a correlation coefficient of 0.80.
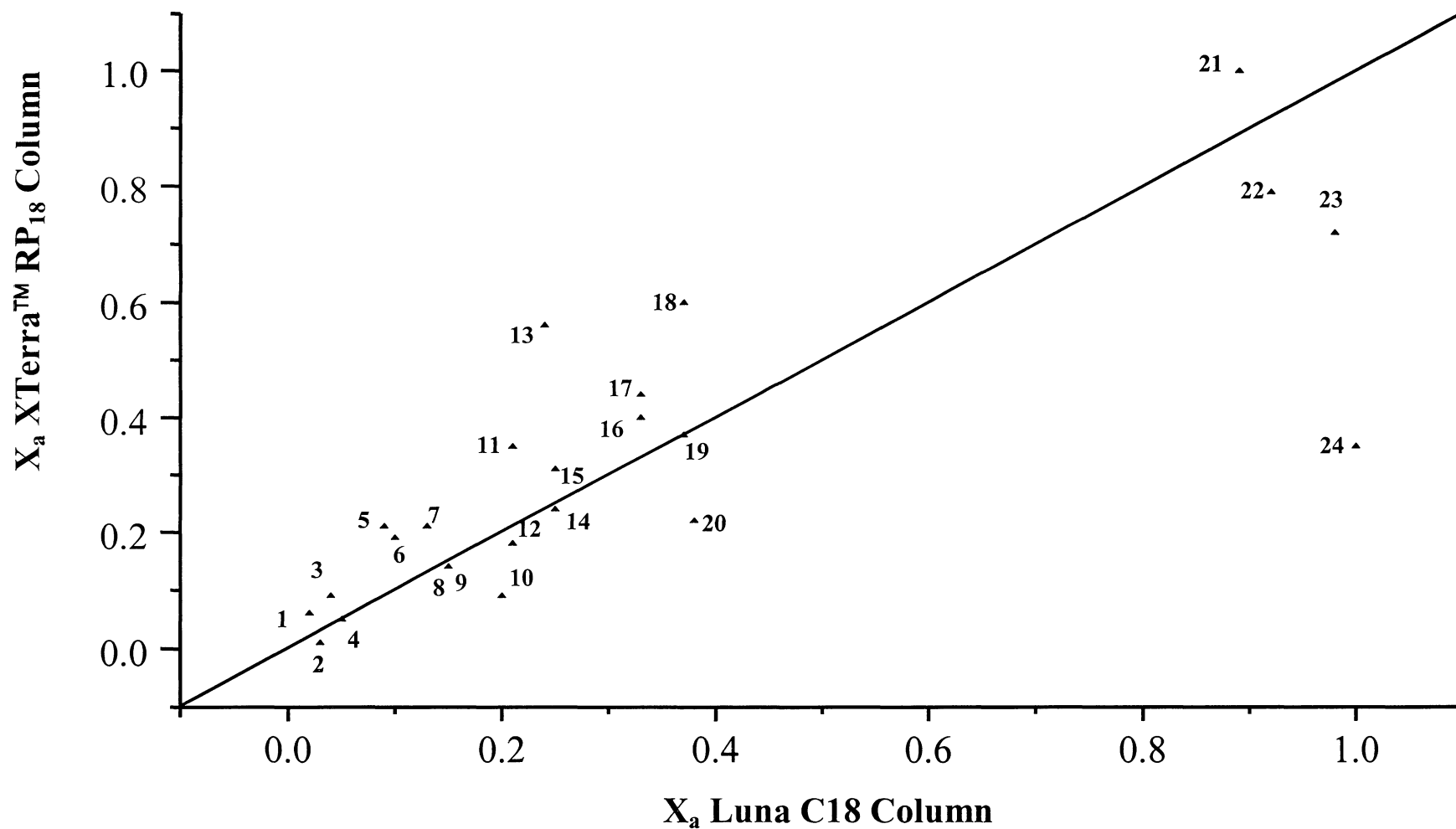
Figure 5.5: Normalised plot of the Luna C18 column versus Waters XTerra™ RP$_{18}$ column, numbered according to elution order on the Luna C18.

Peak Capacity of Luna C18 column
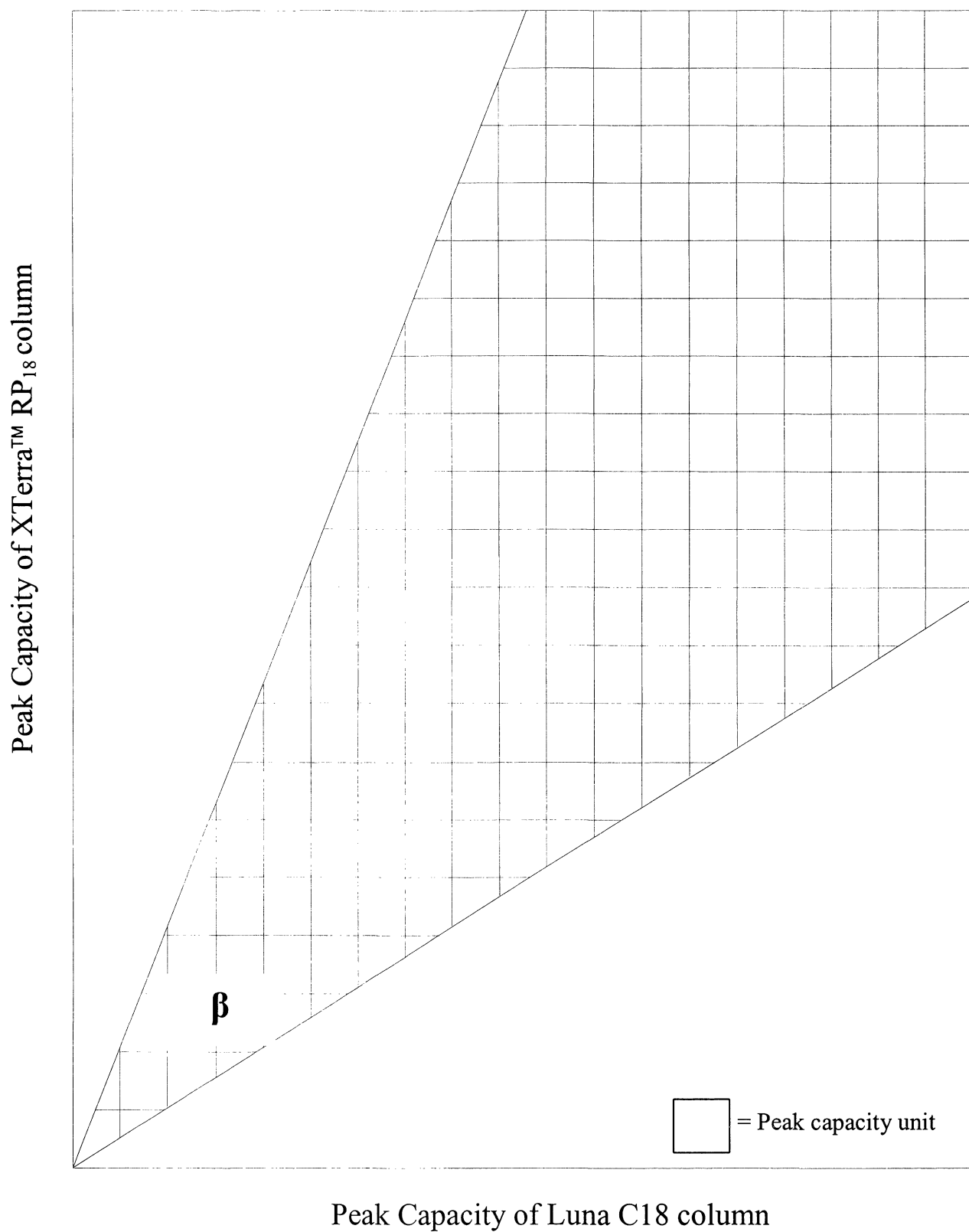
Figure 5.6: Geometric plot showing the practical peak capacity for the Luna C18 column versus the Waters XTerra™ RP$_{18}$ column.

Figure 5.7 shows the normalised retention plot of the Luna C18 column versus the Aqua C18 column. On inspection of the retention plot it can be seen that the data was more ordered along the diagonal compared to the previous two column couples discussed, with a higher degree of data overlap and clustering with an informational similarity of 0.99. The %synentropy was 72.1% (see Table 5.2) displaying the highest degree of retention mechanism equivalency for this study. The geometric plot shown in Figure 5.8 indicates the peak spreading angle to be 31.1 , with the practical peak capacity and the theoretical peak capacity calculated to be 166 and 380, respectively. This is representative of 43.5% usage of the separation space. The correlation factor of 0.86 was approaching the value of unity and indicates a high degree of correlation between these two columns and was in fact the highest reported in this study. Essentially the Luna C18 and Aqua C18 columns provided highly similar chromatographic information.

The Luna C18 column and the Synergi polar RP column were compared and the normalised retention plot for these two columns is shown in Figure 5.9. The retention plot once again showed a moderate degree of alignment along the diagonal with a %synentropy of 50.0%, which was slightly less than the %synentropy for the Luna C18/ Aqua C18 couple (72.1%). This indicated a high degree of overlap and clustering between these columns that was reflected in the informational similarity value of 0.99. Geometric factor analysis was used to calculate the peak spreading angle (45.0) that is indicated on the geometric plot of the practical peak capacities of both of these columns shown in Figure 5.10. Comparison of the Luna C18 and XTerra™ RP$_{18}$ columns
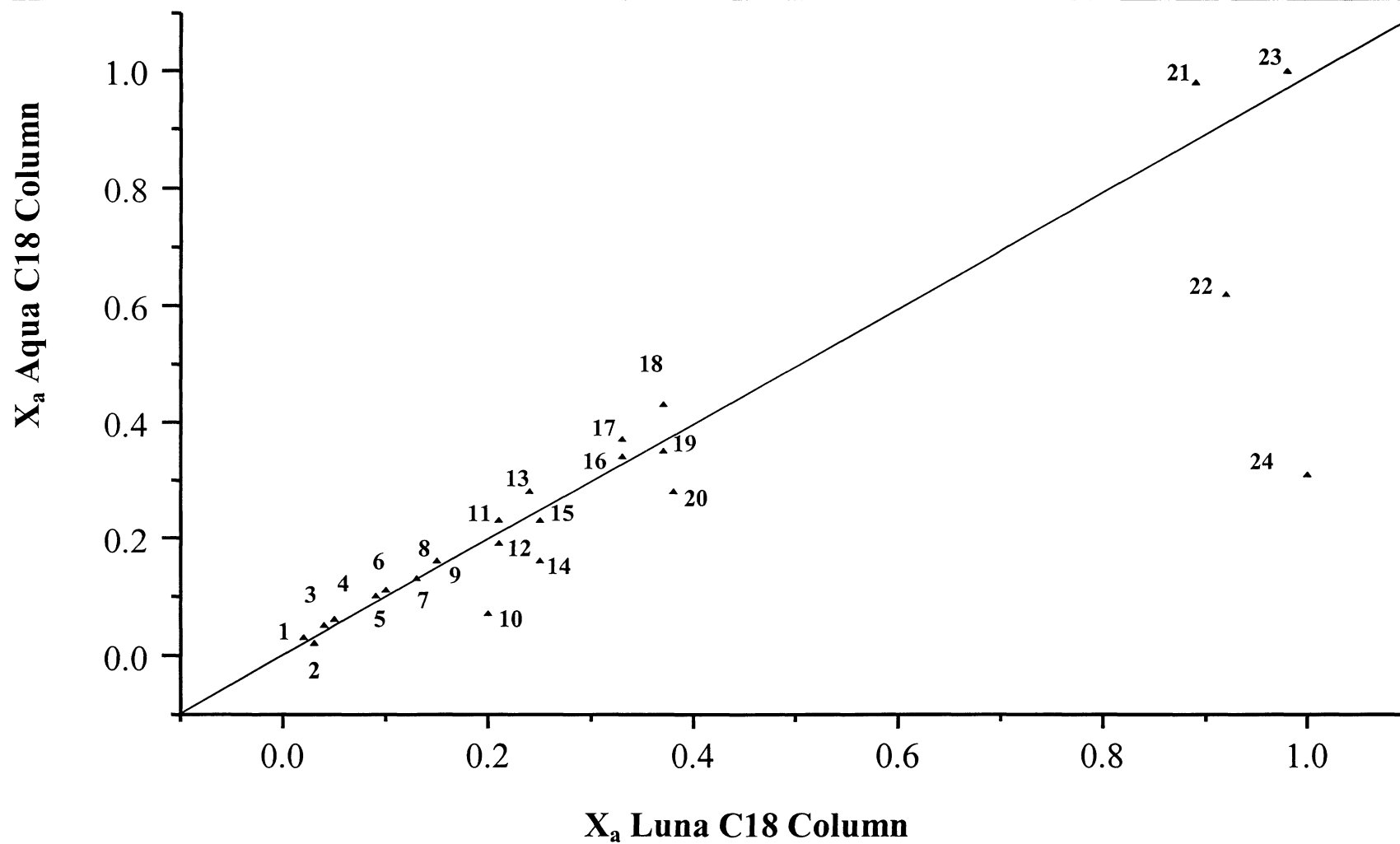
Figure 5.7: Normalised plot of the Luna C18 column versus Aqua C18 column, numbered according to elution order of the Luna C18.

Peak Capacity of Luna C18 column
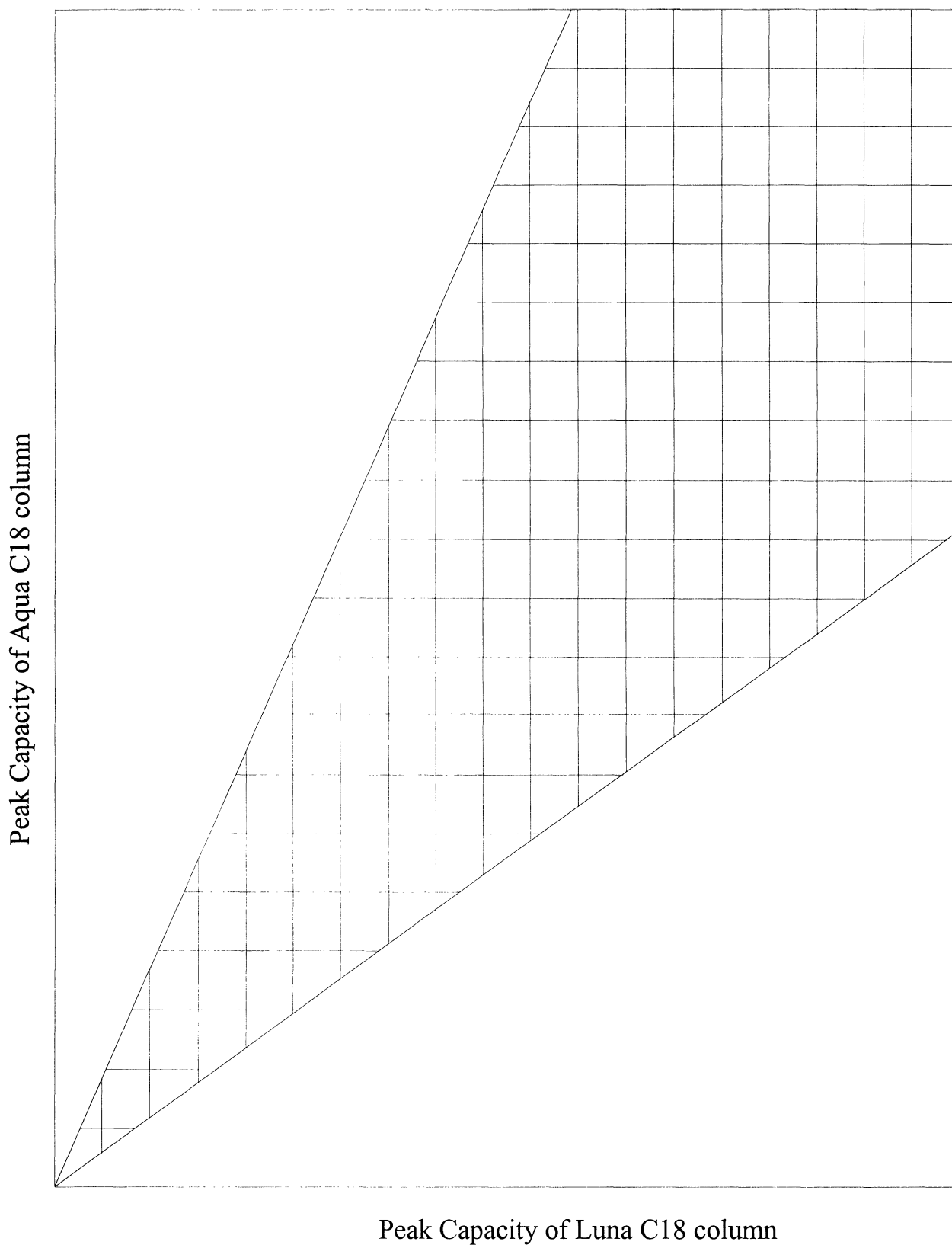
Figure 5.8: Geometric plot showing the practical peak capacity for the Luna C18 column versus the Aqua C18 column.
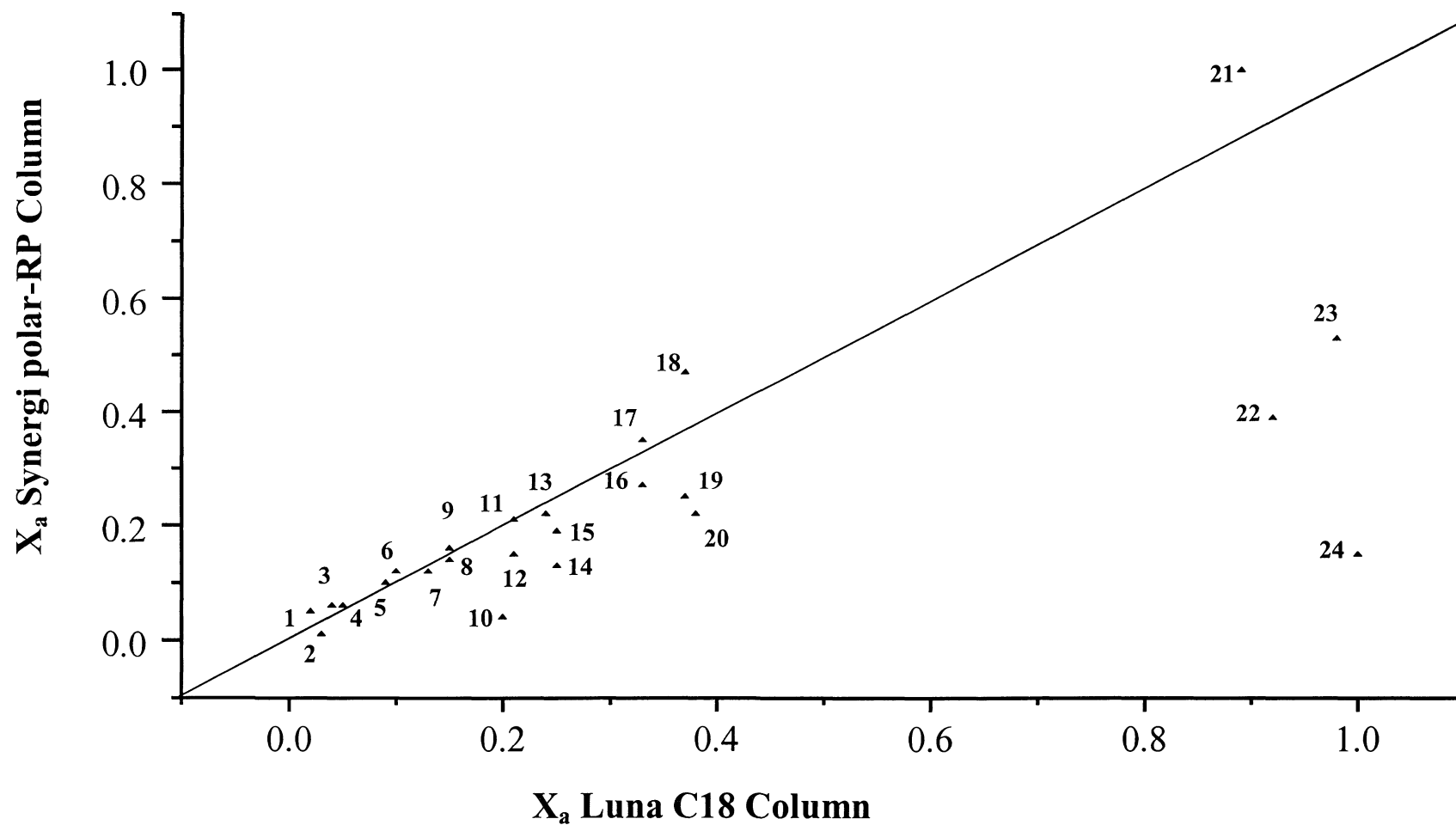
Figure 5.9: Normalised plot of the Luna C18 column versus Synergi polar-RP column, numbered according to the elution order of the Luna C18.
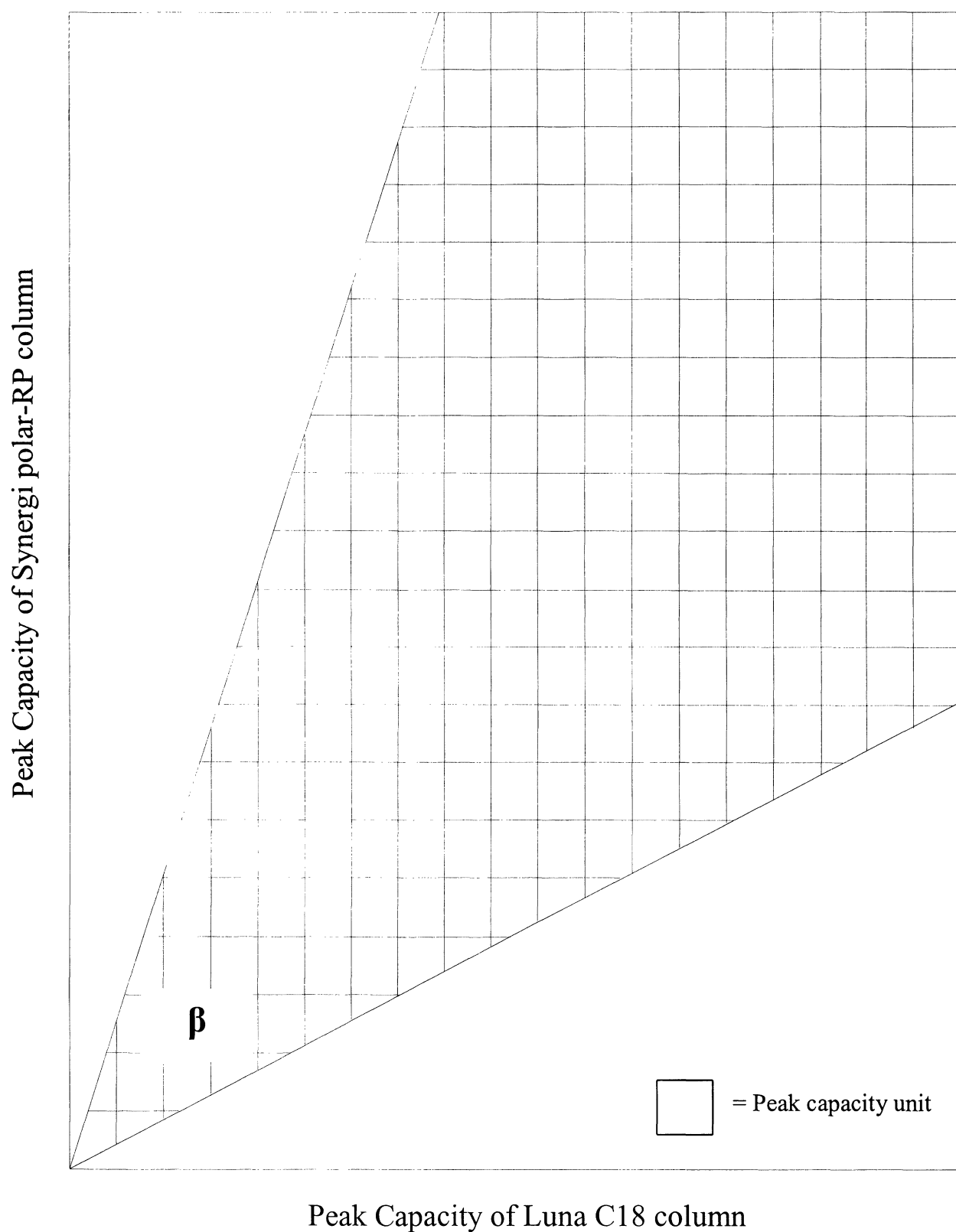
Figure 5.10: Geometric plot showing the practical peak capacity for the Luna C18 column versus the Synergi polar-RP column.

showed that the practical peak capacity was 225 and the theoretical peak capacity was found to be 380. The retention correlation coefficient was 0.70, indicating moderately high system correlation and a 59.0% usage of the separation space.

5.3. COMPARISON OF BAND SHAPE

Evaluating the statistical distribution of the compounds in a hypothetical separation space only goes part way to assessing the performance of these columns with respect to that of the Luna C18 reference. In IT and factor analysis very little attention is paid to the true band shape of the eluting solutes. Peak tailing effects could, for example, transform an apparently useful separation system as measured by IT and factor analysis, into one that is essentially impractical in reality. Hence the study would be incomplete without paying due regard to the physical nature of the band shape.

On examination of the chromatograms for each of the standards separated on all five of the columns studied, obvious differences in peak shape were observed. For example, Figure 5.11 and Figure 5.12 show the separation of phthalic acid and 1,2,4-benzenetricarboxylic acid, respectively, on the five chromatographic columns studied here. Figure 5.11 and 5.12 show that there exists significant differences in the peak shape for both phthalic acid and 1,2,4-benzenetricarboxylic acid. The physical nature of the band shape of each of the standards differed in terms of both the peak width at
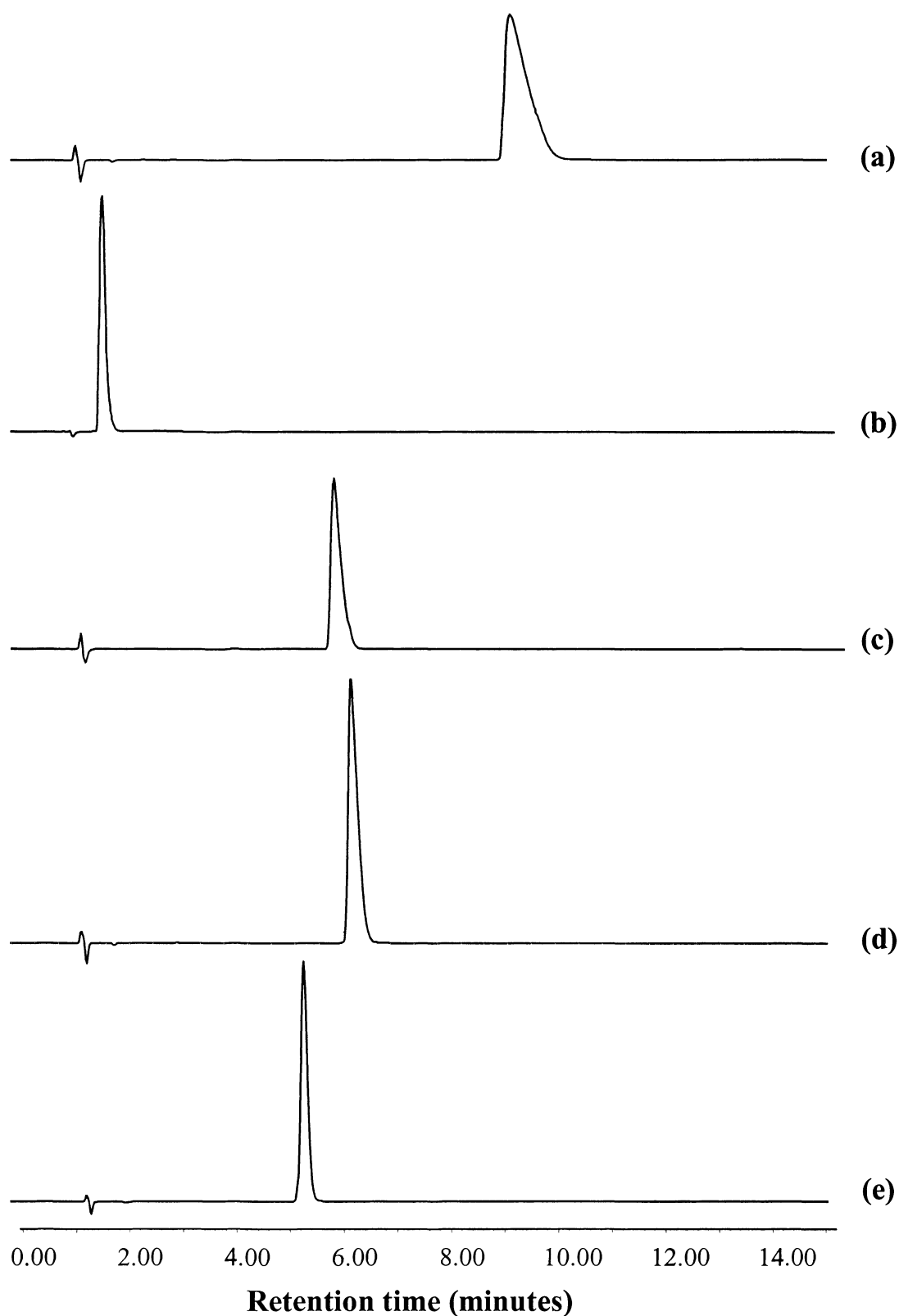
Figure 5.11: HPLC chromatograms for the separation of phthalic acid on (a) Luna C18, (b) Luna cyano, (c) Xterra™ RP$_{18}$, (d) Aqua C18 and (e) Synergi polar-RP.
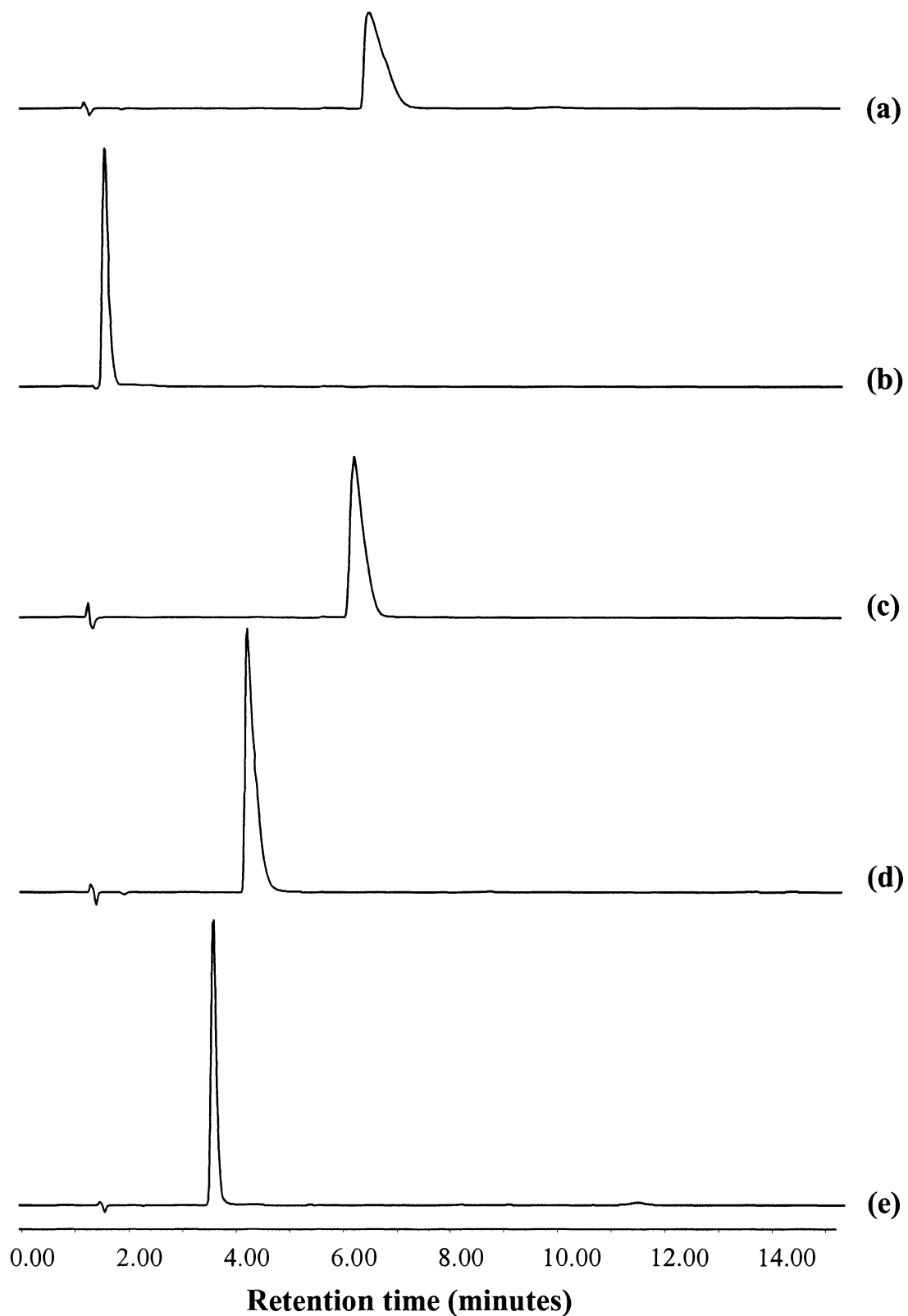
Figure 5.12: HPLC chromatograms for the separation of 1,2,4-benzenetricarboxylic acid on (a) Luna C18, (b) Luna cyano, (c) Xterra™ RP$_{18}$, (d) Aqua C18 and (e) Synergi polar-RP.

half height and peak tailing. Peak width at half height was calculated using Waters Millennium[32] system suitability software [159]. Refer to Appendix A for details on calculation. The asymmetry of the peaks was determined using the United States pharmacopoeia (USP) tailing factor and was calculated using Waters Millennium[32] system suitability software [159]. Refer to Appendix B for details on calculation.

Table 5.3 and 5.4 report the peak width at half height and the USP tailing factors respectively for the five columns studied. When studying the peak shape of the standards on the five different columns, overall the Synergi polar-RP column gave the best results for peak width at half height and USP tailing factors, followed by the Aqua C18 column. The Luna C18 compared to the other four columns gave the worst results for peak shape with higher USP tailing factors and peak width at half height values. For example, the averaged USP tailing factor for all test compounds on the Synergi polar-RP column was 1.47 compared to 2.20 on the Luna C18. This was further highlighted by comparing the peak width at half height and USP tailing factors obtained on the Luna C18 and Synergi polar-RP columns for a number of the standards. Table 5.3 shows that the peak width at half height for 2,5-dihydroxybenzoic acid, 1,2,4-benzenetricarboxylic acid and 1,2,4,5-benzenetetracarboxylic acid dianhydride were six, three and five times, respectively, larger on the Luna C18 than they were on the Synergi polar-RP column. The USP tailing factors in Table 5.4 showed an increase of more than two times for 2,5-dihydroxybenzoic acid, 1,2,4-benzenetricarboxylic acid and 1,2,4,5-benzenetetracarboxylic acid dianhydride between the Luna C18 and Synergi

Table 5.3: Summary of the peak width at half height values for each of the chromatographic columns studied.

Compound name	Peak width at half height				
	Luna C18	Luna Cyano	XTerra™ RP$_{18}$	Aqua C18	Synergi polar-RP
Oxalic acid	0.162	0.117	0.071	0.092	0.053
Catechol	0.101	0.154	0.116	0.097	0.096
Glutaric acid	0.073	0.107	0.076	0.068	0.069
3-hydroxybenzoic Acid	0.199	0.175	0.260	0.165	0.147
4-hydroxybenzoic Acid	0.165	0.164	0.259	0.143	0.138
2,3 – dihydroxy benzoic acid	0.272	0.169	0.253	0.173	0.147
3,4 – dihydroxy benzoic acid	0.109	0.150	0.159	0.103	0.090
2,6 – dihydroxy benzoic acid	3.537	0.293	1.478	1.132	0.576
2,5 –dihydroxy benzoic acid (gentisic acid)	0.236	0.157	0.228	0.136	0.130
3,5 –dihydroxy benzoic acid	0.097	0.140	0.175	0.090	0.092
Phthalic acid	0.460	0.147	0.189	0.191	0.135
3 –hydroxy, 4 – methoxybenzoic acid	0.207	0.205	0.287	0.194	0.192
2,4,6 – trihydroxybenzoic acid	0.067	0.122	0.082	0.065	0.065
3,4,5 – trihydroxybenzoic acid	0.092	0.151	0.130	0.095	0.092
2,3,4 – trihydroxybenzoic acid	0.130	0.139	0.167	0.098	0.101
Suberic acid	0.584	0.147	0.473	0.384	0.274
3,4 – dimethoxybenzoic Acid	0.483	0.263	0.578	0.182	0.483
Sorbitol	0.109	0.137	0.113	0.221	0.095
4 –Hydroxyisophthalic acid	0.971	0.170	0.638	0.384	0.237
5 –Hydroxyisophthalic acid	0.191	0.196	0.384	0.182	0.171
3,5 – dimethoxy, 4 – hydroxybenzoic acid	0.233	0.213	0.384	0.221	0.252
1,2,4 – benzenetricarboxylic acid	0.388	0.115	0.256	0.181	0.107
1,2,3 – benzenetricarboxylic acid	0.175	0.120	0.159	0.124	0.114
1,2,4,5 – benzenetetracarboxylic acid dianhydride	0.435	0.088	0.173	0.199	0.080

Table 5.4: Summary of the USP tailing factors for each of the chromatographic columns studied.

Compound name	USP Tailing Factor				
	Luna C18	Luna Cyano	XTerra™ RP$_{18}$	Aqua C18	Synergi polar-RP
Oxalic acid	2.086	1.018	1.154	2.537	1.972
Catechol	1.266	1.610	1.089	1.059	1.103
Glutaric acid	1.212	1.609	1.089	1.084	1.135
3-hydroxybenzoic Acid	1.391	1.650	1.176	1.144	1.127
4-hydroxybenzoic Acid	1.568	1.639	1.391	1.395	1.247
2,3 – dihydroxy benzoic acid	1.762	1.697	1.216	1.188	1.065
3,4 – dihydroxy benzoic acid	1.264	1.615	1.151	1.105	1.079
2,6 – dihydroxy benzoic acid	12.873	1.972	12.690	11.936	6.733
2,5 –dihydroxy benzoic acid (gentisic acid)	1.990	1.640	1.321	1.288	1.086
3,5 –dihydroxy benzoic acid	1.294	1.628	1.215	1.145	1.120
Phthalic acid	2.836	1.607	1.604	2.115	1.199
3 –hydroxy, 4 – methoxybenzoic acid	1.351	1.689	1.147	1.127	1.120
2,4,6 – trihydroxybenzoic acid	1.173	2.090	1.083	1.078	1.099
3,4,5 – trihydroxybenzoic acid	1.149	1.608	1.104	1.166	1.120
2,3,4 – trihydroxybenzoic acid	1.358	1.654	1.122	1.118	1.099
Suberic acid	1.570	1.634	1.548	2.607	1.358
3,4 – dimethoxybenzoic Acid	1.347	1.698	1.184	1.279	1.282
Sorbitol	1.203	1.454	1.075	1.173	1.037
4 –Hydroxyisophthalic acid	2.840	1.694	2.180	2.607	1.678
5 –Hydroxyisophthalic acid	1.484	1.734	1.251	1.279	1.157
3,5 – dimethoxy, 4 – hydroxybenzoic acid	1.387	1.712	1.179	1.173	1.140
1,2,4 – benzenetricarboxylic acid	2.884	1.460	2.092	2.784	1.410
1,2,3 – benzenetricarboxylic acid	1.664	1.489	1.119	1.339	1.094
1,2,4,5 – benzenetetracarboxylic acid dianhydride	3.952	2.307	2.264	5.393	1.704

Liquid chromatographic analysis of geological organic substances of industrial importance

polar-RP. The polar endcapping agent or the embedded polar group within the bonded phase ligand appears to improve the shape of these polar organic compounds.

5.4. COMPARISON OF ELUTION ORDER

There were a number of significant changes in elution order when comparing the Luna C18 column with the other four columns used in this study. Table 5.5 illustrates the elution order changes for the four chromatographic columns in comparison to the order of elution for the Luna C18 column. For example, on the Luna C18 1,2,4-benzenetricarboxylic acid eluted fourteenth, but on the XTerra™ RP$_{18}$, Synergi polar-RP, Aqua C18 and Luna Cyano it eluted thirteenth, ninth, eleventh and fourth, respectively. The Synergi polar-RP and Aqua C18 columns had similar elution orders to each other but still differed when compared to the Luna C18 elution order. The XTerra™ RP$_{18}$ and Luna Cyano columns differed the most from all the other columns showing significant re-ordering of all the standards.

5.5. REVERSED PHASE COLUMN SELECTION

The analysis of the four couples using informational theory allowed us to examine the retention mechanism equivalency between the Luna C18 and the other four columns in

Table 5.5: Elution order comparison of the Luna C18 column with the four chromatographic columns chosen for this study.

Compound elution on Luna C18 Column	Elution order comparison			
	XTerra™ RP$_{18}$	Synergi polar-RP	Aqua C18	Luna Cyano
(1) 2,4,6 – trihydroxybenzoic acid	2	2	2	2
(2) Oxalic acid	4	10	1	10
(3) 3,4,5 – trihydroxybenzoic acid	1	1	3	4
(4) Glutaric acid	10	3	4	14
(5) 3,5 –dihydroxy benzoic acid	3	4	10	12
(6) 3,4 – dihydroxy benzoic acid	9	5	5	3
(7) 2,3,4 – trihydroxybenzoic acid	8	6	6	1
(8) Catechol	12	7	7	7
(9) Sorbitol	6	14	9	6
(10) 1,2,4,5 – benzenetetracarboxylic acid dianhydride	5	8	8	5
(11) 4-hydroxybenzoic Acid	7	12	14	13
(12) 1,2,3 – benzenetricarboxylic acid	20	24	12	20
(13) 5 –Hydroxyisophthalic acid	14	9	15	9
(14) 1,2,4 – benzenetricarboxylic acid	15	15	11	24
(15) 2,5 –dihydroxy benzoic acid (gentisic acid)	24	11	20	8
(16) 3-hydroxybenzoic Acid	11	13	13	15
(17) 3 –hydroxy, 4 – methoxybenzoic acid	19	20	24	23
(18) 3,5 – dimethoxy, 4 – hydroxybenzoic acid	16	19	16	11
(19) 2,3 – dihydroxy benzoic acid	17	16	19	22
(20) Phthalic acid	13	17	17	19
(21) 3,4 – dimethoxybenzoic Acid	18	22	18	16
(22) 4 –Hydroxyisophthalic acid	23	18	22	18
(23) Suberic acid	22	23	21	17
(24) 2,6 – dihydroxy benzoic acid	21	21	23	21

this study with the ultimate aim to find a reversed phase column that could be used in the development of a multidimensional HPLC method for the separation of Bayer humic substances.

The values for the informational similarity were almost identical for all four comparisons approaching a value of 1.00 indicating high solute crowding. These appear to be in conflict with the other reported system attributes, but it is important to remember that the information similarity is a measure of the crowding of the system, not a measure of the difference in retention behaviour. For that matter, the normalised retention plots showed a significant degree of solute grouping within the 2D separation plane, especially along the main diagonal for the Luna C18/Aqua C18 couple. This high degree of solute crowding masked some of the differences between each of the systems even though there were obvious visual differences. The values for the %synentropy on the other hand indicated that there were changes in the mechanisms by which these columns separate in comparison to the Luna C18 column. This was also supported by what we see on examining the normalised plots as well as the changes in the elution order of the standards as compared to the Luna C18.

Although the information provided by the informational theory (IT) and the factor analysis is different, with IT reporting the retention mechanism equivalency of the Luna C18 column compared to the other four columns and factor analysis determining the similarity of the chromatographic information provided by each of the columns studied, both are related and can be combined to determine any similarity or differences between the Luna C18 and the Luna Cyano, XTerra™ RP_{18}, Aqua C18 and Synergi polar-RP

columns. The correlation coefficient, calculated using factor analysis, is impacted by the combined effects of solute crowding as reported by the informational similarity, the selectivity equivalency reported by the %synentropy and the alignment of the data with respect to the diagonal represented on the normalised retention plots.

The informational similarity for the Luna C18/ Luna Cyano couple was 0.98 reflecting a system where the solute crowding was high. On examination of the normalised retention plot in Figure 5.3 we see that although the solute crowding was high, the majority of the bands were crowded to the left, above the diagonal. This scatter in the data resulted in the %synentropy being relatively low (12.5%). The three combined effects; high solute crowding, low %synentropy and the crowding of data away from the diagonal overall resulted in a low correlation coefficient of 0.56.

For the Luna C18/XTerra™ RP$_{18}$ couple the informational similarity was higher at 1.00 but in this case the bands were more evenly distributed either side of the diagonal on the normalised retention plot (Figure 5.5) with a higher degree of scatter. This resulted in a moderately low %synentropy value of 34.0%. The increase in the %synentropy and the informational similarity for the Luna C18/ XTerra™ RP$_{18}$ couple as compared to the Luna C18/Luna Cyano couple, as well as the redistribution of the bands around the diagonal had an accumulative effect on the correlation coefficient and this resulted in a higher correlation of 0.80.

The informational similarity for both the Luna C18/Aqua C18 couple and the Luna C18/Synergi polar-RP couple was 0.99, however the %synentropy for each couple

differed significantly with the Luna C18/Aqua C18 reporting the highest selectivity similarity at 72.1% whereas the Luna C18/Synergi polar-RP couple only had a value of 50.0%. Although both systems exhibited high solute crowding, the difference in the %synentropy values was seen in the normalised retention plots for both cases. The %synentropy value of 72.1% for the Luna C18/Aqua C18 couple was a result of greater alignment and ordering of the bands along the diagonal as seen in the normalised retention plot in Figure 5.7. Whereas the Luna C18/Synergi polar-RP couple exhibited more alignment along the diagonal compared with the Luna C18/Luna Cyano and Luna C18/ XTerra™ RP$_{18}$ couples, the majority of bands fell below the diagonal in the normalised retention plot shown in Figure 5.9, resulting in a lower %synentropy of 50.0%. Due to the higher %synentropy value of the Luna C18/Aqua C18 couple as well as the greater order in the distribution of the bands along the diagonal, the correlation coefficient for this system was higher at 0.86 than that of the Luna C18/Synergi polar-RP couple, whose lower %synentropy and more chaotic distribution of the bands below the diagonal resulted in a lower correlation of 0.70.

When considering the correlation coefficients, the Luna Cyano seemed to show the greatest difference in retention mechanism and in the chromatographic information provided. However these results can be quite misleading. On examining the retention data for the Luna Cyano separation most of the standards eluted close to the void within the first three minutes of the separation displaying little resolution and an overall decrease in peak shape compared to the other columns studied. As such employing the Luna Cyano column for the separation of these types of compounds would yield limited separation.

Of all the columns studied the Luna C18/Aqua C18 gave the highest correlation coefficient of 0.86 followed closely by the Luna C18/ XTerra™ RP$_{18}$ couple that had a correlation of 0.80. Both these columns displayed a high degree of retention mechanism equivalency and provided similar chromatographic information to the Luna C18 column.

The Luna C18/Synergi polar-RP couple gave the best results with a moderate correlation coefficient of 0.70. Thus use of the Synergi polar–RP column provided the best results in terms of both peak shape as well as a low degree of retention mechanism equivalency compared to the Luna C18 column. In other words it provided different chromatographic information as compared to the Luna C18 column. The Synergi polar-RP column is therefore a better alternative than the Luna C18 column for the separation of polycarboxylic acids and polyphenols and hence may be an alternative for the separation of humic substances.

5.6. CONCLUSIONS

Following the analysis of retention information and using factor analysis and information theory it has been shown that the Phenomenex Aqua C18 column and the conventional Phenomenex Luna C18 column display the highest degree of retention mechanism equivalency, for a series of polycarboxylic acids and polyphenols providing very similar chromatographic information. The Phenomenex Aqua C18 column also yielded the worst overall performance in terms of peak shape. Further, the Phenomenex Aqua C18 and the Waters XTerra™ RP$_{18}$ offered little as an alternative to

that of a conventional Luna C18 column in terms of the separation of polycarboxylic acids and polyphenols.

Although the differences in selectivity and retention mechanism equivalency were maximised between the Luna C18 and Luna Cyano columns, the overall retention of the test solutes employed in this study on the Luna Cyano column was limited with most eluting near the column void volume. Consequently the Luna Cyano column is not recommended for the separation of polycarboxylic acids and polyphenols.

Overall the Phenomenex Synergi polar-RP column displayed the best performance for the separation of the test solutes. Band shapes generally exhibited less peak tailing and IT and factor analysis indicated that there was a moderate correlation coefficient of 0.70 compared to that of the Luna C18 column. Consequently the Phenomenex Synergi polar-RP column would provide a good alternative for separating polycarboxylic acids and polyphenols compared to the conventional C18 column and hence probably humic material.

In Chapter 4 a C18 column was used in the development of a one-dimensional HPLC separation for Bayer humic substances. As already indicated, this method was not ideal and that a multidimensional approach to the separation problem was required. Chapter 6 now details the development of a two-dimensional HPLC separation incorporating a reversed column in the second dimension separation. From the above results the Synergi polar-RP column was found to be better alternative to a C18 column and was subsequently chosen as the column for the second dimension.

CHAPTER 6

Unravelling the complexity of Bayer humic substances using multidimensional HPLC

6.1. INTRODUCTION

In Chapter 4 the separation of Bayer humic substances using ion-paired reversed phase high-performance liquid chromatography (HPLC) was reported. Analysis times greater than ten hours were required and even then limited resolution was achieved as the peak capacity of the separation system was vastly exceeded. This separation highlighted the complexity of the isolation problem and showed that one-dimensional reversed phase HPLC was inadequate to separate such a mixture.

Despite advances in instrumentation and column technology, one-dimensional HPLC cannot completely resolve complex samples. It has been predicted that if the component peaks were uniformly spaced, the maximum number of randomly distributed peaks that could be separated in a one-dimensional HPLC separation is only approximately 37% of the theoretical limit and single component peaks only 18% under the most favorable conditions [110-113]. It has also been shown that a chromatogram should be approximately 95% vacant in order to provide 90% probability that a given component of interest will appear as an isolated peak [112]. The statistical limitations on separating complex samples using a one-dimensional HPLC separation indicate that to successfully separate such a sample a multidimensional HPLC approach must be taken.

It was the aim of this study to improve the separation process for Bayer humic substances by expanding the peak capacity of the system using a multidimensional HPLC approach to the separation problem and developing a two-dimensional HPLC

separation. Ideally each dimension of the separation would employ a stationary phase that would generate orthogonal retention behaviour for the solutes being studied and as a result, maximise the peak capacity of the system [118]. In reality, at least some retention correlation does exist between the dimensions and this to some extent decreases the optimum resolution and peak capacity that could be achieved. In order to take full advantage of the expanded separation space afforded by multidimensional systems the number of system dimensions should equal the number of definable sample attributes [160]. That is, if two factors can be used to describe the sample (for example molecular size and polarity) two separation steps should be employed that are designed to take advantage of each sample attribute.

The results of the two-dimensional technique for the isolation of constituents in Bayer humic substances are presented here. By identifying the various aspects that could be used to describe the Bayer humic sample, such as size and polarity, a separation system that incorporated columns having retention mechanisms corresponding to the defining aspects was designed. Undertaking the separations in a heart-cutting mode, instead of comprehensive, further limited the complexity of the resulting separations.

6.2. DEVELOPMENT OF A TWO-DIMENSIONAL HPLC SEPARATION FOR BAYER HUMIC SUBSTANCES

The first separation process incorporated a Phenomenex BioSep-S2000 size-exclusion column with a sodium nitrate (0.05 M) mobile phase. The second separation process employed a Phenomenex Synergi polar-RP reversed phase column running a curved gradient using formic acid (0.1%) and acetonitrile. Each of the separation dimensions could be operated independently, which improved the separation speed. This is of particular importance when scaling to preparative isolation.

The first attribute chosen to describe the Bayer humic sample was molecular size and a BioSep-S2000 size-exclusion column was used for the separation in the first dimension. Size-exclusion separations are based on entropic exclusion principles and are related to their molecular size where the larger molecules elute first and the smaller molecules elute last. For these types of solutes it is difficult to completely eliminate solute adsorption to the surface of the size-exclusion media and hence secondary retention processes occur. There are a number of reported problems associated with the separation of humic substances using size-exclusion chromatography. The most common problems arise due to possible charge interactions that could produce attractive or repulsive effects between the matrix and the humic substances, leading to a possible overestimation or underestimation of the elution volume and sorption reactions that also result in an overestimation of the elution volume [63]. To some extent the addition of sodium nitrate to the mobile phase limits these secondary adsorption effects but they can never be entirely eliminated [56, 62-65]. Nevertheless, for the most part we

assume that the dominant retention process is entropically driven rather than enthalpy driven.

A reversed phase separation was chosen for the second dimension where the retention process was governed by the chemical interactions between the solute and the stationary phase. In Chapter 5 we investigated alternative reversed phase columns for the separation of humic substances using a set of polycarboxylic acids and polyphenol compounds. Traditionally the C18 column has been used as the column of choice for separating humic substances, however there has been little work published on the use of alternative columns despite the fact that there are a number of new generation columns available on the market that could provide a better alternative and therefore improved resolution. We also showed in Chapter 5 that the Phenomenex Synergi polar-RP column provided a better alternative to the C18 column and was chosen in this study as the column for the second dimension. The Synergi polar-RP column is essentially an ether-linked phenyl base with polar endcapping. The Synergi phase was developed for separating extremely polar aromatic analytes or mixtures and is reported to improve the peak shape of both acids and bases and is stable in 100% aqueous conditions. Consequently two different elution mechanisms (at least in principle) function in both dimensions and this leads to a substantial increase in the separation space and hence an increase in the peak capacity of the system.

The design of the two-dimensional chromatographic system used for the separation of the Bayer humic sample incorporated two 6-port, 2-position switching valves and there operation is illustrated in Figure 6.1. The Bayer humic sample was injected (250 µL) into the first dimension where the sample was separated according to the principles of
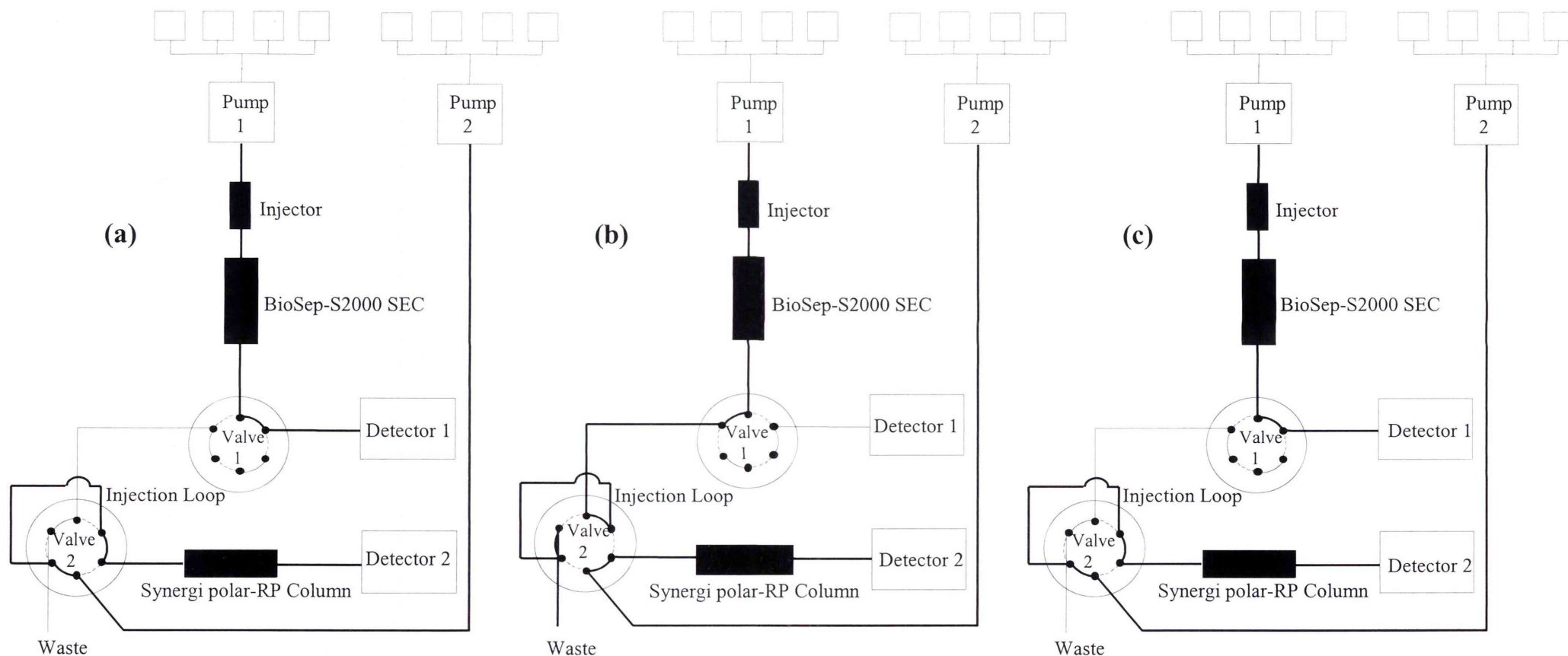
Figure 6.1: Schematic diagram of two-dimensional HPLC column switching system; (a) System configuration for the separation of the Bayer humic sample on BioSep-S2000 SEC; (b) system configuration for the "heart-cutting" of the elution band in the first dimension and; (c) flushing of the sample loop onto the Synergi polar-RP column.

size-exclusion chromatography (Figure 6.1(a)). The peak eluting in the first dimension was cut at 200 μL intervals across the entire band. In total, the size-exclusion band was divided into ninety different sections. Each cut was subsequently transferred to an injection loop using the switching valves that were programmed to periodically 'heart-cut' the solute from the first dimension (Figure 6.1(b)) [161]. The injection loop was then back flushed to load the sample onto the second dimension (Figure 6.1(c)), which was a Synergi polar-RP column where the sample components were further separated according to the retention mechanism of the second dimension chromatographic column. Refer to the attached Chapter 6 CD for a diagrammatic representation of the operation of the switching valves. The total analysis time (90 × 200 μL fractions) was in the order of seven days of continuous operation.

The chromatograph shown in Figure 6.2 illustrates the separation that was achieved in the first dimension on the BioSep-S2000 size-exclusion column. The retention time at which the volume of solvent was equivalent to the interstitial column volume (V_o) was at 2.20 minutes and the retention time at which the volume of solvent was equivalent to the total of the interstitial column volume plus the pore volume (V_t) was at 7.20 minutes. These limits define the exclusion range of the column, which is equivalent to a molecular weight range of 1,000-300,000 Da with respect to the manufacturers specifications. In the chromatogram shown in Figure 6.2 there is a single broad band eluting virtually throughout the entire exclusion range of the column, with some secondary retention phenomena obviously apparent. The broad elution profile indicates that there exists a substantial size distribution of the Bayer humic substances with the majority of the sample eluting around 3.80 minutes.
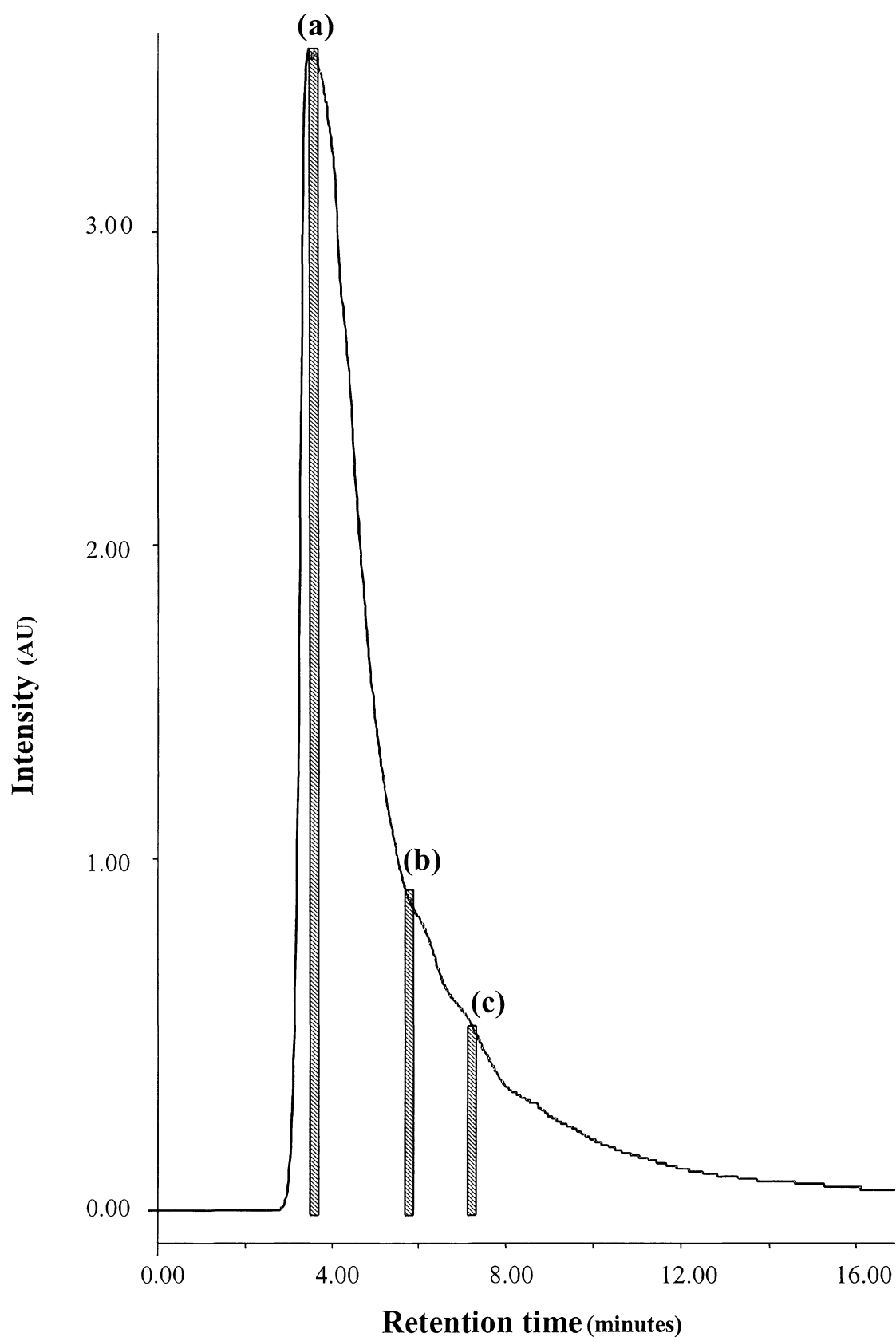
Figure 6.2: Separation of the Bayer humic sample on the BioSep-S2000 size-exclusion

column in the first dimension. AU=arbitrary units.

The shaded regions in Figure 6.2 indicate three fractions (200 µL cuts) that were heart-cut from the first dimension at 3.80 (a), 5.88 (b) and 7.08 (c) minutes and loaded onto the second dimension for further separation. While a total of ninety fractions were effectively heart-cut to the second dimension, only three fractions have been used as examples to illustrate the methodology. The separation in the first dimension and the ninety chromatograms from the second dimension can be viewed on the attached Chapter 6 CD. The chromatograms depicted in Figure 6.3 (a-c) illustrate the elution of the three heart-cut Bayer humic fractions in the second dimension. Minitab software was used to develop a three-dimensional surface representation (Figure 6.4) of the three fractions cut from the first dimension that were separated in the second dimension and clearly illustrate the complexity of the fractions.

Figure 6.3 shows that it is possible to resolve uniform band profiles that show promise of being essentially pure individual components. In the three fractions that have been heart-cut from the first size-exclusion dimension we have isolated at least 18 components resolved to baseline in the second dimension, with many other peaks exhibiting less resolution. As there are a number of major bands that display excellent resolution, isolation at the preparative level should be a seamless process using a goal focused separation approach [161]. Once preparative isolation has been undertaken the task of structural elucidation using NMR can begin at a level never before undertaken.
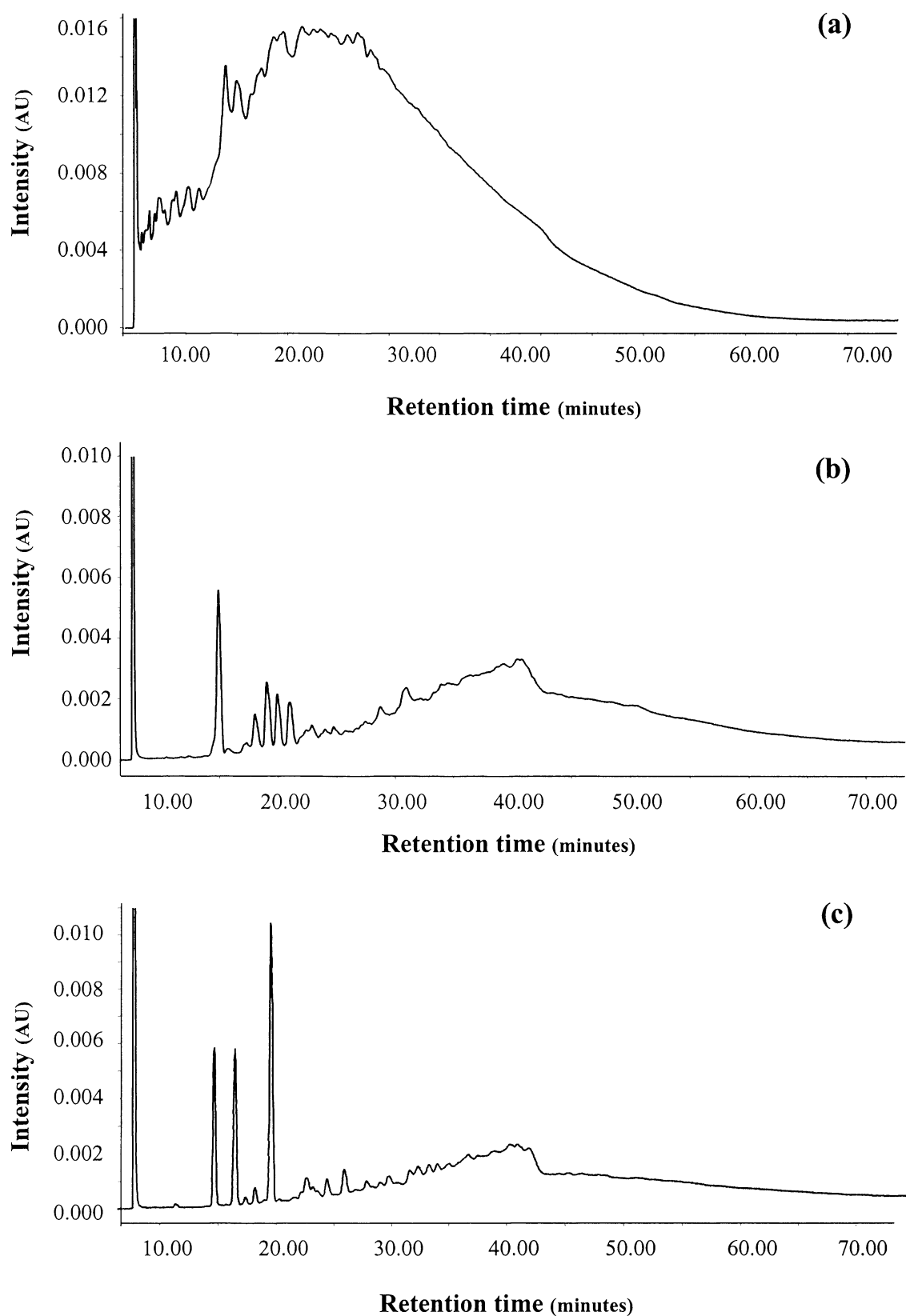
Figure 6.3: Bayer humic fractions cut from the first dimension at 3.80min (a), 5.88min (b) and 7.08min (c) and separated in the second dimension on the Synergi polar-RP column. AU=arbitrary units.

8.00

50.00

Retention time (minutes)
Synergi Polar-RP column

Retention time (minutes)
**BioSep-S2000 Size-exclusion
column**

0.00
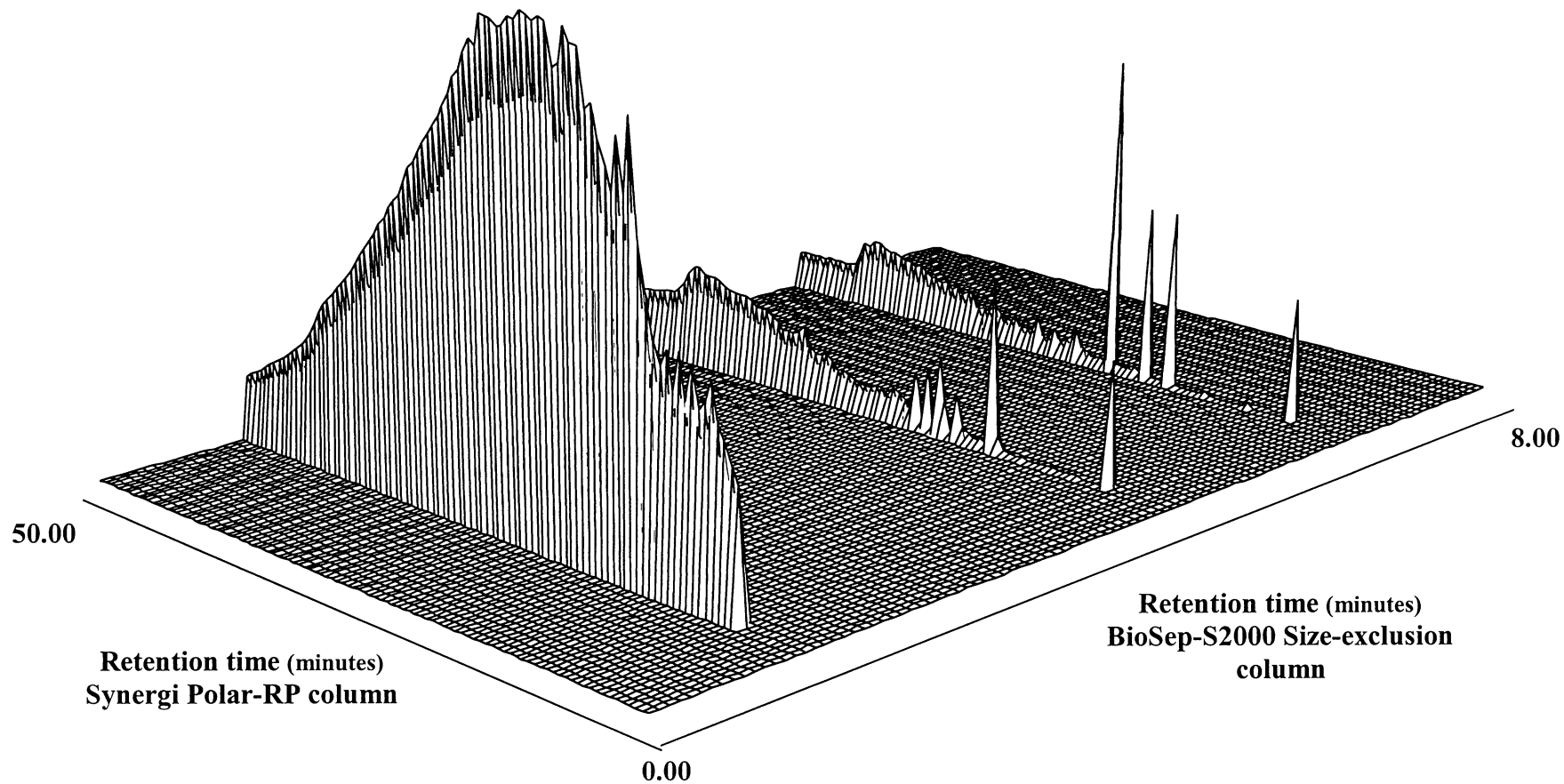
Figure 6.4: Three-dimensional surface representation of the three fractions cut from the first dimension at 3.80min, 5.88min and 7.08min that were subsequently separated in the second dimension.

6.3. MASS SPECTROMETRY ANALYSIS OF SECOND

DIMENSIONAL BANDS

The most intense bands in the second dimension cut fractions were collected on an analytical scale for further analysis by flow injection liquid chromatography/mass spectrometry. The second dimension chromatogram shown in Figure 6.5 is of the cut fraction taken at 6.92 minutes from the first dimension. The chromatogram displays three major bands at 15.25 (1), 17.30 (2) and 20.20 (3) minutes. The three two-dimensional bands were collected on an analytical scale for further analysis by mass spectrometry. Initially, the concentration of the bands was found to be too low to achieve sufficient ion intensity and as a consequence each had to be collected approximately twenty-five times, freeze dried and made up to 50 µL in a 10% methanol solution prior to analysis.

The negative ion electrospray ionisation (ESI) mass spectra were obtained for the three bands collected from the second dimension at 15.25 (1), 17.30 (2) and 20.20 (3) minutes. For all three bands the spectra showed ions predominately at low m/z values. Band 1 shown in Figure 6.6 displayed predominant ions at m/z values of 137, 181 and 249 Da. Product ion spectra obtained under collision-induced decomposition (CID) conditions were obtained for each of these ions and are shown in Figure 6.7. The product ion spectra for each of the selected ions in band 1 showed characteristic fragmentation patterns associated with substituted aromatics. The product ion spectrum of the ion at m/z 181 Da showed an ion peak at m/z 113 Da that corresponds
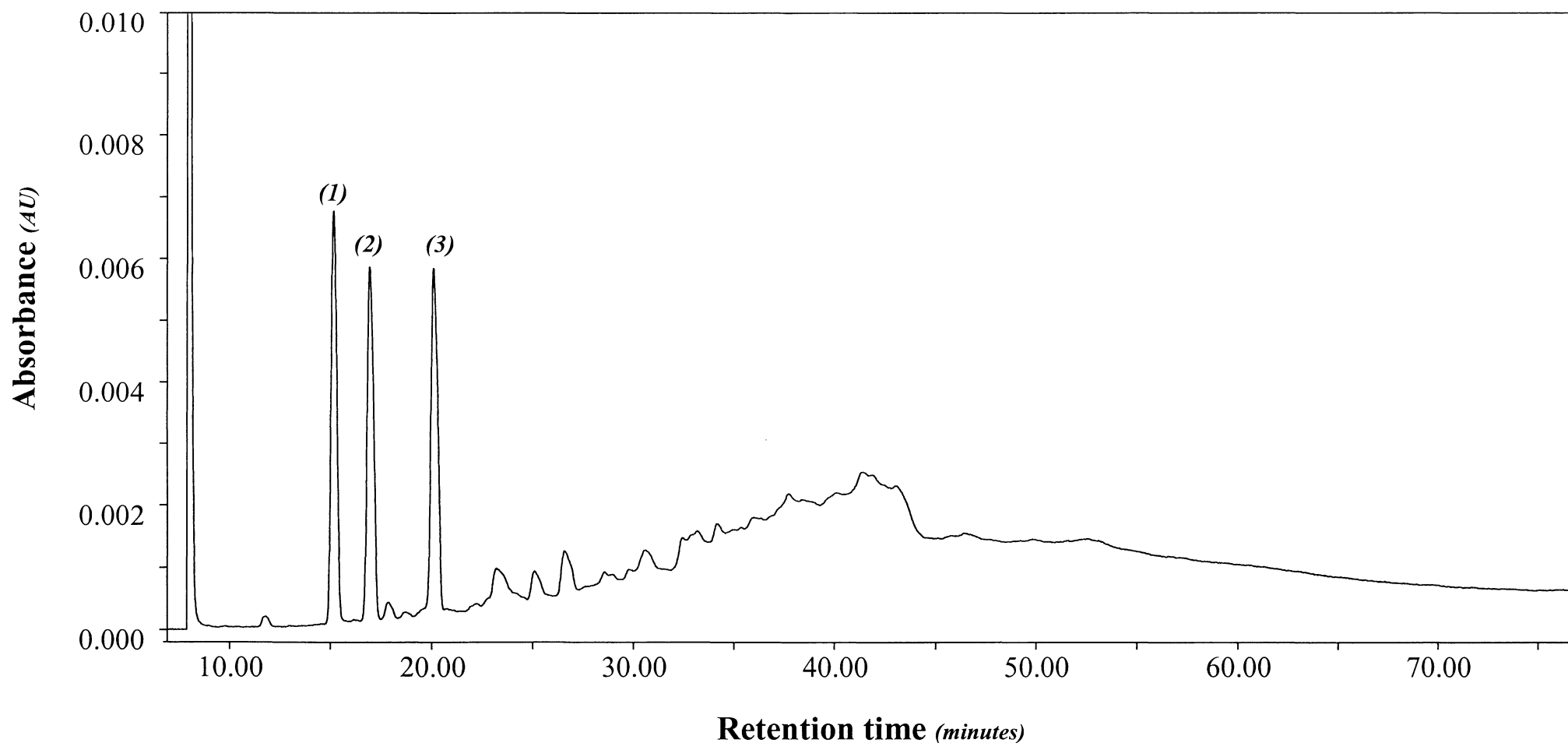
Figure 6.5: HPLC chromatogram of the fraction cut at 6.92 minutes in the first dimension that was subsequently separated in the second dimension. Bands at 15.25 (1), 17.30 (2) and 20.20 (3) minutes were collected for further analysis by mass spectrometry. AU=arbitrary units.
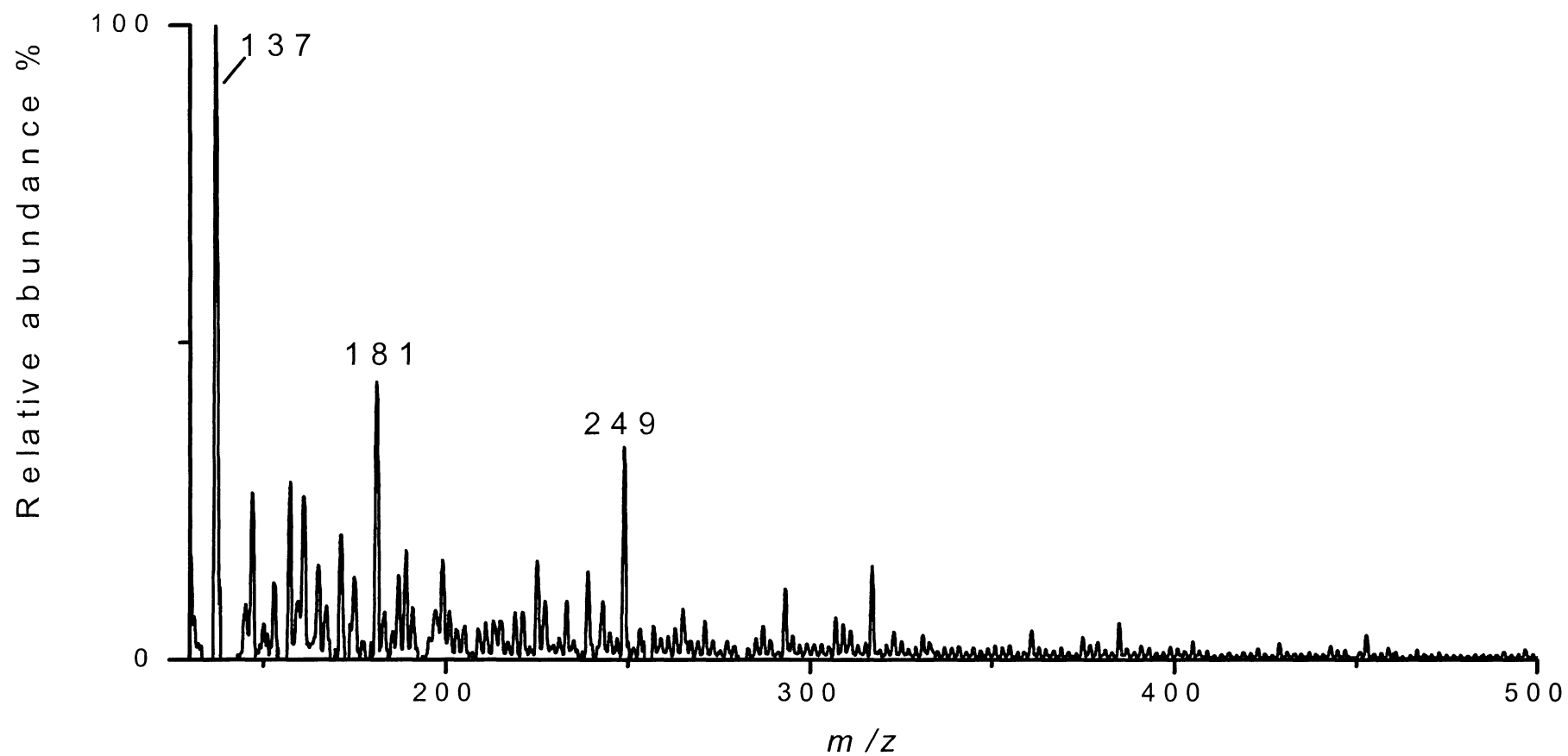
Figure 6.6: Negative ion ESI mass spectrum of the band collected at 15.25 minutes from the second dimension fraction cut at 6.92 minutes.
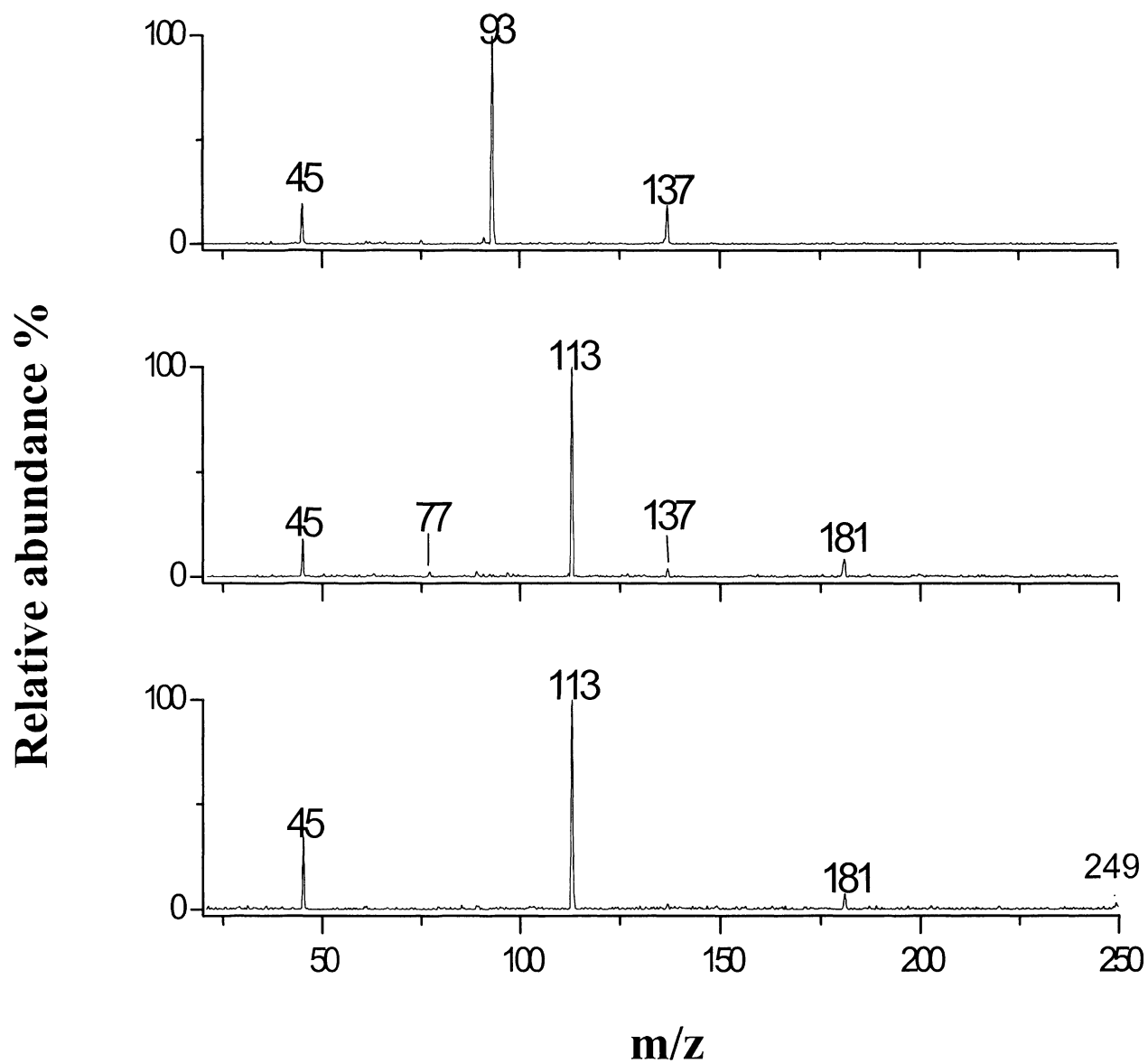
Figure 6.7: CID product ion spectra of band 1 collected at 15.25 minutes.

to the presence of hydroxybutanoic acid.

In band 2 (collected at 17.30 minutes), ions at m/z values of 137 and 153 Da were relatively more intense as shown in the negative ion ESI mass spectrum in Figure 6.8. Figure 6.9 shows the product ion spectra of the ions at m/z values of 137 and 153 Da. The product ion spectrum of the peak at m/z 137 Da confirms the presence of hydroxy benzoic acid and the product ion spectrum of the peak at m/z 153 is characteristic of a methylbenzene due to the presence of the fragment ion of m/z 91 Da.

The negative ion ESI mass spectrum of band 3 (Figure 6.10) showed predominant ions at m/z values of 157, 161 and 167 Da. Figure 6.11 shows the product ion spectra of the ions at m/z values of 157, 161 and 167 Da. The product ion spectra of the ions at m/z 157 and 161 Da appear to indicate the presence of small carboxylic acids with m/z 89 Da corresponding to a hydroxypropanoic acid fragment. The spectrum of the ion at m/z 161 Da is characteristic of a methyl ester due to a loss of m/z 32 Da in the product ion spectrum corresponding to the loss of methanol. A loss of 15 associated with the loss of a methyl group from a methoxyl group was observed in the product ion spectrum of the peak at m/z 167 Da. Along with an ion at m/z 91 Da corresponding to a methylbenzene fragment this indicates the presence of methoxybenzoic acid.
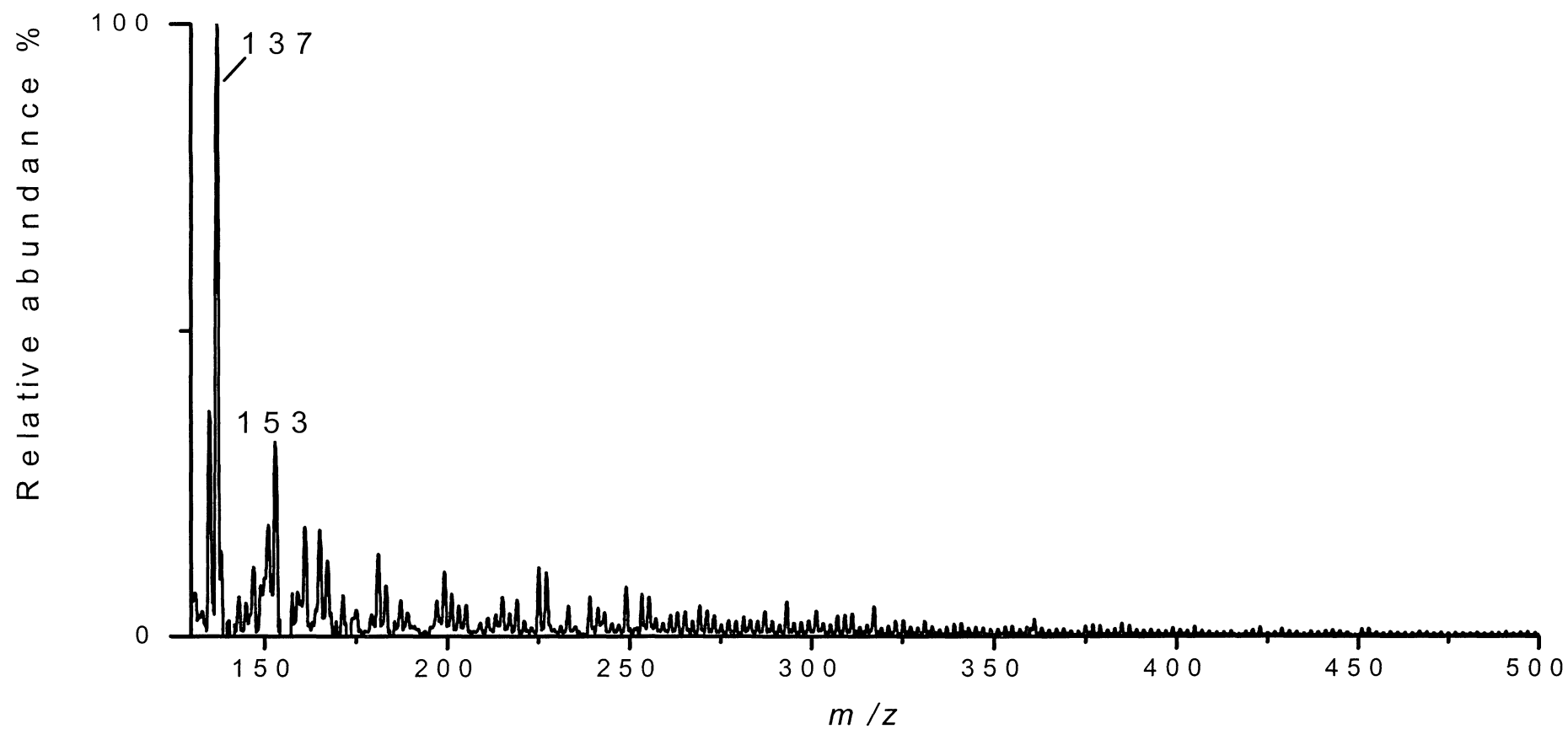
Figure 6.8: Negative ion ESI mass spectrum of the band collected at 17.30 minutes collected from the second dimension fraction cut at 6.92 minutes.
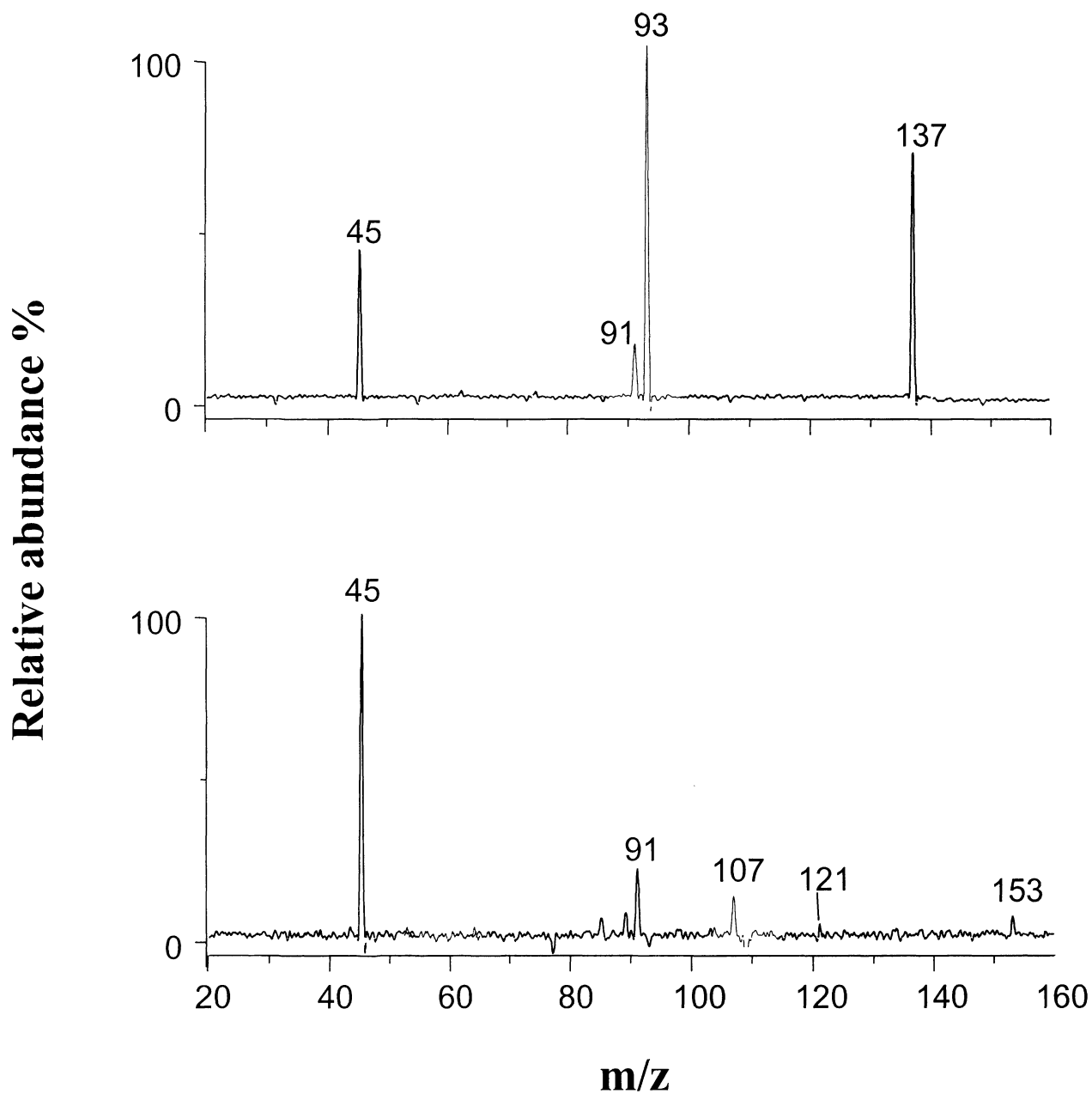
Figure 6.9: CID product ion spectra of band 2 collected at 17.30 minutes.
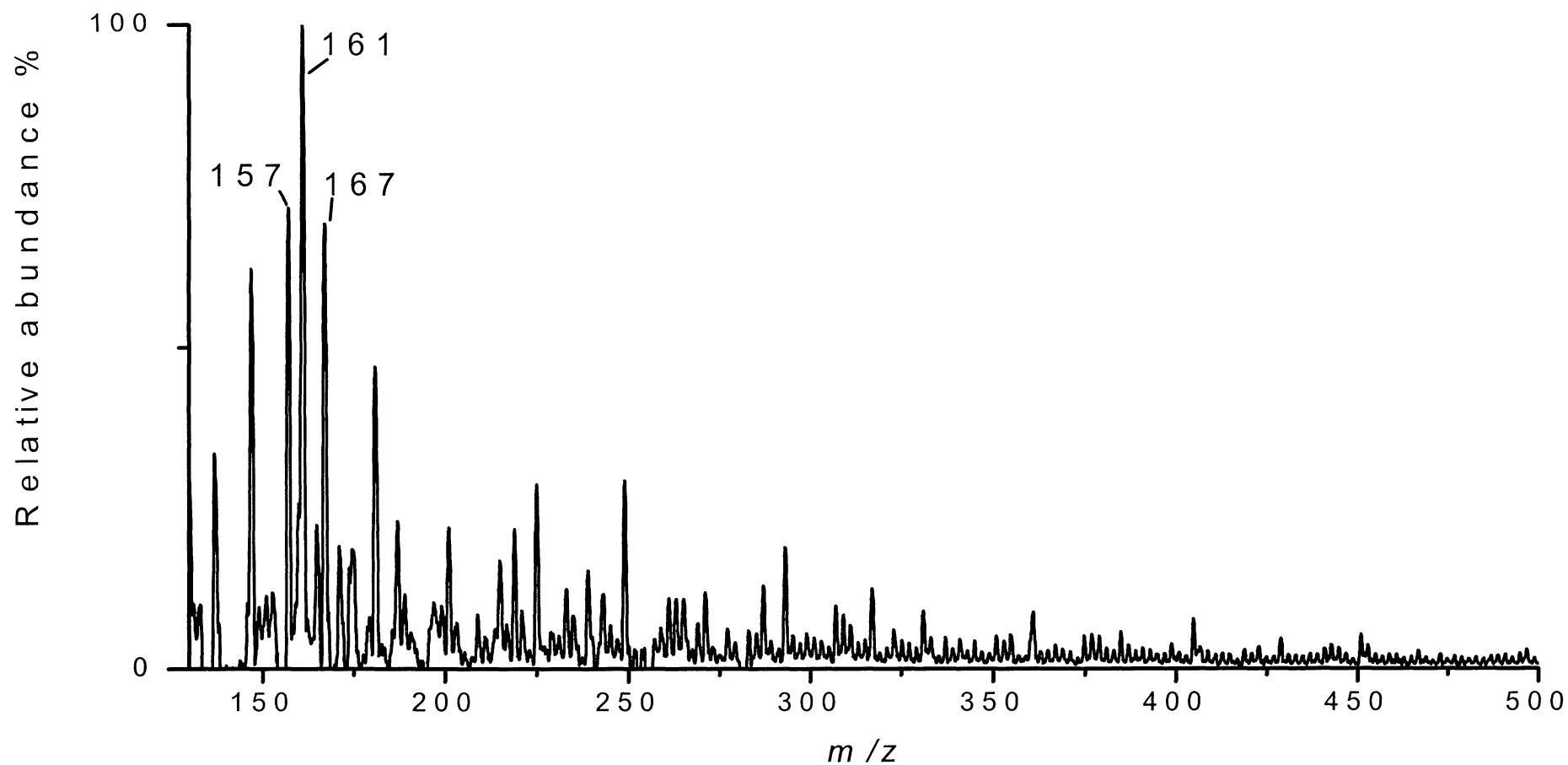
Figure 6.10: Negative ion ESI mass spectra of the band at 20.20 minutes collected from the second dimension fraction cut at 6.92 minutes.
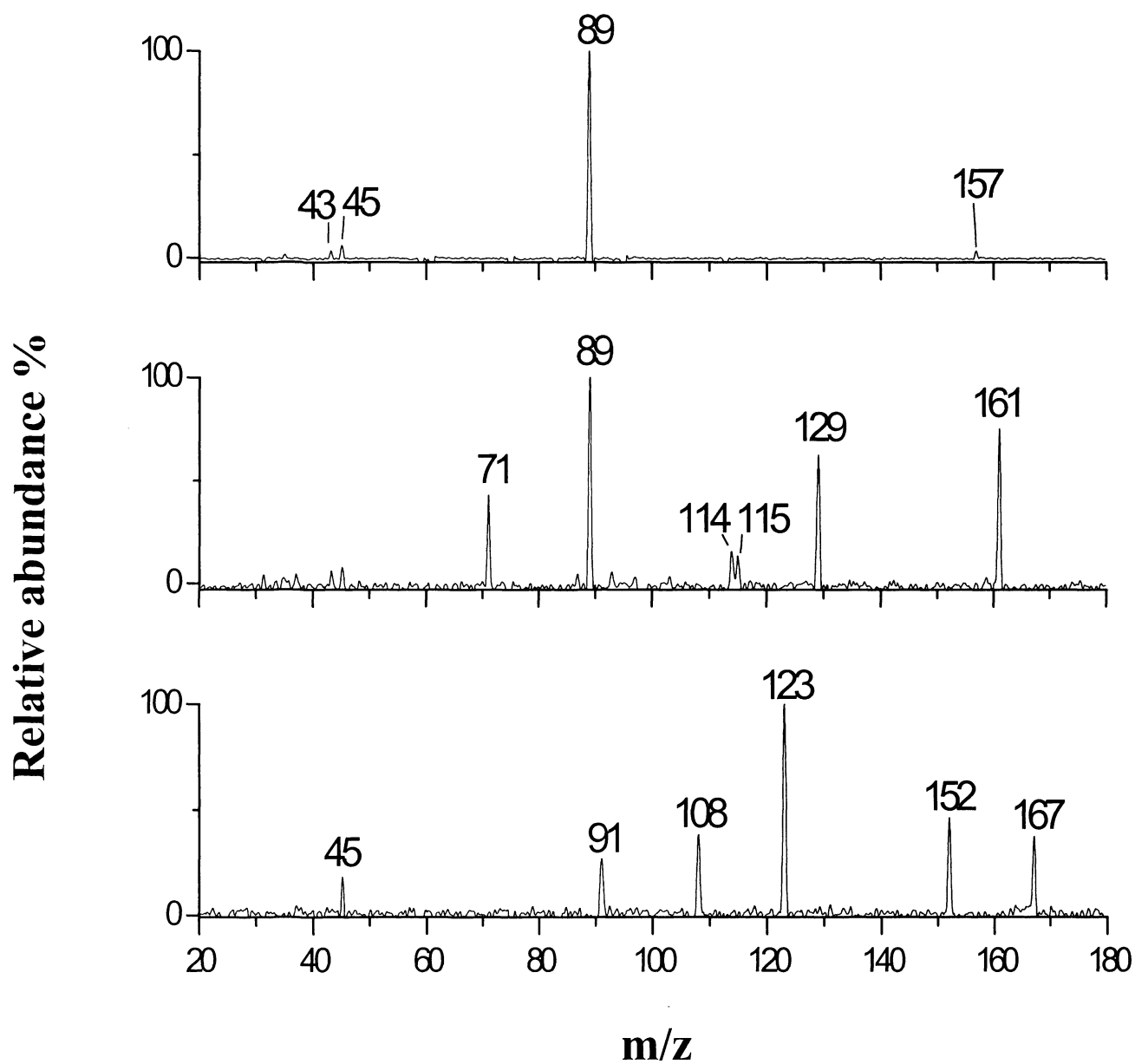
Figure 6.11: CID product ion spectra of band 3 collected at 20.20 minutes.

6.4. SEPARATIONS AND HUMIC SUBSTANCES BEHAVIOUR

The contour plot in Figure 6.12 and the three-dimensional surface representation in Figure 6.13 represent the separation in the second dimension of fractions cut between 3.00 – 8.00 minutes from the first dimension. Although ninety fractions were cut from the first dimension and separated in the second, the contour plot and three-dimensional representation only show cuts taken at 3.32, 3.64, 3.80, 4.20, 4.68, 5.08, 5.48, 5.88, 6.28, 6.68, 7.08, 7.48 and 7.88 minutes. The contour plot and three-dimensional representation illustrate the complexity of the Bayer humic substances even after undergoing separation in the second dimension. Despite taking only 200 µL fractions for separation from the first dimension, the second dimension fraction cuts are obviously still quite complex.

To a large extent the separation in the second dimension was based on polarity. As can be seen from Figure 6.12 and 6.13, the second dimension separation of the 200 µL fractions cut from the first dimension are complex with each fraction cut containing a number of compounds and in some cases, individual species can be seen to be resolved. Analysis of the three bands collected from the second dimension fraction cut at 6.92 minutes by mass spectrometry clearly indicated that they contained some compounds that are of simple structure. This begs the question why are small molecular weight compounds present in molecular weight fractions which are supposed to be of larger molecular weight, and are they present as some sort of structure that when separated in the second dimension disaggregate? The results presented here would suggest so.
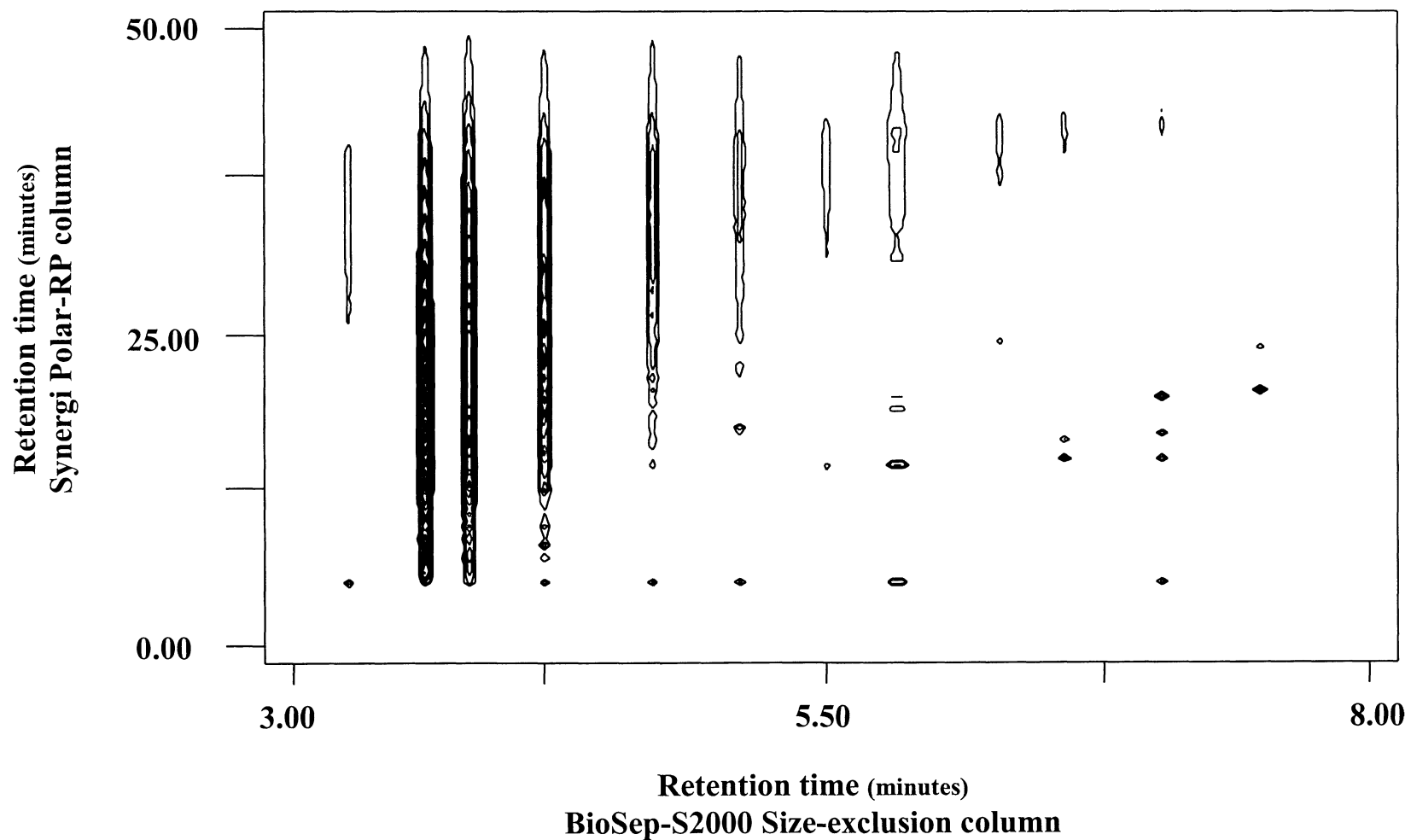
Figure 6.12: Contour plot of the fractions cut from the first dimension at 3.32, 3.64, 3.80, 4.20, 4.68, 5.08, 5.48, 5.88, 6.28, 6.68, 7.08, 7.48 and 7.88 minutes that were subsequently separated in the second dimension.
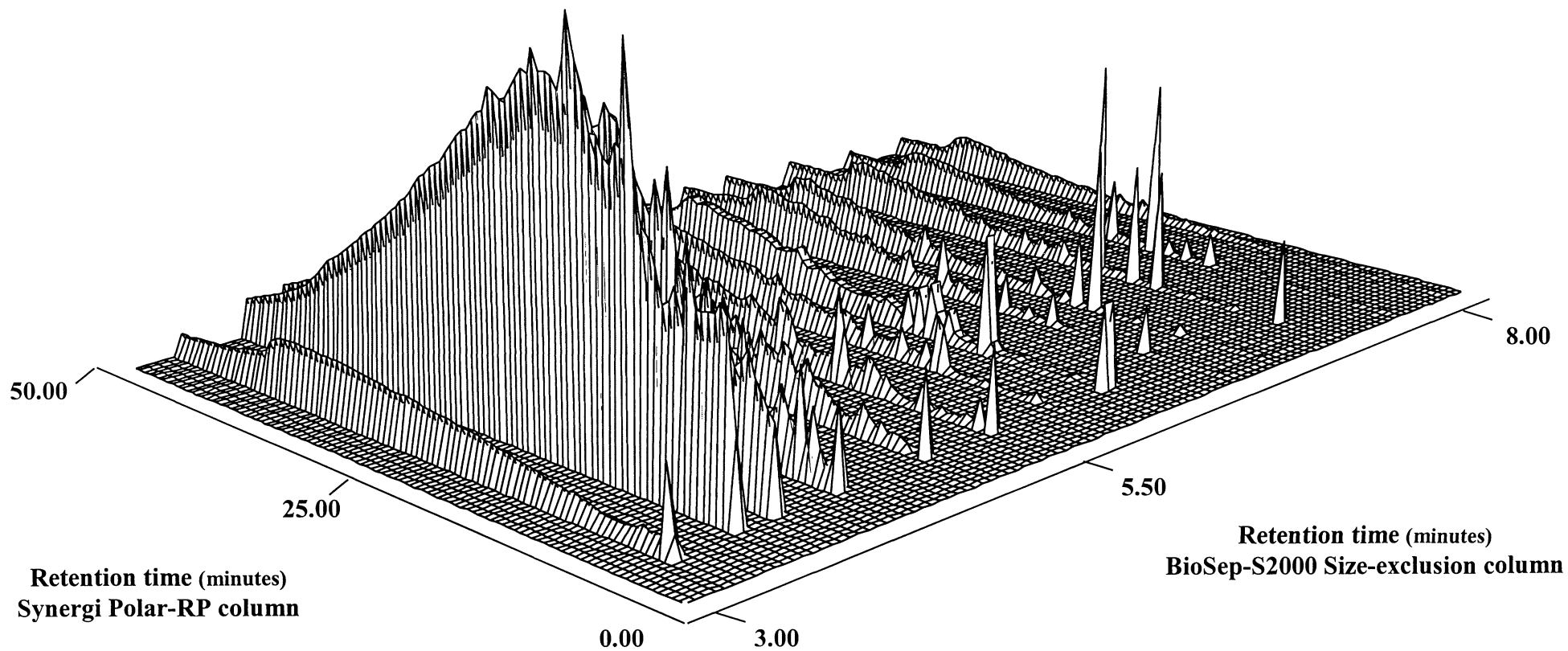
Figure 6.13: Three-dimensional surface representation of the fractions cut from the first dimension at 3.32, 3.64, 3.80, 4.20, 4.68, 5.08, 5.48, 5.88, 6.28, 6.68, 7.08, 7.48 and 7.88 minutes that were subsequently separated in the second dimension.

The results of the mass spectrometric analysis of the second dimensional bands collected from the fraction cut at 6.92 minutes from the first-dimension (Figure 6.5) were significant as they indicated the presence of low molecular weight material. While it is impossible to assign accurate molecular weights for humic substances based on the available calibration standards for size-exclusion chromatography, which include proteins, polystyrenes and polysaccharides, the cut at 6.92 minutes has to be greater than 1000 Da as it was cut within the exclusion range of 1000-300,000 Da as stated for the column. The mass spectrometric analysis however showed them to be of molecular weights of less than 250 Da. The results also indicated that each of the three bands analysed consisted of more than one component despite the fact that each was expected to be a single-component band. The shape and resolution of the three two-dimensional bands that were collected indicated that they were more likely to be single-component. Figure 6.14 shows the chromatograms of five consecutive cuts taken between 6.34 and 7.16 minutes that have been adjusted to compensate for delays due to the times at which cuts were taken. On examination of these chromatograms it can be seen that the three bands increase and decrease in intensity as we cut across the size-exclusion peak, increasing the likelihood that each band is single-component in nature. If they were multi-component they would not simply change in intensity but side bands would in all probability start to appear. It is therefore appropriate to question why, what is expected to be single-component bands, consist of more than one low molecular weight compound? A reasonable explanation for the observed phenomena is that the small molecules must be bound to the larger molecules before being separated by the reversed phase column.

Retention time (minutes)
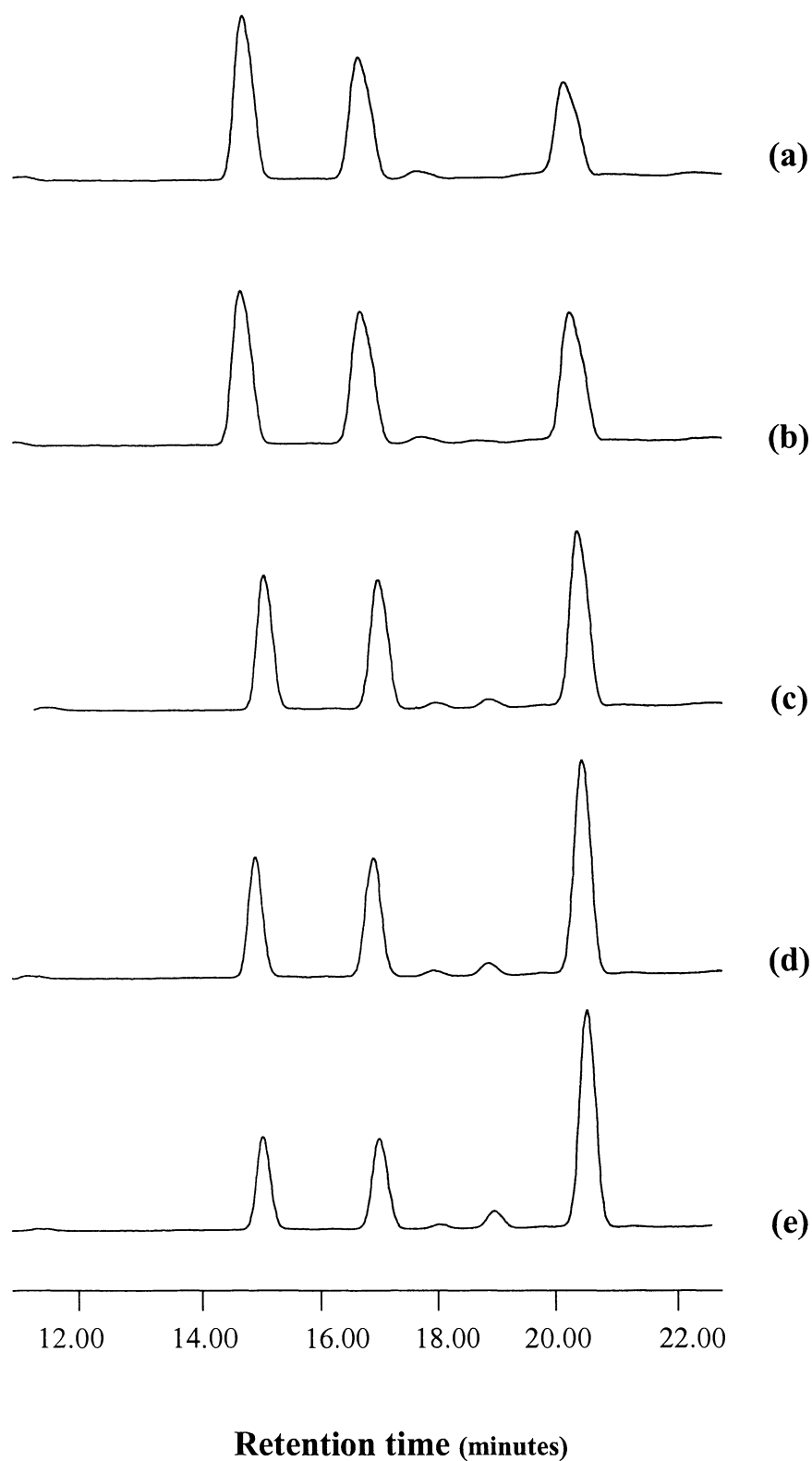
Figure 6.14: Chromatograms of consecutive fractions cut form the first dimension at 6.34 (a), 6.92 (b), 7.00 (c), 7.08 (d) and 7.16 (e) minutes and separated in the second dimension.

There are two possible explanations for this that were introduced in Chapter 4. Firstly small molecules were entrapped in a complex of larger molecules and were transported through the size-exclusion column, eluting entrapped with the larger molecules, which has been referred to as the "hidden host guest model". Alternatively, small molecules were interbound to each other but could not be separated from the host complex during transportation through the size-exclusion column, which has been referred to as the "micellar host guest model". Elsewhere our research group [81, 85] has offered other evidence for these types of structures but have not previously been able to distinguish between them. Nevertheless the excellent work of Piccolo et al. [23, 60, 65-66] strongly supports the latter model. Piccolo et al. proposed a model of molecular association of small molecules held together by hydrophobic forces, which control conformation. Both the conformational work by that group and the results of two-dimensional heart-cutting HPLC separation presented here are supportive of the micellar host guest model.

It is significant that the Bayer humic substances that were eluting closest to exclusion (the chromatograph of which is shown in Figure 6.3(a) at 3.80 minutes) contained less of the discrete molecular material than what was eluting at 5.88 minutes as shown in Figure 6.3(b). In turn this contained less material than the lower molecular weight Bayer humic substances what were eluting towards the end of the exclusion range (1,000-300,000 Da) at 7.08 minutes (Figure 6.3(c)). This shows the complexes are different and not just larger entities with the same components. It also suggests that the lower molecular weight material separated in Figure 6.3(c) is capable of entrapping the small guests more than the larger molecular weight material for which the

chromatogram is shown in Figure 6.3(a). It is unlikely that small molecules hide best inside lower molecular weight material. Rather the results suggest a micellar host guest model is more convincing where molecules bind together through similar functional groups. In Chapter 4, evidence was also presented that supports this micellar host guest model.

The host-guest complexes formed by these highly oxidised humic molecules are unlikely to exist in the caustic environment of the Bayer process however they would form at the lower pH conditions that were used for this HPLC separation. In Bayer liquor the carboxylic groups located on the fatty acids and in the humic macromolecules would be deprotonated, as will phenolic and other acidic groups. The deprotonated groups would not form strong hydrogen bonds under these conditions due to repulsion forces of similarly charged species. During precipitation however, intramolecular hydrogen and intermolecular hydrogen bonding may occur. In the large molecules, voids may be formed which could occlude other molecules. It may well be true that some of these occluded molecules hydrogen bond to larger macromolecules.

The work shown here does illustrate the two-dimensional HPLC can now be applied to advance not only our knowledge of Bayer liquors but also the structure and role of geochemical macromolecules in other systems. Collection of fractions on a preparative level would allow structural elucidation by techniques such as NMR spectroscopy that could further advance our knowledge on the structure and dynamics of Bayer humic substances.

6.5. CONCLUSIONS

In this Chapter, a two-dimensional HPLC method was developed for the separation of Bayer humic substances. Using this technique we have successfully been able to resolve uniform band profiles that show promise of being essentially pure individual components. There are a number of major bands that display excellent resolution with isolation at a preparative level being a seamless process using a goal focused separation approach. In the three sections that have been heart-cut from the first size-exclusion dimension we have isolated at least 18 components resolved to baseline in the second dimension, with many other peaks exhibiting less resolution.

Mass spectrometric analysis of the three second dimensional bands collected from a fraction cut from the first dimension at 6.92 minutes showed the presence of a number of low molecular weight material below 250 Da despite the fact they were collected in a fraction that was cut within the specified exclusion range of 1,000-300,000 Da and from what was assumed to be single-component bands. It is concluded that small molecules are held in some way in some supramolecular structure by larger molecules (host guest complexes). The results also suggest that the lower molecular weight material is capable of holding small guests more than larger molecular weight material making the supposition that the micellar host guest model is more probable than a model where hosts hide within the guests.

CHAPTER 7

Overview

This thesis discussed recent advances in our knowledge of the structure of organic material introduced with the bauxite ore to the Bayer process during the industrial scale production of alumina. In the past there has been a concerted effort into the investigation of the organic material present in the bauxite ore, organic material introduced from plant matter, the effect of organic matter on crystal formation and in solution. Much of this work has lead to the identification of a number of low molecular weight compounds, with work on the characterisation of larger molecular weight material focusing more on the measurement of bulk spectroscopic and chemical properties such as acidity, aromaticity and functional and structural group content. At the start of this thesis we proposed that liquid chromatography could further extend our understanding of Bayer humic substances as little work has previously been undertaken to try and identify humic material larger than 1200 Da using HPLC techniques. The application of liquid chromatography could greatly assist in the identification of these organic substances, which would then lead to the development of methodology for there removal. In this thesis we have made some progress as outlined below.

7.1. DIFFICULTIES WITH ONE-DIMENSIONAL HPLC SEPARATIONS OF BAYER HUMIC SUBSTANCES

As outlined in Chapter 4, there are a limited number of references in the literature on the liquid chromatographic (LC) analysis Bayer humic substances with overall limited success in separation. Here we have developed a one-dimensional HPLC method for

the separation of Bayer humic substances using ion-pair chromatography. Firstly three modes of HPLC separation were investigated; reversed phase, ion-suppression and ion-pair chromatography. Ion-pair chromatography displayed significantly greater selectivity compared to the other two chromatographic modes discussed. The humics from the Bayer liquor were retained for longer and greater resolution was achieved. As ion-pair chromatography offered the greatest potential to vary the separation selectivity, time was further spent in developing this method.

Figure 7.1 (reproduced from Figure 4.6, Chapter 4) shows the optimum separation, with respect to resolution, that was achieved for the separation of the Bayer humic substances by running a gradient using PIC A [5 mM]/acetonitrile, running isocratically for 10 minutes on PIC A [5 mM] and then a linear gradient from 100% PIC A [5 mM] to 18% acetonitrile at a rate of change of 0.056% per minute. The gradient continued running from 82% PIC A [5 mM] and 18% acetonitrile to 57% PIC A [5 mM] and 43% acetonitrile at a rate of change of 0.083% per minute. The gradient was then changed to 50% PIC A [5 mM] and 50% acetonitrile over 5 minutes. The solvent composition was then held for 10 minutes. The separation discussed in Chapter 4 and shown here in Figure 7.1 was highly significant since it represented the first recorded liquid chromatographic method in which Bayer humic substances that contained a range of low to high molecular weight material have been separated into groups of different polarity. It also demonstrated that the material is not randomly polymeric and there are discrete structural types, which chromatograph differently.
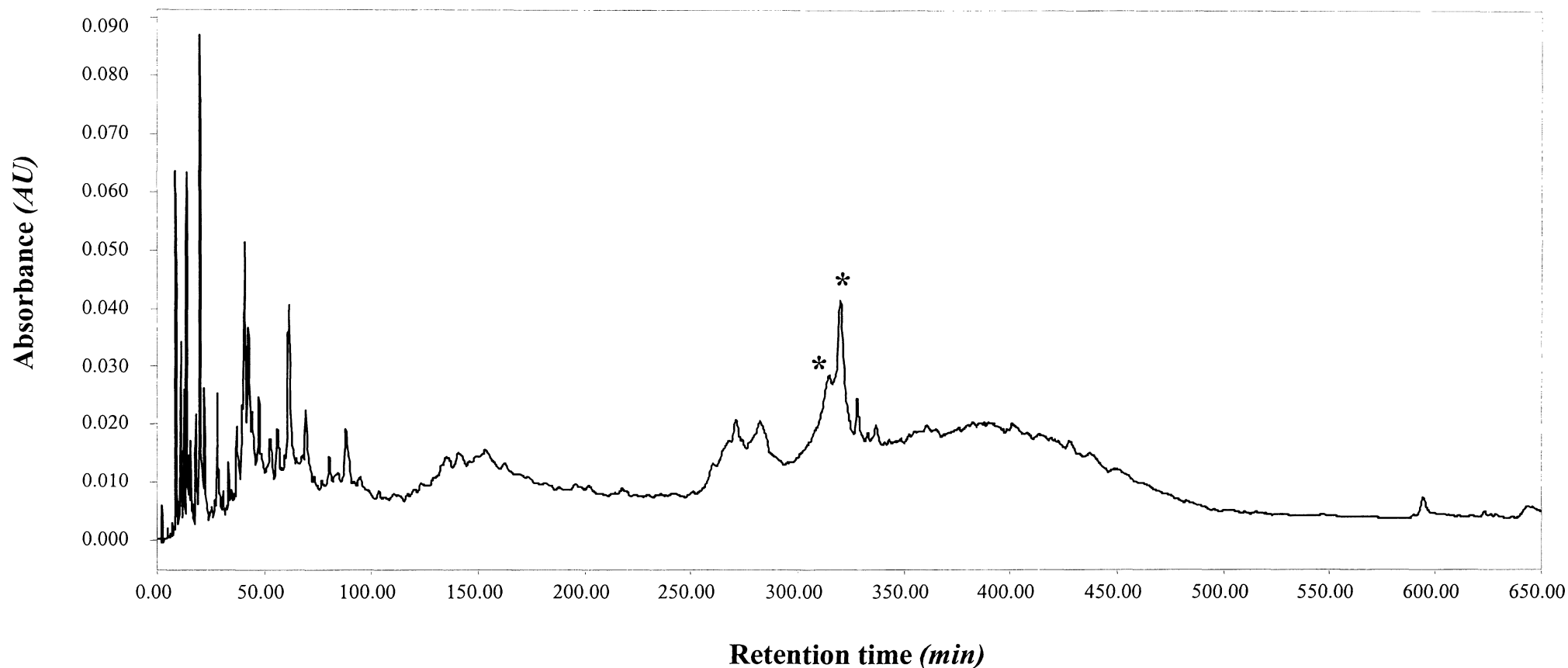
Figure 7.1: Optimum HPLC separation of the Bayer humic sample. Isocratic PIC A [5mM]/acetonitrile for 10min followed by a linear gradient from 100% PIC A[5mM] to 18% acetonitrile at 0.056% min^{-1}, then 82% PIC A [5mM] and 18% acetonitrile to 57% PIC A [5mM] and 43% acetonitrile at 0.083% min^{-1}, then 50% PIC A [5mM] and 50% acetonitrile for 5min. AU=arbitrary units. * =solvent change artefact.

As discussed in Chapter 4, it was interesting that the material did not elute as a continuum, but rather as clusters of peaks. They could represent micellar like aggregates of different amounts of polar groups like the rapidly eluted material, but of higher molecular weight and with less polar functionality. In other words it must be that only certain configurations are stable otherwise the chromatograph in Figure 7.1 would be a continuum.

Despite having developed a one-dimensional HPLC separation for Bayer humic substances that achieved a level of separation previously unreported in the literature, there still exists several inherent problems in the one-dimensional liquid chromatographic analysis of Bayer humic substances. The separation did take over ten hours and even then limited resolution was achieved as the peak capacity of the separation system was vastly exceeded. This separation did however highlight the complexity of the isolation problem. It showed that Bayer humic substances are too complex to separate using a one-dimensional HPLC separation. The statistical limitations on separating Bayer humic substances using a one-dimensional HPLC separation indicated that to successfully separate such a sample a multidimensional HPLC approach must be taken.

7.2. REVERSED PHASE COLUMNS FOR SEPARATIONS OF BAYER

HUMIC SUBSTANCES

To successfully separate Bayer humic substances the peak capacity of the separating system needed to be expanded using a multidimensional HPLC approach and required the development of a two-dimensional HPLC system. In a two-dimensional chromatographic system sample components are displaced along two axes of separation. The first dimension separation process was based on molecular size incorporating a size-exclusion column and separation in the second dimension was based on polarity incorporating a reversed phase column. Traditionally the C18 column has been used as the column of choice for separating humic substances however there has been little work published on the use of alternative columns despite the fact that there are a number of new generation columns available on the market that could provide a better alternative and therefore improved resolution. In Chapter 5 we investigated alternative reversed phase columns for the separation of humic substances using a set of polycarboxylic acids and polyphenol compounds as models.

In this work we used a systematic investigation into the relative separation performance of five reversed phase chromatography columns for a series of polycarboxylic acids and polyphenols. Information theory and factor analysis, together with basic evaluation of retention information (band shape, retention factor and elution order) were used to compare the conventional Phenomenex Luna C18 column with Phenomenex Luna Cyano, Waters

XTerra™ RP$_{18}$, Phenomenex Aqua C18 and Phenomenex Synergi Polar-RP columns. The results showed that there was very little difference in retention behaviour between the Aqua C18 column, the Xterra RP C18 column and the conventional Luna C18 column. However, there were notable differences in retention processes between the polar embedded stationary phase (Synergi polar-RP column) compared to the Luna C18 column. The most significant differences however were observed between the Luna C18 column and a Cyano column, although because of the limited degree of retention of these compounds on the Cyano column it would find limited use for these types of separations and therefore was considered to be inappropriate as a column for the separation of Bayer humic substances.

Overall the best results were achieved for the Phenomenx Synergi polar-RP column, with IT and factor analysis reporting to give a moderate correlation coefficient of 0.70. The Phenomenex Synergi polar-RP column reported the best peak shape and change in elution order and would provide a better alternative for separating polycarboxylic acids and polyphenols compared to the conventional C18 column and hence Bayer humic substances.

7.3. TWO-DIMENSIONAL HPLC SEPARATIONS OF BAYER HUMIC SUBSTANCES

A two-dimensional HPLC separation for the isolation of constituents in Bayer humic substances was reported in Chapter 6. By identifying the various aspects that describe the

Bayer humic sample, such as size and polarity, we were able to design a separation system

that incorporated columns that had retention mechanisms that correspond to those defining

aspects. The first dimension incorporated a BioSep-S2000 size-exclusion column with a

sodium nitrate (0.05M) mobile phase. The second dimension employed a Synergi polar-

RP column, as recommended from the findings of the reversed phase column study in

Chapter 5, running a curved gradient using formic acid (0.1%) and acetonitrile. The Bayer

humic sample (60 mg/mL) was injected (250 μL) into the first dimension that operated at a

flow rate of 2.5 mL/min. The size-exclusion peak eluting in the first dimension was cut at

200 μL intervals across the entire band. In total, the size-exclusion band was divided into

ninety different sections with each cut subsequently transferred to the second dimension.

The total analysis time (90×100 μL fractions) was in the order of seven days of continuous

operation. This resulted in a number of major bands that displayed excellent resolution

and in the three fractions alone shown in Figure 6.3 it could be seen that we had isolated at

least 18 components resolved to baseline in the second dimension, with many other peaks

exhibiting less resolution. The second dimensional bands that showed greatest resolution

were collected for further analysis by mass spectrometry.

The three-dimensional surface representation of twelve fractions cut in the first dimension

between 3.00-8.00 minutes and separated in the second dimension shown in Figure 7.2

(reproduced from Figure 6.13, Chapter 6) illustrated the complexity of the Bayer humic

substances. Despite taking only 200 μL fractions for separation from the first dimension,

the second dimension fraction cuts were still quiet complex, with each fraction cut
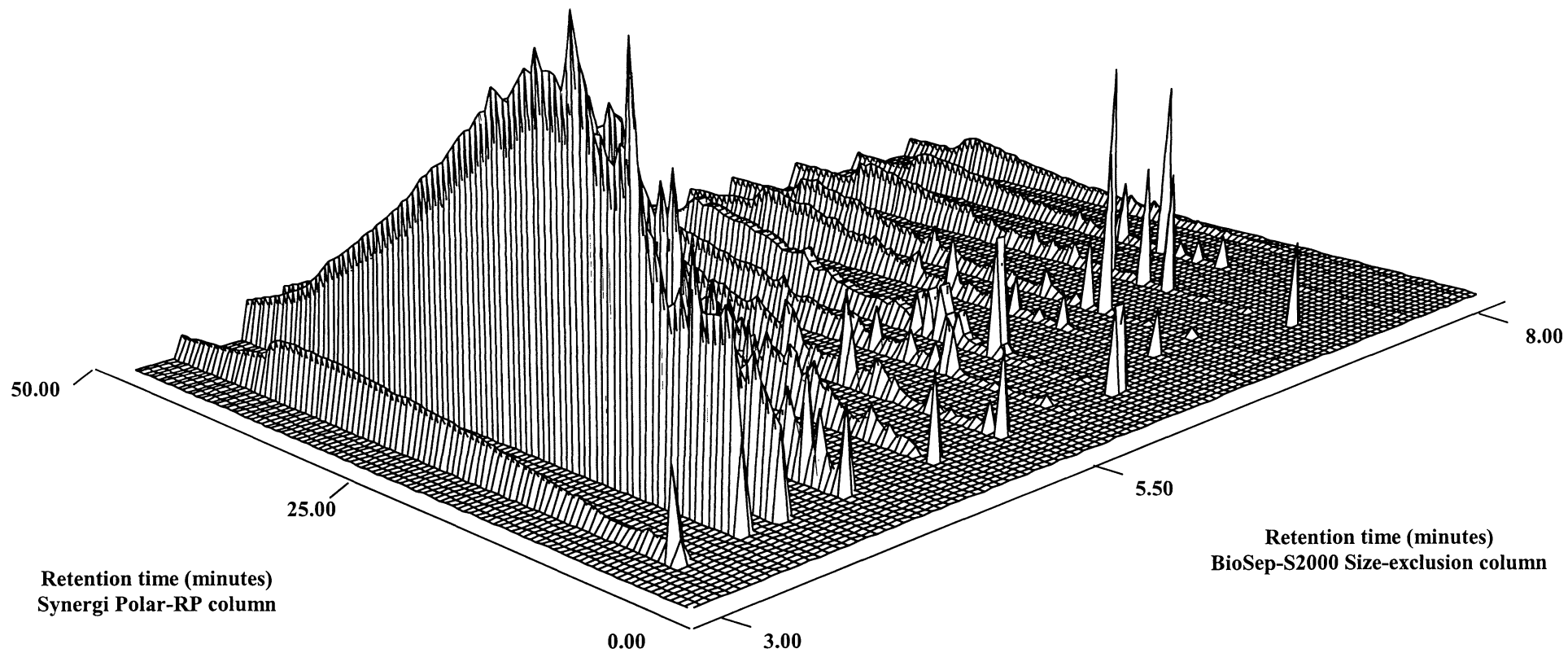
Figure 7.2: Three-dimensional surface representation of the fractions cut from the first dimension at 3.32, 3.64, 3.80, 4.20, 4.68, 5.08, 5.48, 5.88, 6.28, 6.68, 7.08, 7.48 and 7.88 minutes that were subsequently separated in the second dimension.

containing a number of compounds and in some cases, individual species can be seen to be resolved.

As noted in Chapter 6, analysis of the three bands collected from the second dimension fraction cut at 6.92 minutes by mass spectrometry clearly indicated that they contained some compounds that are of simple structure. The question was asked why are small molecular weight compounds present in molecular weight fractions which are of larger molecular weight, and are they present as some sort of structure that when separated in the second dimension disaggregate?

The results of the mass spectrometry analysis of the three second dimensional bands collected from the fraction cut at 6.92 minutes from the first-dimension were significant. They indicated the presence of low molecular weight material (< 250 Da), despite the fact that the fraction cut had to be greater than 1000 Da as it was cut within the exclusion range of 1000-300,000 Da as stated for the column.

Two reasonable explanations for this observed phenomena were put forward in Chapter 6. Firstly that small molecules were entrapped in a complex of larger molecules and were transported through the size-exclusion column, eluting entrapped with the larger molecules; this scenario was referred to as a "hidden host guest model". Alternatively, small molecules were interbound to each other but could not be separated from the host complex during transportation through the size-exclusion column and this scenario was referred to as

the " micellar host guest model". Evidence to support the latter model was put forward and discussed.

As noted in Chapter 6, it was significant that the Bayer humic substances that were eluting closest to exclusion (2.20 minutes) contained the smallest amount of discrete molecular material compared to the lower molecular weight Bayer humic substances what were eluting towards the end of the exclusion range (1,000-300,000 Da) at 7.20 minutes. This showed that the complexes are different and not just larger entities with the same components. It also suggested that the lower molecular weight material separated was capable of entrapping the small guests more than the larger molecular weight material. It is unlikely that small molecules hide best inside lower molecular weight material. Rather the results suggested a micellar host guest model was more convincing where molecules bind together through similar functional groups. This was also supportive of the conclusions found in Chapter 4 that also suggested a micellar host guest model.

The work shown in Chapter 6 did illustrate that two-dimensional HPLC can now be applied to advance not only our knowledge of Bayer liquors but also the structure and role of geochemical macromolecules in other systems. Collection of fractions on a preparative level would allow structural elucidation by techniques such as NMR spectroscopy that could further advance our knowledge on the structure and dynamics of Bayer humic substances.

7.4. CONCLUSIONS

Analysis of the Bayer humic substances by one-dimensional HPLC allowed the following conclusions to be drawn;

1. A high-performance liquid chromatographic method was developed which separated the Bayer humic substances into compound classes. The optimum separation was achieved by running a gradient using PIC A [5 mM]/acetonitrile, running isocratically for 10 minutes on PIC A [5 mM] and then a linear gradient from 100% PIC A [5 mM] to 18% acetonitrile at a rate of change of 0.056% per minute. The gradient continued running from 82% PIC A [5 mM] and 18% acetonitrile to 57% PIC A [5 mM] and 43% acetonitrile at a rate of change of 0.083% per minute. The gradient was then changed to 50% PIC A [5 mM] and 50% acetonitrile over 5 minutes. The solvent composition was then held for 10 minutes.

2. Solvent separation of the humic material yielded compound classes that were then correlated with the optimum separation achieved for the Bayer humic substances. The most polar material concentrated in the least polar solvents indicating that the humic material has a micellar like structure in that polar groups are concentrated to avoid solvent interaction in fractions soluble in the least polar solvents. Two structural models were proposed based on the results, "hidden host guest model" and the "micellar host guest model". Both structural models were discussed further in Chapter 6.

3. Small molecules and three discrete clusters of macromolecules were observed. Within these clusters there was some degree of further resolution. From this it was concluded that only certain configurations are stable otherwise the separation would have shown a continuum of peaks rather than clusters. Four discrete fractions were observed in the separation of the Bayer humic substances under the optimum HPLC conditions which represented certain stable configurations of molecular weights that are controlled by polarity through intramolecular binding and provided strong evidence for a supramolecular structure to humic material rather than the existence of random conformational material.

4. One-dimensional HPLC separations are inadequate to separate complex samples such as Bayer humic substances as the peak capacity of the system was vastly exceeded. Therefore a multidimensional approach must be adopted to separate Bayer humic substances.

From the study of five new generation reversed phase columns for the separation of model humic compounds in, the following conclusions can be made:

1. The analysis of retention information and using factor analysis and information theory the Phenomenex Aqua C18 column and the conventional Phenomenex Luna C18 column displayed the highest degree of retention mechanism equivalency, for a series of polycarboxylic acids and polyphenols. These two columns provided very similar

chromatographic information. The Phenomenex Aqua C18 column also yielded the worst overall performance in terms of peak shape. Further, the Phenomenex Aqua C18 and the Waters XTerra™ RP$_{18}$ offered little as an alternative to that of a conventional Luna C18 column in terms of the separation of polycarboxylic acids and polyphenols.

2. Although the differences in selectivity and retention mechanism equivalency were maximised between the Luna C18 and Luna Cyano columns, the overall retention of the test solutes employed in this study on the Luna Cyano column was limited with most eluting near the column void volume. Consequently the Luna Cyano column was not recommended for the separation of polycarboxylic acids and polyphenols.

3. Overall the Phenomenex Synergi polar-RP column displayed the best performance for the separation of the test solutes. Band shapes generally exhibited less peak tailing and IT and factor analysis indicated that there was a moderate correlation coefficient of 0.70 compared to that of the Luna C18 column. Consequently the Phenomenex Synergi polar-RP column was recommended as an alternative to the conventional C18 column and was used in a multidimensional HPLC system for the separation of Bayer humic substances.

The development of a two-dimensional HPLC separation for Bayer humic substances resulted in the following:

1. A two-dimensional HPLC method was developed for the separation of Bayer humic substances. Using this technique uniform band profiles were resolved that showed promise of being essentially pure individual components. There were a number of major bands that display excellent resolution with future isolation at a preparative level being a seamless process using a goal focused separation approach. In the three sections that were heart-cut from the first size-exclusion dimension with at least 18 baseline resolved components isolated in the second dimension, with many other peaks exhibiting less resolution.

2. Mass spectrometric analysis of the three second dimensional bands collected from a fraction cut from the first dimension at 6.92 minutes showed the presence of a number of low molecular weight material below 250 Da despite the fact they were collected in a fraction that was cut within the specified exclusion range of 1,000-300,000 Da and from what was assumed to be single-component bands. These results provided strong support for a host guest model for these compounds. It was concluded that small molecules are held in some way in some supramolecular structure by larger molecules (host guest complexes). The results suggested that the lower molecular weight material was capable of holding small guests more than larger molecular weight material making the supposition that micellar host guest model is more probable than a model where hosts hide within the guests.

REFERENCES

1. Australian aluminium council. Australian aluminium industry. *Website:* http://www.aluminium.org.au/Pubs.html, **2000**.

2. Hind A.R., Bhargava S.K. and Grocott S.C. The surface chemistry of Bayer process solids: a review. *Colloids and surfaces A: Physicochemical and Engineering Aspects*, **1999**, 146, 359-374.

3. Evans A.M. (ed). Ore geology and industrial minerals an introduction. Blackwell Scientific Publications, London, UK, **1993**.

4. Wefers K. and Misra C. Oxides and hydroxides of aluminium. Alcoa Laboratories, Alcoa Technical Paper No.19, **1978.**

5. Solomom M., Groves D.I. and Jaques A.L. (eds). The geology and origin of Australia's mineral deposits. Oxford University Press, New York, USA, **1994**.

6. Grocott S.C. and Rosenberg S.P. Soda in alumina. Possible mechanisms for soda incorporation. *Proceedings of the second International Alumina Quality Workshop*, Gladstone, Australia, **1988**, 271-287.

7. Armstrong L. Bound soda incorporation during hydrate precipitation. *Proceedings of the Third International Alumina Quality Workshop*, Hunter Valley, Australia, **1993**, 282-292.

8. Atkins P. and Grocott S.C. The impact of organic impurities on the production of refined alumina. *Proceedings of Science, Technology and Utilisation of Humic acids*, CSIRO Division of Coal and Energy Technology, Sydney, Australia, **1988**, 85-94.

9.   Moolenaar R.J., Evans J.C. and Mc Keever L.D.   The structure of the aluminate ion in solutions at high pH. *Journal of Physical Chemistry*, **1970**, 74, 3629-3636.

10.   Wilson M.A., Collin P.J. and Akitt J.W.   Composition of aluminum phosphate solutions. Evidence from Aluminium-27 and Phosphorus-31 Nuclear Magnetic Resonance spectra. *Analytical Chemistry*, **1989**, 61, 1253-1259.

11.   Bradley S.M. and Hanna J.V. ^{27}Al and ^{23}Na MAS NMR and powder X Ray diffraction studies of sodium aluminate speciation and mechanistic of aluminium hydroxide precipitation upon acid hydrolysis. *Journal of the American Chemical Society*, **1994**, 116, 7771-7783.

12.   Power G.P. and Tichbon W.   Sodium Oxalate in the Bayer Process: Its origin and effects. *Proceedings of the second International Alumina Quality Workshop*, Perth, Australia, **1990**, 99-115.

13.   Lever G.   Identification of organics in Bayer liquor. *Light Metals*, **1978**, 71-83.

14.   Sang J.V.   Factors affecting residual Na_2O in precipitation products. *Light Metals*, **1988**, 147-155.

15.   The P.J. and Bush J.F.   Solubility of sodium oxalate in Bayer liquor and a method of control. *Light Metals*, **1987**, 5-10.

16.   Stevenson F.J. (ed).   Humus Chemistry. Genesis, Composition, Reactions.   John Wiley and Sons Inc., New York, USA, **1982**.

17.   Schnitzer M.   Humic substances: chemistry and reactions. *In:* Soil organic matter. Schnitzer M. and Khan S.U. (eds).   Elsevier scientific publishing company, Amsterdam, The Netherlands, **1978**, 1-136.

18.   Senesi N. and Loffredo E.   The chemistry of soil organic matter. *In:* Soil Physical Chemistry. Sparks D. (ed).   CRC Press, New York, USA, **1998**, 241-370.

19. Senesi N. Nature of interactions between organic chemicals and dissolved humic substances and the influence of environmental factors. *In:* Organic substances in soil and water: Natural constituents and their influences on contaminant behaviour. Beck A.J., Jones K.C., Hayes M.H.B. and Mingelgrin U. (eds). Royal Society of Chemistry, Cambridge, UK, **1993**, 73-101.

20. Davies G. and Ghabbour E.A. (eds.). Humic Substances: Structures, Properties and Uses. Royal Society of Chemistry, Cambridge, UK, **1998**.

21. Wilson M.A., Kannangara G.S. and Smeulders D.E. Funeral arrangements for plants. *Journal and Proceedings of the Royal Society of New South Wales*, **2000**, 133(3-4), 71-85.

22. Shevchenko S.M. and Bailey G.W. Life after death: Lignin-humic relationships re-examined. *Critical Reviews in Science and Technology*, **1996**, 26, 95-153.

23. Piccolo A., Conte P. and Cozzolino A. Effects of mineral and moncarboxylic acids on the molecular association of dissolved humic substances. *European Journal of Soil Science*, **1999**, 50, 687-694.

24. Wilson M.A., Ellis A.V., Lee G.S.H., Rose H.R., Lu X. and Young B.R. Structure of molecular weight fractions of Bayer humic substances. 1. Low temperature products. *Industrial & Engineering Chemistry Research*, **1999**, 38(12), 4663-4674.

25. Lobartini J. and Tan K. Differences in humic acid characteristics as determined by carbon-13 nuclear magnetic resonance, scanning electron microscopy and infrared analysis. *Soil Science Society of America Journal*, **1988**, 52, 125-130.

26. Tan K., Lobartini J., Himmelsbach D. and Asmussen L. Composition of humic acids extracted under air and nitrogen atmosphere. *Communications in Soil Science and Plant Analysis*, **1991**, 22(9/10), 861-877.

27. Ogner G. P-NMR(13) spectra of humic acids: a comparison of four different raw humus types in Norway. *Geoderma*, **1983**, 29, 215-219.

28. Santos E.B.H. and Duarte A.C. The influence of pulp and paper mill effluents on the composition of the humic fraction of aquatic organic matter. *Water Research*, **1998**, 32(3), 597-608.

29. Lu X.Q., Hanna J.V. and Johnson W.D. Evidence of chemical pathways of humification: a study of aquatic humic substances heated at various temperatures. *Chemical Geology*, **2001**, 177(3-4), 249-264.

30. Schmidt M.W.I., Skjemstad J.O., Gehrt E. and Kogel-Knaber I. Charred organic carbon in German chernozemic soils. *European Journal of Soil science*, **1999**, 50(2), 351-365.

31. Kogel-Knabner I. ^{13}C and ^{15}N NMR spectroscopy as a tool in soil organic matter studies. *Geoderma*, **1997**, 80, 243-270.

32. Wilson M.A. (ed). NMR techniques and applications in geochemistry and soil chemistry. Pergamon Press, Oxford, UK, **1987**, 62-94.

33. Wilson M.A. Analysis of functional groups in soils by nuclear magnetic resonance spectroscopy. *In:* Soil analysis: modern instrumental techniques. K.A. Smith (ed.). Marcel Dekker, New York, USA, **1991**, 601-645.

34. Preston C.M. Applications of NMR to soil organic matter analysis – history and prospects. *Soil Science*, **1996**, 161, 144-166.

35. Knicker H. and Skjemstad J.O. Nature of organic carbon and nitrogen in physically protected organic matter of some Australian soils as revealed by solid-state ^{13}C and ^{15}N NMR spectroscopy. *Australian Journal of Soil Research*, **2000**, 38, 113-127.

36. Liu X. and Ryan K. Analysis of fulvic acids using HPLC/UV coupled to FT-IR spectroscopy. *Environmental Technology*, **1997**, 18, 417-424.

37. Lobartini J., Orioli G. and Tan K. Characteristics of soil humic acid fractions separated by ultrafiltration. *Communications in Soil Science and Plant Analysis*, **1997**, 28(9/10), 787-796.

38. Tan K.H. and McCreery R.A. The infrared identification of a humo-polysaccharide ester in soil humic acid. *Soil Science and Plant Analysis*, **1970**, 1(2), 75-84.

39. Hatcher P.G., Rowan R. and Mattingly M.A. ^{1}H and ^{13}C NMR of marine humic acids. *Organic Geochemistry*, **1980**, 2, 77-85.

40. Sihombing R., Greenwood P.F., Wilson M.A. and Hanna J.V. Composition of size exclusion fractions of swamp water humic and fulvic acid fractions as measured by solid-state NMR and pyrolysis-gas chromatography-mass spectrometry. *Organic Geochemistry*, **1996**, 24, 859-873.

41. Saiz-Jimenez C. Analytical pyrolysis of humic substances: pitfalls, limitations and possible solutions. *Environmental Science and Technology*, **1994**, 28(11), 1773-1780.

42. Saiz-Jimenez C. and de Leeuw J.W. Chemical characterisation of soil organic matter fractions by analytical pyrolysis-gas chromatography-mass spectrometry. *Journal of Analytical and Applied Pyrolysis*, **1986**, 9, 99-119.

43. Saiz-Jimenez C., Hermosin B. and Ortega-Calvo J.J. Pyrolysis/methylation: A method for structural elucidation of the chemical nature of aquatic humic substances. *Water Research*, **1993**, 27, 1693-1696.

44. Chiavari G., Torsi G., Fabbri D. and Galletti G. Comparative study of humic substances in soil using pyrolytic techniques and other conventional chromatographic methods. *Analyst*, **1994**, 119, 1141-1150.

45. Almendros G., Martin F. and Gonzalez-Vila F. Effects of fire on humic and lipid fractions in a Dystric Xerochrept in Spain. *Geoderma,* **1988**, 42(2), 115-127.

46. Garrison A., Schmitt P. and Kettrup A. Capillary electrophoresis for the characterization of humic substances. *Water Research,* **1995**, 29(9), 2149-2159.

47. Masselter S., Zemann A. and Bobleter O. Analysis of lignin degradation products by capillary electrophoresis. *Chromatographia,* **1995**, 40(1-2), 51-57.

48. Garrison A., Schmitt P. and Kettrup A. Capillary electrophoresis for the characterization of humic substances. *Water Research,* **1995**, 29(9), 2149-2159.

49. Haddad P., Harakuwe A. and Buchberger W. Separation of inorganic and organic anionic components of Bayer liquor by capillary zone electrophoresis. I. Optimisation of resolution with electrolyte-containing surfactant mixtures. *Journal of Chromatography A,* **1995**, 706(1-2), 571-578.

50. Rigol A., Lopez-Sanchez J.F. and Rauret G. Capillary zone electrophoresis of humic acids. *Journal of Chromatography A,* **1994**, 664, 301-305.

51. Pompe S., Heise K.H. and Nitsche H. Capillary electrophoresis for a "finger-print" characterization of fulvic and humic acids. *Journal of Chromatography A,* **1996**, 723, 215-218.

52. Swift R.S. Macromolecular properties of soil humic substances: fact, fiction and opinion. *Soil Science,* **1999**, 164(11), 790-802.

53. De Nobili M. and Chen Y. Size exclusion chromatography of humic substances: Limits, perspectives and prospectives. *Soil Science,* **1999**, 164(11), 825-833.

54. Rausa R., Mazzolari E. and Calemma V. Determination of molecular size distributions of humic acids by high-performance size-exclusion chromatography. *Journal of Chromatography A,* **1991**, 541, 419-429.

55. Varga B., Kiss G., Galambos I., Gelencser A., Hlavay J. and Kirvacsy Z. Secondary structure of humic acids. Can micelle-like conformation be proved by aqueous size exclusion chromatography?. *Environmental Science and Technology*, **2000**, 34, 3303-3306.

56. Conte P. and Piccolo A. Conformational arrangement of dissolved humic substances. Influence of solution composition on association of humic molecules. *Environmental Science and Technology*, **1999**, 33, 1682-1690.

57. Chin Y.P., Alken G. and O'Laughlin E. Molecular Weight, Polydispersity, and Spectroscopic Properties of Aquatic Humic Substances. *Environmental Science and Technology*, **1994**, 28, 1853-1858.

58. Engebretson R.R., Amos T. and von Wandruszka R. Quantitative Approach to Humic Acid Associations. *Environmental Science and Technology*, **1996**, 3, 990-997.

59. Trubetskoj O.A., Trubetskaya O.E., Afanaseva G.V., Reznikova O.I. and Saiz-Jimenez C. Polyacrylamide gel electrophoresis of soil humic acid fractionated by size-exclusion chromatography and ultrafiltration. *Journal of Chromatography A*, **1997**, 767, 285-292.

60. Conte P. and Piccolo A. High pressure size exclusion chromatography (HPSEC) of humic substances: Molecular sizes, analytical parameters, and column performance. *Chemosphere*, **1999**, 38, 517-528.

61. Lin C.F., Lin T.Y. and Hao O.J. Effects of humic substance characteristics on UF performance. *Water Research*, **2000**, 34, 1097-1106.

62. Cozzolino A., Conte P. and Piccolo A. Conformational changes of humic substances induced by some hydroxy-, keto-, and sulfonic acids. *Soil Biology and Biochemistry*, **2001**, 33(4-5), 563-571.

63. Perminova I.V. Size exclusion chromatography of humic substances: Complexities of data interpretation attributable to non-size exclusion effects. *Soil Science*, **1999**, 164(11), 834-840.

64. Perminova I.V., Frimmel F.H., Kovalevskii D.V., Abbt-Braun G., Kudryavtsev A.V. and Hesse S. Development of a predictive model for calculation of molecular weight of humic substances. *Water Research*, **1998**, 32(3), 872-881.

65. Piccolo A. and Conte P. Molecular size of humic substances. Supramolecular associations versus macromolecular polymers. *Advances in Environmental Research*, **2000**, 3, 508-521.

66. Piccolo A. The macromolecular structure of humic substances. *Soil Science*, **2001**, 166(11), 810-832.

67. Ellis A.V., Wilson M.A. and Forster P. Degradation of Klason lignin in sodium hydroxide at 145°C. *Industrial & Engineering Chemistry Research*, **2002**, 41, 6493-6502.

68. Ellis A.V., Wilson M.A. and Kannangara G.S.K. Bayer Poisons: Degradation of angiosperm and gymnosperm water-soluble extracts in sodium hydroxide at 145°C. *Industrial & Engineering Chemistry Research*, **2002**, 41, 2842-2852.

69. Skjemstad J.O., Reicosky D.C., Wilts A.R. and McGowan J.A. Charcoal carbon in US agricultural soils. *Soil Science Society of America Journal*, **2002**, 66(4), 1249-1255.

70. Schmid E.M., Skjemstad J.O., Glaser B., Knicker H. and Kogel-Knabner I. Detection of charred organic matter in soils from a Neolithic settlement in Southern Bavaria, Germany. *Geoderma*, **2002**, 107(1-2), 71-91.

71.   Schmidt M.W.I, Skjemstad J.O., Czimcizik C.I., Glaser B., Prentice K.M., Gelinas Y. and Kuhlbusch T.A.J. Comparative analysis of black carbon in soils. *Global Biogeochemical Cycles*, **2001**, 15(1), 163-167.

72.   Marshall C.P., Kannangara G.S.K., Alvarez R. and Wilson M.A. Characterisation of insoluble char in Weipa bauxite. *Carbon*, **2003**, *(submitted)*.

73.   Baker A.R. and Greenway A.M. Comparison of bauxite and Bayer liquor humic substances by ^{13}C Nuclear Magnetic Resonance Spectroscopy. Implications for the fate of humic substances in the Bayer process. *Industrial & Engineering Chemistry Research*, **1988**, 37, 4198-4201.

74.   Given P.H. and Marzec A. Protons of Differing Rotational Mobility. *Fuel,* **1988**, 67, 242-244.

75.   Redlich P.J., Jackson W.R. and Larkins F.P. Hydrogenation of brown coal Part 9. Physical characterisation and liquefaction potential of Australian coals. *Fuel*, **1985**, 64, 1383 –1389.

76.   Fetsch D., Hradilova M., Mendez E.M.P. and Havel J. Capillary zone electrophoresis study of aggregation of humic substances. *Journal of Chromatography A*, **1998**, 817(1-2), 313-323.

77.   Ong H.L. and Bisque R.E. Coagulation of humic colloids by metal ions. *Soil Science*, **1968**, 106, 220-224.

78.   Havel J., Fetsch D., Peoa-Mendez E.M., Lubal P. and Havli J. Recent developments in humic acid characterisation. Acidobasic and complexation properties, separation and reliable fingerprints by capillary electrophoresis and MALDI-TOF mass spectrometry. *Proceedings of the 9th international meeting of the international humic substances society*, Adelaide, Australia, **1998**, 103-107.

79.   Frimmel F.H.   Impact of light on the properties of aquatic natural organic matter. *Environment International*, **1998**, 24, 559-571.

80.   Smeulders D.E., Wilson M.A. and Armstrong L.   Insoluble organic compounds in the Bayer process. *Industrial & Engineering Chemistry*, **2001**, 40, 2243-2251.

81.   Smeulders D.E., Wilson M.A., Patney H. and Armstrong L.   Structure of molecular weight fractions of Bayer humic substances. II. Pyrolysis behaviour of high temperature products. *Industrial & Engineering Chemistry*, **2000**, 39, 3631-3639.

82.   Harakuwe A., Haddad P. and Jackson P.   Quantitative determination of oxalate in Bayer liquor by capillary zone electrophoresis - a validative study.   *Journal of Chromatography A*, **1996**, 739(1-2), 399-403.

83.   Jackson P.   Analysis of oxalate in Bayer liquors - a comparison of ion chromatography and capillary electrophoresis.   *Journal of Chromatography* A, **1995**, 693(1), 155-161.

84.   Susic M. and Armstrong L.G.   High-performance liquid chromatographic determination of humic acid in sodium aluminate solution.   *Journal of Chromatography A*, **1990**, 502, 443-44.

85.   Smeulders D.E., Wilson M.A. and Kannangara G.S.K.   Host-guest interactions in humic materials. *Organic Geochemistry,* **2001**, 32, 1357-1371.

86.   Wilson M.A., Jones A.J. and Williamson B.   Nuclear magnetic resonance spectroscopy of humic materials. *Nature*, **1978**, 276, 487-500.

87.   Wilson M.A., Collin P.J. and Tate K.R. ^{1}H nuclear magnetic resonance study of a soil humic acid. *Journal of Soil Science*, **1983**, 34, 297-304.

88.   Lee G.S.H., Wilson M.A. and Young B.   The application of the "WATERGATE" suppression technique for analysing humic substances by nuclear magnetic resonance. *Organic Geochemistry*, **1998**, 28(9-10), 549-559.

89. Hatcher P.G., Rowan R. and Mattingly M.A. ^{1}H and ^{13}C NMR of marine humic acids. *Organic Geochemistry*, **1980**, 2, 77-85.

90. Wilson M.A. and Goh K.M. Comment on the paper: ^{1}H and ^{13}C NMR studies on the importance of aromatic structures in fulvic and humic acids. *Geochimica et Cosmochim Acta*, **1981**, 45, 489-490.

91. Preston C.M. and Ripmeester J.A. Application of solution and solid-state ^{13}C NMR to four organic soils, their humic acids, fulvic acids, humins and hydrolysis residues. *Canadian Journal of Spectroscopy*, **1982**, 27, 99-105.

92. Wilson M.A., Farquharson G.J., Tippett J.M., Quezada R.A. and Armstrong L. Aluminophilicity of the humic degradation product of 5-hydroxybenzene-1,3-dicarboxylic acid. *Industrial and Engineering Chemistry Research*, **1998**, 37, 2410-2415.

93. Nagar B.R. Examination of the structure of soil humic acids by pyrolysis-gas chromatography. *Nature*, **1963**, 199, 1213-1222.

94. Wershaw R.L. and Bohner G.E.(Jr). Pyrolysis of humic and fulvic acids. *Geochimica et Cosmochim Acta*, **1969**, 33, 757-762.

95. Kimber R.W.L. and Searle P.L. Pyrolysis gas chromatography of soil organic matter. I. Introduction and methodology. *Geoderma*, **1970**, 4, 47-55.

96. Kimber R.W.L. and Searle P.L. Pyrolysis gas chromatography of soil organic matter. II. The effect of extractant and soil history on the yields of products from pyrolysis of humic acids. *Geoderma*, **1970**, 4, 57-71.

97. Saiz-Jimenez C. and de Leeuw J.W. Chemical characterisation of soil organic matter fractions by analytical pyrolysis-gas chromatography mass-spectrometry. *Journal of Analytical and Applied Pyrolysis*, **1986**, 9, 99-119.

98. Saiz-Jimenez C. and de Leeuw J.W. Chemical structure of a soil humic acid as revealed by analytical pyrolysis. *Journal of Analytical and Applied Pyrolysis*, **1987**, 11, 367-376.

99. Schulten H.R., Plage B. and Schnitzer M. A chemical structure of humic substances. *Naturwissenschaften*, **1991**, 78, 311-313.

100. Schulten H.R. and Schnitzer M. Structural studies on soil humic acids by Curie Point pyrolysis-gas chromatography-mass spectrometry. *Soil Science*, **1992**, 153, 205-216.

101. Challinor J.M. A pyrolysis-derivatisation-gas chromatography-mass spectrometry technique for the structural elucidation of some synthetic polymers. *Journal of Analytical and Applied Pyrolysis*, **1989**, 16, 323-333.

102. Janos P. Separation methods in the chemistry of humic substances. *Journal of Chromatography A*, **2003**, 983, 1-18.

103. Stevenson F.J. and Goh K.M. Infrared spectra of humic acids and related substances. *Geochimica et Cosmochim Acta*, **1971**, 35, 471-483.

104. Braithwaite A. and Smith F.J. (ed). Chromatographic Methods. Chapman and Hall, Glasgow, UK, **1996**.

105. Weston A. and Brown P.R. (eds). HPLC and CE. Principles and practice. Academic Press, New York, USA, **1997**.

106. Snyder L.R. and Kirkland J.J. (ed). Introduction to modern liquid chromatography. John Wiley and Sons Inc, New York, USA, **1979**.

107. Skoog D.A., West D.M. and Holler F.J (eds). High-performance liquid chromatography. *In*: Fundamentals of Analytical Chemistry. Saunders college publishing, New York, USA, **1992**, 712-736.

108.   Robards K., Haddad P.R. and Jackson P.E. (eds).   Principles and Practice of Modern Chromatographic Methods.   Academic Press, London, UK, **1994**.

109.   Dorsey J.G., Cooper W.T., Wheeler J.F., Barth H.G. and Foley J.P.   Liquid Chromatography: Theory and Methodology.   *Analytical Chemistry*, **1994**, 66(12), 500R-546R.

110.   Davis J.M. and Giddings J.C.   Statistical theory of component overlap in multicomponent chromatograms.   *Analytical Chemistry*, **1983**, 55(3), 418-424.

111.   Davis J.M. and Giddings J.C.   Statistical method for estimation of number of components from single complex chromatograms: theory, computer-based testing and analysis of errors.   *Analytical Chemistry*, **1985**, 57(12), 2166-2177.

112.   Giddings J.C.   Maximum number of components resolvable by gel filtration and other elution chromatographic methods.   *Analytical Chemistry*, **1967**, 39(8), 1027-1028.

113.   Rowe K. and Davis J.M.   Relaxation of Randomness in two-dimensional statistical model of overlap: Theory and verification.   *Analytical Chemistry*, **1995**, 67(17), 2981-2993.

114.   Martin M.M., Herman D.P. and Guiochon G.   Probability distributions of the number of chromatographically resolved peaks and resolvable components in mixtures.   *Analytical Chemistry*, **1986**, 58, 2200-2207.

115.   Martin M.M. and Guiochon G.   Analogy between the depolymerization and separation processes. Application to the statistical evaluation of complex chromatograms.   *Analytical Chemistry*, **1985**, 57, 289-295.

116.   Cortes H.J. (ed).   Multidimensional chromatography: Techniques and applications.   Marcel Dekker Inc., New York, USA, **1990**.

117. Sweeney A.P., Wong V. and Shalliker R.A. The separation of Diastereoisomers of polystyrene oligomers in reversed phase HPLC. *Chromatographia*, **2001**, 54(1/2), 24-30.

118. Liu Z.Y. and Lee M.L. Comprehensive two-dimensional separations using microcolumns. *Journal of Mircocolumn Separations*, **2000**, 12(4), 241-254.

119. Kohne A.P. and Welsch T. Coupling of a microbore column with a column packed with non-porous particles for fast comprehensive two-dimensional high-performance liquid chromatography. *Journal of Chromatography A*, **1999**, 845, 463-469.

120. Slonecker P.J., Li X., Ridgway T.H. and Dorsey J.G. Informational orthogonality of two-dimensional chromatographic separations. *Analytical Chemistry*, **1996**, 68(4), 682-689.

121. Sweeney A.P., Wyllie S.G. and Shalliker R.A. The separation of stereoisomers from oligomers of low molecular weight polystyrene on a carbon clad zirconia column using a reversed phase multidimensional HPLC system. *Journal of Liquid Chromatography and Related Technology*, **2001**, 24(17) 2559-2581.

122. Bushey M.M. and Jorgenson J.W. Automated instrumentation for comprehensive two-dimensional high-performance liquid chromatography/capillary zone electrophoresis. *Analytical Chemistry*, **1990**, 62(10), 978-984.

123. Murphy R.E., Schure M.R. and Foley J.P. Effect of sampling rate on resolution in comprehensive two-dimensional liquid chromatography. *Analytical Chemistry*, **1998**, 70, 1585-1594.

124. Opiteck G.J., Jorgenson J.W. and Anderegg R.J. Two-dimensional SEC/RPLC coupled to mass spectrometry for the analysis of peptides. *Analytical Chemistry*, **1997**, 69, 2283-2291.

125. Lemmo A.V. and Jorgenson J.W. Transverse flow grating interface for the coupling of microcolumn LC with CZE in a comprehensive two-dimensional system. *Analytical Chemistry,* **1993,** 65, 1576-1581.

126. Hooker T.F. and Jorgenson J.W. A transparent flow grating interface for the coupling of microcolumn LC with CZE in a comprehensive two-dimensional system. *Analytical Chemistry,* **1997,** 69, 4134-4142.

127. Zhang X.M., Hu H.L., Xu S.Y., Yang X.H. and Zhang J. Comprehensive two-dimensional capillary LC and CE for resolution of neutral components in traditional Chinese medicines. *Journal of Separation Science,* **2001,** 24(5), 385-391.

128. Opiteck G.J., Ramirez S.M., Jorgenson J.W. and Moseley (III) M.A. Comprehensive two-dimensional high-performance liquid chromatography for the isolation of overexpressed proteins and proteome mapping. *Analytical Biochemistry,* **1998,** 258, 349-361.

129. Clarke N.J., Crow F.W., Younkin S. and Naylor S. Analysis of in vivo-derived amyloid-beta polypeptides by on-line two-dimensional chromatography-mass spectrometry. *Analytical Biochemistry,* **2001,** 298(1), 32-39.

130. Issaq H.J. The role of separation science in proteomics research. *Electrophoresis,* **2001,** 22(17), 3629-3638.

131. Wang H., Xu H. and Guan Y. Characterization and source identification of hydrocarbons in water samples using multiple analytical techniques. *Journal of Chromatography A,* **2002,** 971(1-2), 173-184.

132. Raglione T.V. and Hartwick R.A. Liquid chromatography-gas chromatography interfacing using microbore high-performance liquid chromatography with a bundled capillary stream splitter. *Analytical Chemistry,* **1986,** 58, 2680-2683.

133. Mondello L., Dugo P., Dugo G., Lewis A.C. and Bartle K.D. High-performance liquid chromatography coupled on-line with high resolution gas chromatography state of the art. *Journal of Chromatography A*, **1999**, 842(1-2), 373-390.

134. Bieganowska M. and Petruczynik A. Ion-pair chromatography and its application in analysis of pharmaceuticals. *Chemia Analityczna*, **1994**, 39(5), 525-541.

135. Bidlingmeyer B., Deming S., Price W., Sachok B. and Petrusek M. Retention mechanism for reversed-phase ion-pair liquid chromatography. *Journal of Chromatography A*, **1979**, 186, 419-434.

136. Haddad P. and Jackson P (eds). Ion-interaction chromatography. *In:* Ion Chromatography: Principles and applications. Elsevier, New York, USA, **1990**, 165-193.

137. Bidlingmeyer B. Separation of ionic compounds by reversed-phase liquid chromatography: An update of ion-pairing techniques. *Journal of Chromatographic Science*, **1980**, 18, 525-539.

138. Stothers J. (ed). Carbon-13 NMR Spectroscopy, Academic Press, New York, USA, **1972**.

139. Neue U.D., Phoebe C.H., Tran K., Cheng Y. and Lu Z. Dependence of reversed-phase retention of ionisable analytes on pH, concentration of organic solvent and silanol activity. *Journal of Chromatography A*, **2001**, 925, 49-67.

140. Majors R.E. A review of HPLC column packing technology. *American Laboratory*, **2003**, October, 46-54.

141. Rabel F., Cabrera K. and Lubda D. Advancing separation science with monolithic silica HPLC columns. *American Laboratory*, **2000**, December, 20-22.

142. Neue U.D. (ed). HPLC Columns: Theory, Technology and Practice. Wiley-VCH, New York, USA, **1997**.

143. Kele M. and Guiochon G. Repeatability and reproducibility of retention data and band profiles on reversed-phase liquid chromatography columns. I. Experimental protocol. *Journal of Chromatography A*, **1999**, 830, 41-54.

144. Kele M. and Guiochon G. Repeatability and reproducibility of retention data and band profiles on reversed-phase liquid chromatographic columns. II. Results obtained with Symmetry C_{18} columns. *Journal of Chromatography A*, **1999**, 830, 55-79.

145. Kele M. and Guiochon G. Repeatability and reproducibility of retention data and band profiles on reversed-phase liquid chromatography columns. III. Results obtained with Kromasil C_{18} columns. *Journal of Chromatography A*, **1999**, 855, 423-453.

146. Kele M. and Guiochon G. Repeatability and reproducibility of retention data and band profiles on reversed-phase liquid chromatography columns. IV. Results obtained with Luna C_{18} (2) columns. *Journal of Chromatography A*, **2000**, 869, 181-209.

147. Kele M. and Guiochon G. Repeatability and reproducibility of retention data and band profiles on reversed-phase liquid chromatography columns. V. Results obtained with Vydac 218TP C_{18} columns. *Journal of Chromatography A*, **2001**, 913, 89-112.

148. Kele M. and Guiochon G. Repeatability and reproducibility of retention data and band profiles on six batches of monolithic columns. *Journal of Chromatography A*, **2002**, 960, 19-49.

149. Majors R.E. and Przybyciel M. Columns for reversed-phase LC separations in highly aqueous mobile phases. *LC-GC Europe*, **2002**, December, 2-7.

150. Huber J.F.K., Kenndler E., Reich G., Hack W. and Wolf J. Optimal selection of gas chromatographic columns for the analytical control of chemical warfare agents

by application of information theory to retention data. *Analytical Chemistry*, **1993**, 65(20), 2903-2906.

151. Dupuis F. and Dijkstra A. Application of information theory to analytical chemistry. Identification by retrieval of gas chromatographic retention indices. *Analytical Chemistry*, **1975**, 47(3), 379-383.

152. Huber J.F.K., Kenndler E. and Reich G. Quantitation of the information content of multidimensional gas chromatography and low-resolution mass spectrometry in the identification of doping drugs. *Journal of Chromatography*, **1979**, 172, 15-30.

153. Massart D.L., Vandeginste B.G.M., Deming S.N., Michotte Y. and Kaufman L. (eds). Chemometrics: a Textbook. Elsevier Science, London, UK, **1988**.

154. Steuer W., Grant I. and Erni F. Comparison of high-performance liquid chromatography, supercritical fluid chromatography and capillary zone electrophoresis in drug analysis. *Journal of Chromatography*, **1990**, 507, 125-140.

155. Gray M., Dennis G.R., Wormell P., Shalliker R.A. and Slonecker P. Two-dimensional reversed-phase – reversed-phase separations. Isomeric separations incorporating C_{18} and carbon clad zirconia stationary phases. *Journal of Chromatography A*, **2002**, 975, 285-297.

156. Rummel R.J. Understanding factor analysis. *The Journal of Conflict Resolution*, **1967**, 444-480.

157. Reese C.E. and Lochmuller C.H. Introduction to factor analysis. *Website:* http://www.chem.duke.edu/-reese/tutor1/factucmp.html, **1994**.

158. Liu Z. and Patterson D.G. Geometric approach to factor analysis for the estimation of orthogonality and practical peak capacity in comprehensive two-dimensional separations. *Analytical Chemistry*, **1995**, 67(21), 3840-3845.

159. Waters Corporation (eds). Waters Millennium[32]® system suitability software manual. Waters Corporation, Milford, USA, 1997.

160. Giddings J.C. Sample dimensionality: A predictor of order-disorder in component peak distribution in multidimensional separation. *Journal of Chromatography A,* **1995**, 703, 3-15.

161. Wong V. and Shalliker R.A. Isolation of the active constituents in natural materials by 'heart-cutting' isocratic reversed-phase two-dimensional liquid chromatography. *Journal of Chromatography A,* **2004**, 1036, 15-24.

APPENDIX A

Peak width @ half height as calculated by Waters Millennium[32] system suitability software

$$x_{rt} \, y_{rt}$$

$$x_1 \, y_1 \qquad\qquad x_2 \, y_2$$

Width @ 50%

$$x_s \, y_s \qquad\qquad x_f \, y_f$$

Start   Finish
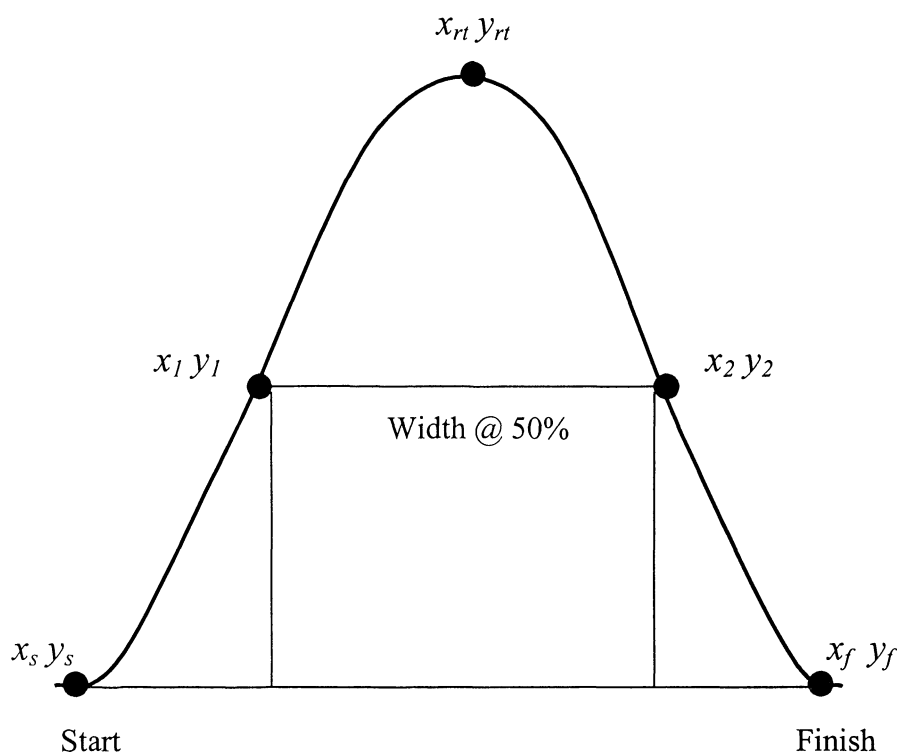
$$width@50\% = (x_2 - x_1)$$

Where: $$y_1 = \frac{1}{2}(y_{rt} - y_f) + y_f$$

$$y_2 = \frac{1}{2}(y_{rt} - y_s) + y_s$$

x_1 = Interpolated point on the chromatogram from x_s to x_{rt} where $y = y_1$

x_2 = Interpolated point on the chromatogram from x_{rt} to x_f where $y = y_2$

APPENDIX B

USP tailing factor as calculated by Waters Millennium[32] system suitability software

Retention time
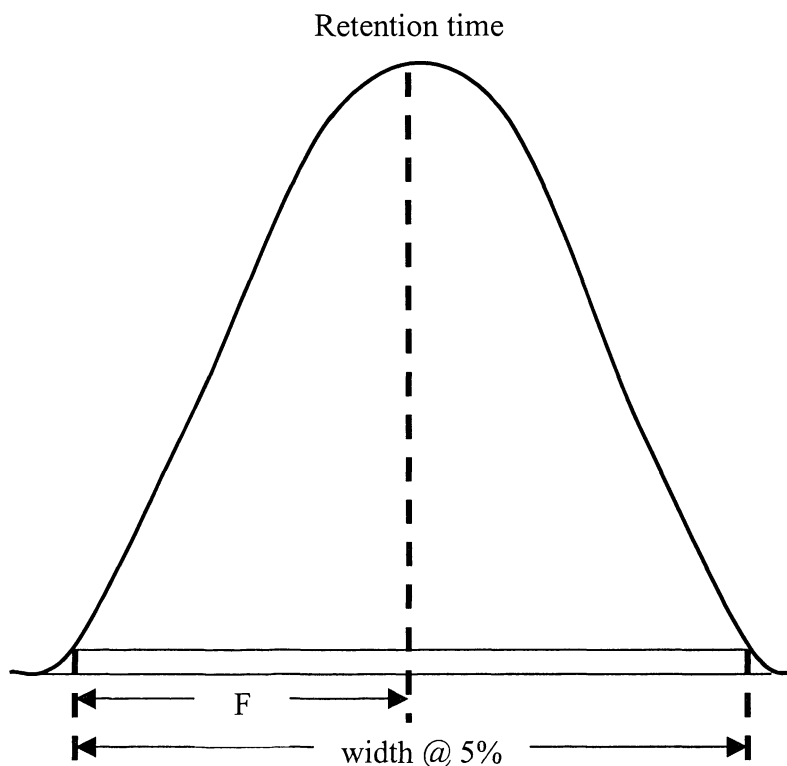
USP tailing factor, T, was defined as the distance between the leading edge and tailing edge of the peak at a width of 5% of the peak height divided by twice the distance, F, between the peak maximum and the leading edge of the peak at 5% of peak height.   The USP tailing factor is calculated using the following equation:

$$T = \frac{W}{2 \times F}$$

T = USP tailing factor,

W = Peak width at 5% of peak height and

F = time from width start point at 5% of peak height to the retention time

APPENDIX C

The following manuscripts were submitted and accepted during the course of this thesis.

Whelan T.J., Ellis A., Kannangara G.S.K., Marshall C., Smeulders D. and Wilson M.A. Macromolecules in the Bayer process. *Reviews in Chemical Engineering*, **2003**, 19(5), 431-471.

Whelan T.J., Kannangara G.S.K. and Wilson M.A. Increased resolution in high-performance liquid chromatograph spectra of high molecular weight organic components of Bayer liquors. *Industrial & Engineering Chemistry Research*, **2003**, 42(26), 6673-6681.

Whelan T.J., Gray M., Shalliker R.A. and Wilson M.A. Study of the selectivity of reversed phase columns for the separation of polycarboxylic acids and polyphenols. *Journal of Chromatography A*, **2004**, *(In Press).*

The following manuscript was submitted during the course of this thesis.

Whelan T.J., Shalliker R.A., McIntyre C. and Wilson M.A. Unravelling the complexity of Bayer humic substances using multidimensional HPLC. *Industrial & Engineering Chemical Research*, **2004**.

Reprinted from

REVIEWS IN CHEMICAL ENGINEERING

Editors:

Dan Luss
University of Houston
Department of Chemical Engineering
Houston, TX 77004, U.S.A.

N. Brauner
Tel Aviv University
Department of Fluid
Mechanics and Heat Transfer
Faculty of Engineering
Ramat Aviv, Israel 69978

MACROMOLECULES IN THE BAYER PROCESS

Thelma J Whelan[1], Amanda Ellis[1], G. S. Kamali Kannangara[2], Craig P Marshall[3], Damian Smeulders[2] and Michael A Wilson[2,*]

[1]Department of Chemistry, Materials and Forensic Science University of Technology, Sydney, Broadway 2007, [2]Office of the Dean, College of Science Technology and Environment, University of Western Sydney, Locked Bag 1797, Penrith South DC, NSW 1797 Australia, [3]Australian Centre for Astrobiology, Department of Earth and Planetary Sciences Macquarie University, Sydney NSW 2109 Australia

ABSTRACT

Organic matter enters the Bayer process during the formation of alumina from bauxite ore via dissolution in concentrated sodium hydroxide at high temperatures. This organic matter interferes with the crystallisation process in a number of ways. The nature of this organic matter is reviewed on the basis of molecular weight. While its function is not fully established, and the prevention of its role has yet to be achieved, much is known about its interaction. Two principle new discoveries have been made, namely 1) a host guest structure to the organic matter, and 2) that a variety of structures exist at different molecular weights. Rather than molecular weight fractions being simple polymers or alike macromolecules, they vary considerably in chemical structure from char to benzoic in nature. This means that organic matter exhibits an array of interactions modes during the crystallization of alumina.

Key words: Bauxite, alumina refining, macromolecules, humic material, sodium oxalate, poisoning

---

* To whom correspondence should be addressed

1. INTRODUCTION

This review discusses recent advances in our knowledge of the role and structure of organic matter introduced with bauxite ore when producing alumina from that ore. Some details on the ore are first described, and then the type of organic matter present However, the main part of the review is concerned with the nature of the organic matter in the process and how it interferes with processing.

1.1. Bauxite

In weathered materials aluminium accumulates in clay minerals or in purely aluminous minerals such as, gibbsite, boehmite, and diaspore, which are the principal minerals of bauxite. Bauxite is a general term for a rock composed of hydrated aluminium oxides and is the material from which alumina is made. It was discovered 175 years ago by Pierre Berthier, a French mineralogist and is the only workable ore of aluminium (see review /1/)

The most popular model proposed for bauxite ore genesis is that bauxite is a residual sedimentary material formed by selective concentration of alumina after the dissolution of carbonate and silicate rocks in subtropical regions. High rainfall areas with pronounced dry seasons such as tropical monsoon and some Mediterranean climates produce saturation and drying of the surface, which results in intensive weathering. This intensive weathering leaches most of the minerals from the top few metres of the soil and leaves the insoluble components such as, iron and aluminium oxides, clay minerals and quartz. This weathering product is termed laterite. Bauxite is laterite enriched in aluminium and most deposits are of the post-Mesozoic age (225-70 Ma).

The amount of the various minerals in bauxite deposits depends on age. Young bauxite deposits are mostly gibbsite, and with age gibbsite gives way to boehmite and diaspore. Gibbsite occurs in monoclinic crystals in bauxites that are mostly of Tertiary (70 Ma) or younger age /1, 2/. Boehmite occurs in orthorhombic crystals in bauxites that are found in deposits of Tertiary and Upper Cretaceous (100-70 Ma) age /1, 2/. Diaspore occurs in orthorhombic crystals in bauxites of older deposits and metamorphic rocks formed by high pressure and elevated temperature /1,2/.

The mineralogical properties of bauxites largely determine the processing conditions for the recovery of alumina. Diaspore is the most difficult to process, and boehmite is more difficult to process than gibbsite. To be classified as economical to mine by today's technology, the bauxite grade must contain over 27% of aluminium oxides /1/. In addition, the amount of inert material, iron oxides, titanium dioxide and non-reactive quartz determines the size of the separation circuits for the removal of this material (collectively termed red mud). These circuits can be very expensive and hence could have an impact on economic viability. Furthermore, the quantity of kaolinite and reactive silica largely determines whether bauxite is classified as commercial or not. At present, if bauxite contains more than 8% silica, it is classed as "not commercial" to process /3/. One more important consideration in bauxite processing is the organic matter content. Significantly, Australian bauxite has the highest organic matter content in the world (0.05-0.5% w/w) /4/. The organic matter has numerous adverse effects on the process, which are discussed in this chapter.

1.2. Bayer Process

The Bayer process (/4/ and refs therein) is used for the industrial-scale production of alumina from the ore bauxite. A processing plant is essentially a three-stage device for heating and cooling bauxite in a large recirculating stream of a highly alkaline solution. In the first major stage, bauxite is added to 3.5-5 M sodium hydroxide at high temperatures (145-245°C) in sealed vessels, termed digesters. The product liquor, which is supersaturated in sodium aluminate, is filtered to remove insoluble residues, such as oxides of silicon, iron and titanium and a geo-organic fraction, humin. This dark red filtrate is termed "red mud". Although the insoluble organics (humin) are removed in this fraction, alkali soluble organic degradation products remain in the process liquor and accumulate on recycling /5-7/.

For a Bayer process plant to operate cost-effectively, different temperatures and molarities of sodium hydroxide are used due to the variability of alumina found in bauxites (Equations 1-3). For gibbsite, 3.5 M NaOH, and temperatures of 135-150°C are used. Thus

$$\gamma\text{-}Al_2O_3.3H_2O + 2NaOH \rightarrow 2NaAl(OH)_4 \tag{1}$$
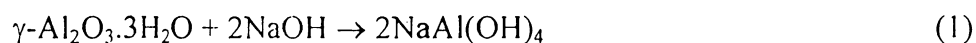
For boehmite, 3.5M NaOH and temperatures of 205-245°C are used. Hence
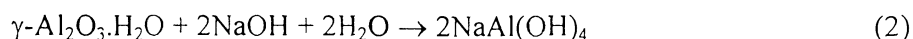
$$\gamma\text{-}Al_2O_3.H_2O + 2NaOH + 2H_2O \rightarrow 2NaAl(OH)_4 \qquad (2)$$

and for diaspore, 5 M NaOH, and higher temperatures are common. Hence

$$\alpha\text{-}Al_2O_3.H_2O + 2NaOH + 2H_2O \rightarrow 2NaAl(OH)_4) \qquad (3)$$
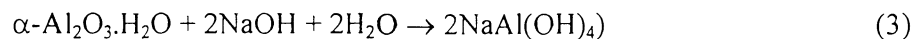
Some modern plants are being designed for the use of higher temperatures.

The next and most critical stage of the process involves cooling the product liquor to approximately 90°C and seeding it to precipitate aluminium hydroxide 'trihydrate'. This involves careful control of conditions to achieve high yields and a good quality product. It is at this point that soluble organic matter contributes detrimentally to the process through suppression of precipitation yields, incorporation of sodium ions, excessive liquor foaming, evolution of odours, increased liquor viscosity and density and effects on alumina crystallisation and agglomeration /5-7/.

After precipitation in the third and final stage, precipitated aluminium hydroxide is calcined at 1200°C to produce alumina (Al_2O_3). Once again, the organics have an adverse effect on the process, causing dusting and decolourisation of the final product.

While a number of technologies have been considered for removing the organics such as photoxidation, prior fractionation of bauxite and post liquor burning, they are all expensive /4/ even though organics have been estimated to be responsible for as much as loss of 20% of production. Organic effects are on each of the processes described below. Methods of removal will be reviewed elsewhere.

1.3. Crystallisation

Crystallisation of alumina from a strongly alkaline solution involves the conversion of the aluminate ion ($AlO_4)^-$ which has tetrahedral geometry to octahedral alumina trihydrate $Al_2O_3.3H_2O$. The process by which this occurs is poorly understood, although there have been suggestions that the aluminate ion dimerises and then addition occurs across the dimer to form a species with octahedral coordination /8/.

Nucleation. A greater understanding of the process can be gained by studying the formation of alumina species at lower pH /9,10/. It is clear that species form polymers either in mildly acidic or mildly basic solution. These

alumina species may be specific such as the Al_{13} species which consists of one tetrahedral aluminium surrounded by twelve octahedral species or long polymer chains, some of which are colloidal, i.e. nanoscale. Five-coordinated aluminium may also be formed transitorily /10/. It would seem logical therefore that nucleation occurs with a number of these species coordinating together so that dimensions of molecules are microsize rather than nanosize. Organic matter with strongly hydrogen bonding groups would coordinate to Al^{3+} species thereby interfering with the process.

Crystal Growth. A second source of interference is during the crystal growth. As the lattice forms, organic molecules may sit on the surface and need to be displaced for further aluminium species to precipitate. These organic molecules may occlude thereby creating lattice defects, or the displacement process may slow down the entire crystallisation. Further, these organic molecules may act as nuclei for other impurities or may prevent individual crystals agglomerating together. Thus some of the compounds present hamper the precipitation of aluminium hydroxide by adversely altering the desired product size distributions and by increasing the amounts of impurities in the product crystals. Organic matter can also affect the crystallisation of other materials in solution, such as sodium oxalate which needs to be removed.

The most important organic contaminant found in highest yield in Bayer liquors is sodium oxalate /11/. At sufficiently high concentrations sodium oxalate may precipitate as fine needles onto which the aluminium hydroxide 'trihydrate' co-precipitates. Once the sodium oxalate obtains a high enough concentration, oxalate crystal nuclei form suddenly in the liquor resulting in what is termed "oxalate showers". These nuclei then allow for gibbsite nucleation onto the oxalate surface. This product is useless.

However the presence of some organic matter species in Bayer liquor are beneficial in this role (although detrimental in others) in that they may stabilise the sodium oxalate in solution, hence reducing the likelihood of the above process.

One might think that oxalate removal can be achieved just by calcination since oxalate can readily be decomposed by heat to carbon dioxide. In fact the sodium oxalate is decomposed to carbon dioxide; however the final alumina product is contaminated with high levels of sodium. This creates very small particles of alumina as the sodium reduces proper calcined particle agglomeration. Finely sized alumina (< 11 μm^2) is not acceptable as a material for alumina production.

In order to control the sodium oxalate concentration a side-stream process in which sodium oxalate is precipitated from the spent (unsaturated) liquor is used. The liquor and precipitate are vacuum filtered then passed through a fabric filter press. The resultant liquor now has a sodium oxalate concentration of approximately 2.0 g/L compared with 4.0 g/L prior to oxalate precipitation.

BAUXITE ORGANIC MATTER

2.1. Bauxite Organic Matter Components

The bauxite entering the process contains essentially two types of organic matter. The first type of organic matter is large vascular plant root systems that penetrate deep into the bauxite deposits from overlying trees. These systems contain largely lignin (up to 26% w/w) and carbohydrates (up to 60% w/w). The dissolution of these components under lower temperature Bayer process conditions has been reported /12,13/.

The second type of organic matter is geo-organic matter/humic material, which has accumulated over the history of the bauxite deposit through geochemical and bacterial transformation of plant and animal matter /11, 14/. This includes alkali soluble species that enter and impinge on the process, and any alkali insoluble organic material, humin, being removed with the red mud. These materials are not all plant derived, as many other alkanes and alkenes, polycondensed aromatics, high nitrogen and long chain fatty acids /11-17/, can originate from bacteria, and fungi. The presence of charcoal-like material termed "char" from ancient forest fires has also been observed in soils and humic extracts /15,16,17/ and bauxite /18/. Tests carried out on one of the "char" samples suggest that it is largely insoluble and is expected to be removed along with red mud /18/.

Given the significance of organic matter content to the process, industrial confidentiality restricts reports in the open literature on organic matter distribution in individual bauxite deposits. However there is at least one report on the organic matter in bauxite and this shows it is not unlike that in many soils /19/.

2.2. Host guest theory

It is clear that a myriad of chemical compounds of different molecular weights make up the organic matter in soils and would therefore end up in

bauxite. For organic matter produced in reducing environments, such as coal and lignite, a Host Guest theory has been proposed based on solubility and reactivity /20, 21/. ^{1}H NMR spectral data also revealed the existence of two groups of molecules in bituminous coals with different molecular rigidities, i.e. rigid large hosts and smaller mobile guests, although there will be rapidly moving groups in hosts such as methyl groups which blur the distinction.

It is also probable that these assemblies could exist in soils and in bauxite /22/. Despite attempts to remove low molecular weight organic matter by dialysis, specific molecular weight fractions revealed the presence of low molecular weight organic matter /22/. These host-guest interactions may occur in a variety of humic macromolecular compounds in the environment. The exact mechanism of entrapment is not known but it is likely that the organic guest molecules are included in the host molecule via formation of intermolecular interactions such as hydrogen bonding. Physical entrapment in the large host structure is also possible.

Another method could be through chelation to metal ions. This may be a mechanism of breaking intra or intermolecular interactions, which may create voids or indeed a mechanism of forming other voids. Chelation may release guests or entrap others. Energetically the destruction of host-guest complexes is expected to be less demanding than the destruction of covalent bonds. Indeed it has been demonstrated that humic substances under go facile degradation with UV radiation rather than polymerisation /23-26/. It can be envisioned that a series of events are taking place, for example, oxidation of host component phenols to quinones which removes any possibility of hydrogen bonding and then subsequent release of small molecular weight guests.

2.3. Dissolution of Lignin

In elucidating the role of different organic components in wood and roots it is desirable to separate lignin /27/ from carbohydrate. Klasons lignins *Callitris rhomboidea* (gymnosperm), *Corymbia callophylla* (angiosperm) and *Eucalyptus marginata* (angiosperm) roots have been digested under Bayer laboratory simulated conditions at 145°C /12, 13/.

The dissolution of lignin under highly alkaline conditions is far from trivial. The degree of dissolution is dependent upon the plant species, i.e. gymnosperm or angiosperm. Plant material high in syringyl (angiospermous) monomers (3,5-dimethoxy, 4-ether aryl compounds) in the lignin show an

increase in dissolution in comparison to plants high in guaiacyl (gymnospermous) monomers (3-methoxy, 4- ether aryl compounds). In addition, a variety of linkages, which tether the monomers, make lignin dissolution highly complex. The fact that the kinetics are not single order in lignin and need to be expressed effectively by a series of exponentials suggests that more than one bond is broken during dissolution and that these occur at different rates. It also suggests that either the concentrations of these bonds and /or types of bonds vary in different lignins. This result is important as it means that different plants will behave differently in the Bayer process.

The breakage of β-O-4 linkages is believed to be the rate-determining step for dissolution of lignin in alkali and is initiated through base attack and removal of protons on the oxygen at the α carbon followed by intramolecular nucleophilic displacement of phenolic anions /28/. The polymeric and cross-linked nature of lignin induces physical constraints that make it less reactive toward attacking species after the initial removal of the β-O-4 linkages.

Solid state ^{13}C NMR analysis shows, after correction for relaxation, the amounts of various structural carbon groups in the extracts and residues. This is not particularly useful, except for showing trends in dissolution. However, by combining yield data it is possible to determine changes in structural group content as the original lignin dissolves. The total amount of carbon in a functional group (Σf_C) in solid and solution phase is given in g/100g of original lignin (Equation 4). This data is given in Table 1 for one example.

$$\Sigma f_C = [(\% \, C_{residue} \, f_{C \, residue} \, \%yield_{residue}) / 100] +$$
$$[(\% \, C_{extract} \, f_{C \, extract} \, \%yield_{extract}) / 100] \tag{4}$$

In equation (4), the $\%C_{residue}$ and $\%C_{extract}$ are the percentage carbon in each Klason lignin, in the residue or extract respectively. The parameter f_C is the fraction of a particular carbon type in the residue or extract from integration of relaxation corrected solid-state NMR spectra and % yield$_{residue}$ and % yield$_{extract}$ are the yields of the residue or recovered extract, respectively.

For *Callitris rhomboidea* there appears to be an initial reaction that involves loss of 22% carbon as aromatic and methoxy carbon (Table 1). Aromatic carbon drops by 53% of the original aromatic carbon. Some aromatic carbon must be converted by base to gas, carbonate or carbon dioxide or other small volatile molecules lost during work up. There is however an increase in aliphatic carbon. Hydroxylation of syringyl and

438

related compounds, followed by ring opening with carbon capture, probably occurs by intramolecularly capturing hydrogen that is generated in any base catalysed organic matter oxidation reaction (schematically for a carboxylic salt, $RCH_3 + H_2O + NaOH \rightarrow 6H + RCOONa$). Table 1 shows that only a small amount (5% total) of further gasification occurs for *Callitris rhomboidea* with increasing time. The same initial processes appear to be occurring for *Corymbia calophylla*. and *Eucalyptus marginata*. For these two lignins 11-12% of the carbon is volatilised. The trend in initial loss of aromatic carbon is *Callitris rhomboidea* > *Eucalyptus marginata* > *Corymbia calophylla*. For *Corymbia calophylla* there is virtually no initial loss.

These results are confirmed by the change in methoxy content. There is an initial rapid loss for *Callitris rhomboidea* due to aryl ring opening. After initial dissolution for all three lignins this continues but at a much slower rate, if at all, and aromatic ring decomposition stops. Indeed some aromatic carbon is recovered through later aromatisation reactions.

The most interesting feature of Table 1 is the reduction in alkoxy carbon. *Callitris rhomboidea*, the gymnosperm, which has the lowest apparent content (6.4%), has a value of only 2.0% after 96 hr. *Eucalyptus marginata* has 9.7% carbon of this type but shows a loss to 4.3% and a faster rate of dissolution. On the other hand *Corymbia calophylla* has 13.0% O-alkyl carbon and this reduces to 6.3%. Most of this loss is during the initial dissolution, and for *Corymbia calophylla*, O-alkyl cleavage is almost over after initial reaction but for the other lignins the reaction continues at a slower rate. Although the results show that the rate of dissolution is clearly dependent on the syringyl content, the electron donating ability of a second methoxy group on the aryl ring should however increase the energy of the β-O-4 decomposing transition state through the 4 position, slowing the rate. However it is the gymnosperm that dissolves slowest, not the angiosperms. One possible explanation is that because a di-aryl linkage can replace the methoxy group in gymnosperms, this holds the lignin together, preventing dissolution. However it is difficult to see how hydroxide slowly breaks this linkage and it appears dissolution requires the β-O-4 linkage to hydrolyse. Perhaps, in the early dissolution for gymnosperms there are internal rearrangements of structures with β-O-4 to α-O-4 linkages which then hydrolyse slower. Such reactions have been suggested for other lignin reactions and demonstrated for model lignin dimer hydrolysis /27, 28/.

The degradation products from the lignin monomers are aromatic carboxylic acids, but their side chains and ring opened products are

Table 1

Yield of different carbon types (g/100g original lignin)
in residues and extracts.

Extraction time (hr)	Assignment					
	Alkyl	Methoxy	O-alkyl	Aromatic	Carboxyl	Σ
Callitris rhomboidea[a]	15.1	4.1	6.4	30.4	2.8	58.8
0	21.0	2.8	6.5	14.3	1.2	45.8
1	21.0	3.4	4.9	18.6	0.9	48.8
5	16.1	3.3	5.2	18.1	1.1	43.8
24	20.2	3.5	3.2	18.7	0.8	46.4
50	17.0	2.8	2.1	22.8	1.7	46.4
96	15.6	2.7	2.0	21.2	1.6	43.1

Eucalyptus marginata[a]	13.2	7.0	9.7	27.0	1.0	57.9
0	13.8	6.1	9.6	21.3	0.6	51.4
1	12.8	6.9	6.6	25.7	1.2	53.2
5	13.7	5.8	5.2	24.4	1.3	50.4
24	13.9	5.4	3.4	25.5	0.9	49.1
50	16.2	4.8	4.7	23.4	0.9	50.0
96	14.6	4.2	4.3	27.2	1.1	51.4
Corymbia calophylla[a]	14.3	5.6	13.0	27.0	1.0	60.9
0	10.5	7.5	6.5	28.3	0.8	53.6
1	11.2	5.8	8.8	22.7	0.8	49.3
5	11.1	6.0	6.6	25.0	1.2	49.9
24	14.3	6.7	7.3	23.0	0.5	51.8
50	11.8	6.4	5.5	27.3	0.7	51.7
96	13.1	6.1	6.3	26.3	0.7	52.5

[a] Calculated from solid state ^{13}C NMR spectrum and % carbon in lignin

polyalcohol and polyhydroxy structures. These are known poisons and can interfere with precipitation of both alumina and the by-product sodium oxalate. Formation of aliphatic chain structures under the conditions described could oxidise to alcoholic species, which are undesirable. However, it does seem that the conditions are harsh enough to make minimal impact arising from the lignin component of plant tissue. The results show that the degree of β-O-4 linkages and hence the production of these phenols is plant specific, indeed Klason lignin type specific. Hence any technology that can remove specific plants may be of value.

2.4. Dissolution of Carbohydrates

Carbohydrates are a significant organic input into the process, whether in native plant matter or as bacterial by-products. Cellulose, in particular, decomposes to give glucose units which readily undergo further decomposition processes, even under less severe conditions. Typically the major decomposition products of glucose under Bayer process conditions are sodium formate, sodium acetate and sodium lactate /29,30/.

Isolation of water-soluble native plant carbohydrates that might enter the Bayer process has been achieved /13/ and their dissolution studied. Gas chromatography-mass spectrometry (GC/MS) chromatographs of the tetramethylsilane (TMS) derivatives of these digestion extracts were useful in determining what species are being formed under dissolution. Each carbohydrate extract digestion yielded a wide variety of compounds, the majority of which were mono-, di- and tri- carboxylic and hydroxy aliphatic and aromatic carboxylic acids of low molecular weight and some carbohydrate species.

Compounds can be grouped into several classes according to their formation or destruction kinetics. Those which: 1) decrease in concentration with time, 2) remain constant in concentration with time, 3) increase in concentration with time and have complex profiles. Carbohydrates such as D-xylose (a), β-D-arabofuranose (b), D-mannose (c), α-D-arabopyranose (d), D-lyxose (e), xylitol (f), D-ribose (g), D-glucose (h), D- altrose (i), D-allose (k), and β-D-fructofuranosyl-α-D-glucopyranoside (l), shown in Figure 1, were found to decrease in concentration for all three plant digestions. Furans such as 2-furancarboxylic acid also decrease in concentration. It is well known that furans are derived from thermal decomposition of carbohydrates. Hence they are an intermediate that is rapidly decomposed. However, it is

significant that the carbohydrate glucitol (j) remains almost constant in concentration for all three-plant digestions. This carbohydrate species is characteristic of many virulent precipitate poisons.

Almost all the small substituted aliphatic carboxylic acids increase in concentration. Lactic acid, hydroxyacetic acid, 2-hydroxybutanoic acid, propanedioic acid, 4-hydroxybutanoic acid and 2-hydroxypropanedioic acid are such examples. This is also true of oxalic acid.
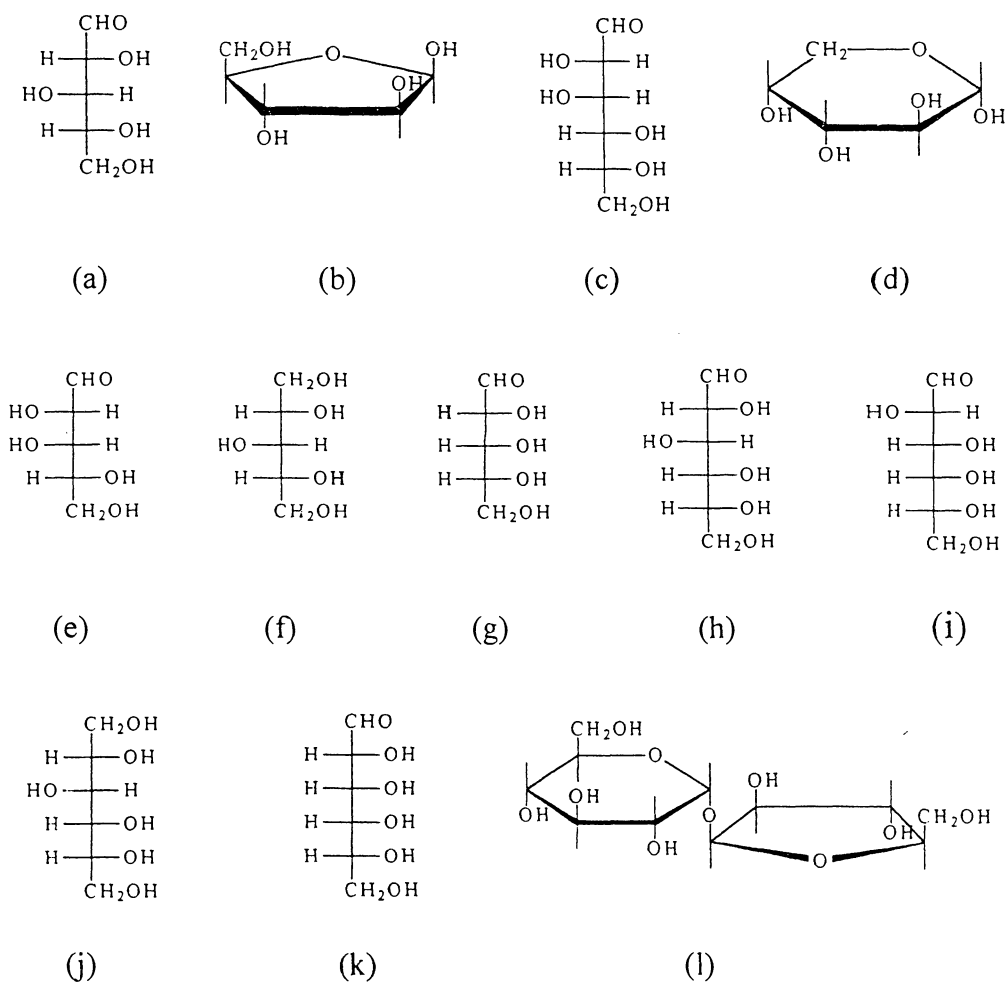
Fig. 1   Structures of carbohydrates such D-xylose (a), β-D-arabofuranose (b), D-mannose (c), α-D-arabopyranose (d), D-lyxose (e), xylitol (f), D-ribose (g), D-glucose (h), D- altrose (i), D-allose (k), and β-D-fructofuranosyl-α-D-glucopyranoside (l).

As noted in section 2.3, the compounds formed from lignin during Bayer processing are different from many of the compounds shown here. Hence it is clear that selective removal of carbohydrates before Bayer processing will influence the nature of organics present in the Bayer liquor and this may affect yields. Water washing is obviously a potential methodology but drying costs could be prohibitive. Another option is thermal maturation.

Like lignins, the mechanism by which carbohydrates yield small molecular weight compounds is by no means trivial, but it is clear from previous work that acetate, formate and lactate are derived from glucose during Bayer processing /29, 30/. The formation of such species is best illustrated by labelling studies, which can indicate where carbons on different parts of the carbohydrate molecule end up. Digestions of unlabeled and labeled 1-^{13}C-D-glucose and 6-^{13}C-D-glucose for 1 hr at 145°C in 3.5 M NaOH have been carried out /30/. Table 2 shows enhanced yields of ^{13}C in products relative to that in the original unlabeled mixture of products.

It is clear that these values are greater than one, and that the label from 1-^{13}C-D-glucose and 6-^{13}C-D-glucose ends up in all carbons in the products. It is also shown in Table 2 that the labeled lactate is the predominant compound formed from both 1-^{13}C-D-glucose and 6-^{13}C-D-glucose under these conditions. The labelling occurs at all three lactate carbons but in different proportions and shows that from 1-^{13}C-D-glucose the production of C1 and C3 labeled lactate is favoured while from 6-^{13}C-D-glucose the production of C3 labeled lactate only is more favoured. The distribution of label in other compounds is also very dependent on the position of label in glucose. In formate the amount of label also depends on the source used. In acetate more label occurs on methyl carbon from 1-^{13}C labeled than 6-^{13}C labeled carbon.

Once formed, the label then becomes indiscriminately scrambled as lactate decomposes. 1-^{13}C-sodium-L-lactate studies showed that ^{13}C labeled carboxylate (COO$^-$) is scrambled equally among carbonate and both carbons in product ethanol molecules. This suggests a common 1,2,3 trihydroxy-cylopropane intermediate. However, decomposition of lactate can be influenced by a number of factors /29/. Agents that inhibit hydride, hydroxy or methyl transfer may be effective since the stability of transition states to the species shown will be sensitive to a number of reaction conditions.

Table 2

^{13}C distribution (%) and enhanced yield in products from unlabeled digested α-D-(+)-glucose and labeled 1-^{13}C-D-glucose and 6-^{13}C-D-glucose digestions in 3.5 M NaOH for 1 hr at 145 °C.

Product	Chemical shift δ (ppm)	Unlabeled α-D-(+)-glucose digestion (1 hr)	1-^{13}C-D-glucose digestion (1 hr)	6-^{13}C-D-glucose digestion (1 hr)	Enhanced yield[a] 1-^{13}C-D-glucose digestion (1 hr)	Enhanced yield[a] 6-^{13}C-D-glucose digestion (1 hr)
Lactate						
COO⁻	185.6	28.7	49.5	24.2	155.2	76.2
CHOH	71.1	24.8	1.0	1.1	3.7	3.7
CH$_3$	23.2	21.6	37.8	33.7	157.9	140.5
Glycolate						
COO⁻	184.6	2.7	3.5	2.9	116.6	96.4
CH$_2$OH	66.5	2.8	0.1	31.7	3.7	1019.2
Acetate						
COO⁻	184.1	0.1	0.1	0.1	90.0	90.0
CH$_3$	26.3	0.1	1.3	0.4	1169.8	359.9

Table 2 (continued)

^{13}C distribution (%) and enhanced yield in products from unlabeled digested α-D-(+)-glucose and labeled 1-^{13}C-D-glucose and 6-^{13}C-D-glucose digestions in 3.5 M NaOH for 1 hr at 145 °C.

Ethanol CH$_2$OH	57.0	3.0	0.1	0.1[b]	2.8	2.8
CH$_3$	17.6	3.2	0.3	0.1	8.3	2.8
Formate HCOO$^-$	173.8	0.1	1.3	0.5	1169.8	449.9
Carbonate CO$_3^{2-}$	170.9	9.7	0.4	0.4	3.7	3.7
Other products		3.2	4.6	4.8	129.5	135.0

[a] Enhanced yield is defined as yield of functional group in ^{13}C labeled experiment (g/100g) / yield in unlabeled experiment (g/100g) = [(% distribution in labeled experiment (g/100g) × fraction of label enhancement in glucose, 0.99) / (% distribution in unlabeled experiment (g/100g) × fraction of natural label enhancement (0.011 for ^{13}C in natural glucose))].

[b] approximate, trace only

3. ORGANIC FRACTIONATION

3.1. Organics in red mud

During the digestion stage of the Bayer process, most organics in the bauxite dissolve but some organic material is insoluble. The insoluble organic matter is removed from the process with the red mud waste product, as an organic rich material on heater tubes in the shell-side of heat exchangers, or adsorbed on aluminium hydroxide precipitate and the sodium oxalate by-product. Sometimes organic matter is also observed in precipitation tank scale and with oxalate-gibbsite co-precipitated fine particles.

It is worthwhile observing the differences in chemical structure between the organic matter that was insoluble in sodium hydroxide that ends up in the red mud, with the organic material in the original bauxite as this provides an insight into the changes taking place during digestion. However, simple pyrolysis-GC/MS is insufficient to compare the two components in the red mud and bauxite because the iron oxide, but not the alumina species, catalyses the decomposition of the organics /31/.

The methanol soluble products are different in the red mud and bauxite as shown by pyrolysis. The pyrolysis products from the methanol solubles from the red mud contained various alkanes, alkenes, aromatic carboxylic acids, and aliphatic carboxylic acids. Some examples include methyl benzoate, methyl esters of saturated C_4 - C_{20} carboxylic acids and C_{11} - C_{23} alkenes. Few aromatic compounds were seen in the extracts /31/. Some of the species released from the red mud were also released from the bauxite when it was analysed under the same conditions, however the compounds were present in very different amounts. These results highlight that the composition of the organic materials in the bauxite and red mud are intrinsically different.

It is clear from the above results that the dissolution of organic matter in the Bayer process is selective. That is, the molecular structure of the organic matter in the red mud differs from that in the bauxite and also from the soluble compounds that dissolve in the Bayer liquor. Surprisingly some of the most polar compounds including the short chain carboxylic acids concentrate in the red mud despite their solubility in sodium hydroxide. These results suggest that the red mud acts as an adsorbent for these compounds.

3.2. Other insoluble organics

As noted in Section 3.1, insoluble organic material (Table 3) is removed at several other stages of the Bayer process including as an organic rich material on heater tubes in the shell-side of heat exchangers, on aluminium hydroxide precipitated crystals, the sodium oxalate by-product, as well as in precipitation tank scale and with oxalate-gibbsite co-precipitated fine particles.

After digestion, the first cooling event occurs at the heat exchanger units. Here an organic material forms on the shell-side of heater tubes and contains enough carbon to be analysed by ^{13}C CP/MAS NMR. The material is highly aromatic, and the aromaticity [fraction of carbon that is aromatic, (f_a)] is 0.40 /31/. The absence of carboxylic carbon at or about 175ppm chemical shift shows that this material is not humic like. Pyrolysis-GC/MS data on the same material identified the sample as having the composition of a light pitch or tar.

Solid-phase sodium oxalate plays a minor role in the sodium content of product alumina, but it has a critical role in gibbsite nucleation in precipitation operations, determining crystal size and particle numbers /5,6/. The presence of organic matter in the Bayer liquor stabilises the oxalate in solution to some extent; however, once oxalate precipitation begins the oxalate surface adsorbs some of the organics from the liquor promoting further precipitation. This phenomenon, known as 'oxalate showers', disturbs the orderly precipitation of aluminium hydroxide, causing excess nucleation leading to fines in the circuit and poor quality alumina with a high sodium content /5,6/. Most alumina refineries use an oxalate removal circuit to control the process and minimise the impact of this material. As a result, the crystallised oxalate is also a material that removes insoluble organic material from the Bayer process.

Crystallised aluminium hydroxide also contains insoluble organic material. These aluminophilic organics play a role in the poisoning of the Bayer process by altering the growth of gibbsite crystals from the Bayer liquor.

The solid state ^{13}C NMR spectra of the insoluble carbon in the sodium oxalate and aluminium hydroxide are similar. The NMR spectra contain three main regions – a distinct aromatic region (100-150 ppm), a less intense aliphatic region consisting of carbon substituted with electron donating groups (50-100 ppm) and a series of peaks in the region between 160-180

Table 3

Organic matter in solution and in deposits from a refinery operating at 250-255°C

	C-Alkyl 0-50 (ppm) %	O-Alkyl 50-100 (ppm) %	Aromatic 100-160 (ppm) %	Carboxylic 160-190 (ppm) %	Carbonyl 190-220 (ppm) %
Deposits					
Heat exchanger scale	60.0	0	40.0	0	0
Sodium oxalate	13.0	0	33.5	53.5	0
Aluminium hydroxide	22.5	0	35.5	42.0	0
Precipitation tank scale	28.6	0	55.8	15.6	0
Oxalate-gibbsite co-precipitation fines	25.7	0	34.9	39.4	0
Molecular weight fractions (kDa) in solution					
<1.2	20.6	2.4	52.9	23.1	1.0
1.2-6	22.4	4.3	55.9	16.7	0.7
6-12	18.8	10.9	56.8	12.2	1.3
12-25	13.0	6.6	62.9	16.2	1.4
25-50	11.8	8.4	58.3	20.6	1.2
50-100	14.6	0.1	67.3	16.9	1.1
100-300	23.2	7.2	58.7	10.1	0.9
>300	26.3	6.9	58.7	7.8	0.4

ppm due to the presence of carboxylic carbon and oxalate /31/.

Sodium oxalate and aluminium hydroxide produced several common pyrolysis products including alkanes, alkenes and long chain aliphatic carboxylic acids (predominantly with C_{14} to C_{16} carbon chain lengths), as well as short chain (C_4-C_7) aliphatic mono-, di- and tri- carboxylic acids. The main difference is that the aluminium hydroxide pyrolysates also contain large amounts of fluorene, biphenyl and methyl-substituted naphthalenes, as well as low concentrations of methyl-substituted phenanthrenes and anthracenes and two alkanes, C_{20} and C_{21}.

Oxalate-gibbsite co-precipitation fines are a network of aluminium hydroxide and sodium oxalate crystals that do not settle from the Bayer liquor. This product gave pyrolysis products including alkanes, alkenes, aromatic compounds including substituted benzenes, alkylbenzenes, napthalenes as well as substituted anthracenes, phenanthrenes and fluorenes. The solid state ^{13}C NMR spectrum of the oxalate-gibbsite co-precipitation fines showed the presence of aliphatic and aromatic carbon. NMR spectra of oxalate-gibbsite co-precipitation fines show a range of structural groups including aromatic and methoxy /31/. The presence of such a wide range of chemical groups may poison further precipitation and growth of the crystals. This may explain why the crystals of aluminium hydroxide and sodium oxalate fines were prevented from growing sufficiently large to be settled from the Bayer process by gravity separation.

Precipitation tank scale contains both precipitated sodium oxalate and aluminium hydroxide. The ^{13}C NMR spectrum of the precipitation tank scale appeared quite similar to the NMR spectra obtained for dissolved humic substances with the proportions of the different carbon types also being similar /31/.

4. ORGANICS IN SOLUTION

4.1. Process differences due to temperature

Typical concentrations of organics in Bayer liquors which are extracted from the bauxite into the Bayer process liquor during digestion range from a few grams per litre up to 40 g/L, /5/ and they have molecular weights from less than 100 Da to greater than 300 kDa /32, 33/. As already noted this geo-organic matter causes numerous problems in the operation of alumina

refineries. The compositions of organic materials obtained from a low temperature Bayer refinery (145-150°C) and a high temperature refinery (250-255°C) have been compared /32, 33/.

Typical chemical compositions of the organic molecular weight fractions are detailed in Tables 3 and 4 but they vary with refinery /32, 33/. Table 4 also shows compositions of whole liquor organics prior (pregnant) and post (spent) precipitation of alumina hydrate. Table 4 shows the smallest molecular weight fraction, the <1.2 kDa fraction, accounting for 87% of the recovered organic material from a refinery operating at 250-255°C. Structurally the <1.2 kDa fraction contains mainly hydroxybenzene carboxylic acids /32, 33/. The 12-25 kDa and 25-50 kDa fractions appear to resemble material more akin to kerogen, while the highest molecular weight organic material (>300 kDa) behaves as a soluble char /32, 33/.

Table 4 shows that the acidities of the organic fractions are highly variable. The two whole organic fractions, from the pregnant and spent liquors, as well as the <1.2 kDa fraction are the most acidic. The pH of each fraction generally increases with increasing molecular weight; however, the 12-25 kDa fraction is an exception. Acidity of the fractions is an important factor during precipitation testing as this affects local ionic strengths of the Bayer solutions, which has an impact on oxalate stability, and precipitation yields.

4.2. Small molecular weight molecules

The amount of less than 1.2 kDa molecules is highly dependent on temperature, bauxite geological history and species of native plant matter as previously described. This is the most acidic fraction containing the highest proportion of carboxylic carbon (20%, 145°C and 23.1%, 245°C), compared with >300 kDa higher molecular weights (9.8%, 145°C and 7.8%, 245°C) /15-18/. Much of this fraction comprises of very low molecular weight species, such as, oxalate and lactic, acetic and formic acids and a range of benzene carboxylic acids /5-7/. They are well documented by Lever /34/. Table 5 shows comparative py-GC/MS data between compounds found in the lowest molecular weight fraction isolated from a low temperature (145°C) /32/ and high temperature (245°C) /33/ processes which shows clear differences in volatiles upon pyrolysis.

It is clear that the presence and thus the formation of compounds in the low molecular weight fractions isolated from Bayer liquors are Bayer plant

Table 4

Yields, acidity and elemental analysis of the Bayer humic substance fractions

(dry ash free basis) from a refinery operating at 250-255°C

Fraction No.	Molecular weight fraction (kDa)	%C	%H	%N	%S	%O Difference	O/C	H/C	N/C	S/C	pH at 5g/litre in water	Mass yield (%)[a]
PL[b]	<1.2 to >300	56.32	3.67	0.36	0.23	39.42	0.53	0.78	0.0055	0.0015	2.43	100.00
SL[b]	<1.2 to >300	53.13	3.58	0.11	0.11	43.07	0.61	0.80	0.0018	0.00078	2.39	100.00
1	<1.2	50.79	4.22	0.56	0.17	44.26	0.65	0.99	0.0095	0.0013	2.48	87.0
2	1.2-6	48.25	3.78	1.87	0.32	45.78	0.71	0.93	0.033	0.0025	2.96	3.3
3	6-12	54.32	4.23	3.22	0.60	37.62	0.52	0.93	0.051	0.0041	3.39	0.6
4	12-25	53.87	3.67	1.39	0.44	40.62	0.57	0.81	0.022	0.0031	2.90	1.6
5	25-50	55.58	5.41	3.69	0.42	34.90	0.47	1.16	0.057	0.0028	3.79	1.0
6	50-100	48.85	4.05	4.92	0.68	41.50	0.64	0.99	0.086	0.0052	3.99	3.8
7	100-300	49.13	4.85	5.92	0.99	39.11	0.60	1.18	0.10	0.0075	4.64	0.7
8	>300	54.52	3.78	2.05	0.42	39.24	0.54	0.83	0.032	0.0029	4.36	2.0

a) The weight of fraction over total weight of material recovered. b) PL = pregnant liquors, SL = spent liquors

Table 5

Comparison of py-GC/MS data at 450 °C between low molecular weight (<1.2 kD) fraction from a low temperature and high temperature Bayer liquor. Selective relative abundance (%) to phenol.

Compound	Low temperature process (145 °C) <1.2 kD	High temperature process (245 °C) <1.2 kD
Toluene	35.3	
1,2-dimethylbenzene	44.9	
1,2,3-trimethylbenzene	27.7	
5-methoxy-2-methyl-1H-indole	90.1	99
4-hydroxybenzonitrile		51
Phenol	100	100
2-methylphenol	16.8	
3-methylphenol	31.8	
2-methoxyphenol	55.5	
2-naphthalenol		125
2-coumaranone	54.4	63
2-methyl -1,3-isobenzofurandione		61
4-hydroxyphenyl-1-pentanone		23
1H-isoindole-1,3(2H)-dione		87
4,7-dimethyl-1,3-isobenzofurandione		170
5,6-dimethyl-1,3-isobenzofurandione		59
Benzoic acid	50.1	83
3-methylbenzoic acid	29.2	41
4-methylbenzoic acid	34.0	
4-methyl-1,2-benzenecarboxylic acid		100
3-hydroxy-4-methylbenzoic acid		287
Trimethylbenzaldehyde	49.3	

dependent. Interestingly, Table 5 shows that the high temperature process contains a higher proportion of ketones, diones and nitrogen containing compounds. This is in contradiction with the low temperature process in which methylbenzenes, phenols, and benzoic acids predominate. Temperature may play a role in this discrepancy, in that high temperatures produce more highly oxidised species. However, it is also likely that the differing geo-histories of the bauxite deposits produce different organic inputs to the processes.

4.3. Intermediate molecular weight molecules

There is little literature on the interaction of intermediate (1.2-100 kDa) molecular weight humic substances with alumina, although it is known that this material plays an important role in the Bayer process.

Attempts have been made to characterise and quantify these intermediate organic molecules present in the Bayer liquor by using a number of chromatographic techniques. GC-MS spectral analysis has been successfully used to identify and quantitate a number of smaller molecular components such as monocyclic aromatic carboxylic acids and alkanes and fatty acids /32,33/. Liquid chromatographic (LC) analysis of the humic acid component has been less successful. LC methods for the monitoring of known organic and inorganic ions that accumulate in the process liquor have been reported /35- 37/. Any further reported attempts at analysing the humic acids found in the Bayer liquor have been restricted to the quantitative analysis of the humic acids present /38/. The development of a High-Performance Liquid Chromatographic (HPLC) method for resolving these intermediate molecular weight components into molecular entities or even compound classes would be of considerable industrial importance /39,40/. Two-dimensional HPLC methods show promise.

4.4. Large molecular weight molecules

The higher molecular weight organics (>50 kDa), although present in low concentrations in Bayer process liquor, have a range of structures. The largest are char like /15-18/. In principle because they are large compounds it would be expected that these would have large surface covering effects and therefore inhibit precipitation in this way. As hosts they may also contain many guests, which might be prevented from playing a role in precipitation.

They can effectively alter the equilibrium concentration between an adsorbing guest on a crystal surface and a free guest in solution. Char like materials can be in the original bauxite /18/ but solubility studies suggest this material ends up largely as insolubles in the red mud. Thus char like materials are probably also synthesised in the process.

4.5. Host guests in Bayer liquor extracts

It is clear that a myriad of chemical compounds of different molecular weights compose the organic mixture that makes up the organic matter in Bayer liquors. Many have extremely high molecular weights with values for some components as high as 300 kDa. Dialysis of humic organic matter separates the material into molecular weight fractions or more correctly, fractions that can pass through specifically sized pores. Despite attempts to separate organic matter into molecular weight fractions by dialysis, specific higher molecular weight fractions were obtained which still contained low molecular weight organic material. Material of molecular weight of 50 kDa or greater will have voids in its packing quite capable of occluding smaller molecular weight material so that the smaller materials are in fact guests. It was clear that these small molecules appeared to be bound to much larger macromolecules by physical entrapment and/or hydrogen bonding.

One new finding for oxidising environments is the concept of host-guest structures where smaller molecules reside within a framework of a macromolecular host primarily derived from lignin /41/. The guests within the host cannot be removed by physical separation techniques. The structure of the host can be determined by py-GC/MS and NMR techniques. Differential thermal analysis, calorimetry, methylation and NMR data can be used to identify the guests. Some of the guests are probably held by hydrogen bonding but others are true prisoners in that they are alkanes and hence have no binding sites.

In differential thermal gravimetric analysis studies on various dialysed high molecular weight (>25 kDa) fractions, the loss of mass up to 200°C was attributed to loss of volatile organics as well as surface and bound water /33,41/. These molecules are trapped in the macromolecular matrix. If the amount of water and volatile organics adsorbed on a humic extract solid is calculated and compared with that calculated by summing that for each molecular weight fractions adjusted for mass, the numbers differ. This shows that the water and volatile organic holding capacity for the different fractions

changes when the different molecular weight materials are separated. It suggests that the various humic molecular weight fractions agglomerate together in structures where some of the water or volatile organic binding sites, on each humic substance, are held by other humic species. This is depicted in Figure 2 (left side), where both water and small organic volatiles (circles) occupy binding sites and the bound molecules can bridge macromolecules (rectangles). After separation by dialysis (Figure 2, right side) the large molecules are separated and this process generates more sites for adsorption of small molecules. Thus the water and volatile content of the unseparated material is not the same as the mass weighted sum of the water content of the separated materials. Mass loss data expressed as first derivative plots (differential thermal gravimetric analysis, DTG) indicates temperatures at which rapid mass loss occurred and this allows further information to be gained. Such plots also show that secondary volatile material is present which gives superimposed inflections in DTG plots.
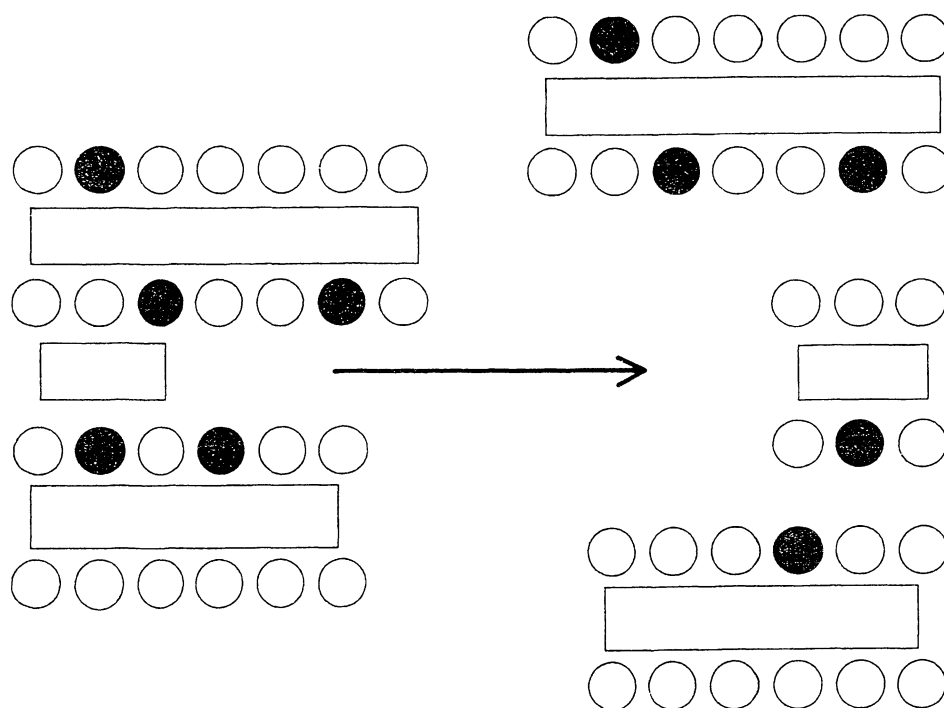

Fig. 2: Model to explain the water and volatile holding capacity of humic substances before and after fractionation. Rectangles = humic substance, length equivalent to molecular weight, o = water, • = organic volatile. The arrow represents the process of dialysis.

Enthalpy can also assist in identification. However, thermal events are not discrete for geo-organic matter, since a variety of materials may be volatilising at the same time or changing phase in some other way. Since the ΔH of vaporisation of water is known (44 kJ mol^{-1}), it is possible to determine whether the thermal events at lower temperatures are due to loss of water or not. Thus there is considerable evidence for volatile material other than water being present from enthalpy data. This is additional evidence that the events are evaporations and not decompositions and arise from trapped species.

^{1}H and ^{13}C NMR analysis of molecular weight fractionated material is very useful in supporting this proposition /41/. Discrete resonances should not be observed for macromolecules, yet they are seen in high molecular weight fractions. In larger molecular weight fractions these are mainly confined to the aliphatic region. The ^{1}H NMR spectrum of all fractions of molecular weight greater than 25 kDa showed few discrete resonances in the aromatic region. These fractions >25 kDa appear to form molecular aggregates with alkanes and aliphatic fatty acids. Discrete aromatic resonances were not seen for >300 kDa molecular weight fractions, indicating that there were no small aromatic compounds in this fraction.

When the fractions were methylated with tetramethyl ammonium hydroxide (TMAH) /42/ and subsequently analysed by GC/MS, a wide variety of compounds were identified including benzenecarboxylic acids, *n*-alkanes, and fatty acids. These three families of compounds represented the majority of the compounds released by the fractions. Many of the compounds released from the Bayer organic fractions by methylation were analysed as methyl esters, particularly the fatty acids and benzenecarboxylic acids.

Methylation with TMAH acts to release small molecules trapped in the macromolecules by forming esters and ethers with carboxylic and phenolic groups respectively, thereby breaking the hydrogen bonding that holds the molecules in place. Without methylation the molecules are held tightly in the macromolecular matrix. When the un-methylated fractions were analysed by GC/MS no small molecules were detected; only the internal standard (C_{20}) was identified. This result indicates that the small molecules are tightly hydrogen bonded in the macromolecule structures by forming molecular aggregates.

n-Alkanes were identified in the chromatograms of the methylated fractions with carbon chain lengths ranging from C11 to C29. n-Alkanes are derived from algal, microbial and higher plant sources. The distribution of the n-alkanes in these fractions suggests that they were derived from the

waxes of higher plants. Fatty acids were found to be one of the main chemical classes released by the methylation of the Bayer organic fractions. Fatty acids with carbon chain lengths ranging from C7 to C22 were identified as products of the fractions. Fatty acids that were identified were found to have both monocarboxylic and dicarboxylic acids on their structures as well as unsaturations in several of the products. Numerous C18 isomers were identified as products from the organic fractions. Numerous substituted benzene mono- and di-carboxylic acid compounds were identified as methylation products from the Bayer organic fractions.

It is not clear that the host-guest complexes formed by these highly oxidised humic molecules also exist in solution. The deprotonated conjugate bases, phenoxide and carboxylate would not form strong hydrogen bonds under these conditions due to repulsion forces of similarly charged species under strongly basic conditions but under neutral pH they may still hydrogen bond. In either case, during precipitation intra molecular hydrogen and intermolecular hydrogen bonding may occur. In the process large molecules voids may be formed which could occlude other molecules. It may well be true that some of these occluded molecules also hydrogen bond but the presence of alkanes shows that for some molecules this is not always the case.

5. POISONING

5.1. Ionic strength effects

In high ionic strength solutions molecules do not behave as free ions but exist in tight ion pairs. Thus in Bayer solutions the surface probably resembles the sort of phenomenon that exists in an electrical double layer at a surface or in molten salts. In this process the adsorption of an ion results in the immediate replacement of it with another of same charge from further out in solution. The kinetics of adsorption are dependent on interactions between ions not just the interaction with the surface. Likewise in nucleation the forces acting in chelation are different because molecules must move in tightly bound ion pairs. Thus it is not possible to directly extrapolate the effects of various ion concentrations without understanding activity. Poisoning experiments must be done at constant ionic strength if the effects of activity changes are not to be observed. Examples are cases where a

carboxylic acid might locally consume hydroxide ion, thereby altering the local ionic strength, and thus the effect on alumina hydrate yield is due to an ionic strength change and not due to adsorption.

5.2. Aluminophilicity and poisoning

By aluminophility we mean the desire for a molecule to adsorb on the alumina surface. It has been shown conclusively that this does not correlate with poisoning activity /43/. This is clear evidence for a role of organic matter in influencing nucleation rather than just altering surface coverage.

5.3. Precipitation experiments

Table 6 illustrates typical poisoning experiments /44,45/. The first set of experiments (Group A) was run with the organic fractions added at the concentrations recovered from the process using caustic washed seed. This was obtained by taking the seed crystal slurry from the refinery and extensively (5x) washing it with hot ~5M NaOH, and then water rinsed and air-dried. The second sets of experiments (Group B) were performed with equal concentrations of the organic fractions (Table 7) and hot water washed seed (seed crystals were prepared by five hot water washings of typical refinery seed).

Experiments were carried out under model conditions in which Bayer refinery additives were present such as carbonate oxalate and chloride ions /44, 45/. Different molecular weight fractions of the humic substances were found to have different detrimental affects on precipitation yields of aluminium hydroxide and these did not correlate with changes in crystal surface area.

The results for Group A experiments (Table 6) conducted with the organic fractions at the concentrations recovered from the Bayer process liquor showed few negative impacts from the presence of the organics. Table 6 shows little inhibition of the precipitation of aluminium hydroxide, with the yields of aluminium hydroxide for samples containing organic species being almost identical to the blank sample. In some cases the yield was higher than the blank, possibly as a result of the humic acids decreasing the concentration of the sodium hydroxide by protonation of hydroxide ion, thereby providing a greater driving force for precipitation and therefore higher precipitation yields. The largest decrease in yield was observed for the 12-25 kDa fraction

Table 6

Results from dose rate experiments with humic molecular weight fractions under pseudo-Bayer plant conditions (Group A experiments) on aluminium hydroxide precipitation using caustic-washed seed

Organic fraction	Organic dose (g/L)	Difference in yield of alumina (g) relative to blank	% Change in product with surface area <20 μm^2 relative to blank	% Change in surface area of product relative to blank	% Change in oxalate concentration relative to blank
<1.2kD	2.48	0.86	+0.79	-0.82	+11.20
1.2-6kD	0.095	0.12	+0.66	+4.06	-8.86
6-12kD	0.018	-0.05	+0.57	+3.25	-12.68
12-25kD	0.046	-0.43	+0.05	+9.76	-12.73
25-50kD	0.018	0.08	+0.32	-6.50	-6.69
50-100kD	0.108	-0.01	+0.14	-2.80	+11.10
100-300kD	0.020	0.56	+0.16	-0.82	+15.00
>300kD	0.065	0.54	+0.23	-0.82	+8.60

Table 7

Results from constant dose rate experiments with humic molecular weight fractions at 0.1g/L (Group B experiments) on aluminium hydroxide precipitation using hot water washed seed

Organic fraction	Organic dose (g/L)	Difference in yield of alumina (g) relative to blank	% Change in product with surface area <20 μm² relative to blank	% Change in surface area of product relative to blank	% Change in oxalate concentration relative to blank
<1.2kD	0.1	-0.11	+3.16	-16.65	0
1.2-6kD	0.1	-0.31	-2.68	+27.30	+0.40
12-25kD	0.1	-0.75	-2.91	+28.87	+3.66
50-100kD	0.1	-0.71	-2.87	+28.63	+9.40
>300kD	0.1	-1.68	-1.70	+20.46	+16.60

(-0.43 g) which appears to have quite different properties from the other organic fractions.

Table 6 shows no correlation between surface area of crystals and the yield. However the greatest increase in surface area was exhibited by the 12-25 kDa fraction which also inhibited the yield the most. The 25-50 kDa fraction produced a decrease in surface area. These results do not translate directly to particle size because of agglomeration and microcavities. All fractions increased the percentage of very fine crystals with surface areas less than $20\mu m^2$, with the largest increase seen for the <1.2 kDa fraction. This fraction produced a 0.79% increase in the amount of fine material. Interestingly the 12-25 kDa fraction, which reduced yield and increased surface area, produced the smallest change in very fine crystals. Thus the role of these small and intermediate molecular weight organics is complex and is not simply one of inhibiting growth of crystals. Rather they also affect nucleation and agglomeration as well as growth in rather subtle ways.

Group B experiments used hot water washed seed crystals to promote crystallisation, Each fraction clearly had an effect on yield (Table 7), with the least poisonous fraction being the <1.2 kDa fraction. However, although the small molecular weight material did not strongly affect the yield of aluminium hydroxide crystals, the <1.2 kDa fraction had a strong influence on crystal size, decreasing the surface area of the product aluminium hydroxide while increasing the amount of very fine crystals ($20\mu m^2$).

It is clear from Table 7 that the higher molecular weight organics (>12 kDa), although present in low concentrations in Bayer process liquor, have particularly strong adverse affects on the precipitation of aluminium hydroxide. Group B experiments showed that the higher molecular weight humic materials acted as precipitation poisons with the most poisonous fraction being the >300 kDa material (Table 7).

Table 7 showed that, although the yield of the aluminium hydroxide product was decreased by the larger humic material, the material actually increased the size of the precipitated crystals by increasing the surface area of the crystals and decreasing the amount of very fine crystals. In addition, Tables 6 and 7 showed that the larger molecular weight humic materials also have an important role to play in oxalate stability. All fractions >50 kDa substantially increased the concentration of oxalate in solution with the >300 kDa fraction having the largest effect. These higher molecular weight organic fractions increased oxalate stability in synthetic Bayer liquor by up to 20% (see below, section 5.5).

5.4. Stressed systems

Mitchell *et al.* /46/ discovered that precipitation yields could be improved if poisoning organic species were adsorbed onto calcined alumina. Caustic washing of the seed crystals was examined to determine whether the creation of a clean crystal surface through the dissolution of the outer crystal layers, along with contaminating organics, would act to improve precipitation yields by providing sites for the poisoning organics to bind. Caustic seed washing would provide a greater number of binding sites for poisoning organic species to adsorb while still providing free precipitation sites to allow precipitation to continue.

The effects of various molecular weight fractions (<1.2 kDa to >300 kDa) of organic matter on precipitation yields were maximised under system stress. That is, when there is competition for the number of sites at which new alumina carrying species or humic material can bind the impact on precipitation is increased, as a result the organic fractions impacted strongly on precipitation when hot-water washed seed was used. The preparation of seed crystal is therefore very important and because of competition, effects are concentration dependent.

These concepts are supported by comparative experiments on seed. Group A experiments with caustic washed seeds show a much greater tolerance to humic material which suggests that caustic washing increases the number of sites at which new alumina carrying species or humic materials can bind. Thus if humic materials bind there are plenty of sites left to grow alumina. Indeed Group A experiments (caustic washed seed) showed much less variation in the surface area of the product crystals. Group A experiments showed a maximum change in the surface area of the product crystals of ± 10%, with many organic fractions producing a change of less than 4% (Table 6). From these results it appears that changes in surface area can be minimised through the use of caustic washed seed, which may negate many of the detrimental impacts of the poisoning organic species.

5.5. Sodium Oxalate

Solid-phase sodium oxalate plays a minor role in the sodium content of product alumina, but has a critical role in gibbsite nucleation and fines balance in precipitation operations, determining crystal size and particle numbers /5,6/. Bayer alumina refineries typically operate an oxalate

precipitation stage to control the level of oxalate build up in the liquor, so as to minimise the impact of this organic degradation product via precipitation at unwanted parts of the process. The presence of organic matter in the Bayer liquor stabilises the oxalate in solution to some extent /45/. However, once oxalate precipitation begins the oxalate surface adsorbs some of the organics from the liquor, promoting further precipitation. This phenomenon disturbs the orderly precipitation of aluminium hydroxide, causing excess nucleation leading to fines in the circuit and poor quality alumina with a high sodium content /5,6/.

Table 6 shows results from the oxalate concentrations in the Group A experiments (caustic washed seed). They reveal that the small molecular weight organic species (<50 kDa) decreased oxalate stability by up to 13%, with the exception being the <1.2 kDa fraction that showed a slight increase in oxalate stability (11%). These experiments were performed with the organic fractions at the concentrations recovered from the process liquor. The larger molecular weight organic species (>50 kDa), although added at low concentrations, were each seen to increase oxalate stability by between 9-15%, including the 100-300 kDa fraction (15%). The materials from the pregnant and spent liquor also increased oxalate stability, with the pregnant material increasing stability by 33% and the spent material by 24%.

For stressed systems (Table 7), oxalate concentration in solution was shown to depend on organic dose /44/ but oxalate stability was significantly increased by the 12-25 kDa, 50-100 kDa and >300 kDa organic fractions with the oxalate concentration being increased by more than 16% for the largest molecular weight fraction (>300 kDa). The smallest molecular weight fraction (<1.2 kDa) when added at similar concentration produced no effect on the oxalate concentration. This suggests that there is some relationship between humic molecular weight and capacity to stabilise oxalate in solution. This may be because the oxalate may aggregate with the large organic macromolecules via hydrogen bonding, forming host-guest complexes in much the same way as small molecular weight Bayer humic substances may aggregate. The formation of such complexes prevents the oxalate from agglomerating into a form where it can be precipitated from solution, leading to increased concentrations of the oxalate in solution, i.e. stabilisation.

6. RELATIVE ACTIVITIES

Studies with model compounds have shown that many small hydroxy-organic compounds act as poisons to the Bayer process /47-52/. Model hydroxybenzene carboxylic acid compounds, similar in structure to those isolated in the smallest molecular weight fraction of the Bayer humic substances, were found to be effective aluminium hydroxide precipitation poisons. The present study supports the findings of the tests with model compounds, revealing that the small molecular weight compounds do affect precipitation yields, as do the larger molecular weight materials. Studies with model compounds have determined that hydroxy organic compounds produce decreases in particle size of product crystals. These findings were supported by the results obtained, as the small molecular weight material isolated from the Bayer process had very strong adverse effects on product sizing, leading to the generation of excessive amounts of fine aluminium hydroxide crystals. However such effects are only seen when there is a deficiency of sites for newly settling alumina carrying species and humic material to bind. Caustic washed seed (group A experiments) was found to minimise the decreases in yield caused by the poisoning of the precipitation of aluminium hydroxide by the Bayer organic fractions. The reductions in yield when caustic washed seed was used were much smaller than those obtained using hot water washed seed (group B experiments), even when the organic fractions were present in roughly equivalent concentrations (1.2-6 kDa, 12-25 kDa, 50-100 kDa and >300 kDa). Caustic washed seed also minimised the changes in crystal size due to the presence of organic compounds, producing crystals of a similar size to the crystals produced with no organics present.

Hot water washed seed (Group B experiments) would already contain significant amounts of bound organics on the crystal surfaces reducing the number of potential sites for aluminate ions to precipitate from solution. Moreover the presence of additional organic compounds in solution would bind with the remaining free precipitation sites on the hot water washed seed effectively preventing further aluminium hydroxide precipitation, thus resulting in a decrease in precipitation yields. The caustic washed seed (Group A experiments) acts to decrease the inhibition caused by process organics by providing more free sites to precipitate aluminate ions. Caustic washing removes the outer crystal surfaces and bound organics from the seed crystals, thus providing additional aluminate ion precipitation sites that were previously occupied by the process organics.

7. CONCLUSIONS

1. The organic matter in Bayer fractions varies considerably with molecular weight. This variation is due to the nature of the organic material that enters the process, but also depends on the conditions of processing. The type of vegetation can affect this organic matter and the rate at which it dissolves in Bayer liquors. Clear differences between Angiosperms and Gymnosperm lignins have been observed. Carbohydrates are in general unstable but some such as xylitol can have longer half-lives so they may influence the process. Carbohydrates form lactic acid and other small organic molecules which themselves can influence the process in complex ways.

2. All molecular weight fractions from <1.2 kDa to >300 kDa of Bayer organic matter affect precipitation yields, particle sizes and surface areas of product alumina; however, the effects only occur when there is competition for the number of sites at which new alumina carrying species or humic material can bind. The preparation of seed crystal is therefore very important and because of competition, effects are concentration dependent.

3. Higher molecular weight fractions (>50 kDa) were found to be the most detrimental to the precipitation of aluminium hydroxide from Bayer process liquor decreasing product yields significantly. The >300 kDa fraction had the largest effect. The higher molecular weight organic fractions were also seen to have the largest impact on oxalate stability, increasing oxalate stability in synthetic Bayer liquor by up to 20%. These molecules are probably largely synthesised in situ.

4. Yield, particle size and surface area of alumina from the spent liquor does not add up to the weighted sum of the respective yields, particle sizes and surface areas from the individual molecular weight fractions. Thus the humic materials must interact with each other in producing precipitation effects or interact in tandem with the surface. It is probable that initially ligand exchange of water occurs at the surface followed by a fast process where small molecular weight species occupy binding sites. These molecules are then displaced by irreversibly adsorbing large macromolecular organic species. This would suggest that all the molecular weight fractions play a role in the poisoning process, with the largest molecular weight material having a displacement role.

5. Oxalate stabilisation in solution is promoted by higher molecular weight fractions, especially under conditions in which the system is deficient in binding sites. The highest molecular weight fraction (>300 kDa) is the most effective. These results support a model in which humic material can capture oxalate and make it unavailable to the precipitation pool by forming host guest complexes.

8. REFERENCES

1. Evans AM. *Ore Geology and Industrial Minerals: An Introduction.* London: Blackwell Scientific Publications, 1993: 389.

2. Wefers K and Misra C. *Oxides and Hydroxides of Aluminium.* Alcoa Laboratories, Alcoa Technical Paper No. 19, 1978.

3. Solomom M, Groves DI and Jaques AL. *The Geology and Origin of Australia's mineral deposits.* New York: Oxford University Press, 1994: 772.

4. Hind AR, Bhargava SK and Grocott SC. The surface chemistry of Bayer process solids: a review. *Colloids and Surfaces, A: Physicochemical & Engineering Aspects,* 1999; 146: 359-374

5. Grocott SC, Rosenberg SP. Soda in Alumina. Possible mechanisms for soda incorporation. *Proceedings of the Second International Alumina Quality Workshop,* Gladstone, Australia, 1988; 271-287.

6. Armstrong L. Bound soda incorporation during hydrate precipitation. *Proceedings of the Third International Alumina Quality Workshop,* Hunter Valley, Australia, 1993; 282-292.

7. Atkins P, Grocott SC. The impact of organic impurities on the production of refined alumina. *Proceedings of Science, Technology and Utilisation of Humic Acids,* CSIRO Division of Coal and Energy Technology, Sydney, Australia, 1988; 85-94.

8. Moolenaar RJ, Evans JC and Mc Keever LD. The structure of the aluminate ion in solutions at high pH. *Journal of Physical Chemistry,* 1970; 74: 3629-3636.

9. Wilson MA, Collin PJ and Akitt JW. Composition of aluminum phosphate solutions. Evidence from Aluminium-27 and Phosphorus-31 Nuclear Magnetic Resonance spectra. *Analytical Chemistry,* 1989; 61: 1253-1259.

10. Bradley SM And Hanna JV. 27Al and 23Na MAS NMR and powder X Ray diffraction studies of sodium aluminate speciation and mechanistics of aluminum hydroxide precipitation upon acid hydrolysis. *Journal of the American Chemical Society*, 1994; 116: 7771-7783.

11. Power G.P. and Tichbon W. Sodium Oxalate in the Bayer Process: Its origin and effects. In *Proceedings of the Second International Alumina Quality Workshop,* Perth Australia, 1990, p99-115.

12. Ellis AV, Wilson MA, Forster P. Degradation of Klason lignin in sodium hydroxide at 145°C. *Industrial & Engineering Chemistry Research*, 2002; 41, 6493-6502.

13. Ellis AV, Wilson MA, Kannangara GSK. Bayer Poisons: Degradation of angiosperm and gymnosperm water-soluble extracts in sodium hydroxide at 145°C. *Industrial & Engineering Chemistry Research,* 2002; 41: 2842-2852.

14. Swift RS. Macromolecular properties of soil humic substances: Fact, fiction and opinion. *Soil Science*; 1999; 164: 790-802.

15. Skjemstad JO, Reicosky DC, Wilts AR and Mc Gowan JA. Charcoal carbon in US agricultural soils. *Soil Science Society of America Journal,* 2002; 66(4):1249-1255.

16. Schmid EM, Skjemstad JO, Glaser B, Knicker H and Kogel-Knabner I. Detection of charred organic matter in soils from a Neolithic settlement in Southern Bavaria, Germany. *Geoderma,* 2002; 107(1-2):71-91.

17. Schmidt MWI, Skjemstad JO, Czimcizik CI, Glaser B, Prentice KM, Gelinas Y and Kuhlbusch TAJ. Comparative analysis of black carbon in soils. *Global Biogeochemical Cycles,* 2001; 15(1):163-167.

18. Marshall CP, Kannangara GSK, Alvarez R, Wilson MA. Characterisation of insoluble char in Weipa bauxite. *Carbon,* 2004; Submitted.

19. Baker AR, Greenway AM. Comparison of bauxite and Bayer liquor humic substances by [13]C Nuclear Magnetic Resonance Spectroscopy. Implications for the fate of humic substances in the Bayer process. *Industrial & Engineering Chemistry Research,* 1988; 37: 4198-4201.

20. Given PH and Marzec A. Protons of Differing Rotational Mobility. *Fuel,* 1988; 67: 242.

21. Redlich PJ, Jackson WR and Larkins FP. Hydrogenation of brown coal Part 9. Physical characterisation and liquefaction potential of Australian coals. *Fuel,* 1985; 64: 1383 –1389.

22. Wilson MA, Kannangara GSK and Smeulders DE. Funeral arrangements for plants: An essay in organic geochemistry. *Journal and Proceedings of the Royal Society of New South Wales*, 2000; 133: 71-85.

23. Fetsch D, Hradilova M, Mendez EMP and Havel J. Capillary zone electrophoresis study of aggregation of humic substances. *Journal of Chromatography A.*, 1998; 817(1-2): 313-323.

24. Ong HL and Bisque RE. Coagulation of humic colloids by metal ions. *Soil Science*, 1968; 106: 220-224.

25. Havel J, Fetsch D, Peoa-Mendez EM, Lubal P and Havli J. Recent developments in humic acid characterisation. Acidobasic and complexation properties, separation and reliable fingerprints by capillary electrophoresis and MALDl-TOF mass spectrometry. *Proceedings of the 9th International Meeting of the International Humic Substances Society*, Adelaide, Australia, 1998; 103-107.

26. Frimmel FH. Impact of light on the properties of aquatic natural organic matter. *Environment International*, 1998; 24: 559-571.

27. Higuchi T. Lignin structure and morphological distribution in plant cells walls. *Lignin Biodegradation: Microbiology, Chemistry and Potential Applications*. Boca Raton; CRC Press, 1981.

28. Criss DL, Ingram Jr LL and Schultz TP. A low-temperature internal nucleophilic aromatic substitution reaction on a β-O-4 lignin model dimer. *Journal of Organic Chemistry*, 1997; 62: 7885-7888.

29. Ellis AV, Kannangara GSK and Wilson MA. Chemistry of sodium lactate formation under simulated alumina refinery conditions. *Industrial & Engineering Chemistry Research*, 2003; 42:3185-3189.

30. Ellis AV and Wilson MA. Carbon exchange in hot alkaline degradation of glucose. *Journal of Organic Chemistry*, 2002; 67: 8469-8474.

31. Smeulders DE, Wilson MA, Armstrong L. Insoluble organic compounds in the Bayer process. *Industrial & Engineering Chemistry*, 2001; 40: 2243-2251.

32. Wilson MA, Ellis AV, Lee GSH, Rose HR, Lu X, Young BR. Structure of molecular weight fractions of Bayer humic substances I. Low-temperature products. *Industrial & Engineering Chemistry Research*, 1999; 38: 4663-4674.

33. Smeulders DE, Wilson MA, Patney H, Armstrong L. Structure of molecular weight fractions of Bayer humic substances II. Pyrolysis behaviour of high temperature products. *Industrial & Engineering*

Chemistry, 2000; 39: 3631-3639.

34. Lever G. Identification of organics in Bayer liquor. *Light Metals*, 1978, 71-83.

35. Harakuwe A, Haddad P and Jackson P, Quantitative determination of oxalate in Bayer liquor by capillary zone electrophoresis - a validative study. *Journal of Chromatography*, 1996; 739(1-2): 399-403.

36. Susic M and Armstrong LG. High-performance liquid chromatographic determination of humic acid in sodium aluminate solution. *Journal of Chromatography*, 1990; 502: 443-44.

37. Whelan TJ, Wilson MA and Kanangara GSK. HPLC investigation of humics found in Bayer liquors. *Proceedings of the Australian Organic Geochemistry Conference*, CSIRO Marine Research Laboratories, Hobart, Australia, 2002; 77-78.

38. Jackson P. Analysis of oxalate in Bayer liquors - a comparison of ion chromatography and capillary electrophoresis. *Journal of Chromatography*, 1995; 693(1): 155-161.

39. Wilson MA, Ellis AV, Kannangara GSK and Whelan TJ. Transformation of organics inputs to alumina refineries. *Proceedings of the 6ᵗʰ International Alumina Quality Workshop*, AQW Inc. Ltd., Brisdane, Australia, 2002; 67-72.

40. Whelan TJ, Kannangara GSK and Wilson MA. Increased resolution in High-Performance Liquid Chromatography spectra of high molecular weight organic components of Bayer liquors. *Industrial & Engineering Chemistry Research*, 2004, in press.

41. Smeulders DE, Wilson MA and Kannangara GSK. Host-guest interactions in humic materials. *Organic Geochemistry*, 2001; 32: 1357-1371.

42. Hatcher PG, Nanny MA, Minard RD, Dible SD and Carson DM. Comparison of two thermochemolytic methods for the analysis of lignin in decomposing gymnosperm wood: The CuO oxidation method and the method of thermochemolysis with tetramethylammonium hydroxide (TMAH). *Organic Geochemistry*, 1995; 10: 881-888.

43. Wilson MA, Farquharson GJ, Tippett JM., Quezada RA And Armstrong L. Aluminophilicity of the humic degradation product of 5-hydroxybenzene-1,3-dicarboxylic acid. *Industrial and Engineering Chemistry Research*, 1998; 37: 2410-2415.

44. Smeulders DE and Wilson MA. Crystal surface and humic material effects on crystallisation. *Proceedings of the International Humic*

Substance Society, Boston, United States of America, 2002; 478-480

45. Smeulders DE, Wilson MA and Armstrong L. Poisoning of aluminum hydroxide precipitation by high-molecular-weight fractions of Bayer organics. *Industrial & Engineering Chemistry Research*, 2001; 40: 5901-5907.

46. Mitchell CH, Alamdari A, Wainwright MS and Raper JA. Improvement of batch precipitation of alumina trihydrate from Bayer pretreated with calcined aluminas. *Proceedings of the Nineteenth Australasian Chemical Engineering Conference (Chemeca 91)*, Newcastle, Australia, 1991; 114-121.

47. Atkins P and Grocott SC. The impact of organic impurities on the production of refined alumina. *Proceedings of the Science, Technology and Utilisation of Humic Acids*. CSIRO Division of Coal and Energy Technology, Sydney, Australia, 1988; 85-94.

48. Watling HR, Smith PG and Loh J. Comparative effects of model organic compounds on gibbsite crystallisation. *Proceedings of the Fourth International Alumina Quality Workshop*, Darwin, Australia, 1996; 553-555.

49. Smith PG, Watling HR and Crew P. The effect of model organic compounds on gibbsite crystallization from alkaline aluminate solutions: polyols. *Colloids Surfaces A: Physicochemical and Engineering Aspects*, 1996; 111: 119-130.

50. The PJ. The effect of glucoisosaccarinate on the Bayer precipitation of alumina trihydrate. *Light Metals*, 1980; 119-130.

51. Alamdari A, Raper JA and Wainwright MS. Poisoning of the precipitation of alumina trihydrate by mannitol. *Light Metals*, 1993; 143-149.

52. Coyne JF, Wainwright MS, Cant NW and Grocott SC. Adsorption of hydroxy organic compounds on alumina trihydrate. *Light Metals*, 1994; 39-45.

Increased Resolution in High-Performance Liquid Chromatograph Spectra of High-Molecular-Weight Organic Components of Bayer Liquors

Thelma J. Whelan, G. S. Kamali Kannangara, and
Michael A. Wilson

Department of Chemistry, Materials and Forensic Science, University
of Technology Sydney, P.O. Box 123, Broadway 2007, Sydney,
Australia, and Deans Unit, College of Science, Technology and
Environment, University of Western Sydney, Locked Bag 1797,
Penrith South DC NSW 1797, Sydney, Australia

APPLIED CHEMISTRY

Increased Resolution in High-Performance Liquid Chromatograph Spectra of High-Molecular-Weight Organic Components of Bayer Liquors

Thelma J. Whelan,[†] G. S. Kamali Kannangara,[‡] and Michael A. Wilson*,[‡]

Department of Chemistry, Materials and Forensic Science, University of Technology Sydney, P.O. Box 123, Broadway 2007, Sydney, Australia, and Deans Unit, College of Science, Technology and Environment, University of Western Sydney, Locked Bag 1797, Penrith South DC NSW 1797, Sydney, Australia

A high-performance liquid chromatographic (HPLC) method has been developed to study the chemistry of higher-molecular-weight components (>1200 Da) of humic materials in an alumina refinery (Bayer process). The optimum separation was achieved using a Nova-Pak C18 column at a flow rate of 0.5 mL/min. A step gradient was developed using tetrabutylammonium hydrogen sulfate (PIC A) as the ion-pairing reagent and acetonitrile. Extraction of the humic material with a series of solvents differing on the basis of polarity yielded solvent extracts, which were then characterized and correlated with the optimum HPLC separation. The carboxylic-rich components concentrated in the material that eluted first, as expected for reverse-phase separations, thus confirming the validity of the methodology. To account for the solubilities and the absence of a continuum in the elution of the Bayer humics, it is suggested that the organic matter is associated in solution as micelles or other clusters.

1. Introduction

Humic substances are loosely defined as alkali-soluble geo-organic matter found in the environment. They are important in the Bayer process because of their adverse effect on the industrial-scale production of alumina from bauxite. During the Bayer process, the bauxite is subjected to a high-temperature caustic digestion using 3.5–5 M sodium hydroxide. Most of the organic matter associated with the bauxite (up to 0.3%) ends up in the liquor,[1,2] although some organics are removed with the insoluble material termed "red mud", which contains oxides of silicon, iron, and titanium. The soluble organic species can accumulate in the process liquor as the caustic solution is recycled for the digestion of fresh bauxite after the precipitation of the aluminum hydroxide trihydrate. Repetitive caustic digestion transforms some of the organics to a multitude of low-molecular-weight aliphatic and aromatic carboxylic acids.[2–7]

Typical concentrations of Bayer liquor organics range from a few grams to 40 g of carbon/L.[8] They range in molecular weight from less than 100 to over 300 000 Da. Low-molecular-weight organic molecules such as formate, acetate, oxalate, and simple aromatic polycarboxylic acids and phenols can be readily molecularly characterized both quantitatively and qualitatively after methylation by gas chromatography/mass spectrometry.[2,3] However, the molecular characterization of humic compounds of molecular weights above 1200 Da has

yet to be achieved. Rather, work has been focused on the measurement of bulk spectroscopic or chemical properties such as acidity, aromaticity, and structural group components determined by pyrolysis gas chromatography/mass spectroscopy (py GC/MS) and solid-state nuclear magnetic resonance (NMR) spectroscopic techniques.[4–7]

The analysis of humic compounds of molecular weights above 1200 Da is of considerable industrial importance. This is because many of these compounds have a poisoning effect that reduces the yields of alumina and oxalate precipitation and causes agglomeration and a range of other phenomena during processing.[8–13] Poisoning effects vary from plant to plant, because of the variation in the nature of the poisonous compounds. Species containing relatively acidic hydroxycarboxylic acid functionalities and alcohols have been implicated. Even for low-molecular-weight materials, the role is complex. Although it was believed that the poisoning effect increased as the number of polar groups increased, 5-hydroxybenzene-1,3-dicarboxylic acid has recently been shown to be inactive.[14] The poisoning effects of the C-5 polyols, ribitol, arabinitol, and xylitol also differ and *meso*-tartaric acid is unusually active.[15,16]

Research on natural systems[17] has demonstrated that the adsorption mechanism of humic substances is sequential. Ligand exchange of water occurs initially at the surface, followed by a fast adsorption process involving the low-molecular-weight material. Rapidly adsorbing low-molecular-weight compounds are then successively displaced from the surface by slow irreversibly adsorbing compounds of higher molecular weight. There is thus a progressive and selective immobilization

---

* To whom correspondence should be addressed. E-mail: MA.Wilson@uws.edu.au.
† University of Technology Sydney.
‡ University of Western Sydney.

of high-molecular-weight humic substances that can have an impact on crystallization. The effects of various molecular weight fractions (<1200 to >300 000 Da) of organic matter introduced into alumina refineries with bauxite have been studied.[13] Effects are maximized under system stress.[18] It is clear that the higher-molecular-weight organics (>50 000 Da), although present in low concentrations in Bayer process liquor, have particularly strong adverse affects on the dynamics of the precipitation of aluminum hydroxide.[13] These higher-molecular-weight organics were also found to stabilize sodium oxalate in solution.

Liquid chromatographic (LC) analysis of the humic acid component of Bayer liquors has so far not been reported, although LC methods have been successfully developed for the monitoring of known simple organic and inorganic ions that accumulate in the process liquor. Oxalate, which is of prime importance given that its stability and removal can control refinery productivity, as well as chloride and sulfate have been analyzed using either ion chromatography (IC) or capillary electrophoresis (CE).[19,20] For the determination of oxalate, chloride, and sulfate in Bayer liquors, CE was found to be preferable to IC, allowing for the complete resolution of all of the ions from the matrix in a run time of less than 6 min.[20] Any further reported attempts at analyzing the humic acids found in the Bayer liquor have been restricted to the quantitative analysis of the humic acids present. Susic et al.[21] reported the first use of an HPLC method with fluorometric detection for the quantitative humic acid analysis of a Bayer liquor. A method by which the humic acid concentration could be routinely monitored was supposedly developed; however, not all humic material fluoresces, and therefore, this approach offers limited full detection.

The work presented in this paper aims to develop an LC method that would separate some of the larger organic species (>1200 Da) present into compound classes. Liquid chromatography is routinely used for the determination of ionic and nonionic compounds, although LC of ionic samples tends to be more complicated and difficult to interpret. Therefore, several strategies are employed to simplify the analysis of ionic samples. There is a choice of three LC modes of separation: reverse-phase, ion-suppression, and ion-pair chromatography. Reverse-phase HPLC is usually the most appropriate starting point because of its simplicity compared to the other modes of separation. If reverse-phase chromatography proves to be inadequate, the application of ion suppression or the addition of an ion-pairing reagent can be considered.

2. Experimental Section

2.1. Preparation of Organic Material for Analysis. 2.1.1. Bulk Material.
This procedure has been described in detail elsewhere[5] but is repeated briefly here for completeness. An aliquot of Bayer liquor (200 mL) from digestion of bauxite at 145–150 °C at the Kwinana Alcoa refinery, Western Australia, was diluted at a volume ratio of about 1:10 (v/v) with distilled water and acidified to pH 1.5 with 1:1 (v/v) hydrochloric acid/water mixture. The soluble fulvic acid fraction was decanted and then filtered through a glass microfiber paper (Whatman 15.0 cm GF/C) and filtered again through a sintered glass filter (porosity 4) to remove undissolved particles in the acidified Bayer liquor. The pH of the precipitated humic acid fraction was gradually

Table 1. Continuous Solvent Extraction Percentage Yields and Solvents to Separate Humic Material

fraction	solvent	mass yield (%, w/w)
F1	diethyl ether	54
F2	ethyl acetate	8
F3	isopropyl alcohol	13
F4	water	25

increased to 4 with sodium hydroxide (1 M) to solubilize the humic acid. This solution and the fulvic acid solution were combined and adsorbed onto an XAD-7 resin as described below.

Extraction of the humic substances in the Bayer liquor was then carried out on a prewashed and acidified Amberlite XAD-7 resin column (6 × 2 cm, 200 g of resin). The humic substances in the acidified Bayer liquor solution (above) (1 L) were absorbed onto the column by passing the solution through the XAD-7 column at a flow rate of approximately 1 mL/min until the outlet liquor became yellow in color. The column was washed with 2 L of 0.1 M hydrochloric acid and then with 1 L of doubly distilled deionized water until the pH of the outlet water was neutral. The column was eluted with 0.1 M KOH solution (450 mL), and the concentrated (brown-colored) humic substances were collected (400 mL). The protonated form of the Bayer humic substances was obtained by passing 200 mL of the alkaline humic substances solution through a prewashed (doubly distilled deionized water) cation-exchange resin (Amberlite 120, 60 cm × 2 cm). The humic substances were washed from the column with one column volume of doubly distilled deionized water (120 mL) to yield the protonated form (humic and fulvic acids). The procedure was repeated 20 times using 200-mL aliquots of the initial Bayer liquor solution, and the solutions were combined to form 2.4 L of combined solution. This solution was then filtered through a 0.45-μm Millipore glass fiber filter, and 16 aliquots of 60 mL each were removed for molecular weight separation. The rest of the material was freeze-dried and stored. The yield of organic material from the Bayer liquor was 11.6 g/L.

2.1.2. Solvent Fractionated Material.
A continuous solvent extraction procedure with varying solvent polarity was used to separate the bulk Bayer humic material into four fractions. The Bayer humic material (2g) was placed in a glass microfiber extraction thimble 919 × 90 mm and used in a Soxhlet extractor. The extraction was carried out starting with diethyl ether (150 mL) and then ethyl acetate (150 mL), isopropyl alcohol (150 mL) and finally milli-Q water (150 mL), with each solvent being allowed to extract for 12 h. The diethyl ether, ethyl acetate, and isopropyl alcohol extracts were rotor-evaporated to dryness and dried under vacuum overnight, whereas the water extract was freeze-dried. Yields are given in Table 1.

2.2. Characterization Methods.
The pH was measured at 25 °C on a Radiometer Pacific Copenhagen pH meter using a glass electrode. The pH of the entire Bayer humic sample was obtained by redissolving the humic material (50 mg) in 10 mL of distilled water to make up a solution of 5.0 g/L. The pH of the Bayer humic sample is listed in Table 2. The carbon, hydrogen, and nitrogen compositions were determined using a Carlo Erba EA1108 CHNS–O elemental analyzer after the samples had been vacuum-dried for 4 h in an oven at 60 °C. Other elements were not measured. The Microanalytical Unit of the Australian National Uni-

Table 2. Acidity and Elemental Analysis of the Bayer Humic Substance[a]

% C	% H	% N	% O difference	O/C	H/C	N/C	pH at 5 g/L in water
50.25	4.24	0.67	44.84	0.67	1.01	0.011	2.4

[a] Analyses are given to two decimal places but error is ±0.05.

versity performed all elemental analyses in-house. The elemental composition of the Bayer humic sample is summarized in Table 2.

Solution ^{1}H NMR spectra were recorded on a Bruker DRX 300-MHz instrument fitted with field gradient coils. The Bayer humic material (2 mg) was dissolved in dimethyl sulfoxide-d_6 (DMSO-d_6, 99.8 atom % D, Aldrich, 0.6 mL). The clear amber solution was removed by pipet to a 5-mm NMR tube. The choice of solvent DMSO-d_6 was based on complete solubility of Bayer humic material and better resolution of the proton peaks, especially the exchangeable protons. All spectra were recorded at a temperature of 300 K unless a higher temperature (320 K) was used to distinguish the exchangeable protons (hydrogens attached to oxygen and/ or nitrogen atoms). At higher temperatures, the exchangeable protons are shielded (peaks shift to a lower chemical shift) because of the weakening of the hydrogen bonding. All nondecoupled proton experiments were obtained with a 90° pulse of 7.4 μs, 4000 sweep width, a recycle delay of 2 s, and an acquisition time of 4.09 s. The data were collected in 8k of memory and then Fourier transformed using line-broadening factors of 0.3 Hz. The chemical shifts are referenced externally to a solution of tetramethylsilane (TMS, 0 ppm). Two-dimensional NMR experiments such as [1]H−[1]H homonuclear correlation spectroscopy (COSY) spectra were obtained to confirm the spin−spin coupling between the protons and to assist in assignments. Acquisition parameters for the [1]H−^{1}H COSY 2-D NMR experiments included a spectral width of 4000 Hz, a recycle delay of 2 s, 1024 data points (time domain), and 16 scans per experiment. ^{1}H NMR spectra were collected for all four solvent extracts using the above experimental conditions.

Solid-state ^{13}C cross-polarization magic-angle spinning nuclear magnetic resonance (CP/MAS NMR) spectra were obtained on a Bruker DPX200W Advance 200-MHz instrument operating at 50.3 MHz. Approximately 200 mg of the Bayer humic sample was analyzed using the cross-polarization technique with magic-angle spinning (CP/MAS). The solid samples (powder) were packed into a 4-mm zirconia rotor with a Kel-F cap, and the rotors were spun at the magic angle (54.74°). The spinning speed was 5 kHz, and spectra were recorded at ambient temperature. Pulse widths of 4 μs were used, with a 2-s recycle time, and a contact time of 1.5 ms; 20 480 scans were collected in 16k points and Fourier transformed with a line broadening of 20 Hz to obtain the frequency-domain spectrum. The chemical shifts were expressed relative to tetramethylsilane (TMS) using adamantane as an external reference (the CH_2 peak of adamantane was assigned to 38.3 ppm downfield from the 0.00 ppm TMS peak). The frequency-domain ^{13}C spectrum was analyzed to determine approximately the different structural groups present using established literature methods as outlined below. ^{13}C NMR spectra were collected for all four solvent extracts using the above experimental conditions.
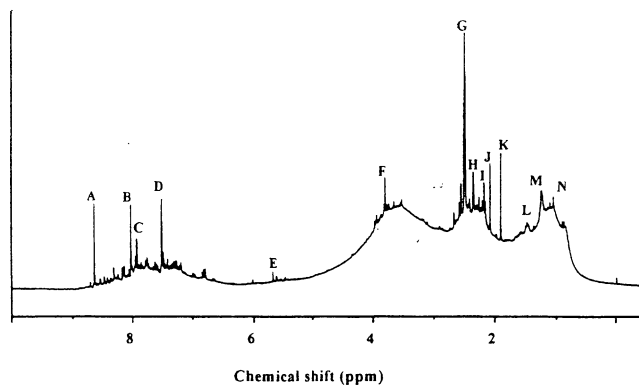

Figure 1. Solution ^{1}H NMR spectrum of the Bayer humic substance. Resonances A−N are assigned in the text.

Fourier transform infrared spectra were recorded from 4000 to 400 cm^{-1} using a Nicolet Magna-IR 760 spectrometer with 64 scans and a resolution of 4 cm^{-1}. Samples were prepared as KBr disks with a diameter of 16 mm (2 mg of sample/250 mg of KBr). All spectra were recorded by subtracting background.

Solvent fractions were methylated and analyzed by GC/MS. Approximately 0.5 mg of the humic sample and each of the four solvent fractions were placed in a 2-mL glass ampule. One hundred microliters of a solution made from 5 mL of 25% tetramethylammonium hydroxide in methanol and 1 mL of 0.05% (w/v) of an internal standard, C19 alkane, in methanol was added. The methanol was evaporated to dryness under vacuum, and the ampules were sealed under vacuum. The ampules were placed in an oven at 200 °C for 30 min. After being cooled, the ampules were opened and thoroughly washed out with dichloromethane (~100 μL). The solution was then analyzed by GC/MS.

An HP 5890 GC/MS instrument interfaced to an HP 5970 mass-selective detector was used. One microliter of the solution was injected onto a DB5MS capillary column (30 m × 0.25 mm i.d.). The oven was programmed to have an initial temperature of 60 °C. After an initial holding time of 5 min, the oven was heated at a rate of 5°/min to 290 °C. Mass spectral analysis was carried out in full-scan mode over a range of m/z 60−600.

2.5. High-Performance Liquid Chromatography (HPLC). All HPLC separations were performed using a Waters 2690 Alliance system equipped with a Waters 996 photodiode array (PDA) detector. Separations were performed on a Waters Nova-pak C18, 4-μm particle size, 3.9 × 150 mm (60-Å pore size) column at a flow rate of 0.5 mL/min. The Bayer humic material sample was redissolved in water/methanol (80/20, v/v) using an ultrasonic bath (5 min), and 50 μL of the solution (concentration 1500 mg/L) was injected. All chromatograms were analyzed over the wavelength range of 190−400 nm. The mobile-phase composition (acetonitrile, water, formic acid, tetrabuytlammonium hydroxide) and the elution program (isocratic and gradient) varied throughout this study. All four samples obtained from the continuous solvent extraction procedure were subjected to similar HPLC analyses.

3. Results and Discussion

3.1. Structure of Humic Material. Figure 1 shows the ^{1}H NMR spectrum obtained in deuterated dimethylsulfoxide (DMSO-d_6). The NMR spectrum represents

two main regions, the aliphatic (0–6 ppm) and the aromatic (7–10 ppm). The individual resonances with relatively high intensities with chemical shifts of 8.63, 8.03, 7.95, 7.51, 5.65, 3.79, 2.49, 2.35, 2.19, 2.07, 1.90, 1.47, 1.24, and 1.05 ppm are labeled A–N sequentially. Many of these peaks have been previously assigned in other humic materials.[22,23] The signals at 3.79 and 2.49 ppm (peaks F and G, respectively) were attributed to water in DMSO and methyl signals of trace amounts of nondeuterated DMSO, respectively. The signals at 8.63 ppm (A) and 1.9 ppm (K) were assigned to hydrogen of formate (HCOO⁻) and the methyl group of acetate (CH₃COO⁻), respectively.

The presence of a number of singlets between 7 and 9 ppm can be attributed to isolated proton spin systems, most likely on substituted aromatic rings. The protons on an aromatic ring with electron-donating substitutions such as ethers and hydroxy groups will be shielded and will therefore appear between 6.5 and 7 ppm. Some alkene protons are observed at 5.6 ppm (peak E, Figure 1). Despite the broad DMSO peak between 3 and 4 ppm, a number of smaller peaks can be seen that indicate the presence of protons attached to carbons directly bonded to electronegative groups such as ether and alkoxy groups in the humic macromolecules or from furan-type molecules. The tetrahydrofurans, which are formed during the Bayer process from the rearrangement of carbohydrates, will have protons in this region.

The ^{1}H–^{1}H homonuclear correlation (COSY) NMR spectrum is shown in Figure 2 and revealed information on the extent of the spin–spin coupling among the protons. The aliphatic region, between 0.8 and 2.4 ppm, exhibits two distinct correlations. These peaks are obscured by the broad hump in the region. The triplet at 2.19 ppm in Figure 2b (see peak I, Figure 1) is coupled to the protons (multiplet) at 1.47 ppm, and the protons at 1.47 ppm is further coupled to protons at 1.24 ppm. Although the splitting pattern of the peak at 1.24 ppm is not visible because of the superimposition of the broad peak, it is most likely to be a terminal methyl group. The triplet at 2.19 ppm can be attributed to methylene protons in close proximity to an electron-withdrawing group such as carboxylic acid. The singlets at 2.07 and 1.90 ppm (peaks J and K, respectively, Figure 1) are not present in Figure 2 and hence can be assigned to proton-isolated methyl ketone substituent, i.e., CH₃–CO–C–, and acetate, i.e., CH₃COO⁻, respectively.

Several correlations can be observed in the aromatic region. The two sets of doublets at 6.80 and 6.82 (Figure 2a) show correlations to protons at 7.75 and 7.43 ppm, respectively. It is most likely that the peaks at 6.80 and 7.75 ppm correspond to the protons on 4-hydroxybenzoic acid and that the 6.82 and 7.43 ppm peaks belong to the adjacent protons of 3,4-dihydroxybenzoic acid. In both instances, the proton adjacent to the hydroxy group will be shielded and hence will appear at high field. Another correlation between the protons at 7.50 and 7.95 ppm suggests an electron-deshielded environment and was assigned to 1,2-benzene dicarboxylic acid. The singlet at 8.03 ppm belongs to isolated, electron-deficient protons and was assigned to 1,4-benzene dicarboxylic acid. The symmetry of the molecule gives rise to only a single peak in the NMR spectrum. The doublet peak at 8.15 ppm in Figure 2b and the other two protons giving signals at 8.47 and 7.65 ppm showed the 1,3,4-trisubtituted benzene ring system where the proton at 8.15 ppm is coupled to both the protons at 8.47 and 7.65 ppm.
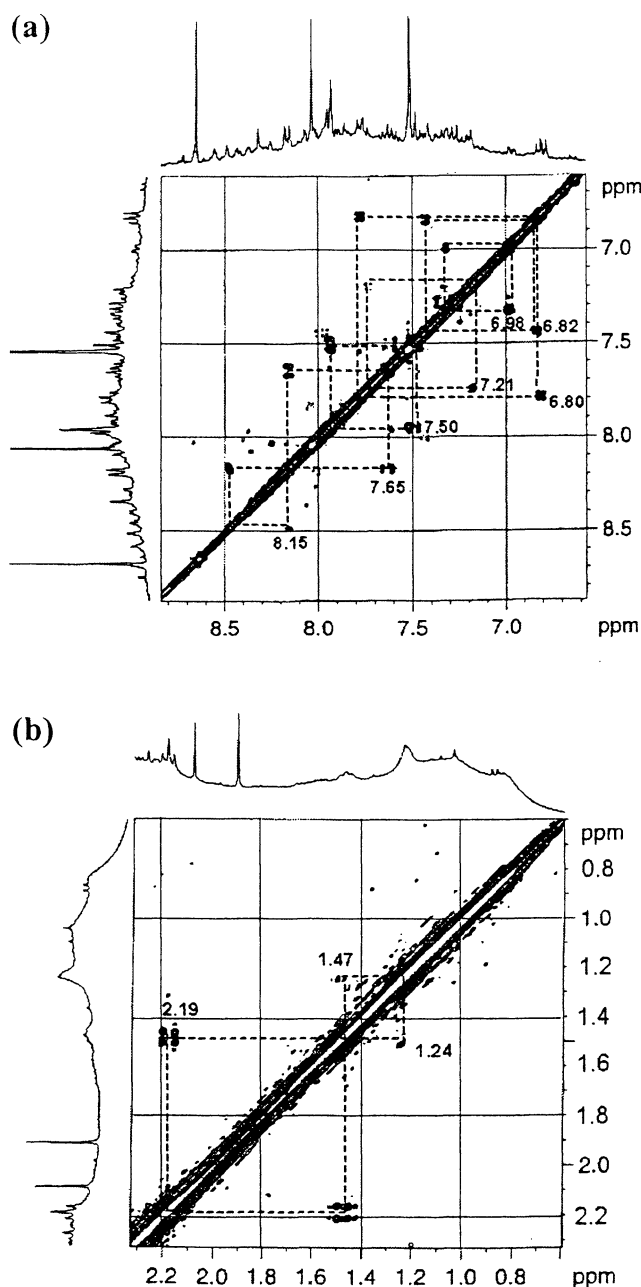
(a)

(b)

Figure 2. ^{1}H–^{1}H homonuclear 2-D correlation (COSY) spectrum of the Bayer humic substance: (a) aromatic region, (b) aliphatic region. Assignments are described in the text.

In summary, the results of the 1-D and 2-D ^{1}H NMR spectra give information on the type and pattern of substitution of the protons in the molecular components.

The ^{13}C solid-state CP/MAS NMR spectrum is shown in Figure 3, and the assignments of carbons belonging to different functional groups are summarized in Table 3. The spectrum shows four broad regions that can be assigned to aliphatic carbon groups unsubstituted with O (C-alkyl, 0–50 ppm), carbon attached to a methoxy group (55 ppm) and all other aliphatic carbons attached to alkoxy and hydroxy groups (O-alkyl, 50–100 ppm), carbons with two alkoxy groups and aromatic carbons (acetal and aromatic, 100–160 ppm), and carbonyl carbons in carboxyl groups (160–190).[22,23] Table 3 also indicates the percent composition of the different carbon groups in the Bayer humic sample, which was calculated by integration of the different regions in the ^{13}C solid-state NMR spectrum.
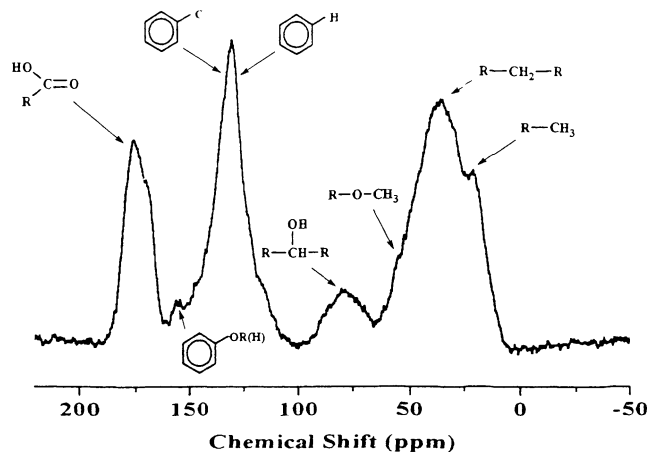
Figure 3. Cross-polarization (1-ms) ^{13}C solid-state NMR spectrum of the Bayer humic substance. Structural groups are assigned.

Table 3. Percentage Composition of Different Carbon Types in the Bayer Humic substance as measured by Solid-State ^{13}C NMR Spectroscopy[a]

percent composition (%)	chemica shift (ppm)	humic substance	F1[b]	F2[c]	F3[d]	F4[e]
C-alkyl	0-50	42.4	35.7	39.4	36.5	37.4
O-alkyl	50-100	5.4	5.4	5.5	6.2	4.6
acetal, aromatic	100-160	31.3	33.9	31.3	35.0	41.3
carboxyl	160-190	20.9	25.0	23.8	22.5	16.7
carboxyl ratio	180/175	1.22	0.8	0.9	1.0	2.0

[a] Solvent peaks have been not been integrated, error is ± 0.5. [b] Diethyl ether fraction. [c] Ethyl acetate fraction. [d] Isopropyl alcohol fraction. [e] Water fraction.

Overall, the IR spectrum in Figure 4a reflects the preponderance of oxygen-containing functional groups, that is, CO$_2$H, OH, and C=O, in the humic material. The broad absorption at 3433 cm^{-1}(A) is due to the O–H stretching of the H-bonded OH groups. The bands in the region of 2900–3000 cm^{-1} (B) are attributed to the asymmetric and symmetric stretching vibrations of aliphatic C–H bonds in CH$_3$ and CH$_2$ groups and are a common feature in most humic samples. The distinct band at 1709 cm^{-1} (C) is the C=O stretching vibration, which is due to carboxyl groups present in the Bayer humic sample. The band at 1616 cm^{-1} (D) is due to C=C vibration of aromatic compounds, the hydrogen-bonded C=O of carbonyls or quinones, and the COO$^-$ symmetric stretching. The absorption band at 1403 cm^{-1} (E) can be assigned as the OH deformation and C–O stretching of phenolic OH, the C–H deformation of CH$_2$ and CH$_3$ groups, and the COO$^-$ antisymmetric stretching. The broad band at 1237 cm^{-1} (F) is attributed to C–O stretching and the OH deformation of COOH groups and stretching of aryl ethers and phenols. The weak bands at 933 (G) and 772 (H) cm^{-1} are due to the out-of-plane bending of the aromatic C–H and C–H of long-chain aliphatics.[22-24]

3.2. Structure of Solvent-Fractionated Material. Similar and additional studies were carried out on the solvent-fractionated material. ^{1}H NMR spectra showed that small molecules concentrated in the diethyl ether and ethyl acetate fractions. This is best illustrated by Figure 5, which shows small molecules observed by GC/MS after methylation. Compounds identified by library matching are listed in Figure 5.

The infrared spectra of the solvent fractions are shown in Figure 4. Differentiation occurs primarily in the number of structural carboxylic acid groups ob-
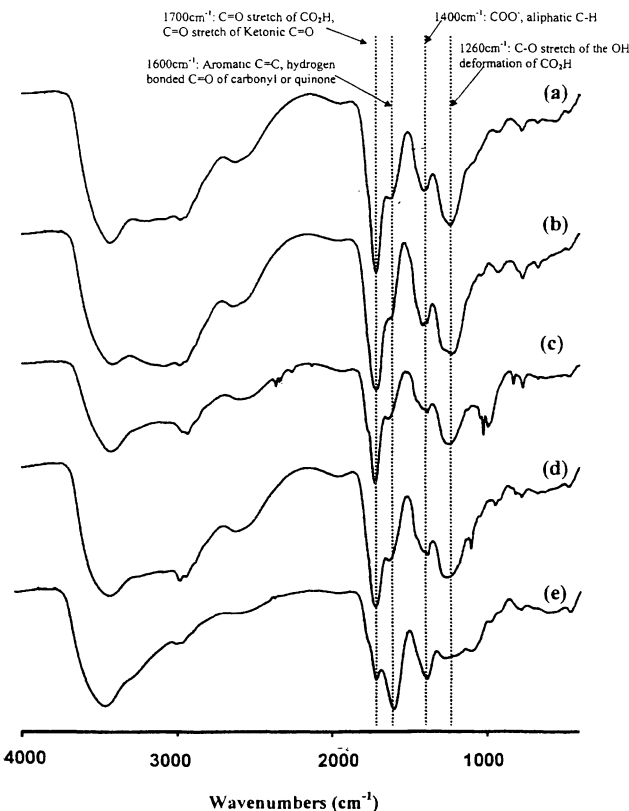

Figure 4. FT-IR spectra of the solvent fractions: (a) Bayer humic sample, (b) diethyl ether fraction, (c) ethyl acetate fraction, (d) isopropyl alcohol fraction, and (e) water fraction. Absorptions are (A) 3433, (B) 2974, (C) 1709, (D) 1616, (E) 1403, (F) 1237, (G) 933, and (H) 772 cm^{-1} in the whole Bayer humic sample.

served in the infrared spectra. A decrease in the intensity of the absorption band at 1700 cm^{-1} can be seen in all four fractions from the least polar extract to the most polar. This indicates a decrease in the content of carboxylic groups (C=O stretch at 1700 cm^{-1}) from the diethyl ether fraction (Figure 4b) to the water fraction (Figure 4e). The reduction coincides with a change in magnitude of the C–O stretching vibration at 1260 cm^{-1}. The water extract displayed a considerable reduction in the amount of carboxylic acid functional groups present compared to the diethyl ether extract. Thus, it is clear that the water-soluble extract contains the fewest of polar groups. This might seem strange, but it should be appreciated that the solubility of humic materials is controlled by association, so small molecules that can aggregate by arranging their polar groups internally to produce a more hydrophobic complex are more soluble in organic solvents.[24]

The ^{13}C data are supportive of the infrared data. The frequency-domain ^{13}C spectrum for each extract was analyzed to approximately determine the different structural groups present using the established literature methods previously mentioned. Table 3 summarizes the functional group assignments and indicates the percent composition of the different carbon groups in the Bayer humic sample and the carboxyl ratios calculated by integration of the different regions in the ^{13}C solid-state NMR spectra. The carboxyl content follows the order expected. The carboxyl group is partly resolved into two groups at 175 and 180 ppm, with the aromatic carboxylic acids assigned to the higher chemical shift (this is also evident in Figure 3 for the whole humic material). The diethyl ether extract contains
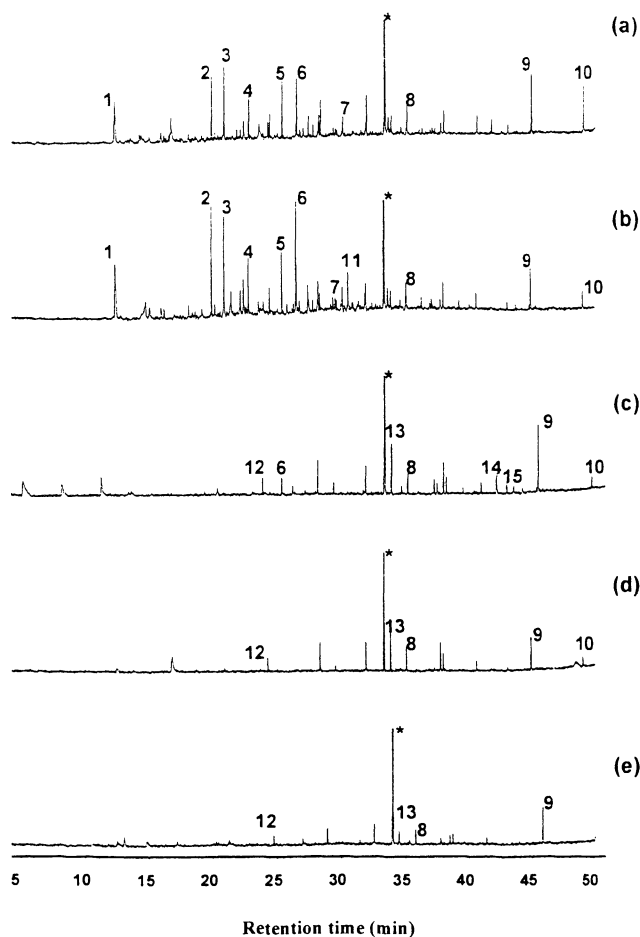
Figure 5. GC/MS results for methylated solvent fractions: (a) Bayer humic sample, (b) diethyl ether fraction, (c) ethyl acetate fraction, (d) isopropyl alcohol fraction, and (e) water fraction. (1) Benzoic acid methyl ester, (2) 3-methoxybenzoic acid methyl ester, (3) 4-methoxybenzoic acid methyl ester, (4) octanedioic acid dimethyl ester, (5) nonanedioic acid dimethyl ester, (6) 3,4-methoxybenzoic acid dimethyl ester, (7) 3,4-dihydro-5-methoxy-3,8-dimethyl-1(2H)-naphthalenone, (8) octadecanoic acid methyl ester, (9) 1,2-benzenedicarboxylic acid bis(2-ethylhexyl) methyl ester, (10) squalene, (11) 3,5-di-tert-butyl-4-hydroxybenzaldehyde, (12) 1,4-benzenedicarboxylic acid methyl ester, (13) hexadecanoic acid methyl ester, (14) 1,2-benzenedicarboxylic acid butyl phenylmethyl ester, and (15) hexanedioic acid bis(2-ethylhexyl) methyl ester. *indicates internal standard, nonadecane.

more of the 175 ppm group and the water extract more of the 180 ppm group.[29] This could be hydrogen-bonded or deshielded carboxylic acids. Hydrogen bonding deshields the COOH group, which is in agreement with the data if the material in the ether extract is complexed in hydrogen-bonded structures, intramolecularly, or in supramolecular structures, whereas that in the water extract is free to bond with the water.[29] However, bearing in mind that the water fraction is more aromatic, as is evident both from the NMR and infrared spectra (as seen by comparing the relative intensities of the 1616 cm^{-1} absorption due to C=C vibrations), these differences could be due to different amounts of aromatic and aliphatic bound carboxylic, respectively.

3.3. Development of a Liquid Chromatographic Method. 3.3.1. Reverse-Phase Chromatography.
Because of the wide range of applicability, the convenience, and the ease with which the selectivity and capacity factor can be altered through the manipulation of the aqueous mobile phase, reverse-phase chromatography was used as the starting point for developing a
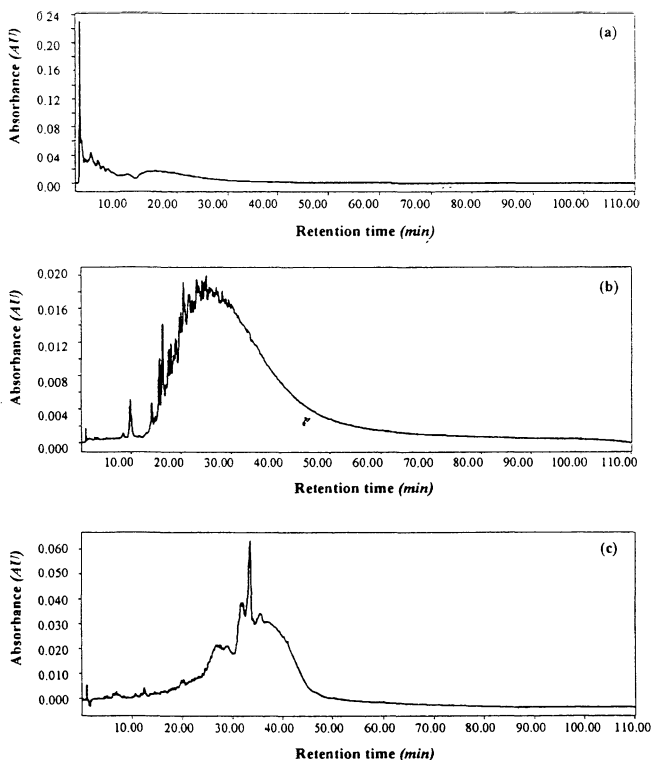

Figure 6. HPLC separation of the Bayer humic sample using (a) reverse-phase chromatography with water and acetonitrile gradient, (b) ion-suppression chromatography with 1% formic acid, and (c) ion-pairing chromatography with PIC A and acetonitrile; linear gradient 1% min^{-1}.

method for the separation of the Bayer liquor humic sample. A water/acetonitrile gradient was used, running isocratic for 10 min on water and then with a linear gradient from 100% water to 100% acetonitrile with a 1% change per minute. The chromatogram in Figure 6a shows that the majority of the Bayer liquor humic sample eluted in the first 20 min, close to the void. From this result, normal reverse-phase chromatography can be seen to be inadequate for separating the Bayer liquor humic sample, and another mode of separation was required.

3.3.2. Ion-Suppression Chromatography. Ionic samples are normally separated by ion-exchange or ion-pair chromatography, but reverse-phase chromatography can be used if the sample contains weak acids or weak bases in addition to neutral compounds. In cases where the sample contains weak acids or weak bases, it is possible to alter the chromatographic retention by adjusting the pH of the eluent with the addition of a buffer to the mobile phase. This mode of separation termed "ion suppression", controls chromatographic retention through suppression of the ionization of an ionic sample. The ionization of an acid or the protonation of a base is suppressed by adjusting the pH, thereby allowing the sample to be chromatographed on a reverse-phase column using methanol or acetonitrile plus a buffer solution as the mobile phase and incresing the retention of the sample.[5]

In this case, the aqueous component of the mobile phase was adjusted to a lower pH with 1% formic acid, which suppressed the ionization of the weak acid solutes, thus allowing for improved retention on the hydrophobic stationary phase. A 1% formic acid/acetonitrile gradient was used, running isocratically for 10 min on 1% formic acid and then with a linear gradient
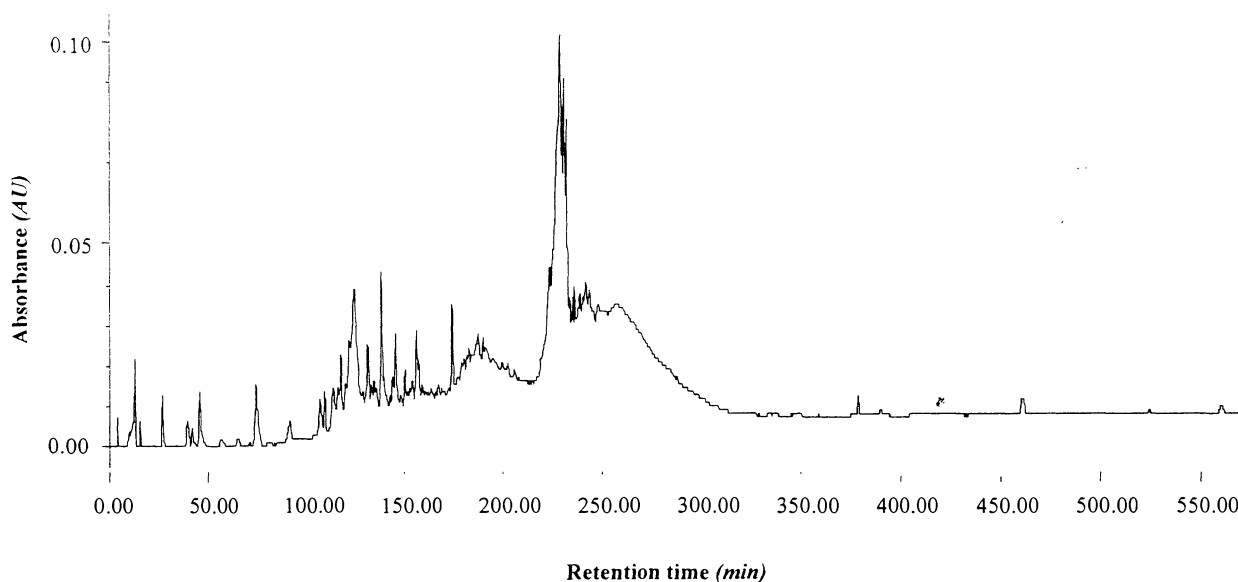
Figure 7. HPLC gradient separation of the Bayer humic sample using reverse-phase chromatography with water and acetonitrile gradient of 0.25% min^{-1}.

from 1% formic acid to 100% acetonitrile with a 1% change per minute. The chromatogram in Figure 6b shows the humics from the Bayer liquor being retained for longer extents, allowing further separation to occur. Through adjustment of the pH of the mobile phase, the ionic equilibrium of the Bayer humic sample has been adjusted to the neutral form, increasing its retention on the hydrophobic stationary phase. The ionized form of the Bayer humic sample is eluted more rapidly in comparison to its neutral form because of the greater affinity the polar ionized form has to the polar aqueous phase, whereas the neutral form has a greater affinity for the hydrophobic stationary phase of the Nova-pak C18 column. The majority of the sample eluted after 20 min with some resolution achieved, but the separation was still poor. To improve the separation, the gradient was altered by slowing the percentage change to a 1% change every 4 min. This had little effect on the resolution, indicating that another mode of separation such as ion-pair chromatography would be more appropriate.

3.1.3. Ion-Pair Chromatography. In cases where the sample contains strong acids or bases and in the case of polar solutes of small molecules, the method of ion suppression might not be adequate.[25,26] Improved control of retention and selectivity on a reverse-phase column in these cases is obtained with the application of an ion-pairing reagent.[27] Ion-pairing chromatography is an extension of the principles discussed for ion-suppression chromatography. An organic water-soluble ionic compound (ion-pairing reagent) is added to the mobile phase and forms an ion pair with a sample component of the opposite charge. Addition of an ion-pairing reagent can alter the retention of the ionic compounds in the sample but will not affect the retention of the neutral compounds.[25,26] Uncertainty still exists over the retention mechanism of this mode of separation; however, it is believed that an electrical double layer is formed at the stationary phase surface by the lipophilic ion-paring reagent ions, thus establishing a dynamic equilibrium with the eluent and stationary phases.[25-28] It is generally observed that the retention of the oppositely charged solute ions increases with increased concentration and hydrophobicity of the pair-

ing ion in the mobile phase and can be further altered by adjusting the percentage of the organic eluent or the pH.[27]

For organic acids, the added ion-pairing reagent is a strong base, which in this case, was tetrabutylammonium hydrogen sulfate, referred to as PIC A. A gradient was run using PIC A (5 mM)/acetonitrile, running isocratically for 10 min on PIC A (5 mM) and then a linear gradient from PIC A (5 mM) to 75% acetonitrile with a 1% change per minute. The resulting chromatogram in Figure 6c shows that greater resolution was achieved using PIC A, with the humics from the Bayer liquor eluting over the first 50 min of the run. Neutral solutes in the Bayer humic sample pass through the double layer relatively unaffected. Solutes that have an opposite charge to the ion-pairing reagent in the Bayer humic sample show an increase in retention due to an attraction with the electrostatic layer. The solutes in the Bayer humic sample with the same charge as the ion-pairing reagent show a decrease in retention due to repulsion from the electrostatic layer.

Considering all three modes of separation, ion-pairing chromatography displayed significantly greater selectivity compared to the two other chromatographic modes discussed. The humics from the Bayer liquor were retained for longer times, and greater resolution was achieved. As ion-pairing chromatography offered the greatest potential to vary the separation selectivity, time was further spent in developing this method.

To improve on the initial separation seen in Figure 6c, where a PIC A (5 mM)/acetonitrile gradient was used, the gradient was slowed from a 1% change every 1 min to a 1% change every 6 min. As a result of the decrease in the gradient, the Bayer humic sample was retained longer, increasing the interaction of the sample with the stationary phase and eluent. This resulted in greater resolution being achieved in the first 100 min of the chromatographic run. A step gradient was then developed to improve this result. Figure 7 shows the HPLC separation achieved. It is clear that individual small molecules present can be resolved at the start of the chromatogram and that other material elutes much later at 100 min. The small molecules are those seen
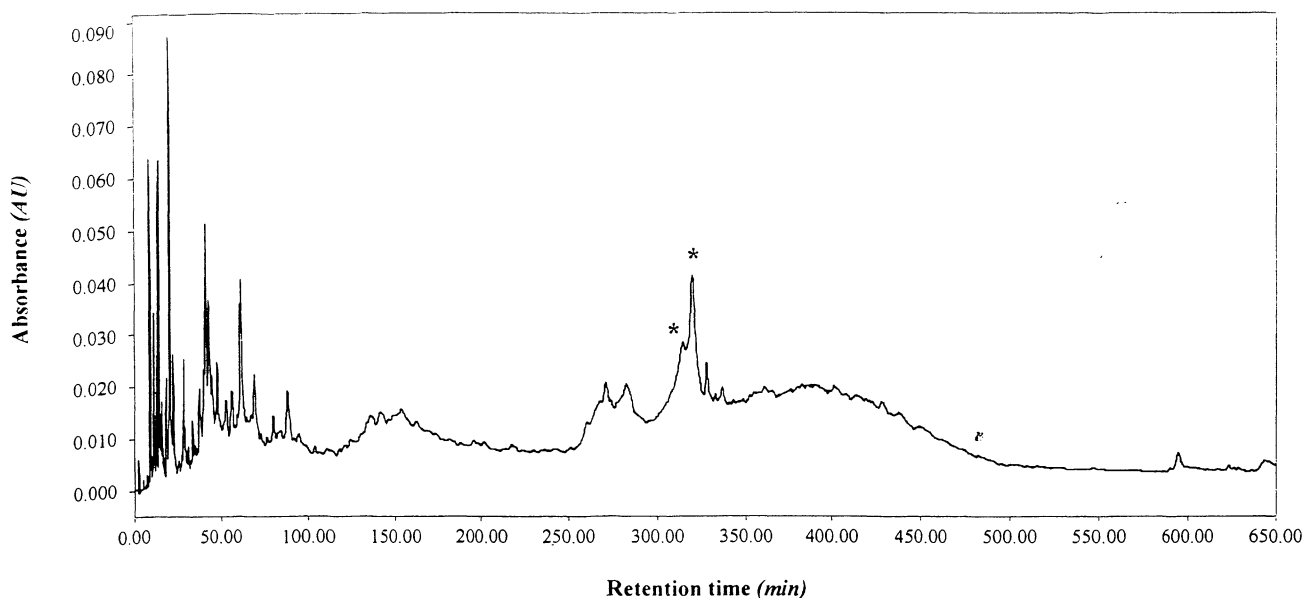
Figure 8. Optimum HPLC separation of the Bayer humic sample. Isocratic PICA (5 mM)/acetonitrile for 10 min, followed by a linear gradient from 100% PIC A (5 mM) to 18% acetonitrile at 0.056% min^{-1}, then 82% PIC A (5 mM) and 18% acetonitrile to 57% PIC A (5 mM) and 43% acetonitrile at 0.083% min^{-1}, and then 50% PIC A (5 mM) and 50% acetonitrile for 5 min. * = solvent change artifact.

by NMR spectroscopy and are the parent molecules to those observed by mass spectroscopy.

Of more novelty is the high-molecular-weight material. Figure 8 shows the optimum separation achieved for the Bayer humic sample. There is a slight loss of resolution in the separation in Figure 8 compared to the separation under the conditions shown in Figure 7. The separation shown in Figure 8, however, is the optimum, as it achieved baseline resolution for four groupings: the highly resolved low-molecular-weight material at 0–100 min, a second grouping of material at 100–200 min, the partly resolved material at 250–280 min, and the hump from 280 to 500 min. To achieve the separation in Figure 8, a gradient was run using PIC A (5 mM)/acetonitrile, running isocratically for 10 min on PIC A (5 mM) and then using a linear gradient from 100% PIC A (5 mM) to 18% acetonitrile with a 1% change every 18 min. The gradient continued running from 82% PIC A (5 mM) and 18% acetonitrile to 57% PIC A (5 mM) and 43% acetonitrile with a 1% change every 12 min. The gradient was then changed to 50% PIC A (5 mM) and 50% acetonitrile over 5 min and then held for 10 min. The chromatogram showed that substantial separation was achieved in the first 300 min, with an improvement on the separation between 300 and 650 min.

The chromatograms of the solvent-soluble extracts were analyzed using the optimum conditions developed above. The low-molecular-weight polar material concentrates at the lowest retention time and is concentrated in the diethyl ether fraction, as expected from the spectroscopic data. The material eluting at retention times above 300 min appears to concentrate in the water-soluble extract, which is the least polar, as it does not contain hydrogen-bonded associated organic material. Thus, the validity of the methodology is demonstrated.

The separation in Figure 8 is highly significant because it represents the first recorded liquid chromatographic method in which Bayer humic materials of a higher molecular weight have been separated into groups of different polarities. It also demonstrates that

the material is not randomly polymeric and that there are discrete structural types that chromatograph differently.

It is interesting that the material elutes not as a continuum, but rather as clusters of peaks. These peak clusters could represent micellar-like aggregates of different amounts of polar groups such as the rapidly eluted material, but of higher molecular weight and with less polar functionality. In other words, it must be true that only certain configurations are stable; otherwise, the chromatograph in Figure 8 would be a continuum. An outstanding problem is to determine the molecular weights of these clusters as only certain defined molecular clusters must be allowable.

Conclusions

A high-performance liquid chromatographic method has been developed that separates Bayer humic material into compound classes. The optimum separation was achieved by using a gradient using PIC A (5 mM)/acetonitrile, running isocratically for 10 min on PIC A (5 mM) and then applying a linear gradient from 100% PIC A (5 mM) to 18% acetonitrile with a 1% change every 18 min. The gradient continued running from 82% PIC A (5 mM) and 18% acetonitrile to 57% PIC A (5 mM) and 43% acetonitrile with a 1% change every 12 min. The gradient was then changed to 50% PIC A (5 mM) and 50% acetonitrile over 5 min. The gradient was then held for 10 min.

Solvent separation of the humic material yielded compound classes that were then correlated with the optimum separation achieved as shown in Figure 8. The most polar material concentrates in the least polar solvents, showing that the humic material has a micellar-like structure in that polar groups are concentrated to avoid solvent interaction in fractions soluble in the least polar solvents.

Small molecules and three discrete clusters of macromolecules were observed. Within these clusters, there is some degree of further resolution. It must be the case that only certain configurations are stable; otherwise,

the separation would show a continuum of peaks rather than clusters. Four discrete fractions were observed in Figure 8 that represent certain stable configurations of molecular weights that are controlled by polarity through intramolecular binding and are strong evidence for a supramolecular structure to humic material rather than the existence of random conformational material.

Acknowledgment

Literature Cited

(1) Grocott, S. G. Bayer liquor impurities: Measurement of organic carbon oxalate and carbonate extractions from bauxite digestives. *Light Met.* **1988**, 833–841.

(2) Atkins, P.; Grocott, S. C. Impact of organic impurities on the product of refined alumina. In *Proceedings Science, Technology and Utilisation of Humic Acids*; CSIRO Division of Coal and Energy Technology: Sydney, Australia, 1988; pp 85–94.

(3) Lever, G. Identification of organics in Bayer liquor. *Light Met.* **1978**, 71–83.

(4) Wilson, M. A.; Perdue, M.; Vassallo, A. M.; Reuter, J. H. A. Compositional and Solid State Nuclear Magnetic Resonance Study of Humic and Fulvic Acid Fractions of Soil Organic Matter. *Anal. Chem.* **1987**, *59*, 551–558.

(5) Wilson, M. A.; Ellis, A. V.; Lee, G. S. H.; Rose, H. R.; Lu, X.; Young, B. R. Structure of molecular weight fractions of Bayer humic substances. 1. Low-temperature products. *Ind. Eng. Chem. Res.* **1999**, *38*, 4663–4674.

(6) Smeulders, D. E.; Wilson, M. A.; Patney, H. K.; Armstrong, L. Structure of molecular weight fractions of Bayer humic substances. 2. Pyrolysis behavior of high-temperature products. *Ind. Eng. Chem. Res.* **2000**, *39*, 3631–3639.

(7) Smeulders, D. E.; Wilson, M. A.; Armstrong, L. Insoluble Organic Compounds in the Bayer Process. *Ind. Eng. Chem. Res.* **2001**, *40*, 2243–2251.

(8) Grocott, S. C.; Rosenberg, P. R. Soda in Alumina. Possible mechanisms for soda incorporation. In *Proceedings of the Third International Alumina Quality Workshop, Gladstone, Australia*; 1988; pp 271–287.

(9) Armstrong, L. Bound soda incorporation during hydrate precipitation. *Proceedings Third International Alumina Quality Workshop, Hunter Valley, Australia*; 1993; pp 282–292.

(10) Alamdari, A.; Raper, J. A.; Wainwright, M. S. Poisoning of the precipitation of alumina trihydrate by mannitol. *Light Met.* **1993**, 143–149.

(11) Coyne, J. F.; Wainwright, M. S.; Cant, N. W.; Grocott, S. C. Adsorption of hydroxy organic compounds on alumina trihydrate. *Light Met.* **1994**, 39–45.

(12) Tran, T.; Kim, M. J.; Emanuel, H. J.; Wong, P. L. M., The effect of 3,4-dihydroxybenzoic acid (3,4-DHBA) on the precipitation and attrition of alumina trihydrate. *In Fourth International Alumina Quality Workshop, Darwin, NT, Australia*, 1996; pp 292–300.

(13) Smeulders, D. E.; Wilson, M. A.; Armstrong, L. Poisoning of the precipitation of aluminium hydroxide by molecular weight fractions of Bayer humic substances. *Ind. Eng. Chem. Res.* **2001**, *40*, 5901–5907.

(14) Wilson, M. A.; Farquharson, G. J.; Tippett, J. M.; Quezada, R. A.; Armstrong, L. Aluminophilicity of the humic degradation product of 5-hydroxybenzene-1,3-dicarboxylic acid. *Ind. Eng. Chem. Res.* **1998**, *37*, 2410–2415.

(15) Watling, H. R.; Smith, P. G.; Loh, J.; Crew, P.; Shaw, M. Comparative effects of model organic compounds on gibbsite crystallisation. In *Fourth International Alumina Quality Workshop, Darwin, NT, Australia*, 1996; pp 553–555.

(16) Smith, P. G.; Watling, H. R.; Crew, P. The effects of model organic compounds on gibbsite crystallisation from alkaline aluminate solutions: Polyols. *Colloids Surf. A: Physicochem. Eng. Aspects* **1996**, *111*, 119–130.

(17) Ochs, M.; Cosovic, B.; Stumm, W. Coordinative and hydrophobic interaction of humic substances with hydrophilic Al_2O_3 and hydrophobic mercury surfaces. *Geochim. Cosmochim. Acta* **1994**, *58*, 639–650.

(18) Smeulders, D. M.; Wilson, M. A. Crystal Surface and humic material effects on crystallisation. In *Proceedings of the 10th Humic Substances Society Conference*; International Humic Substances Society, St. Paul, MN; pp 478–480.

(19) Jackson, P. Analysis of oxalate in Bayer liquors—A comparison of ion chromatography and capillary electrophoresis. *J. Chromatogr.* **1995**, *693*, 155–161.

(20) Harakuwe, A.; Haddad, P.; Jackson, P. Quantitative determination of oxalate in Bayer liquor by capillary zone electrophoresis—a validative study. *J. Chromatogr.* **1996**, *739*, 399–403.

(21) Susic, M.; Armstrong, L. G. High-performance liquid chromatographic determination of humic acid in sodium aluminate solution. *J. Chromatogr.* **1990**, *502*, 443–44.

(22) Lee, G. S. H.; Wilson, M. A.; Young, B. R. The application of the "WATERGATE" suppression technique for analysing humic substances by nuclear magnetic resonance. *Org. Geochem.* **1998**, *28*, 549–559.

(23) Wilson, M. A.; Collin, P. J.; Malcolm, R. L.; Perdue, M.; Cresswell, P. Low molecular weight species in humic and fulvic fractions. *Org. Geochem.* **1988**, *12*, 7–12.

(24) Smeulders, D. E; Wilson, M. A.; Kannangara, G. S. K. Host–guest interactions in humic materials. *Org. Geochem.* **2001**, *32*, 1357–1371.

(25) Bieganowska, M.; Petruczynik, A. Ion pair chromatography and its application in analysis of pharmaceuticals. *Chem. Anal.* **1994**, *39* (5), 525–541.

(26) Bidlingmeyer, B.; Deming, S.; Price, W.; Sachok, B.; Petrusek, M. Retention mechanism for reversed-phase ion-pair liquid chromatography. *J. Chromatogr. A* **1979**, *186*, 419–434.

(27) Haddad, P.; Jackson, P. Ion-interaction chromatography. In *Ion Chromatography: Principles and Applications*; Elsevier: New York, 1990; Vol. 46, pp 165–193.

(28) Bidlingmeyer, B. Separation of ionic compounds by reversed-phase liquid chromatography: An update of ion-pairing techniques. *J. Chromatogr. Sci.* **1980**, *18*, 525–539.

(29) Stothers, J. *Carbon-13 NMR Spectroscopy*; Academic Press: New York, 1972.